ELECTROCHEMICAL DETECTION OF DNA USING POLY(VINYLFERROCENIUM) MODIFIED ELECTRODES

POLİ(VİNİLFERROSENYUM) MODİFİYE ELEKTROTLAR KULLANILARAK ELEKTROKİMYASAL DNA TAYİNİ

FİLİZ KURALAY

Submitted to Institute of Sciences of Hacettepe University

as a partial fulfilment to the requirements for the award of the degree of

DOCTOR OF PHILOSOPHY

in

CHEMISTRY

2009

Graduate School of Natural and Applied Sciences,

This is to certify that we have read this thesis and that in our opinion it is fully adequate, in scope and quality as a thesis for degree of Doctor of Philosophy in Chemistry.

Chairman :.....

Prof. Dr. Adil DENİZLİ

Member (Advisor) :.....

Prof. Dr. Haluk ÖZYÖRÜK

Member :.....

Prof. Dr. Handan GÜLCE

Member :.....

Assoc. Prof. Dr. Nuray Öğün ŞATIROĞLU

Member (Co-advisor) :.....

Assoc. Prof. Dr. Serdar ABACI

APPROVAL

This thesis has been certified as a thesis for the degree of Doctor of Philosophy by the above Examining Committee Members on ...../...../.....

...../...../.....

Prof. Dr. Erdem YAZGAN
Director of the Graduate School of
Natural and Applied Sciences

TO MY PRECIOUS FAMILY

ELECTROCHEMICAL DETECTION OF DNA USING POLY(VINYLFERROCENIUM) MODIFIED ELECTRODES

Filiz Kuralay

ABSTRACT

Electroactive redox polymer, poly(vinylferrocenium) (PVF^+), modified platinum (Pt), gold (Au) and pencil graphite (PG) working electrodes were used in this study for the preparation, application and characterization of electrochemical DNA biosensor. The electroactive redox polymer provided an appropriate matrix for DNA interaction and hybridization studies. PVF^+ could directly report the electrochemical behavior at low potentials, selectively. Thus, there was no need for an extra indicator to monitor the electrochemical behavior of DNA immobilized polymer modified electrode.

The changes at the oxidation peak currents of polymer and electroactive DNA bases (adenine, guanine) were sensitively monitored by using cyclic voltammetry (CV) and differential pulse voltammetry (DPV) techniques in the absence/presence of DNA on Pt, Au and PG working electrodes. Optimization studies were performed in order to obtain more selectivite and sensitive electrochemical measurements. After the optimum working conditions were obtained, DNA hybridization was performed. PVF^+ modified electrode and DNA immobilized PVF^+ modified electrode were characterized by scanning electron microscopy (SEM), scanning tunneling microscopy (STM), raman spectroscopy, X-ray photoelectron spectroscopy (XPS), fourier transform infrared-attenuated total reflentance (ATR) spectroscopy and alternating current (AC) impedance measurements. The changes in the electrochemical behavior of dsDNA/ssDNA immobilized polymer modified electrodes were investigated after anticancer drug, Mitomycin C (MC) interaction.

Keywords: Poly(vinylferrocenium) modified electrode, polymer, electrochemical DNA biosensor, DNA, guanine, adenine.

Advisor: Prof. Dr. Haluk Özyörük, Hacettepe University, Department of Chemistry, Analytical Chemistry Division
Co-advisor: Assoc. Prof. Dr. Serdar Abacı, Hacettepe University, Department of Chemistry, Analytical Chemistry Division

POLİ(VİNİLFERROSENYUM) MODİFİYE ELEKTROTLAR KULLANILARAK ELEKTROKİMYASAL DNA TAYİNİ

Filiz Kuralay

ÖZ

Bu çalışmada elektroaktif redoks polimeri, poli(vinilferrosenyum) (PVF^+), ile modifiye edilmiş platin (Pt), altın (Au) ve kalem grafit (PG) çalışma elektrotları elektrokimyasal DNA biyosensörlerinin hazırlanması, uygulanması ve karakterizasyonunda kullanılmıştır. Elektroaktif redox polimeri, DNA etkileşimi ve hibridizasyon çalışmaları için uygun bir matriks ortamı sağlamıştır. PVF^+, düşük gerilimlerde seçici olarak doğrudan elektrokimyasal davranışı belirleyebilmektedir. Bu nedenle DNA immobilize polimer modifiye elektrodun elektrokimyasal davranışını gözlemek için başka bir indikatöre gerek kalmamıştır.

DNA içermeyen ve DNA immobilize polimer modifiye Pt, Au ve PG çalışma elektrotlarında polimerin ve elektroaktif DNA bazlarının (adenin, guanin) yükseltgenme pik akımlarındaki değişiklikler dönüşümlü voltametri (CV) ve diferansiyel puls (DPV) voltametri yöntemleri ile duyarlı bir şekilde ölçülmüştür. Daha seçici ve duyarlı elektrokimyasal ölçümler elde edebilmek için optimizasyon çalışmaları yapılmıştır. Optimum çalışma koşulları belirlendikten sonra DNA hibridizasyonu gerçekleştirilmiştir. PVF^+ modifiye elektrotlar ve DNA immobilize PVF^+ modifiye elektrotlar taramalı elektron mikroskobu (SEM), taramalı tünelleme mikroskobu (STM), raman spektroskopisi, X-ışınları fotoelektron spektroskopisi (XPS), fourier transform infrared azalan tam yansıma spektroskopisi (ATR) ve alternatif akım (AC) impedans ölçümleri ile karakterize edilmiştir. dsDNA/ssDNA immobilize polimer modifiye elektrotların antikanser ilacı, Mitomisin C ile etkileşimden sonra elektrokimyasal davranışındaki değişiklikler incelenmiştir.

Anahtar kelimeler: Poli(vinilferrosenyum) modifiye elektrot, polimer, elektrokimyasal DNA biyosensörü, DNA, guanin, adenin.

Danışman: Prof. Dr. Haluk Özyörük, Hacettepe Üniversitesi, Kimya Bölümü, Analitik Kimya Anabilim Dalı

Eş-Danışman: Doç. Dr. Serdar Abacı, Hacettepe Üniversitesi, Kimya Bölümü, Analitik Kimya Anabilim Dalı

ACKNOWLEDGEMENT

I would like to express my special thanks to:

My advisor **Prof. Dr. Haluk Özyörük,** for his guidance, invaluable help and encouragement throughout this thesis;

My co-advisor **Assoc. Prof. Dr. Serdar Abacı,** for his invaluable contribution and help;

Prof. Dr. Attila Yıldız, for his invaluable ideas;

Prof. Dr. Kadir Pekmez and **Prof. Dr. Handan Gülce** for their invaluable suggestions and ideas;

Prof. Dr. Arzum Erdem Gürsan, for her kind contribution and collaboration at all levels;

My precious cousin **Assist. Prof. Dr. Mutlu Sönmez Çelebi,** for her deepest support and contribution at all times;

My dear friend **Res. Ass. Ayşenur Sağlam,** for her good fellowship and motivation;

My friends **Dr. Lokman Uzun, Dr. Ayşe Uzgören Baran, Yeşeren Saylan, Assist. Prof. Dr. Dursun Ali Köse** and **Res. Ass. Serhat Döker** for their help and friendship;

Hande Torun and Res. Ass. Gülçin Bolat for their support during the study;

All members of **Electrochemistry Research Group** for their support;

And finally, **my father, mother, brother and sister (my precious family)** for their love, support, encouragement, patience and invaluable contribution during all stages of my life.

TABLE OF CONTENTS

LIST OF FIGURES

LIST OF TABLES

LIST OF SCHEMES

1. INTRODUCTION

Deoxyribonucleic acid (DNA) is the largest, naturally occuring, well defined molecule. Considering its biological function, connected with its marvellous, relatively regular structure, it may be considered as the most interesting, and arguably, also the most important molecule of life (Palecek, 2002a, b). DNA plays an important role in the life process because it carries heritage information and intructs the biological synthesis of proteins and enzymes through the process of replication and transcription of genetic information in living cells. It is of great help to understand the structural properties of DNA, the mutation of genes, the origin of some diseases, the action mechanism of some antitumor and antivirus drugs and, therefore, to design new and more efficient DNA targeted drugs to deal with genetic diseases. Moreover, the detection of DNA sequences is of widespread interest in many fields including clinical, forensic, environmental and food applications (Erdem and Ozsoz, 2002; Lucarelli et al., 2004).

Studies on the binding mechanism of some molecules with DNA have been identified as one of the key topics during the past few decades (Korri-Youssoufi and Makrouf, 2001; Palecek and Fojta, 2001). Conventional methods for the analysis of specific gene sequences are based on either direct sequencing or DNA hybridization methods. Because of its simplicity, the second option is more commonly used in diagnostic laboratories (Jelen et al., 2004).

Electrochemical biosensors have emerged as the most commonly used biosensors. They have received considerable attention in the development of DNA biosensors (Lucarelli et al., 2004; Wang, 2002). Electrochemical DNA biosensors are well suited for rapid and direct detection of specific DNA sequences. The viability of DNA biosensors requires an intimate connection between the nucleic acid system and the electronic transducer. Numerous approaches to electrochemical detection have been developed, including direct electrochemistry of DNA, electrochemistry at polymer modified electrodes, electrochemistry of DNA-specific redox reporters, electrochemical amplifications with nanoparticles, and electrochemical devices based on DNA-mediated charge transport chemistry (Wang et al., 1998). The electrochemistry of DNA is irreversible and occurs at highly negative and positive potentials. Therefore, a derivative should be useful as

a DNA probe that undergoes reversible electrode reactions at less-extreme potentials (Nakayama et al., 2002).

DNA can be immobilized onto the different platforms for development of novel sensor by adsorption, entrapment, complexation, covalent attachment, and other methods (Yang et al., 1997). Polymer modified electrodes can provide a suitable interface for the immobilization of DNA. The use of electroactive polymers as the transduction element of hybridization was recently described in the literature (Piro et al., 2005; Ramanavicius et al., 2006).

Poly(vinylferrocenium) (PVF^+) is a redox type polymer containing the ferrocene/ferrocenium centers that are covalently bound to insoluble polymer skeleton. The polymer can be deposited onto the electrode surface by the electrooxidation of the reduced form poly(vinylferrocene) (PVF) by resulting a less soluble polymer (Gülce et al., 1995a, b, c; Gülce et al., 1997). After the electrostatic immobilization of negatively charged biomolecules onto the polymer modified platinum (Pt) electrode surface effectively, it has been found that this polymer modified electrode can be used as a biosensor in order to monitor different molecules (Gündoğan-Paul et al., 2002a, b; Kuralay et al., 2005; Kuralay et al., 2006). It is known that the PVF is a homegenous compact film whereas PVF^+ is inhomogeneous film in which pores and pinholes exist (Inzelt and Backsai, 1992; Peerce and Bard, 1980).

In this study, a new biosensor for the electrochemical detection of DNA using PVF^+ modified electrode was developed. The electrode was prepared in two steps: (1) electrodeposition of $PVF^+ClO_4^-$ onto the platinum (Pt), gold (Au) and pencil graphite (PG) surfaces from the solution of PVF in methylene chloride including tetra-n-butyl-ammonium perchlorate (TBAP) as supporting electrolyte; (2) incorporation of double-stranded DNA (dsDNA), single-stranded DNA (ssDNA), and oligonucleotides (ODNs) onto the polymer matrix.

In the first part of the study, the electrochemical behavior of PVF^+ modified DNA biosensor was investigated in the absence/presence of dsDNA at the surface of Pt electrode as an electrochemical transducer. The investigation of parameters

influencing DNA immobilization onto $PVF^{+}ClO_4^{-}$ film was studied in terms of optimum analytical conditions; such as, the effects of; the polymeric film thickness, concentration of dsDNA, immobilization time of dsDNA, the concentration of buffer solution, different buffer solutions, pH and temperature of the medium, the concentration of ClO_4^{-} ion. The immobilization mechanism of negatively charged DNA onto the positively charged matrix was tested by reducing the polymer if it was mainly because of electrostatic attraction or not. After the optimum working conditions were obtained, the electrochemical behavior of DNA modified polymer electrode by using dsDNA or ssDNA was compared. The effects of some of the parameters given above; such as, polymeric film thickness, concentration of DNA and immobilization time of dsDNA were also investigated at the surfaces of Au and PG electrodes.

In the second part of the study, the effect of different ODN modifications on the response of this DNA sensing method after ODN immobilization step was examined with thiol linked, amino linked, phosphate linked and bare ODNs in respect to their binding performance onto the positively charged polymer matrix. The effects of thiol and amino linked ODNs concentration were also studied. DNA hybridization studies were also carried out including target ODN concentration.

In the third part of the study, polymer modified electrode and DNA immobilized polymer modified electrode were characterized by scanning electron microscopy (SEM), scanning tunneling microscopy (STM), raman spectroscopy, X-ray photoelectron spectroscopy (XPS), fourier transform infrared-attenuated total reflectance (ATR) spectroscopy and alternating current (AC) impedance measurements.

In the last part, the interactions of an anticancer drug, Mitomycin C (MC) with dsDNA/ssDNA immobilized polymer modified electrodes were investigated.

2. DEOXYRIBONUCLEIC ACID (DNA)

2.1. Nucleic Acids

The nucleic acids, deoxyribonucleic acid (DNA) and ribonucleic acid (RNA) are the biologically occuring polynucleotides. They are the molecular repositories for genetic information. The structure of every protein, and ultimately of every cell constituent, is a product of information programmed into the nucleotide sequence of a cell's nucleic acids (Lehninger et al., 1982).

2.2. Structure of DNA

DNA is a very long, threadlike macromolecule made up of a large number of deoxyribonucleotides, each composed of a nitrogenous base, a sugar, and a phosphate group. The bases of DNA molecules carry genetic information, whereas their sugar and phosphate groups perform a structural role (Stryer, 1995). The sugar in a deoxyribonucleotide is deoxyribose. The deoxy prefix indicates that this sugar lacks an oxygen atom that is present in ribose, the parent compound. The nitrogenous base is a derivative of purine or pyrimidine (Figure 2.1). The purines in DNA are adenine (A) and guanine (G), and the pyrimidines are thymine (T) and cytosine (C). The structures of DNA bases are given in Figure 2.2.

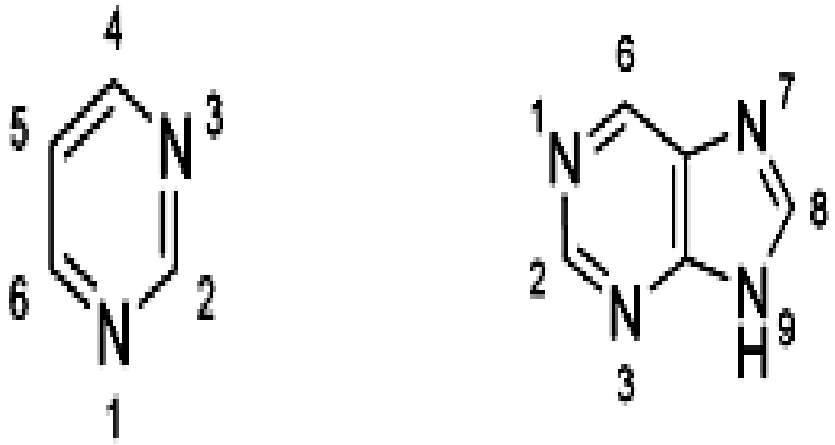

Pyrimidine Purine

Figure 2.1. The parent compounds of the pyrimidine and purine bases of nucleotides and nucleic acids.

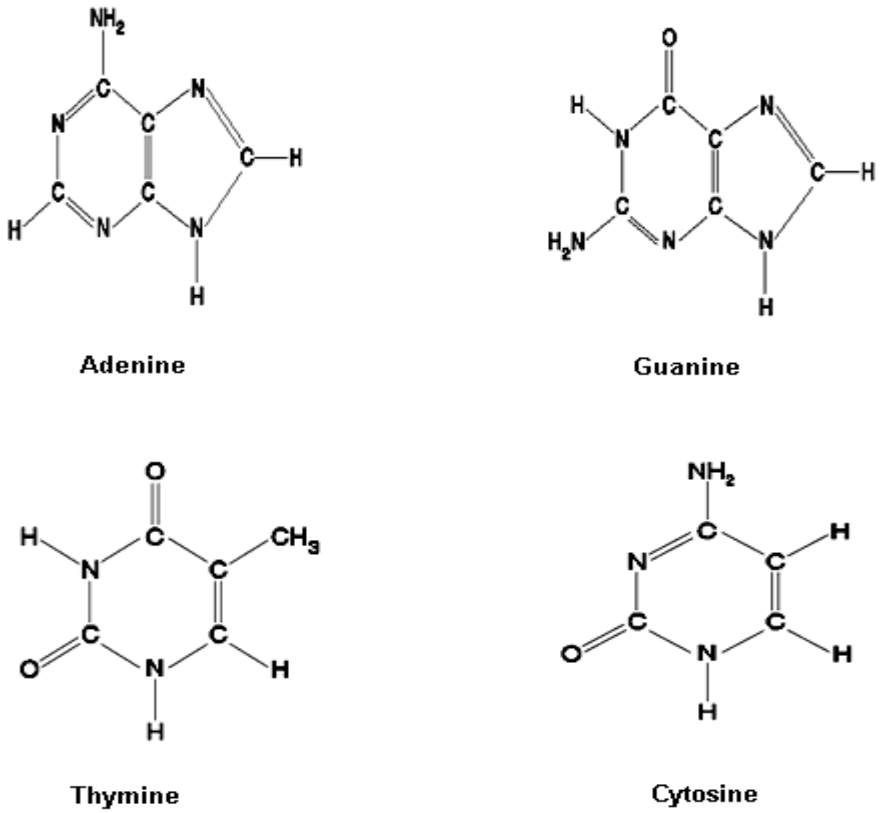

Figure 2.2. Structure of DNA bases.

A nucleoside consists of a purine or pyrimidine base bonded to a sugar. The four nucleoside units in DNA are called deoxyadenosine, deoxyguanosine, deoxythymidine, and deoxycytidine. In a deoxyribonucleoside, N-9 of a purine or N-1 of a pyrimidine is attached to C-1 of deoxyribose. The configuration of this N-glycosidic linkage is β (the base lies above the plane of the sugar). A nucleotide is a phosphate ester of a nucleoside. The common site of esterification in naturally occuring nucleotides is the hydroxyl group attached to C-5 of the sugar. Such a compound is called a nucleoside 5' -phosphate or a 5' -nucleotide. For example, deoxyadenosine 5' -triphosphate (dATP) is an activated precursor in the synthesis of DNA; the nucleotide is activated by the presence of two phosphoanhydride bonds in its triphosphate unit. A primed number of denotes an atom of the sugar, whereas an unprimed number denotes an atom of the purine or pyrimidine ring. The prefix d in ATP indicates that the sugar is deoxyribose to distinguish this compound from ATP, in which the sugar is ribose.

The backbone of DNA, which is invariant throughout the molecule, consists of deoxyriboses linked by phosphate-group bridges. Specially, the 3' -hydroxyl of the sugar moiety of one deoxyribonucleotide is joined to the 5' -hydroxyl of the adjacent sugar by a phosphodiester bridge. Thus the covalent backbones of nucleic acids consist of alternating phosphate and pentose residues, and the characteristic bases may be regarded as side groups joined to the backbone at regular intervals. Also the backbone of DNA is hydrophilic. The hydroxyl groups of sugar residues form hydrogen bonds with water. The phosphate groups in the polar backbone have a pK near 0 and are completely ionized and negatively charged at pH 7; thus DNA is an acid. These negative charges are generally neutralized by ionic interactions with positive charges on proteins, metal ions, and polyamines (Lehninger et al., 1982). The variable part of DNA is its sequence of four kinds of bases (A, G, C, and T). All the phosphodiester linkages in DNA strands have the same orientation along the chain, giving each linear nucleic acid strand a specific polarity and distinct 5' and 3' ends. By definition, the 5' end lacks a nucleotide at the 5' position, and the 3' end lacks a nucleotide at the 3' position. Other groups (most often one or more phosphates) may be present on one or both ends. The nucleotide sequences of nucleic acids can be represented schematically by a segment of DNA having five nucleotide units. The phosphate groups are symbolized by P and each deoxyribose by a vertical line. The carbons in the deoxyribose are represented from 1' at the top to 5' at the bottom of the vertical line. The connecting lines between nucleotides (through P) are drawn diagonally from the middle (3') of the deoxyribose of one nucleotide to the bottom (5') of the next. By convention, the structure of a single strand of nucleic acid is always written with the 5' end at the left and the 3' end at the right; i.e., in the 5'→3' direction. A short nucleic acid is referred to as an oligonucleotide. The definition of short is somewhat arbitrary, but the term oligonucleotide is often used for polymers containing 50 or fewer nucleotides. A longer nucleic acid is called a polynucleotide. The structure of a DNA chain is shown in Figure 2.3 (Stryer, 1995).

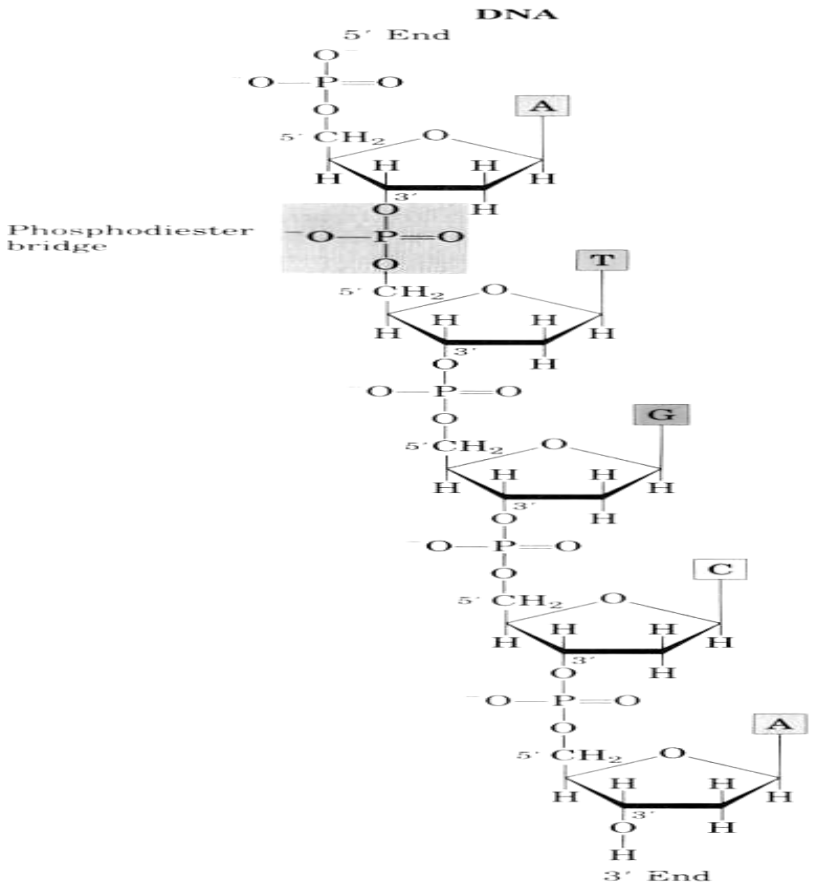

Figure 2.3. The covalent backbone structure of DNA.

2.3. Investigation of DNA

The biochemical investigation of DNA began with Swiss physician Friedrich Miescher, who carried out the first systematic studies of cell nuclei. In 1868 Miescher isolated a phosphorous-containing substance, which he called “nuclein” from the nuclei of pus cells (leukocytes) obtained from discarded surgical bandages. He found nuclein to consist of an acidic portion, which we know today as DNA, and a basic portion, protein. Miescher later found a similar acidic substance in the heads of salmon sperm cells. Although he partially purified the nucleic acid and studied its properties, the covalent (primary) structure of DNA did not become known with certainty until the late 1940s. Miescher and many others suspected that nuclein or nucleic acid was associated with cell inheritance, but first direct evidence that DNA is the bearer of genetic information came in 1944 through a discovery made by Oswald T. Avery, Colin MacLeod, and Maclyn McCarty. These investigators found that DNA extracted from a virulent (disease-

causing) strain of the bacterium Streptococcus pneumoniae, also known as pneumococcus, genetically transformed a nonvirulent strain of this organism into a virulent form. Avery and his colleagues concluded that the DNA extracted from the virulent strain carried the inheritable genetic message for virulence. Not every-one accepted these conclusions, because traces of protein impurities present in the DNA could have been the actual carrier of the genetic information. This possibility was soon eliminated by the finding that treatment of the DNA with proteolytic enzymes did not destroy the transforming activity, but treatment with deoxyribonucleases (DNA-hydrolyzing enzymes) did. A second important experiment provided independent evidence that DNA carries genetic information. In 1952 Alfred D. Hershey and Martha Chase used radioactive phosphorus (^{32}P) and radioactive sulfur (^{35}S) tracers to show that when the bacterial virus (bacteriophage) T2 infects its host cell, E. coli, it is the phosphorus-containing DNA of the viral particle, not the sulfur containing protein of the viral coat, that actually enters the host cell and furnishes the genetic information for viral replication. These important early experiments and many other lines of evidence have shown that DNA is definitely the exclusive chromosomal component bearing the genetic information of living cells (Lehninger et al., 1982).

A most important clue to the structure of DNA came from the work of Erwin Chargaff and his colleagues in the late 1940s. They found that four nucleotide bases in DNA occur in different ratios in the DNAs of different organisms and that the amounts of certain bases are closely related. These data, collected from DNAs of a great many different species, led Chargaff to the following conclusions:

- The base composition of DNA generally varies from one species to another.
- DNA specimens isolated from different tissues of the same species have the same base composition.
- The base composition DNA in a given species does not change with the organism’s age, nutritional state, or changing enviroment.
- In all DNAs, regardless of the species, the number of adenine residues is equal to the number of thymine residues (that is, A=T), and the number of

guanine residues (G=C). From these relationships it follows that the sum of the purine residues the sum of the pyrimidine residues; that is, A+G = T+C.

These quantitative relationships, sometimes called “Chargaff’s rules,” were confirmed by many subsequent researchers. They were a key to establishing the three-dimensional structure of DNA and yielded clues to how genetic transformation is encoded in DNA and passes from one generation to the next (Lehninger et al., 1982).

2.4. Double Helix Form of DNA

To shed more light on the structure of DNA, Rosalind Franklin and Maurice Wilkis used the powerful method of x-ray diffraction to analyze DNA crystals. They showed in the early 1950s that DNA produces a characteristic x-ray diffraction pattern. From this pattern it was deduced that DNA polymers are helical with two periodicities along their long axis, a primary one of 0.34 nm and a secondary one of 3.40 nm. The pattern also indicated that the molecule contains two strands, a clue that was crucial to determining the structure. The problem then was to formulate a three-dimensional model of the DNA molecule that could account not only for the specific A=T and G=C base equivalences discovered by Chargaff and for the other chemical properties of DNA.

In 1953 Watson and Crick postulated a three-dimensional model of DNA structure that accounted for all of the available data (Figure 2.4). It consists of two helical DNA chains coiled around the same axis to form a right-handed double helix. The hydrophilic backbones of alternating deoxyribose and negatively charged phosphate groups are on the outside of the double helix, facing the surrounding water. The purine and pyrimidine bases of both strands are stacked inside the double helix, with their hydrophobic and nearly planar ring structures very close together and perpendicular to the long axis of the helix. The spatial and relationship between these strands creates a major Groove and minor Groove between two strands. Each base of one strand is paired in the same plane with a base of the other strand. Watson and Crick found that the hydrogen-bonded base pairs are those that fit best within the structure, providing a rationale for Chargaff’s rules. It is important to note that three hydrogen bonds can form between G and

C, symbolized G≡C, but only two can form between A and T, symbolized A=T. Other pairings of bases tend (to varying degrees) to destabilize the double-helical structure (Stryer, 1995).

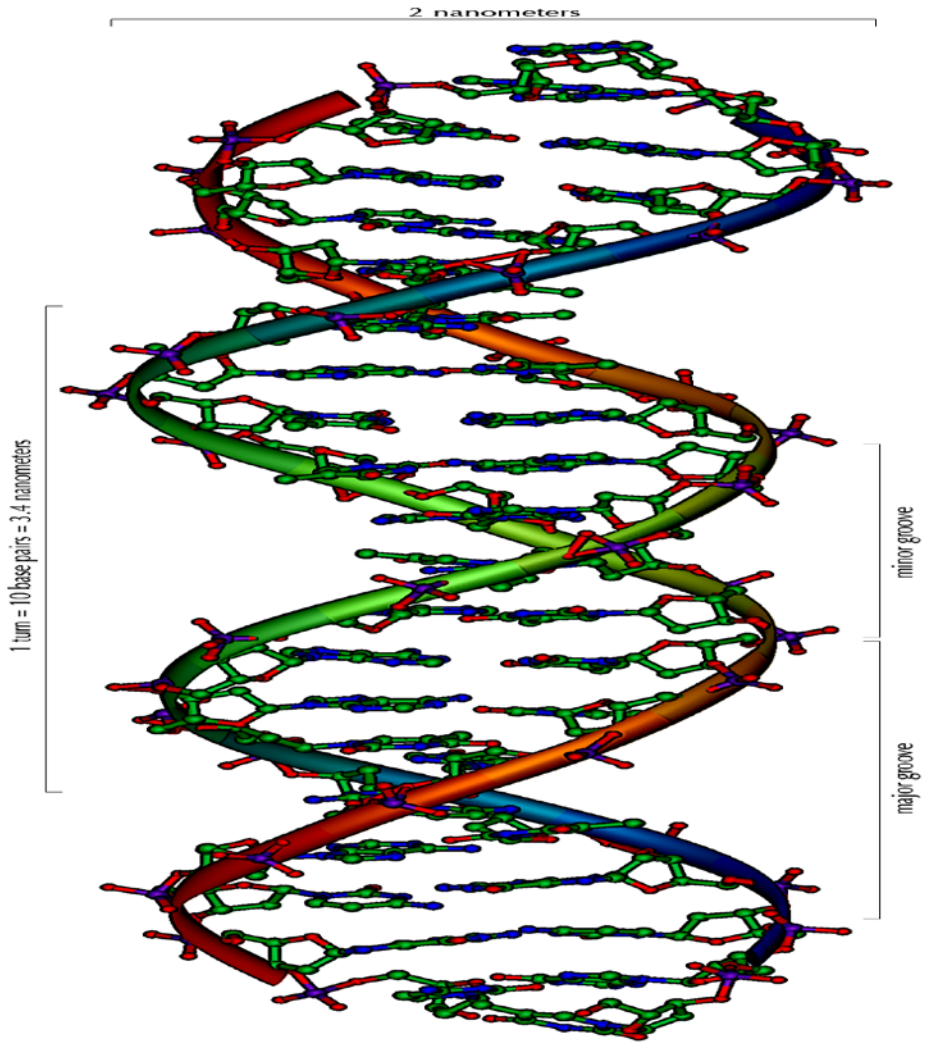

Figure 2.4. The Watson-Crick Model for the structure of DNA.

In the Watson-Crick structure, the two chains or strands of the helix are antiparallel; their 5', 3' –phosphodiester bonds run in opposite directions. Later work with DNA polymerases provided experimental evidence, confirmed by x-ray crystallography, that the strands are indeed antiparallel. To account for the periodicities observed in the x-ray diffraction pattern, Watson and Crick used molecular models to show that the vertically stacked bases inside the double helix would be 0.34 nm apart and that the secondary repeat distance of about 3.40 nm could be accounted for by the presence of 10 (now 10.5) nucleotide residues in

each complete turn of the double helix. The two antiparallel polynucleotide chains of double-helical DNA are not identical in either base sequence or composition. Instead they are complementary to each other. Wherever adenine appears in one chain, thymine is found in the other; similarly, whereever guanine is found in one chain, cystosine is found in the other.

The DNA double helix or duplex is held together by two sets of forces: hydrogen bonding between complementary base pairs and base-stacking interactions. The specificity that maintains a given base sequence in each DNA strand is contributed entirely by the hydrogen bonding between base pairs. The base-stacking interactions, which are largely nonspecific with respect to the identity of the stacked bases, make the major contribution to the stability of the double helix.

The important features of the double-helical model of DNA structure are supported by much chemical and biological evidence. Moreover, the model immediately suggested a mechanism for the transmission of genetic information. The essential feature of the model is the complementarity of the two DNA strands. Making a copy of this structure (replication) could logically proceed by (1) separating the two strands and (2) synthesizing a complementary strand for each by joining nucleotides in a sequence specified by the base-pairing rules stated above. Each preexisting strand could function as a template to guide the synthesis of the complementary strand. These expectations have been experimentally confirmed, and this discovery was a revolution in our understanding of DNA metabolism (Lehninger et al., 1982).

2.5. Different Structural Forms of DNA

DNA is a remarkably flexible molecule. Considerable rotation is possible around a number of bonds in the sugar-phosphate backbone, and thermal fluctuation can produce bending, strectching, and unpairing (melting) in the structure. Many significant deviations from the Watson-Crick DNA structure are found in cellular DNA, and some or all of these may play important roles in DNA metabolism. These structural variations generally do not affect the key properties of DNA defined by Watson and Crick: strand complementarity, antiparallel strands, and the requirement for A=T and G≡C base pairs. The Watson -Crick structure is also

referred to as B-form DNA. The B form is the most stable structure for a random-sequence DNA molecule under physiological conditions, and is therefore the standard point of reference in any study of of the properties of DNA. Two DNA structural variants that have been well characterized in crystal structures are the A and Z forms. The A form is favored in many solutions that are relatively devoid of water. The DNA is still arranged in a right-handed double helix, but the rise per base pair is 0.23 nm. And the number of base pairs per helical turn is 11, relative to the 0.34 nm rise and 10.5 base pairs per turn found in B-DNA. For a given DNA molecule, the A form will be shorter and have a greater diameter than the B form. Z-form DNA is a more radical departure from B structure; the most obvious distinction is the left-handed helical rotation. There are 12 base pairs per helical turn, with a rise of 0.38 nm per base pair. The DNA backbone takes on a zig-zag appearance. Certain nucleotide sequences fold up into left-handed Z helices more readily than do others. Prominent examples are sequences in which pyrimidines alternate with purines, especially alternating C and G or 5-methyl-C and G. Whether A-form DNA actually occurs in cells is uncertain, but there is evidence for some short stretches of Z-DNA in both prokaryotes and eukaryotes. These Z-DNA tracts may play an as yet undefined role in the regulation of the expression of some gene sor in genetic recombination. Comparison of the A, B, and Z forms are given in Figure 2.5 (Lehninger et al., 1982).

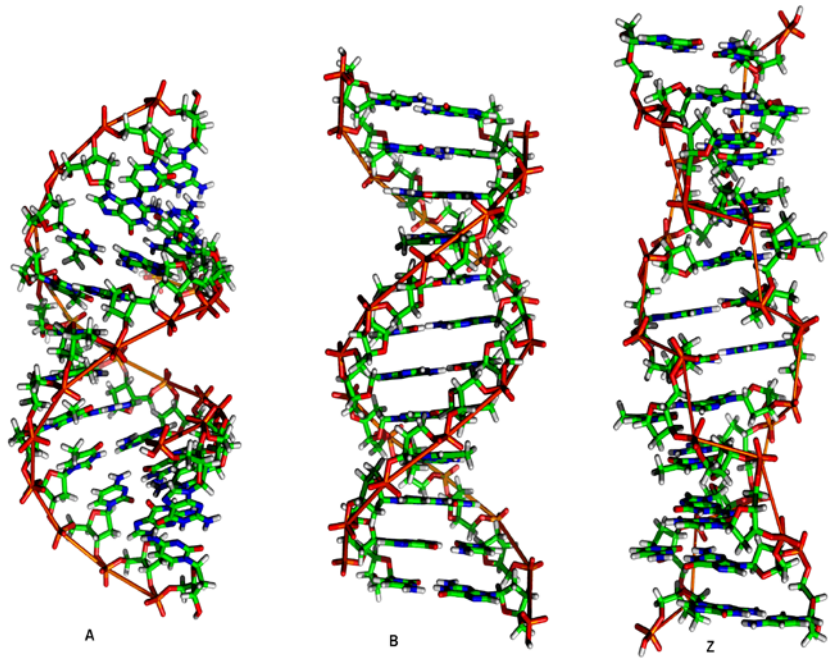

Figure 2.5. Comparison of the A, B, and, Z forms of DNA.

2.6. Denaturation of Double-Helical DNA

Solutions of carefully isolated, native DNA are highly viscous at pH 7.0 and room temperature (20 to 25 °C). When such a solution is subjected to extremes of pH or to temperatures above 80 to 90 °C, its viscosity decreases sharpy, indicating that the DNA has undergone a physical change. Just as heat and extremes of pH cause denaturation or melting of double-helical DNA. This involves disruption of the hydrogen bonds between the paired bases and the hydrophobic interactions between the stacked bases. As a result, the double helix unwinds to form two single strands, completely separate from each other along the entire length, or part of the length (partial denaturation), of the molecule. No covalent bonds in the DNA are broken. Renaturation of DNA is a rapid one-step process as long as a double-helical segment of a dozen or more residues still unites the two strands. When the temperature or pH is returned o the biological range, the unwound segments of the two strands spontaneously rewind or anneal to yield the intact duplex (Figure 2.6). However, if the two strands are completely separated, renaturation occurs in two steps. The first step is relatively slow, because the two strands must first find each other by random collisions and form a short segment of complementary double helix. The second step is much faster: The remaining unpaired bases successively come into register as base pairs, and two strands zipper themselves together to form the double helix (Lehninger et al., 1982).

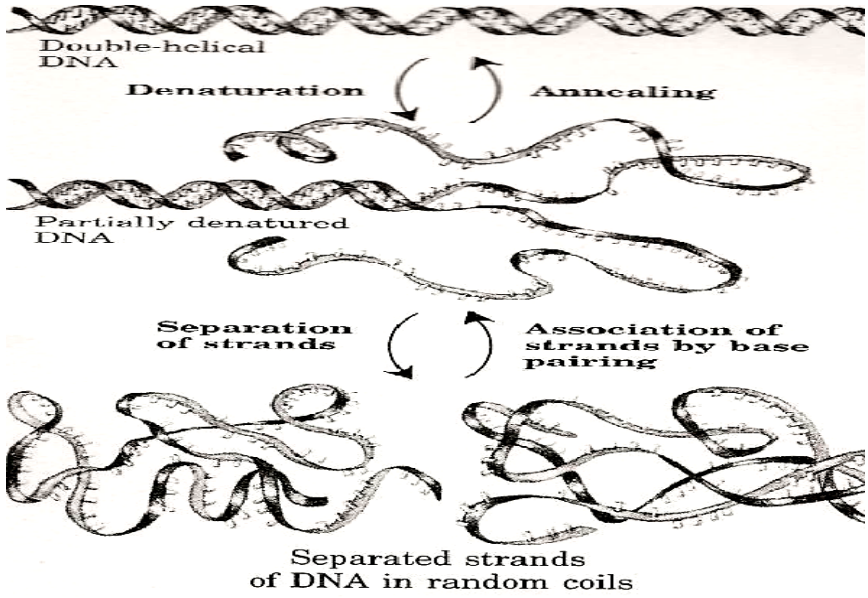

Figure 2.6. Stages in the reversible denaturation and annealing (renaturation) of DNA.

2.7. Hybridization of DNA

The capability of two complementary DNA strands to pair with one another can be used to detect similar DNA sequences in two different species or within the genome of a single species. If duplex DNAs isolated from human cells and from mouse cells are completely denatured by heating, then mixed and kept at 65 °C for many hours, much of the DNA will anneal. Most of the mouse DNA strands anneal with complementary mouse DNA strands to form mouse duplex DNA; similarly, many of the human DNA strands anneal with complementary human DNA strands. However, some strands of the mouse DNA will associate with human DNA strands to yield hybrid duplexes, in which segments of the mouse DNA strand form base-paired regions with segments of the human DNA strand. This reflects the fact that different organisms have some common evolutionary heritage; they generally have some proteins and RNAs with similar functions and, often, similar structures. In many cases, the DNA encoding these proteins and RNAs will have similar (homologous) sequences. The closer the evolutionary relationship between the species, the more extensively will their DNAs hybridize. For example, human DNA hybridizes much more extensively with mouse DNA than with DNA form yeast. The hybridization of DNA strands from different sources forms the basis of a powerful set of techniques essential to the modern practice of molecular genetics. It is possible to detect a specific DNA sequence or gene in the presence of many other sequences if one already has an appropriate complementary DNA strand to hybridize with it. The complementary DNA can be from a different species or from the same species; in some cases it is synthesized in the laboratory (Lehninger et al., 1982).

2.8. Length of DNA Molecules

A striking characteristic of naturally occuring DNA molecules is their length. DNA molecules must be very long to encode the large number of proteins present in even the simplest cells. The dimensions of some of DNA molecules are given in Table 2.1. It should be noted that even the smallest DNA molecules are highly elongate (Stryer, 1995).

Table 2.1.

Sizes of DNA genomes

Organism	Base pairs (in thousands, or kb)	Length (mm)
Viruses		
Polyoma or SV40	5.1	1.7
λ phage	48.6	17
T2 phage	166	56
Vaccinia	190	65
Bacteria		
Mycoplasma	760	260
E. coli	4.000	1.360
Eukaryotes		
Yeast	13.500	4.600
Drosophila	165.000	56.000
Human	2.900.000	990.000

2.9. Chemical Synthesis of DNA

One of the technology that has paved the way for many biochemical advances is the chemical synthesis of oligonucleotides with any chosen sequence. The chemical methods for synthesizing nucleic acids were developed primarly by H. Gobind Khorona in the 1970s. Refinement and automation of these methods has made it possible to synthesize DNA strands rapidly and accurately. The synthesis is carried out with the growing strand attached to a solid support. The efficiency of each addition step is very high, allowing the routine laboratory synthesis of polymers of 70 or 80 nucleotides. In some laboratories much longer strands are synthesized. The availability of relatively inexpensive DNA polymers with predesigned sequences having powerful DNA polymers with predesigned sequences having a powerful impact on all areas of biochemistry (Lehninger et al., 1982).

3. BIOSENSORS

A biosensor is a device having a biological sensing element either intimately connected to or integrated within a transducer. The aim is to produce a digital electronic signal, which is proportional to the concentration of a specific (bio)chemical or set of (bio)chemicals in the presence of interfering species (Gerard et al., 2002). Figure 3.1 shows a general configuration of a biosensor. The development of biosensors is an interdisciplinary area for which sharp limits cannot be drawn easily (Erdem et al., 2000a). It is the result of combined efforts of chemists, biologists, physicists and engineers (Malhotra and Chaubey, 2003). Biosensors have been widely researched and developed as a tool for chemical, biochemical, medical, agricultural and environmental monitoring because of their compact size, real time analysis, nearly reagentless operation, simple pretreatment protocols, low cost of construction, and simplicity of use. A key technology in developing biosensors is combining the biological components to the surface of transducers. The performance of the biosensors is dominated by the combination technique of these two system components. This technique is often called immobilization of biological components or interfacial design (Muguruma and Karube, 1999). The most commonly used techniques of immobilization are adsorption of inert carriers, cross-linking by bifunctional reagents into the macroscopic particles, physical entrapment in gel lattices, covalent binding of water insoluble matrices, microencapsulation within the wall spheres, electrostatic interaction and electrochemical entrapment, etc.

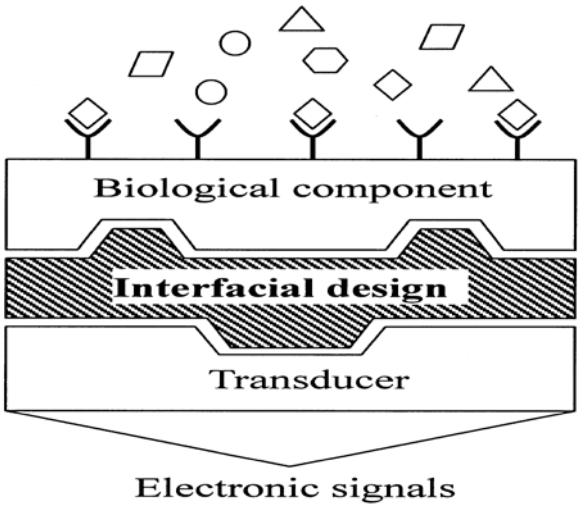

Figure 3.1. Scheme of a biosensor.

3.1. Classification of Biological Recognizers

Biosensors can be classified in aggrement to the type involved active biological component in the mechanism or the mode of signal transduction or combination of these two aspects. Figure 3.2 shows some analytes (substrate) possible to be analyzed immobilizing the biological components, separately, in several transducers. The choice of the biological material and the adjusted transducer depends on the properties of each sample of interest and the type of the physical magnitude to be measure. The type of the biocomponent determines the degree of selectivity or specificity of the biosensor. Thus, the biological recognizers are divided in three groups: biocatalytic, bioaffinity and hybrid receptors (Mello and Kubota, 2002).

3.1.1. Biocatalytic receptors

The biocatalytic recognition element can be systems containing enzyme (mono or multi enzyme), whole cells (microorganisms, such as bacteria, fungi eukaryotic cells, yeast), cells organelles and plant or animal tissues slice. Problems like selectivity and the slow response characteristic of microbial sensors can be overcome by the use of enzymes which, not surprisingly, represent the most commonly used sensing agents due to their selectivity (Davis et al., 1995).

3.1.2. Bioaffinity receptors

The affinity-based biosensors may be chemoreceptors, antibodies or nucleic acid. Affinity-based biosensors provide selectivity interactions with a given ligand to form a thermodynamically stable complex. The potential use of immunosensors is due to their general applicability (any compounds can be analyzed as long as specific antibodies are available) and to the specificity and selectivity of the antigen-antibody reaction and the high sensivity of the method, depending on the detection method used. The antigen-antibody complex may be utilized in all types of sensors. The physichochemical change induced by antigen-antibody binding does not generate an electrochemically detectable signal. Therefore, enzymes, fluorecent compounds, electrochemically active substrates, avidin-biotin complexes are used to label either the antigen or the antibody (Davis et al., 1995).

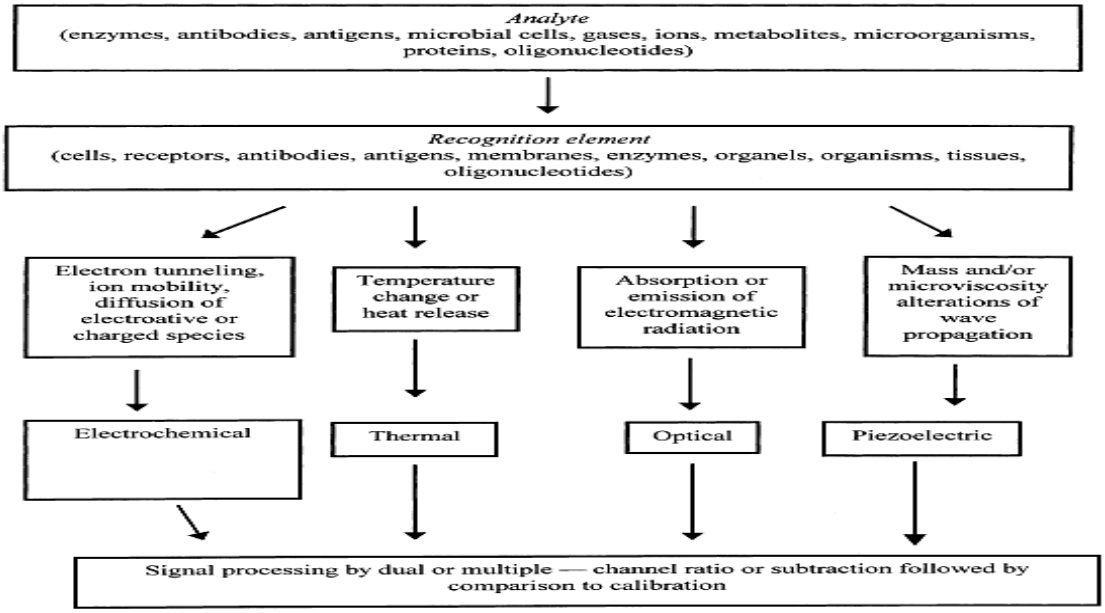

Figure 3.2. Biocomponent and transducers employed in construction of biosensors.

3.1.3. Hybrid receptors

The hybrid receptors such as DNA and RNA probes have shown promising applications. The principle of selective detection is based on the detection of a unique sequence of nucleic acids through hybridization. The nucleic acid structure is a double helix conformation of two polynucleotide strands. Each strand is constituted of a polymeric chain that contain bases: A, T, C, G. These bases are complementary by two through three hydrogen bonds in the C-G base pair and two in the T-A base pair. This base-pairing property gives ability of one strand to recognize its complementary strand to form a duplex. DNA sensors consist to immobilize, onto a solid support, well-defined sequences of single strands as a biological receptor. A DNA probe is added to DNA or RNA from an unknown sample or the reverse process is possible. If the probe hybridizes (combines) with the unknown nucleic acid because of pairing of complementary base recognition, detection and identification are possible (Mello and Kubota, 2002).

3.2. Transducers

The biosensor can be classified in several types according to the transducer: calorimetric, optical, piezoelectric and electrochemical transducers. Optical biosensors are based on the measurement of light absorbed or emitted as a

consequence of a biochemical reaction. In such a biosensor, the light waves are guided by means of optical fibers to suitable detectors (Peterson and Vurek, 1984). They can be used for measurement of pH, O_2 or CO_2 etc. Calorimetric biosensors detect an analyte on the basis of the heat evolved due to the biochemical reaction of the analyte with a suitable enzyme. Different substrates, enzymes, vitamins and antigens have been determined using thermometric biosensors. Piezoelectric biosensors operate on the principle of generation of electric dipoles on the subjecting an anisotropic natural crystal to mechanical stress. They are used for the measurement of ammonia, nitrous oxide, carbon monoxide, hydrogen, methane and certain organophosphorus compounds. All these biosensors suffer from certain drawbacks. For example, optical biosensors, though very sensitive, however, cannot be used in turbid media. Thermal biosensors cannot be utilized with systems with very little heat change. Moreover, they are not easy to handle. Electrochemical biosensors have emerged as the most commonly used biosensors. They have been found the overcome most of the disadvantages, which inhibit the use of other types of biosensors. These biosensors are rapid, easy to handle and are of low cost (Malhotra and Chaubey, 2003).

3.2.1. Electrochemical transducers

Among the chemical sensors electrochemical biosensors hold an important position (Wang, 1994). An electrochemical biosensor is a self-contained integrated device, which is able to provide specific quantitative or semiquantitative analytical information using a biological recognition element (biochemical receptor) which is retained in direct and spatial contact with the transduction element (Thevenot et al., 2001). These are based on the fact that during a bio-interaction process, electrochemical species such as electrons are consumed or generated producing an electrochemical signal, which can in turn be measured by an electrochemical detector. Biosensors based on the electrochemical transducer have the advantage of being economic and present fast response. They can be operated in turbid media, have comparable instrumental sensitivity and are more amenable to miniaturization. Also, possibility of automation allows application in a wide number of samples (Malhotra and Chaubey, 2003).

4. REDOX POLYMERS

Conductive polymers have been the subjects of study for many decades as possible synthetic metals. Many of these polymers, especially those with a conjugated π-bond system, often yield higher conductivity once having undergone the doping process. Four types of polymers possessing electrical conductivity can be distinguished: Composites, ionically conducting polymers, conjugated polymers and redox polymers. Redox polymers are characterized by the presence of specific spatially and electrostatically isolated electrochemically active sites which are in contact with each other and capable of exchanging electrons by hoping mechanism (Yu et al., 2005). Electroactivity in the redox polymer is highly localized, while the electrochemical processes in conjugated polymers lead to a reorganization of the bonds in the molecule itself. Typically, a redox polymer consists of a system where a redox-active transition metal based pendant group is covalently bound to some sort of polymer backbone which may or may not be electroactive (although for synthetic convenience the backbone is frequently formed by the electropolymerization of suitable monomer complexes). A few representative examples are shown in Figure 4.1.

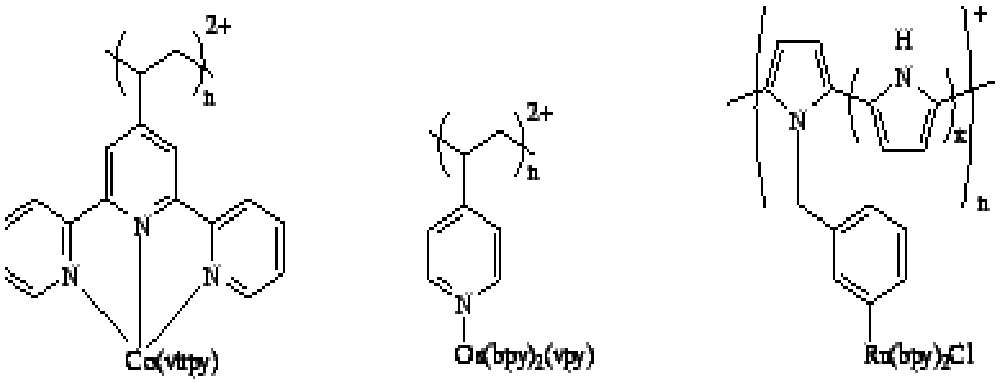

Figure 4.1. Three typical redox polymers.

The widespread interest in these polymers has been spurred by their applicability in the area of chemically modified electrodes (Murray, 1984; Abruna, 1988). One goal of coating electrodes with electroactive polymers is the development of new materials with very active catalytic properties. The bulk of the work has been with systems where the polymer itself is inert and serves only as a support for the electrocatalytic metal sites. The electrocatalyst site functions as a mediator,

facilitating the transfer of electrons between the electrode and the substrate. Electrocatalysis in general is of great economic importance and the aim of these modified electrodes is to drive electrochemical reactions selectively and/or at modest potentials, and with better control than could be possible by the direct interaction between the substrate and the electrode. Embedding electrocatalytic transition metal species in a polymer modified electrode matrix is a means to endow the electrode with the chemical, electrochemical, optical, and other properties of the immobilized molecule (Murray, 1984). A number of additional advantages include:

- Control of the reaction rate by the applied potential or current
- Close proximity of electrocatalytic sites to the electrode
- High concentration of active centres despite low amount of material required
- Cooperative effects stemming from the proximity of other catalyst sites
- Easy removal of the catalyst from the substrate.

Unlike the electronically conducting polymers, redox polymers characteristically exhibit conductivity only over a very narrow potential range, with maximum conductivity occurring when the concentrations of the oxidized and reduced forms are equal in the film, *i.e.,* at the formal potential of the redox centers. This leads to a voltammetric profile such as the one shown in Figure 4.2, with the characteristics of a surface bound redox system (or finite linear diffusion).

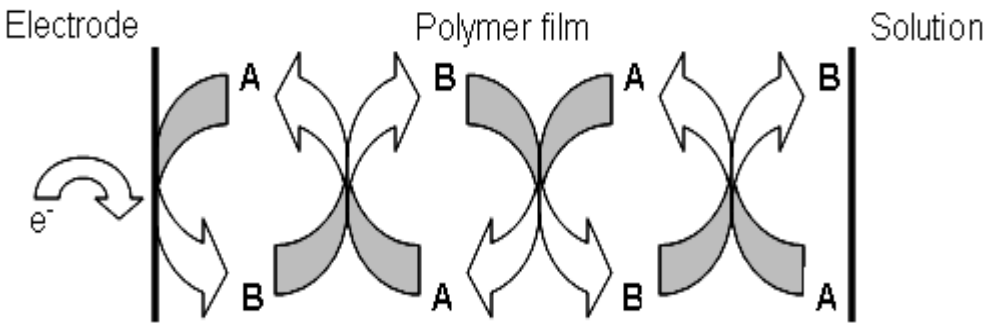

Figure 4.2. Charge propagation by means of quasi-diffusional charge percolation in a redox polymer.

The details of charge transport between the electrode and the supported redox sites are a fundamental consideration. It is commonly held that redox conduction in polymers occurs by the electron hopping process proposed by Kaufman and coworkers (Kaufman and Engler, 1979) whereby electron transfer proceeds as a process of sequential self-exchange steps between adjacent redox groups.

Since electroneutrality in the film must be maintained, the generation of charge at the electrode and the motion of the charge throughout the polymer must be accompanied by the ingress and motion of counterions. This is an important consideration since electroactive polymers are really mixed conductors, displaying both electronic and ionic conductivity. Often the ionic contribution may be safely disregarded, in which case the charge transport diffusion may be ascribed entirely to electron diffusion. However this is not always the case and electron hopping rates can be strongly influenced by the nature of the counter ion (Ren and Pickup, 1994). Full characterization should consider both electronic and ionic conductivities of the material.

4.1. Poly(vinylferrocene) (PVF)

Poly(vinylferrocene) (PVF) prepared in 1955 can be regarded as the first established organometallic polymer in which little electronic communication exists between redox-active metal complex sites. PVF, is a redox polymer, which has long been used as a fundamental conducting polymer system, with the advantages of simple electrochemistry (a reversible one-electron process), high stability (allowing multiple measurements to be made over extended time scale), and the ease of deposition of thin films using a variety of methods (Yu et al, 2005). Chemical structure of neutral form of PVF is presented in Figure 4.3.

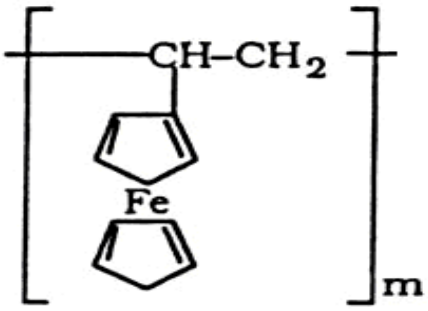

Figure 4.3. Structure of neutral PVF.

5. CHEMICALLY MODIFIED ELECTRODES (CMEs)

Chemically modified electrodes (CMEs) provide an approach to the development of analytical procedures and techniques employing immobilized reagents. With CMEs electrode surfaces are modified in a quest to render an electrochemical function either not possible or difficult to achieve using conventional electrodes. Targeted improvements include increased selectivity, sensitivity, chemical and electrochemical stability, as well as a larger usable potential window and improved resistance to fouling. Furthermore, electrodes with tailored surfaces enhance fundamental studies of interfacial processes. Therefore, the need for improved electrode performance and logically designed interfaces is rapidly growing in many areas of science (Edwards et al., 2007).

5.1. Fabrication of CMEs

5.1.1. Monolayer adsorption

The advantage of this preparation method is its simplicity. Many aromatic organic compounds can adsorb onto graphite; the adsorptive strength increases with increasing numbers of aromatic rings. The adsorption is due to the strong interaction between the basal plane of the graphite and the extended π-electron systems of redox molecules.

5.1.2. Covalent modification

Reagents can easily be attached covalently to surfaces. Analytical applications of covalently modified electrodes have been successful. For instance, silanization reactions have provided Glassy Carbon (GC) electrodes with oxalic acid functional groups (Miwa et al., 1984), which have improved electrode performance compared with non-modified GC electrodes.

5.1.3. Composite formation

The carbon paste electrode (CPE) is an example of a composite electrode, a mixture of components. CPEs are prepared by mixing carbon powder with a suitable pasting (binding) medium such as liquid paraffin or silicone grease (Arrigan, 1994).

5.1.4. Polymer modification

Various methods are used to prepare polymer-film electrodes:

Dip coating. The bare electrode is held in a solution of the polymer, which is deposited via an adsorption process.

Droplet evaporation**.** A small volume (usually a few microlitres) of polymer solution is placed on the electrode surface and the solvent is allowed to evaporate. The polymer is confined to the CME by using the electrode in an electrolyte/solvent in which the polymer is insoluble.

Spin coating**.** The electrode is set spinning after drop of the polymer solution is placed on the surface; the result is an even layer of polymer surface free of pinholes.

Electropolymerization**.** The products of the electrode reaction are polymeric and insoluble in the solvent system used. Electropolymerization of various substituted monomeric compounds can lead to CMEs with interesting analyte-binding and electrical properties.

Oxidative or reductive deposition**.** Relies on the dependence of polymer solubility on ionic state. For example, PVF oxidizes from methylene chloride to give less soluble poly(vinylferrocenium) (PVF^+), which precipitates onto the electrode surface to give a PVF^+ modified electrode. It is known that, on PVF^+ coated electrodes; the polymer undergoes a reversible redox reaction (Umana et al., 1980):

$$PVF \underset{e}{\overset{-e}{\Leftrightarrow}} PVF^+ \qquad (5.1)$$

PVF^+ coated electrodes can be prepared by the constant potential anodic electrolysis of methylene chloride solution of PVF. It has been stated that the electrodeposited polymer was in a partially oxidized state containing ClO_4^- ions as the counter anion, ferrocene and ferrocenium groups (Shirota et al., 1984). Structure of electrochemically doped PVF^+ is given in Figure 5.1.

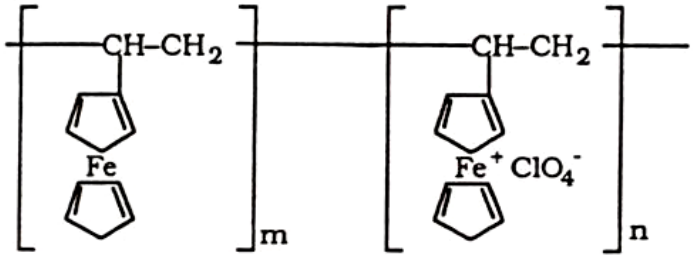

Figure 5.1. Electrochemically doped PVF.

5.2. Analyte-Accumulation Modes on Chemically Modified Electrodes

a. Ion-exchange

Immobilization of an ion exchanger at an electrode surface can allow an ion-exchange reaction to be monitored voltammetrically if one of the ions involved is electroactive. Various ion-exchange CMEs have been prepared from carbon pastes or by coating onto solid electrode surfaces.

b. Complexation

The reaction of a solution metal ion with a surface-bound ligand can yield a surface-bound metal complex:

$$mL_{surface} + M^{n+}{}_{solution} \Leftrightarrow ML_m{}^{n+}{}_{surface} \qquad (5.2)$$

where M^{n+} is the metal ion, L, the ligand, and m, the number of ligands per complex. If the complex is electroactive, it can be measured voltammetrically at the CME surface.

c. Hydrophobic interaction

Hydrophobic analytes can accumulate at an electrode displaying hydrophobic properties. This type of CMEs may be used in the determination of certain compounds in biological fluids.

d. Covalent attachment

Certain functionalized electrodes allow a covalent bond to form between the electrode and the analyte species in solution.

e. Bioaccumulation

Certain biological organisms can accumulate metal ions. It is therefore possible to determine metal ions by voltammetry following a bioaccumulation step at the electrode.

6. ELECTROCHEMICAL DNA BIOSENSORS

Wide-scale genetic testing requires the development of easy-to-use, fast, inexpensive, miniaturized analytical devices. Traditional methods for detecting DNA, such as gel electrophoresis or embrane blots, are too slow and labor intensive. Biosensors offer a promising alternative for faster, cheaper, and simpler DNA assays. DNA biosensors commonly rely on the immobilization of double-stranded DNA (dsDNA), single-stranded DNA (ssDNA) and a ss oligonucleotide probe onto a transducer surface for hybridization with its complementary target sequence. The two major requirements for a successful operation of a DNA biosensor are high specificity and high sensitivity. Even though DNA is a relatively simple molecule, finding the sequence that contains the desired information and distinquishing between perfect matches are very challenging tasks (Wang, 2005).

Electrochemical transducers have received considerable recent attention in connection to the detection of DNA (Gooding, 2002). First reports about the ability of DNA to produce analytically useful electrochemical reduction and oxidation signals were published by the end of the 1950s and in the beginning of the 1960s (Palecek, 2002a). Modern electrochemical DNA biosensors and bioassays offer remarkable sensitivity, compatibility with modern microfabrication technologies, inherent miniaturization, low cost (disposability), minimal power requirements, and independence of sample turbidity or optical pathway. Such devices are thus extremely attractive for obtaining the sequence-specific information in a simpler, faster, and cheaper manner compared to traditional methods. In addition, electrochemistry offers innovative rotes for interfacing DNA recognition system with the signal-generating element and for amplifying electrical signals (Wang, 2005).

Electrochemical DNA sensing has been achieved by three types of approaches, including the use of a DNA probe having an electrochemical signal part, use of an electrochemical DNA ligand, and the monitoring the change in electrochemical characteristics of the surface associated with hybridization (Millan and Mikkelsen, 1993).

DNA-binding metal complexes and intercalating ligands have been reported by many researchers (Takenaka, 2005). Electrochemical gene-detecting method based on ferrocenylnaphthalene diimide as the electrochemical hybridization indicator coupled with a DNA probe-immobilized has studied by Takenaka et al. The performance of ferrocenylnaphthalene diimide has been based on its binding mode for dsDNA in the threading intercalation (Takenaka, et al., 2001). The electrochemical detection of binding of small molecules to DNA and generally DNA damage has been described in earlier reports (Palecek et al., 1998; Fojta et al., 2000; Zhu et al., 2004; Navarro et al., 2004); such as, the intercalation of compound into dsDNA has been observed in the presence of the planar aromatic molecules (e.g; bromine ligands, acridine dyes, etc.) (Tang and Huang, 1999).

Many electrochemical studies are dealing with the interactions of DNA with redox indicators, which are used in determination of the DNA nucleotide sequence. Echinomycin and cobalt-phenanthroline ($[Co(phen)_3]^{3+}$) has been used for this purpose at gold electrodes by Karadeniz et al. In order to minimize the nonspecific adsorption of oligonucleotides, the thiol derivatized oligonucleotides were immobilized onto gold electrode in the presence of 6-mercapto-1-hexanol (Karadeniz et al., 2006). Osmium tetraoxide complexes have been utilized as electroactive markers for DNA hybridization at mercury and carbon electrodes (Kizek et al, 2002; Billova et al., 2002; Fojta et al., 2004; Havran et al., 2004; Yosypchuk et al., 2006). These complexes have been applied as a probe of DNA structure, reacting preferentially with ssDNA and distorted DNA regions. Moreover, DNA-osmium adducts has been determined. The interaction of dsDNA and ssDNA with a ruthenium comlex and methylene blue has been explored at carbon paste electrode by Erdem et al. The structure of DNA has been determined by the magnitudes of the voltammetric peaks of ruthenium bipyridine complex and methylene blue (Erdem et al., 2001).

Using the redox-active DNA conjugate (ferrocene-modified oligonucleotide) as a probe, electrochemical gene sensor has been developed by Nakayama et al. In this study, complementary oligonucleotide to the target has been immobilized onto gold electrode through the specific chemisorption of phoshorothioates and DNA sensing has been achieved based on the ferrocene oxidation (Nakayama et al.,

2002). In another study, synthesis and characterization of ferrocene-labelled oligodeoxynucleotides has been described by Beilstein and Grinstaff. The structure and stability of the DNA duplex has been demonstrated (Beilstein and Grinstaff, 2001).

There has been a great interest for the development of double surface techniques in combination with magnetic separation and DNA sensor systems. The use of monosized magnetic beads gives the convenience of magnetic separation. Wang et al. has been studied the attachment of biotinylated oligonucleotide probes onto streptavidin-coated magnetic beads, followed by the hybridization event, dissociation of the DNA hybrid from beads, and potentiometric stripping measurements at a renewable graphite pencil electrode (Wang et al., 2001). DNA hybridization with magnetic beads based on the enhanced accumulation of purine nucleobases in the presence of copper ions has been also studied in another study (Wang et al., 2002).

Fan et al. has studied voltammetric response and determination of DNA with a silver electrode with low overpotentials. In this study voltammetric response of DNA has been attributed to the redox reaction of purine bases (Fan et al., 1999). Zhao et al. has performed the characterization of DNA-modified gold electrodes by scanning tunneling microscopy (STM), Raman spectroscopy, in situ UV/Vis reflection spectroscopy, X-ray photoelectron spectroscopy (XPS) and alternating current (AC) impedance. In this study the bases and phosphate groups of DNA backbone has interacted with gold electrode surfaces (Zhao et al., 1999).

The number of studies on self-assembled monolayers (SAMs) has grown over the past years. SAMs are molecular layers formed on a surface when it is immersed in a solution containing molecules that specifically interact with this surface. Due to the efficiency and simplicity of the self-assembly technique, immobilization of thiol- or disulfide-modified DNA on gold electrodes has been reported in the literature (Kerman et al., 2002; Sanchez-Pomales et al., 2007; Degefa and Kwak, 2008). SAMs at mercury electrodes have been also reported by Ostatna and Palecek (Ostatna and Palecek, 2006).

The power and scope of nanomaterials can be greatly enhanced by combining them with biological recognition reactions and electrical processes (Storhoff and Mirkin, 1999; Niemeyer, 2001). The performance of glassy carbon and graphite pencil electrodes modified with multiwalled carbon nanotubes has been compared by Erdem et al. for DNA hybridization, based on the direct electrochemical detection of guanine signal (Erdem et al., 2006). Electrochemical detection of DNA hybridization based on silver-enhanced gold nanoparticle DNA probes has been performed by Cai et al. The assay has been relied on the electrostatic adsorption of target oligonucleotides by using glassy carbon electrode (Cai et al., 2002). The electrochemical sensing of DNA has been developed based on the oxidation signals of silver and guanine by using disposable pencil graphite electrodes. In this study the surface modification has been performed by passive adsorption using amino linked oligonucleotide attached onto the surface of silver nanoparticles (Karadeniz et al., 2007a). Chang et al. has been studied DNA hybridization using gold nanoparticles based on assembly of alternating DNA and poly(dimethyldiallylammonium chloride) multilayer films by layer-by-layer electrostatic adsorption (Chang et al., 2008).

The use of electroactive polymers as the transduction element of DNA hybridization has been recently described in the literature. The immobilization of DNA using polymer film is very simple, and the adsorption or covalent binding method can be simultaneously applied for the DNA immobilization (Wang, 2000). The characterization of a biofunctional electroactive polymer, poly(5-hydroxy-1,4-naphthoquinone) (juglone)-co-5-hydroxy-3-thioacetic acid-1,4-naphthoquinone) used for direct electrochemical detection of DNA hybridization has been reported by Piro et al (Piro et al., 2005). Such a bifunctionalized polymer could act as a reagentless sensor, with the quinone group as the transducer between the biomolecule and the electrode, and the carboxylic function as the binding site. Pyrolytic graphite elecrodes with adsorbed poly(4-vinylpyridine) (PVP) and attached Ru(II) complex with 2,2'-bipyridine ligand ($[Ru(bpy)_3]^{2+}$) have given reversible voltammetry and facilitated reusable DNA biosensors. These electrodes have given responses to poly(guanylic) acid and DNA caused by catalytic oxidation of guanine moieties in these polynucleotides (Mugweru and Rusling, 2001).

A conductive polymer, polypyrrole (PPy) is one of the extensively used conducting polymers in design of bioanalytical sensors (Ramanavicius et al., 2006). The dielectric method has been applied to distinguish between polymers containing different dopant and to monitor their ion-exchange occuring when PPy was used for DNA adsorption (Saudi et al., 2000). Biosensing of DNA based on the electrochemical response of ferrocenyl groups grafted to polypyrole has also been studied (Korri-Youssoufi and Makrouf, 2001). Also oligonucleotide modified probes have been developed by grafting them on polypyrrole (Komarova et al., 2005; Qi et al., 2007). Preparation of polyprrole nanofiber modified pencil graphite electrode and its usage in the electrochemical DNA biosensors have been investigated in the presence of methylene blue by Özcan et al. (Özcan et al., 2007). DNA immobilized PP-polyvinysulphonate film at indium-tin-oxide (ITO) has been studied for Mycobacterium tuberculosis by monitoring guanine oxidation and redox indicators; methylene blue and ruthenium complex (Prabhakar et al., 2008a).

Polyaniline (PANI) has been used for the design and development of DNA biosensors. DNA hybridization biosensor based on PANI electrochemically deposited onto Pt disc electrode has been fabricated by Arora et al. using biotin-avidin as indirect coupling agent to immobilize 5'-biotin end-labeled probes to detect complementary target, using both direct electrochemical oxidation of guanine and methylene blue (Arora et al., 2007). PANI-polyvinyl sulphonate (PVS) film has been also fabricated using electrochemically entrapped calf thymus dsDNA for detection of organophosphorus pesticides (Prabhakar et al., 2008b).

In another study a poly(cyclopentadithiophene) matrix modified by DNA covalently fixed to the surface has been designed to study the redox and ion-exchange properties in surface-tethered DNA-conducting polymers. Voltammetric investigations has been showed an improvement in conductivity, originating from DNA modification (Cougnon et al., 2008). Fang et al. has investigated label-free electrochemical method for the detection of DNA-peptide nucleic acid (PNA) hybridization using ferrocene-functionalized polythiophene transducer and ssPNA probes on the nanogold modified electrode (Fang et al., 2008).

Poly-L-lysine/single-walled carbon nanotubes has been also used for electrochemical DNA biosensor. The well-dispersed carboxylic group-functionalized single-walled carbon nanowires has been dripped onto carbon paste electode surface firstly, and poly-L-lysine films has been subsequently electopolymerized by cylic voltammetry (Jiang et al., 2008). In another work, positively charged chitosan (CS) and negatively charged DNA were alternately adsorbed on the surface of pyrolytic graphite (PG) electrodes, forming $(CS/DNA)_n$ layer-by-layer films. In that work by Liu and Hu, CS has been selected as the building component of layer by-layer films with DNA because of its positive charges at suitable pH (Liu and Hu, 2007). Li et al., has been reported chitosan based biosensor with carbon nanotube to detect DNA (Li et al, 2005). The polymer-copper(II) complex samples, $[Cu(phen)(L\text{-}Thr)(BPEI)]ClO_4.2H_2O$ (L-THr = L-theronine, phen = 1,10-phenanthroline and BPEI = branched polyethyleneimine), with varying degrees of copper(II) chelate content in the polymer chain, has been prepared by ligand substitution method in water-ethanol medium by Kumar and Arunachalam. They reported that the polymer-copper(II) chelates could bind to DNA molecules mainly by electrostatic attraction in their study (Kumar and Arunachalam, 2007).

The interaction of DNA with drugs is among the important aspects of biological studies in drug discovery and pharmaceutical development processes (Erdem and Ozsoz, 2002). Wang et al. have studied the interaction of the antitumor drug daunomycin with calf thymus dsDNA in solution and at the carbon electrode (CPE) surface. As a result of intercalation of this drug between the base pairs in dsDNA, daunomycin response has decreased (Wang et al., 1998). The interactions of anticancer drugs, epirubicin (EPR) and mitoxantrone (MTX) with calf thymus dsDNA and calf thymus ssDNA have been studied electrochemically at CPE by Erdem and Ozsoz. The signals for EPR and MTX which bound to DNA through intercalation have been found to decrease in the order of bare CPE, ssDNA-modified and dsDNA-modified CPE (Erdem and Ozsoz, 2001a, b). In another study electrochemical investigation of interaction between anticancer drug, mitomycin C (MC) and DNA in a novel drug-delivery system has been developed by Karadeniz et al. The magnitude of guanine oxidation has been

monitored before and after interaction between MC and dsDNA (Karadeniz et al., 2007b).

There is no doubt that electrochemical methods offer, in addition to the development of the DNA biosensors, a number of interesting possibilities in the contemporary nucleic acid research, including studies of the DNA-protein interactions, DNA damage, highly sensitive nucleic acid determination, effect of surface charge on structure and properties of DNA adsorbed at the surface, highly sensitive detection of impurities in DNA samples, etc. Electrochemical research into DNA is a vast field requiring more researchers with some knowledge both in electrochemistry and biochemistry of nucleic acids (Palecek and Jelen, 2005).

6.1. Definition of Some Terms about DNA Biosensors

Oligonucleotide (ODN): A short nucleic acid is referred to as an oligonucleotide. The term oligonucleotide is often used for polymers containing 50 or fewer nucleotides.

Polynucleotide: A longer nucleic acid, compared to ODN is called a polynucleotide.

Probe: ODN that has certain base sequence is called a probe.

Target: ODN that is exact equivalent of a probe is called a target.

Mismatch (MM): ODN that has one or more different bases from target is called MM.

Noncomplementary (NC): ODN that has completely different base sequence from target is called NC.

7. EXPERIMENTAL TECHNIQUES

7.1. Controlled Potential Electrolysis with Coulometry

In controlled-potential coulometry the total number of coulombs consumed in an electrolysis is used to determine the amount of substance electrolyzed. To enable a coulometric method, the electrode reaction must satisfy the following requirements: (a) it must be of known stoichiometry; (b) it must be a single reaction or at least have no side reactions of different stoichiometry; (c) it must occur with close to 100% current efficiency.

The current-time curve is integrated under conditions such that only a single substance is reduced or oxidized at the surface of the electrode whose potential is controlled, and the electrolysis and integration are prolonged until virtually all of that substance has been consumed. The total quantity of electricity Q_∞ (in coulombs) consumed in reducing or oxidizing N moles of material is then given by Faraday's law:

$$Q_\infty = \int_o^\infty i \, dt = nFN \qquad (7.1)$$

Where i is the current (in amperes) t seconds after the start of the electrolysis, n is number of electrons transferred to or from each molecule or ion of the electroactive substance, and F is the number of coulombs per faraday. Integrating the current with respect to time makes it possible to evaluate n if N is known, or to evaluate N if n is known (Bard and Faulkner, 2001). Controlled potential electrolysis with coulometry (or potentiostatic coulometry) involves maintaining the potential of the working electrode at a constant level such that quantitative oxidation or reduction of the analyte occurs without involvement of less reactive species in the sample or solvent. Here the current is initially high but decreases rapidly and approaches to zero as the analyte is removed from the solution (Figure 7.1) (Skoog and Leary, 1992).

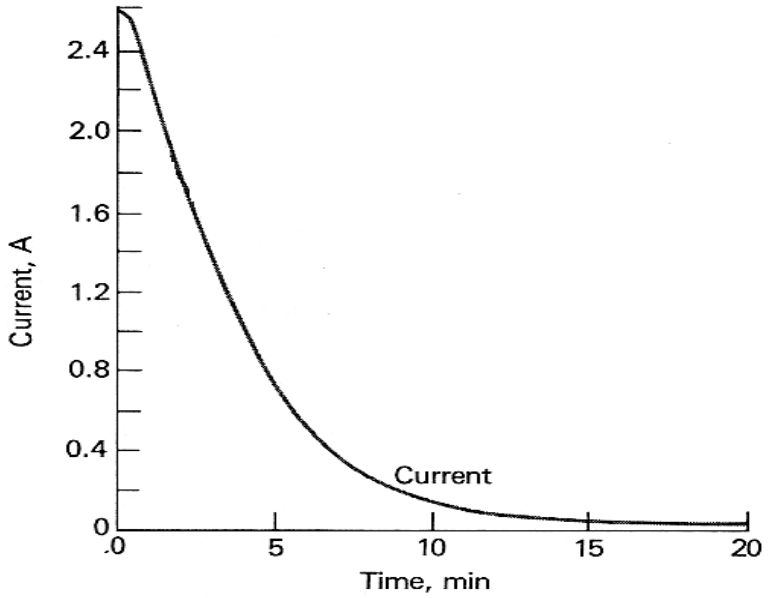

Figure 7.1. Change in current during a controlled-cathode-potential electrolysis.

7.2. Cyclic Voltammetry (CV)

Voltammetry comprises a group of electroanalytical methods in which information about the analyte is derived from the measurement of current as a function of applied potential obtained under conditions that encourage polarization of a working electrode (Skoog and Leary, 1992). Cyclic voltammetry (CV) is a type of potentiodynamic electrochemical measurement.

A simple potential wave form that is often used in electrochemical experiments is the linear wave form i.e., the potential is continuously changed as a linear function of time. In cyclic voltammetry the potential range is scanned in one direction, starting at the initial potential then finishing at the final potential and then the direction of the potential is reversed at the end of the first scan. Thus, the waveform is usually in a triangular wave form. This has the advantage that the product of the electron transfer reaction that occurred in the forward scan can be probed again in the reverse scan. In addition, it is a powerful tool for the determination of formal redox potentials, detection of chemical reactions that precede or follow the electrochemical reaction and evaluation of electron transfer kinetics. The electrode potential ramps linearly versus time are given in Figure 7.2. This ramping is known as the experiment's scan rate (V/s). The potential is measured between the reference electrode and the working electrode and the

current is measured between the working electrode and the counter electrode. This data is then plotted as current (*i*) vs. potential (*E*). As the waveform shows, the forward scan produces a current peak for any analytes that can be reduced (i_{pc}) [or oxidized (i_{pa}) depending on the initial scan direction] through the range of the potential scanned. The current will increase as the potential reaches the reduction potential of the analyte, but then falls off as the concentration of the analyte is depleted close to the electrode surface (Bard and Faulkner, 2001).

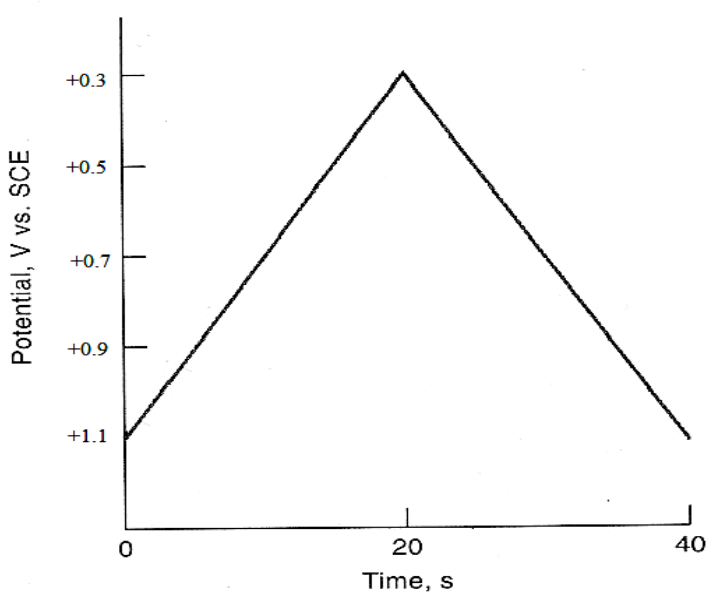

Figure 7.2. Variation of potential with time in cyclic voltammetry.

Cyclic voltammetry is mainly used for studying the reversibility of electrode process and for kinetic observations. If the redox couple is reversible then when the applied potential is reversed, it will reach the potential that will reoxidize the product formed in the first reduction reaction, and produce a current of reverse polarity from the forward scan. This oxidation peak will usually have a similar shape to the reduction peak. As a result, information about the cathodic peak potential (E_{pc}), anodic peak potential (E_{pa}), and also, electrochemical reaction rates of the compounds are obtained. For a reversible system, the peak current is expressed with Randles-Sevcik equation:

$$i_p = k\, n^{3/2}\, A\, D^{1/2}\, C\, v^{1/2} \qquad (7.2)$$

where; i_p : peak current in amperes

n : number of transferred electrons in the electrode reaction

A : area of the working electrode in cm^2

D : diffusion coefficient in $cm^2\ s^{-1}$

C : concentration of the electroactive species in mol cm^{-3}

v : potential scanning rate in V s^{-1}

k : Randles-Sevcik constant ($2.69x10^5$).

The current at the working electrode is plotted versus the applied voltage to give the cyclic voltammogram. A typical cyclic voltammogram (CV) is presented in Figure 7.3. It is known that for a reversible redox process:

$$\Delta E_p = E_{pc} - E_{pa} = (59 / n)\ mV \qquad (7.3)$$

The position of the current peak in this case being independent of the voltage scan rate. The two peaks have equal heights. With increasing irreversibility, ΔE_p becomes greater. For quasi-reversible processes and for slow change of voltage, the difference is about (60/n) mV, but it becomes greater for a faster sweep. For totally irreversibly processes, the reduction product is not reoxidized, so the anodic current peak is not seen.

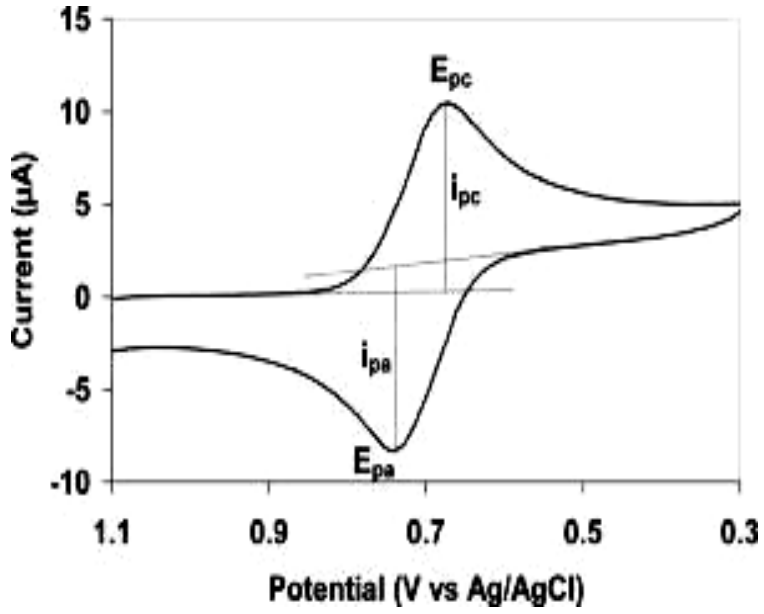

Figure 7.3. Cyclic voltammogram of a reversible electrode reaction.

Cyclic voltammetry is generally used to study the electrochemical properties of an analyte in solution. Cyclic voltammetry, while not used for routine analysis, has become an important tool for the study of mechanisms and rates of oxidation/reduction processes, particularly in organic and inorganic systems. Often, cyclic voltammograms will reveal the presence of intermediates in oxidation-reduction reactions (Skoog and Leary, 1992).

7.3. Differential Pulse Voltammetry (DPV)

By the 1960s, linear-scan voltammetry ceased to be an important analytical tool in most laboratories. The reason for the decline in use of this once popular technique was not only the appearance of several more convenient spectroscopic methods but also the inherent disadvantages of the method, including slowness, inconvenient apparatus, and, particularly, poor detection limits. These limitations were largely overcome by pulse methods. The two most important pulse techniques are differential pulse and square wave voltammetries (Skoog and Leary, 1992).

In differential pulse voltammetry the potential is scanned with a series of pulses. Each potential pulse is fixed, of small amplitude (10 to 100 mV), and is superimposed on a slowly changing base potential. Current is measure at two points for each pulse, the first point (1) just before the application of the pulse and the second (2) at the end of the pulse. These sampling points are selected to allow for the decay of the nonfaradaic (charging) current. The difference between current measurements at these points for each pulse is determined and plotted against the base potential. These measurements can be used to study the redox properties of extremely small amounts of chemicals. The peak current is proportional to the concentration. In these measurements, the effect of the charging current can be minimized, so high sensitivity is achieved. Faradaic current is extracted, so electrode reactions can be analyzed more precisely (Bard and Faulkner, 2001). Potential waveform for differential pulse voltammetry is given in Figure 7.4.

Figure 7.4. Potential waveform for differential pulse voltammetry.

7.4. Electrochemical Impedance Spectroscopy (EIS)

Electrochemical impedance spectroscopy (EIS) can give information on the impedance changes of the electrode surface in the modification process. This technique has grown tremendously in stature over the past few years and is now being widely employed in a wide variety of scientific fields such as biomolecular interaction, electrochemical sensor systems, corrosion studies, fuel cell testing, and microstructural characterization. Impedance is the opposition to the flow of alternating current (AC) in a complex system (Fang et al., 2008).

EIS characterization relies on a system whose electrochemical behavior is dependent on various processes, which are responsive at different rates or frequencies. It is well known that EIS measurements normally take a long time, i.e., it can take from anywhere between ~10 min to more than several hours to collect an EIS spectrum. Obviously, this will depend on the relaxation processes/stability of the system under study, and the frequency range choosen. Not many techniques are available that can easily separate the bulk membrane charge transport processes from the interfacial reactions; however, EIS is one of

very few techniques that is capable of providing this information simultaneously (Pepcic and De Marco, 2006). EIS also provides more prolific information about the barrier properties (Defega and Kwak, 2008).

Electrochemical impedance spectrum (Nyquist plot, *Z''* vs. *Z'*) is composed of a semicircle part in a high frequency region and a linear part in a low frequency region, corresponding to the electron transfer process and the diffusion process, respectively. In EIS, the diameter of the semicircle represents the charge-transfer resistance (R_{ct}), which controls the electron transfer kinetics of the redox probe at the electrode interface. In AC impedance, an amplitude and a frequency range are applied at open circuit potential (Fang et al., 2008). A Nyquist plot is given in Figure 7.5.

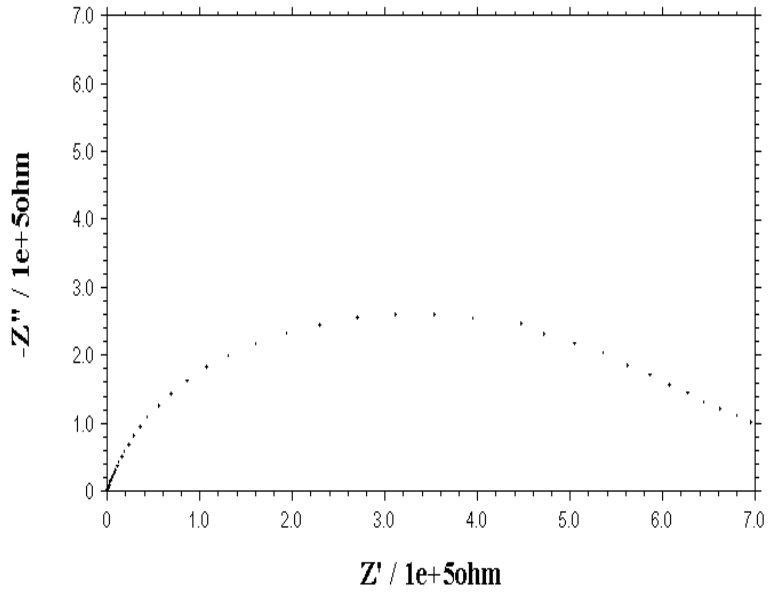

Figure 7.5. A Nyquist plot.

7. 5. Scanning Electron Microscopy (SEM)

In many fields of chemistry, material science, geology, and biology detailed knowledge of the physical nature and chemical composition of the surfaces of solids on a submicrometer scale is becoming of greater and greater importance (Skoog and Leary, 1992). By far the most important on surface structure, at least in the first stage of examination of a sample, comes from the techniques that provide images of structural differentiation in the surface layers. The simplest and most accessible of these techniques is scanning electron microscopy (SEM).

SEM is a type of electron microscope that images the sample surface by scanning it with a high-energy beam of electrons in a raster scan pattern. The electrons interact with the atoms that make up the sample producing signals that contain information about the sample's surface topography, composition and other properties such as electrical conductivity. Secondary electron images can be obtained on all materials identifying surface features, on most instruments, to a limit of ~ 100 nm. Despite the considerable depth of penetration of the incident primary electron beam (e.g. 0.5-5 μm), the re-emitted electrons (as secondary and backscattered electrons) come from mean depths of 50 nm-0.5 μm depending on the density of the material. Hence, the technique is sensitive to the near-surface region. Scanning (or rastering) the beam over the surface minimizes surface damage and surface charging. The surface features in this range include extensive faceting, phase separation, morphology of crystals, the structure of fracture faces, precipitates, pores, distribution of materials in composites, bonding at interfaces and preferential reaction at different sites on the surface. Backscattered electron images can give contrast based on the average atomic number of the region or phase examined. Topographic images, obtained by combining different backscattered electron images, can reveal detail of pits and protusions, precipitates and altered regions on the surface. The SEM is relatively easy to use requiring straightforward specimen preparation and conventional vacuum. The essential elements of an SEM are shown schematically in Figure 7.6. The electron gun, fitted by a W, LaB_6 or Field Emission (FE) gun operates typically over the range 0.1-30 kV accelerating voltage. A condenser lens produces a demagnified image of the electron source, which in turn is imaged by the probe forminglens (often called the objective lens) onto the specimen. The

electron path and sample chamber are evacuated. Scanning coils deflect the probe over a rectangular raster, the size of which, relative to the display screen, determines the magnification. Detectors collect the emitted electron signals, which after suitable amplification can be used to modulate the intensity of a TV-like image tube, which is rastered in synchronism with the probe (Connor et al., 2003).

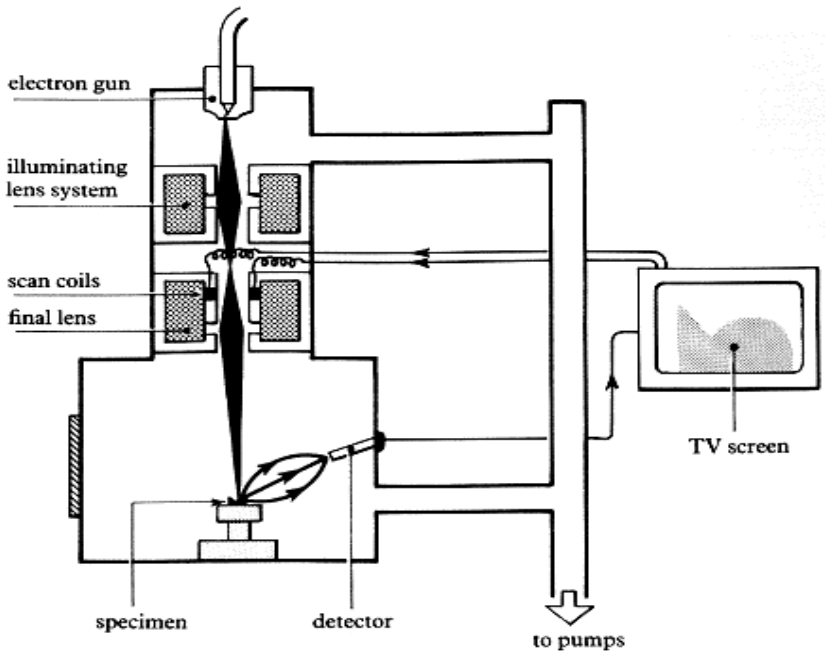

Figure 7.6. Basic features of the SEM.

7.6. Scanning Tunneling Microscopy (STM)

Scanning tunneling microscope (STM) is a powerful technique for viewing surfaces at the atomic level. It uses the low field quantum mechanical tunneling effect, where the tunneling current is an approximately related to the inverse exponential of the barrier thickness (gap width) and the square root of the work function, to produce images with resolution of individual atoms. The current dependence on gap width (*d*) is very sensitive (e.g. a ten-fold change for a change in d of 1 Å). An almost atomically sharp metal tip is used to scan areas as small as 10 x 10 Å to produce the most detailed images of atomic defects on material surfaces. When a conducting tip is brought very near to a metallic or semiconducting surface, a bias between the two can allow electrons to tunnel through the vacuum between them. The vertical resolution is even higher than the lateral resolution, in most cases being better than 0.1 Å. For low voltages,

tunneling current is a function of the local density of states (LDOS) at the Fermi level, E_f, of the sample. Variations in current as the probe passes over the surface are translated into an image. The technique can also be used to study differences in local work function allowing, in principle, identification of chemically different species in the surface (e.g. impurities or defect sites) or adsorbed on the surface. STM also, provides excellent tools for the study of polymer surfaces.

The components of an STM include scanning tip, piezoelectric controlled height and x,y scanner, coarse sample-to-tip control, vibration isolation system, and computer. The tip is often made of tungsten or platinum-iridium, though gold is also used. Tungsten tips are usually made by electrochemical etching, and platinum-iridium tips by mechanical shearing. Due to the extreme sensitivity of tunnel current to height, proper vibration isolation is imperative for obtaining usable results. In the first STM magnetic levitation was used to keep the STM free from vibrations; now spring systems are often used. Additionally, mechanisms for reducing eddy currents are implemented. Maintaining the tip position with respect to the sample, scanning the sample in raster fashion and acquiring the data is computer controlled. The computer is also used for enhancing the image with the help of image processing as well as performing quantitative morphological measurements (Connor et al., 2003). Schematic view of an STM is given in Figure 7.7.

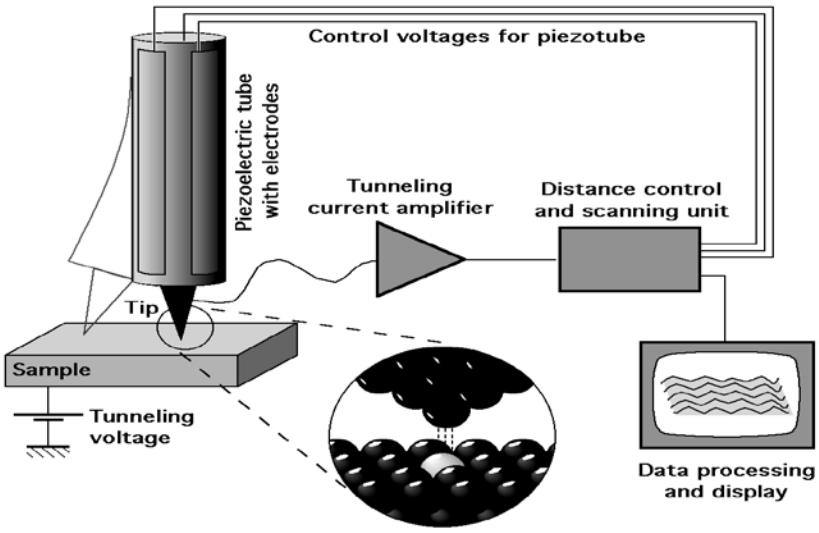

Figure 7.7. Schematic view of an STM.

7.7. Raman Spectroscopy

Raman spectroscopy is a spectroscopic technique used in condensed matter physics and chemistry to study vibrational, rotational, and other low-frequency modes in a system. Raman spectra are obtained by irradiating a sample with a powerful laser source of visible or infrared monochromatic radiation. During irradiation, the spectrum of the scattered radiation is measure at some angle (usually 90 deg) with a suitable spectrometer. Spectral excitation is normally carried out by radiation having a wavelength that is well away from any absorption peaks of the analyte. Scattering involves a momentary distortion of the electrons distributed around a bond in a molecule, followed by reemission of the radiation as the bond returns to its ground electronic state. In its distorted form, the molecule is temporarily polarized; that is, it develops momentarily an induced dipole, which disappears upon relaxation and reemission. The scattered radiation is of three types, namely Stokes, anti-Stokes, and Rayleigh. The last, whose wavelength is exactly that of the excitation source, is significantly more intense than either of the other two types. The intensity of a normal Raman peak depends in a complex way upon the polarizability of the molecule, the intensity of the source, and the concentration of the active group. The theory of Raman scattering shows the phenomenon results from the same type of quantized vibrational changes that are associated with infrared absorption. Thus, the difference in wavelength between the incident and scattered radiation corresponds to wavelengths in the mid-infrared region. Indeed, the Raman scattering spectrum and infrared absorption spectrum for a given species often resemble one another quite closely. There are, however, enough differences between the kinds of groups that are Raman active to make the techniques complementary rather than competitive. An important advantage of Raman spectra over infrared lies in the fact that water does not cause interference. Raman spectra can be obtained from aqueous solutions. In addition, glass or quartz cells can be employed.

Instrumentation for modern Raman spectroscopy consists of three components, namely, a laser source, a sample-illumination system, and a suitable spectrometer (Figure 7.8). The most widely used Raman source is probably a helium/neon laser, which operates in a continuous mode at a power of 50 mW. Laser radiation is produced at 632.8 nm. Argon-ion lasers, with lines at 488.0 and 514.5 nm, the

Nd:YAG laser that emits near-infrared radiation at 1.064 μm, are also employed. A common sample holder for liquid samples is an ordinary glass melting-point capillary. Raman spectra of solid samples are often obtained by filling a small cavity with the sample after it has been ground to a fine powder. Polymers can usually be examined directly with no sample pretreatment. Most Raman spectrophotometers employ double monochromators. In addition, a split-beam design and photomultiplier tubes serve as detectors in most instruments (Skoog and Leary, 1992).

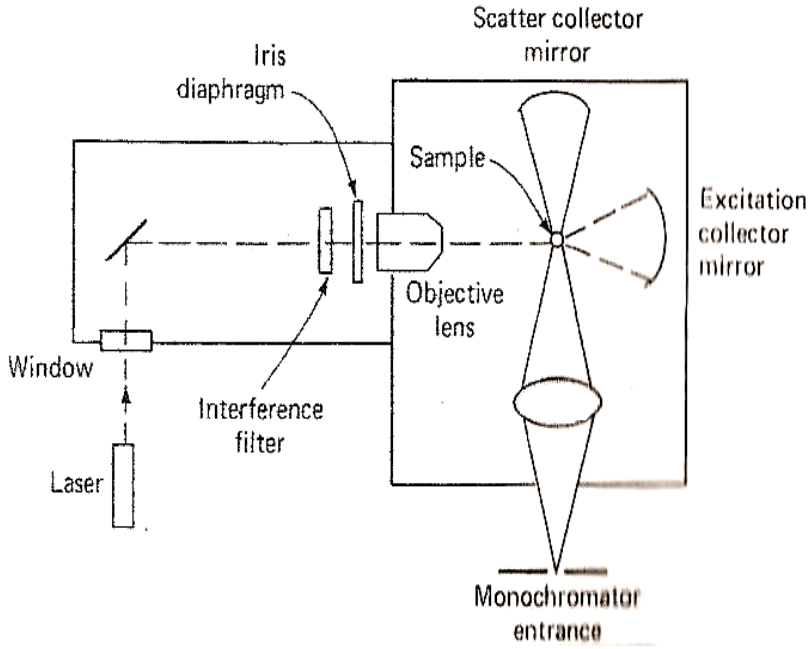

Figure 7.8. Instrumentation for Raman spectroscopy.

7.8. X-Ray Photoelectron Spectroscopy (XPS)

The detection and energy analysis of photoelectrons produced by radiation whose energy exceeds their binding energies is the subject of an extensively used technique known as Photoelectron (PE) Spectroscopy. The most common type, which is based upon irradiation with monochromatic X-radiation, is called X-ray photoelectron spectroscopy (XPS); it is also termed electron spectroscopy for chemical analysis (ESCA). XPS is a quantitative spectroscopic technique that measures the elemental composition, empirical formula, chemical state and electronic state of the elements that exist within a material. XPS spectra are obtained by irradiating a material with a beam of aluminium or magnesium X-rays

while simultaneously measuring the kinetic energy (KE) and number of electrons that escape from the top 1 to 10 nm of the material being analyzed. XPS requires ultra-high vacuum (UHV) conditions.

XPS is a surface chemical analysis technique that can be used to analyze the surface chemistry of a material in its as received state, or after some treatment such as: fracturing, cutting or scraping in air or UHV to expose the bulk chemistry, ion beam etching to clean off some of the surface contamination, exposure to heat to study the changes due to heating, exposure to reactive gases or solutions, exposure to ion beam implant, exposure to ultraviolet light.

Figure 7.9 is a schematic diagram indicating the essential components necessary for performing XPS. These consist of an X-ray source, a sample/support system, an electron energy analyser and an electron detector/multiplier, all maintained under UHV, and suitable electronics to convert the detected current into a readable spectrum (Connor et al., 2003).

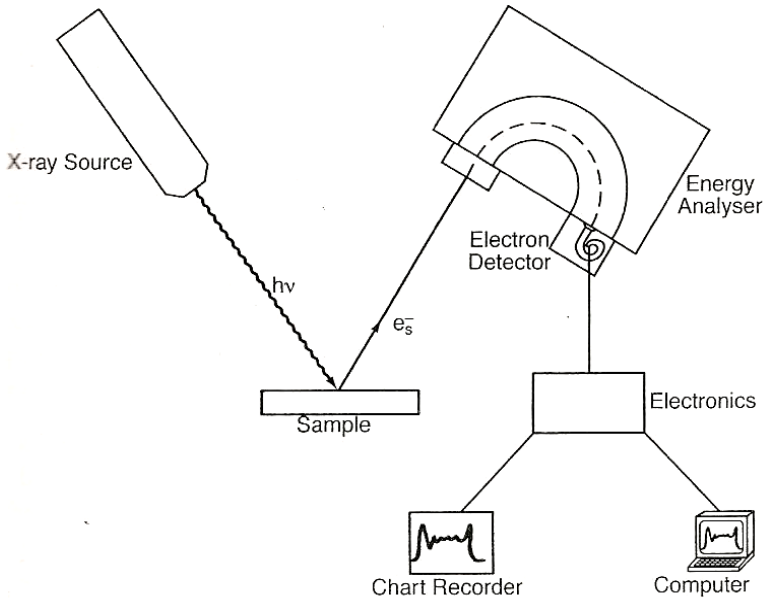

Figure 7.9. Basic components of a XPS system.

7.9. Fourier Transform Infrared-Attenuated Total Reflectance (ATR) Spectroscopy

Infrared spectroscopy has been a widely used technique in industry for the structural and compositional analysis of organic, inorganic and polymeric samples and for quality control of raw materials and commercial products. With the advent of Fourier transform infrared spectroscopy (FTIR) the range of applications and the materials amenable to study has increased enormously, owing to its increased sensitivity, speed, wavenumber accuracy and stability. Conventional infrared spectroscopy relies on the dispersion of an infrared beam via a grating into its monochromatic components, and slowly scanning through the entire spectral region of interest. When a sample is placed in the beam, various wavelengths of infrared radiation are adsorbed by the sample as the beam is scanned, and the result recorded as the infrared spectrum of the sample.

Internal-reflection spectroscopy is a technique for obtaining infrared spectra of samples that are difficult to deal with, such as solids of limited solubility, films, threads, pastes, adhesives, and powders. When a beam of radiation passes from a denser medium, reflection occurs. The fraction of the incident beam that is reflected increases as the angle of incidence becomes larger; beyond a certain critical angle, reflection is complete. During the reflection process the beam acts as if it penetrates a small distance into less dense medium before reflection occurs. The depth of penetration, which varies from a fraction of a wavelength up to several wavelengths, depends upon the wavelength, the index of refraction of the two materials, and the angle of the beam with respect to the interface. The penetrating radiation is called the evanescent wave. If the less dense medium absorbs the evanescent radiation, attenuation of the beam occurs at wavelengths of absorption bands. This phenomenon is known as attenuated total reflectance (ATR). Figure 7.10 shows an apparatus for attenuated total reflectance measurements. As seen from the figure, the sample is placed on opposite sides of a transparent crystalline material of high refractive index; a mixed crystal of thallium bromide/thallium iodide is frequently employed, as are plates of germanium and zinc selenide. By proper adjustment of the incident angle, the radiation passes undergoes multiple internal reflections before passing from crystal to the detector. Absorption and attenuation take place at each of these

reflections. Internal-reflectance spectra are similar but not identical to ordinary absorption spectra. In general, while same peaks are observed, their relative intensities differ. The absorbances, although dependent upon the angle of incidence, are independent of sample thickness, because the radiation penetrates only a few micrometers into the sample (Connor et al., 2003).

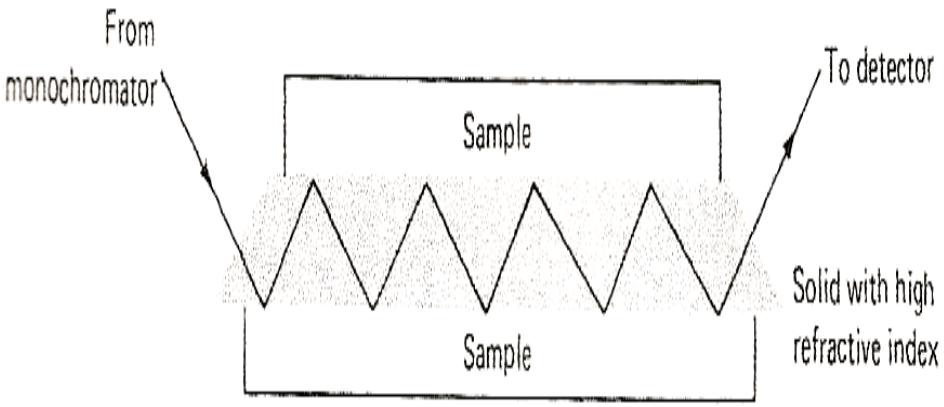

Figure 7.10. Internal reflectance apparatus.

8. EXPERIMENTAL

8.1. Apparatus

8.1.1. Electronic equipment

The potential-controlled coulometric, cyclic voltammetric, differential pulse voltammetric and AC impedance studies were carried out with CH Instruments System; Model 660 B. This system was connected to a personnel computer.

Scanning electron microscope (SEM) images were obtained by Quanta 400-FEI. Scanning tunneling microscope (STM) data were performed under ambient conditions by using a Molecular Imaging Model PicoScan Instrument. In all cases, Pt-Ir tips were used for imaging the surfaces. Raman spectroscopy studies were performed with Labram 800 HR Raman Spectrometer. XPS spectra were recorded on a SPECS ESCA (Berlin, GERMANY) system with Mg/Al dual anode using Mg Kα radiation. FTIR-ATR studies were acquired with Perkin Elmer FT-IR System Spectrum-BX.

Temperature controlled experiments were carried out with PolyScience® digital temperature controller.

8.1.2. Electrodes

Working electrodes: A handmade platinum (Pt) (Aldrich) disc electrode (area: 7.85×10^{-3} cm^2), a handmade gold (Au) (Aldrich) electrode (area: 7.85×10^{-3} cm^2) and a handmade pencil graphite electrode (PGE) were used as the working electrodes in electrochemical studies. A Tombo pencil was used as a holder for the disposable graphite tip (0.5 B Tombo pencil tip). The pencil was held vertically with 1.0 cm of tip immersed in the solution. The experiments except electrochemical studies were performed with Pt foil electrode (0.5 cm x 0.5 cm). Before each experiment, Pt and Au electrodes were polished with slurry of Al_2O_3 with water, then rinsed with triple distilled water, cleaned in ultrasonic bath and dried. Finally, the electrode was washed with solvent (methylene chloride) that was used for the experiment. The shapes of working electrodes are shown in Figure 8.1.

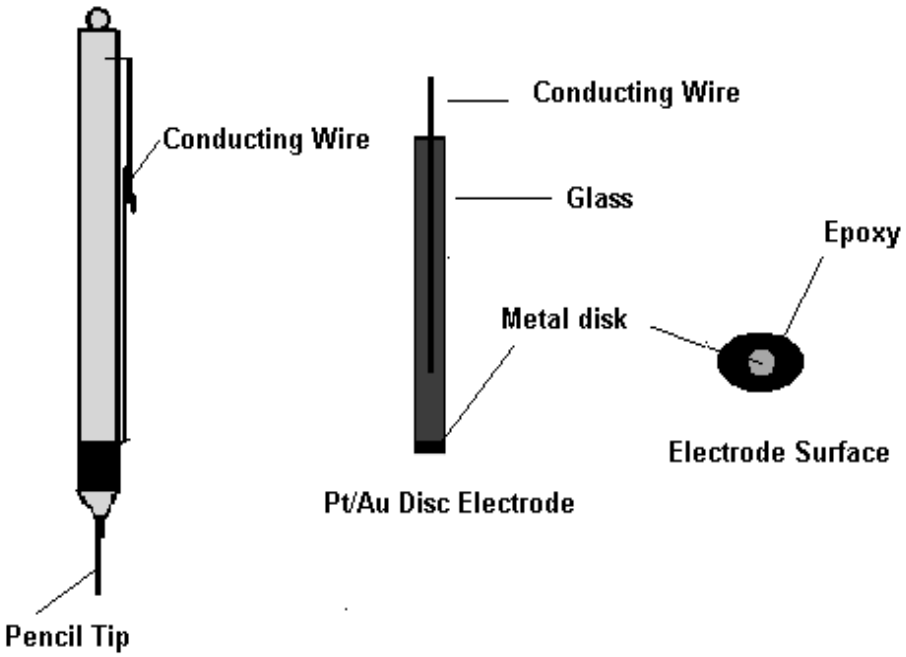

Figure 8.1. Shapes of working electrodes.

Reference electrodes: A handmade Ag/AgCl reference electrode was used for polymer electrooxidation process performed in methylene chloride. It was prepared by anodic electrolysis of a Ag (Aldrich) electrode in 0.1 M HCl solution for 3 hours at + 2.1 V with a current density of 2 mA cm^{-2}. The electrode was immersed in a separate compartment containing methylene chloride/0.1 M tetrabutylammonium perchlorate (TBAP) solution with a saturated amount of AgCl. For the experiments performed in aqueous medium, a saturated calomel electrode (SCE) (BAS) was used as the reference electrode.

Counter electrodes: A handmade Pt wire electrode that was made by using Pt wire (Aldrich) in separate compartment containing methylene chloride/0.1 M TBAP solution was used as the counter electrode for the electrochemical experiments carried out in methylene chloride medium. A Pt electrode that was also made by using Pt wire (Aldrich) with a surface area of 2 cm^2 in spiral form, was used as the counter electrode in the experiments performed in aqueous medium.

8.1.3. Electrochemical cell

An electrochemical cell, which had five inlets, was used for the electrochemical studies. Three of these were used for the electrodes and the other two were used

for nitrogen gas inlet and nitrogen gas outlet. Before electrochemical experiments, the cell was washed with acidic $K_2Cr_2O_7$, distilled water and alcohol. Then it was dried at 100 ^oC. After this washing and drying procedure, it was ready to use for electrochemical experiments. A schematic representation of the cell is given in Figure 8.2.

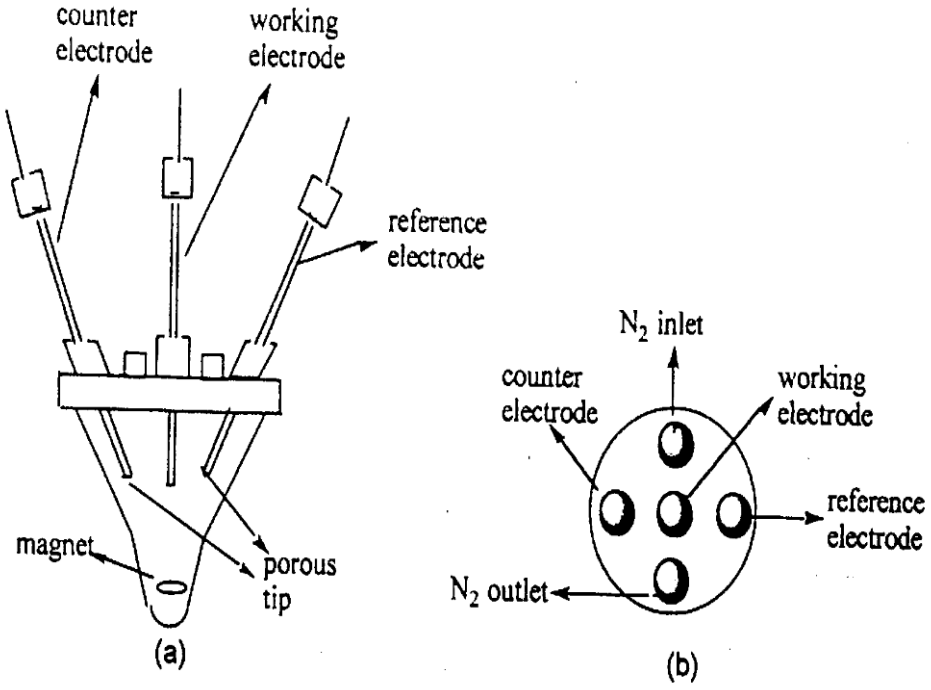

Figure 8.2. An electrochemical cell: a) cross-sectional view, b) top view of the cell.

8.2. Reagents

$NaH_2PO_4.2H_2O$, $Na_2HPO_4.2H_2O$, NaOH, Na_2CO_3, tetra-n-butyl ammonium hydroxide (TBAOH), ethyl alcohol (EtOH) and methanol were purchased from Merck. HPLC grade methylene chloride was obtained from Riedel de Haen. $NaClO_4$ and $Na_2B_4O_7$ were purchased from Sigma-Aldrich. Perchloric acid and benzene were obtained from BDH. Vinylferrocene was purchased from Aldrich. 2,2'-Azo-bis(2-methyl-propionitrile) (AIBN) was Alfa. $NaCH_3COO$ and CH_3COOH were purchased from Fluka.

Fish sperm double-stranded DNA (dsDNA) was obtained from Serva. Calf thymus DNA (ds/ssDNA) and mitomycin C were obtained from Sigma. The 20-23 mer

oligonucleotides (ODNs) were purchased as lyophilized powder from TIB MOLBIOL (Germany). Their base sequences are given below:

Thiol linked probe: 5'-SH-AATACCACATCATCCATATA
Amino linked probe: 5'-NH_2-AATACCACATCATCCATATA
Phosphate linked probe: 5'-PO_4-AATACCACATCATCCATATA
Bare probe: 5'-AATACCACATCATCCATATA
Target: 5'-TATATGGATGATGTGGTATT
Mismatch (MM): 5'-TATGTGGATGATGTGGTATT
Noncomplementary (NC) (23-mer): 5'-AATACCTGTATTCCTCGCCTGTC

The preparation of solutions: Phosphate buffer solutions (PBS, pH: 7.0) which contained 0.1M $NaClO_4$ were prepared from $NaH_2PO_4.2H_2O$ and $Na_2HPO_4.2H_2O$ using triple distilled water. Acetate buffer solutions (ABS, pH: 4.80) were prepared from CH_3COONa and CH_3COOH. Borate buffer solutions (BBS, pH: 9.00) were prepared from $Na_2B_4O_7$.

DNA and ODN stock solutions were prepared with ultrapure tri-distilled water and kept frozen. The diluted solutions of DNA were prepared by using PBS. More diluted ODN solutions were prepared with PBS containing 20 mM NaCl. Mitomycin C was prepared with ultrapure tri-distilled water and kept in refrigerator.

8.3. Supporting Electrolytes

TBAP was used as the supporting electrolyte of the polymer solution, in nonaqueous medium. TBAP was obtained by the reaction of TBAOH (40 % aqueous solution) with perchloric acid and recrystallized from the 1:9 mixture of water and EtOH by volume several times. It was then dried at 120 °C under vacuum for 12 hours. This salt was always kept under nitrogen atmosphere. Buffer solutions were used as the supporting electrolyte in aqueous medium.

8.4. Chemical Polymerization of Vinylferrocene

4.24 g vinylferrocene, 5.00 mL benzene and 0.0328 g initiator [2,2'-Azo-bis(2-methyl-propionitrile) (AIBN)] were charged to a Carious tube. The resulting solution was subjected to several freeze-thaw cycles to degas the solution and it

was lyophilized to remove the benzene. The tube was then sealed in vacuum, and the polymerization was carried out for 20 hours at 70 ^{0}C. The resulting polymer was dissolved in benzene and reprecipitated into methanol; PVF was dried at 60 °C under vacuum for 24 hours (Aso et al., 1969).

8.5. Preparation of Polymer Solution

1.0 mg mL^{-1} poly(vinylferrocene) polymer solution was prepared in methylene chloride/tetra-n-butyl ammonium perchlorate solvent/supporting electrolyte system. The polymer solution was deoxygenated by bubbling pure nitrogen gas (BOS) before electrochemical experiments.

8.6. Electrochemical Procedure

All the experiments were done at room temperature. A new polymer coated electrode and DNA immobilized polymer coated electrode were used in each electrochemical detection cycle. Each test was repeated three times, and the average values were presented in the histograms with the error bars.

9. RESULTS AND DISCUSSION

9.1. The Preparation of PVF^+ Modified Working Electrode

PVF^+ is an electroactive polymer. The polymer can be deposited onto the electrode surface by the electrooxidation of the reduced form, PVF, by resulting a less soluble polymer (Gülce et al., 1995a, 1997). PVF^+ is sensitive to the anions. After the electrostatic immobilization of negatively charged biomolecules onto the polymer modified Pt electrode effectively, it has been found that this polymer modified electrode can be used as a biosensor in order to monitor different molecules (Gülce et al., 1995b, c, 2002a, b ,c, 2003; Aydın et al., 2002, Gündoğan-Paul et al.,2002a, b; Kuralay et al., 2005; Özer et al., 2007).

The PVF^+ modified working electrode (Pt, Au or PGE) was prepared by the electrooxidation of 1.0 mg mL^{-1} PVF on working electrode at +0.7 V vs. Ag/AgCl electrode in methylene chloride/TBAP solvent/supporting electrolyte system. +0.7 V was set in our previous measurements as the optimized potential for the oxidation of PVF to PVF^+ (Kuralay et al., 2005, 2006, 2007). Perchlorate ions (ClO_4^-) in the structure of TBAP are incorporated into the polymeric structure as a counter ion as shown in the equation below:

$$\underset{(\textit{yellow})}{PVF} + ClO_4^- \Leftrightarrow \underset{(\textit{green})}{PVF^+ClO_4^-} + e^- \qquad (9.1)$$

The colour of $PVF^+ClO_4^-$ film is green and the PVF solution is yellow. The uptake of ClO_4^- as the counter anion to the polymer film was shown in a previous study by infrared spectroscopy and differential scanning calorimetry techniques (Gülce et al., 1995a).

Negatively charged biomolecules can be incorporated into $PVF^+ClO_4^-$ film via anion exchange (Gülce et al., 1995b, c; Gündoğan-Paul et al., 2002a, b). Since deoxyribose-phosphate backbone of DNA is negatively charged (Yang et al., 1997), it is believed that the main interaction between the positively charged matrix and DNA molecule is electrostatic interaction.

It is also believed that there is a specific interaction between DNA molecule and PVF^+ ions. It is known from our previous studies, this polymer shows electrocatalytic effect (Gülce et al., 1995a). DNA bases interact with redox couple of the polymer by giving adduct(s) at low potentials because of electrocatalytic oxidations of adenine and guanine in the presence of redox couple (Chen et al., 2007). Additional signals coming from possible adduct(s), besides to the polymer signal are attributed due to the interaction of DNA bases interact with iron forms in the structure of polymer forming electroactive complexes. It is also known that metal ions (such as iron, copper or manganese) react with DNA, frequently yielding strand breaks (Fojta et al., 2002).

The thicknesses of $PVF^+ClO_4^-$ films were controlled by the charge passed during the electroprecipitation step in the study. This charge was considered as an indication of polymeric film thickness. A charge of $1x10^{-3}$ C corresponded to $1.32x10^{-6}$ moles of the oxidized PVF per cm^2 dry thickness of ~300 µm, which corresponds to about $3x10^5$ layers (Peerce and Bard, 1980). Polycyclic voltammogram of 1.0 mC $PVF^+ClO_4^-$ coated Pt electrode in 50 mM PBS containing 0.1 M $NaClO_4$ after immersing it into the blank solution (50 mM PBS + 0.1 M $NaClO_4$) for 1 hour is presented in Figure 9.1. The oxidation potential of PVF to PVF^+ was observed at +0.40 V vs. SCE and the reduction potential of PVF^+ to PVF was measured at +0.23 V vs. SCE. These peaks are assigned to ferrocenium/ferrocene redox couple.

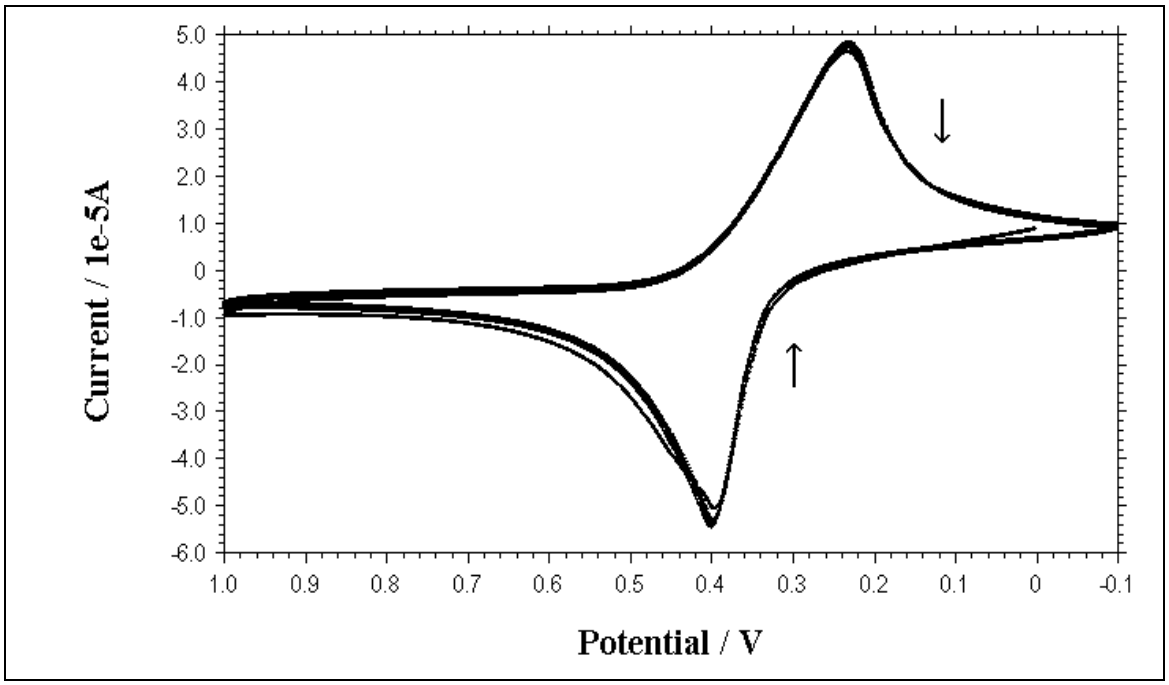

Figure 9.1. Polycyclic voltammogram of $PVF^{+}ClO_4^{-}$ coated Pt electrode corresponding to a film thickness of 1.0 mC in 50 mM PBS containing 0.1 M $NaClO_4$. Scan rate: 100 mV s^{-1}.

9.2. The Preparation of DNA Immobilized PVF^{+} Modified Electrode

The preparation of DNA immobilized electrode was accomplished by immersing the $PVF^{+}ClO_4^{-}$ modified electrode into ds/ssDNA solution. Probe ODN immobilized polymer electrodes were prepared dropping the probe ODN solutions onto the polymer modified Pt/Au electrode. Probe ODN immobilized polymer modified PG electrode was prepared immersing the $PVF^{+}ClO_4^{-}$ modified electrode into probe ODN solution. For Pt/Au electrode, hybridization studies were performed dropping target, NC and MM ODN solutions onto the probe immobilized polymer modified electrode. For PG electrode, hybridization studies were performed immersing the $PVF^{+}ClO_4^{-}$ modified electrode into target, NC and MM ODN solutions. After immobilization of nucleic acid onto the polymer electrode, the electrode was washed by using PBS for 10 seconds to remove the excess DNA, which was not held electrostatically. So-formed electrodes were used as an electrochemical DNA biosensor.

In the study, electrochemical sensing of DNA was performed using the oxidation peak currents of mainly polymer and electroactive DNA bases (guanine, adenine). The oxidation peak current of polymer in the absence/presence of DNA was

measured in 50 mM PBS containing 0.1 M $NaClO_4$ by using CV scanning between -0.1 V and +1.0 V and the oxidation peak currents of polymer, guanine, and adenine were measured by using DPV scanning between +0.0 V and +1.4 V vs. SCE at the pulse amplitude of 50 mV. For hybridization studies, firstly oxidation peak current of probe immobilized polymer and then oxidation peak currents of target, NC and MM immobilized probes were measured using DPV scanning between +0.0 V and +1.4 V vs. SCE at the pulse amplitude of 50 mV.

When the anions exchange with ClO_4^- counter anion in the structure of the polymer, the electroactivity of the film due to ferrocenium/ferrocene sites of the polymer either decreases or vanishes depending upon the type and concentration of the exchanging anion (Gülce et al., 1995a). After DNA immobilization onto the polymer modified electrode, electroactivity of the polymer decreases considerably due to less conductive character of DNA molecule. A significant decrease was observed at the oxidation and reduction peak currents of the polymer in parallel to the results obtained in the literature (Sanchez-Pomales et al., 2007; Prabhakar et al, 2008a, b; Degefa and Kwak, 2008). The decrease at the peak currents can be attributed to blocking of electroactive sites of PVF^+ by DNA molecule. Also, the electroactivity loss in the film upon anion exchange probably arises because of the inhibiting effect of the anion on the rate of the charge transfer process. Similar behaviors of this polymer were also cited in the literature (Inzelt and Szabo, 1986). Oxidation and reduction peak potentials of the polymer were also shifted after DNA immobilization. Polycyclic voltammogram of polymer modified electrode after 1 hour dsDNA immobilization in 50 mM PBS containing 0.1 M $NaClO_4$ is given in Figure 9.2. The oxidation peak potential of PVF to PVF^+ was observed at +0.41 V vs. SCE and the reduction peak potential of PVF^+ to PVF was measured at +0.20 V vs. SCE. There was an adduct measured at +0.07 V by using dsDNA immobilized polymer modified electrode due to the specific interaction between DNA molecule and PVF^+.

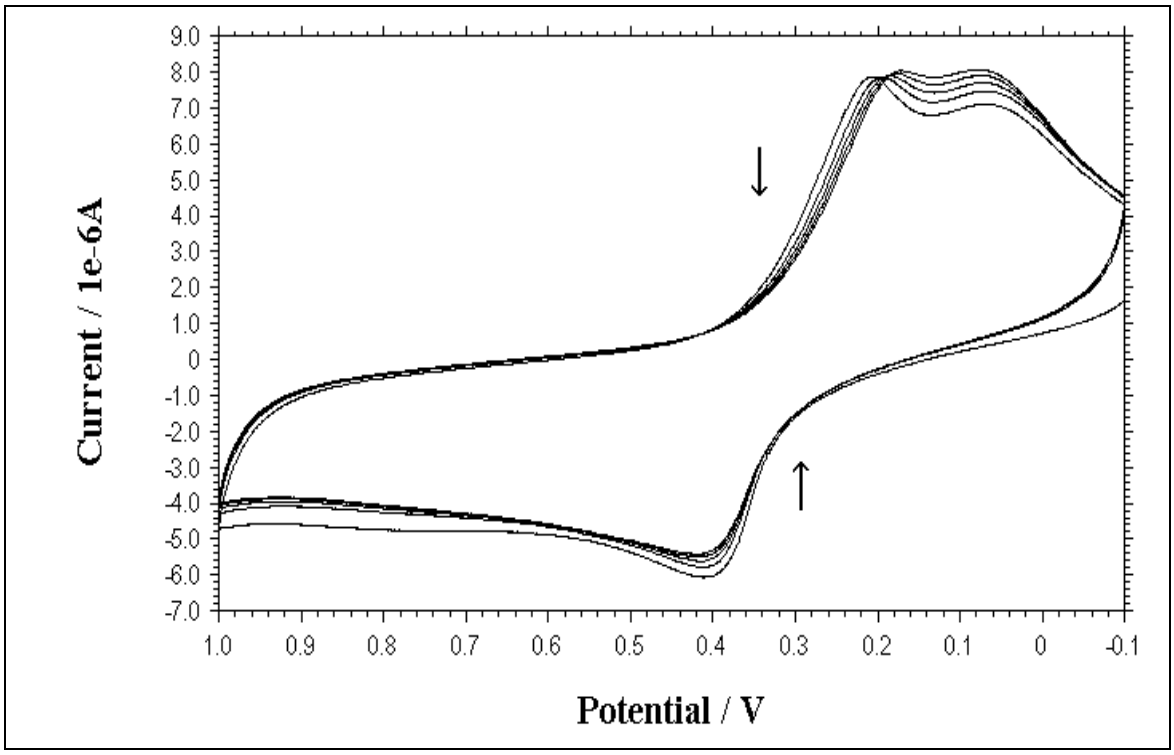

Figure 9.2. Polycyclic voltammogram of $PVF^{+}ClO_4^{-}$ coated Pt electrode corresponding to a film thickness of 1.0 mC in 50 mM PBS containing 0.1 M $NaClO_4$ after 1 hour 2.5 mg mL^{-1} dsDNA immobilization. Scan rate: 100 mV s^{-1}.

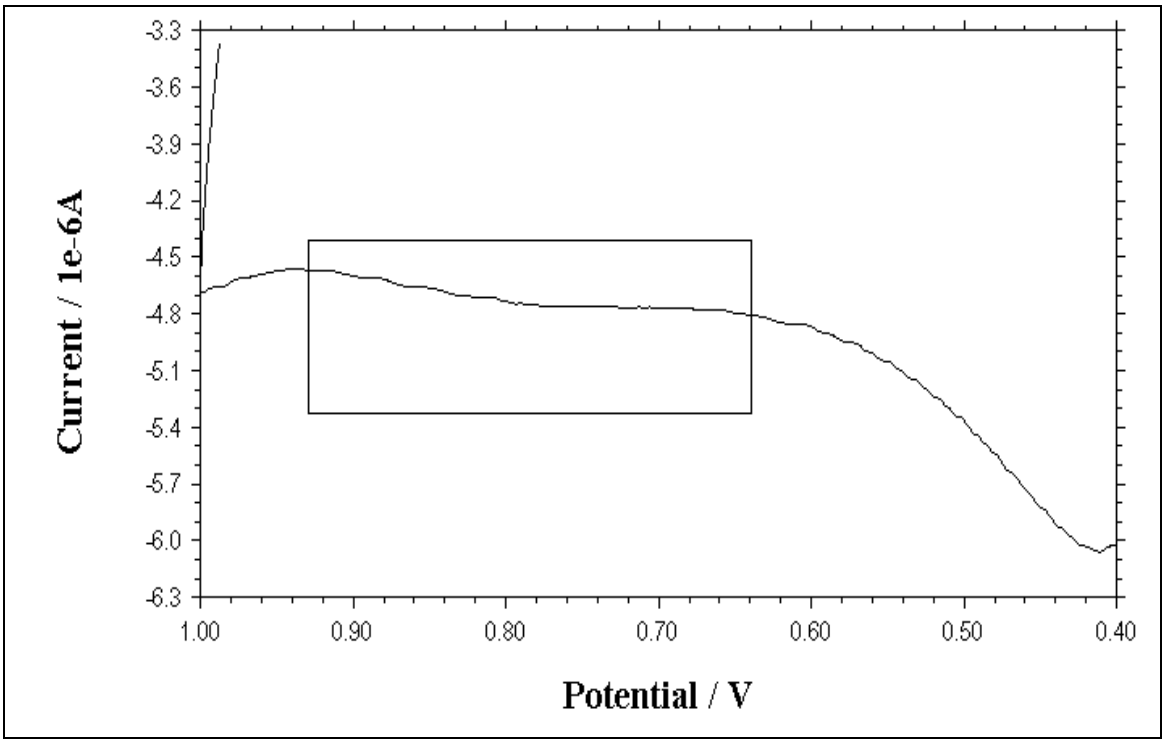

Figure 9.3. Enlarged cyclic voltammogram of $PVF^{+}ClO_4^{-}$ coated Pt electrode corresponding to a film thickness of 1.0 mC in 50 mM PBS containing 0.1 M $NaClO_4$ after 1 hour 2.5 mg mL^{-1} dsDNA immobilization. Scan rate: 100 mV s^{-1}.

There also existed a shoulder shown clearly in Figure 9.3 in the first scan of polycyclic voltammogram of DNA immobilized polymer film at about +0.80 V which could reflect the oxidation signal of guanine in parallel to the reported results (Jelen et al., 2004; Özcan et al., 2007; Prabhakar et al., 2008a).

In Figure 9.4, cyclic voltammetric behaviors of (a) uncoated Pt disc electrode, (b) $PVF^{+}ClO_4^{-}$ film and (c) dsDNA immobilized $PVF^{+}ClO_4^{-}$ film are given in 50 mM PBS containing 0.1 M $NaClO_4$. The purpose of the first period of the study was to develop a simple DNA immobilization strategy which provides a well-defined recognition interface. As can be seen from the figure, the peak currents and peak potentials of both oxidation and reduction peaks of the redox polymer changed and shifted after DNA was immobilized onto the polymer electrode. It can be concluded that immobilization of DNA was achieved using $PVF^{+}ClO_4^{-}$ surfaces.

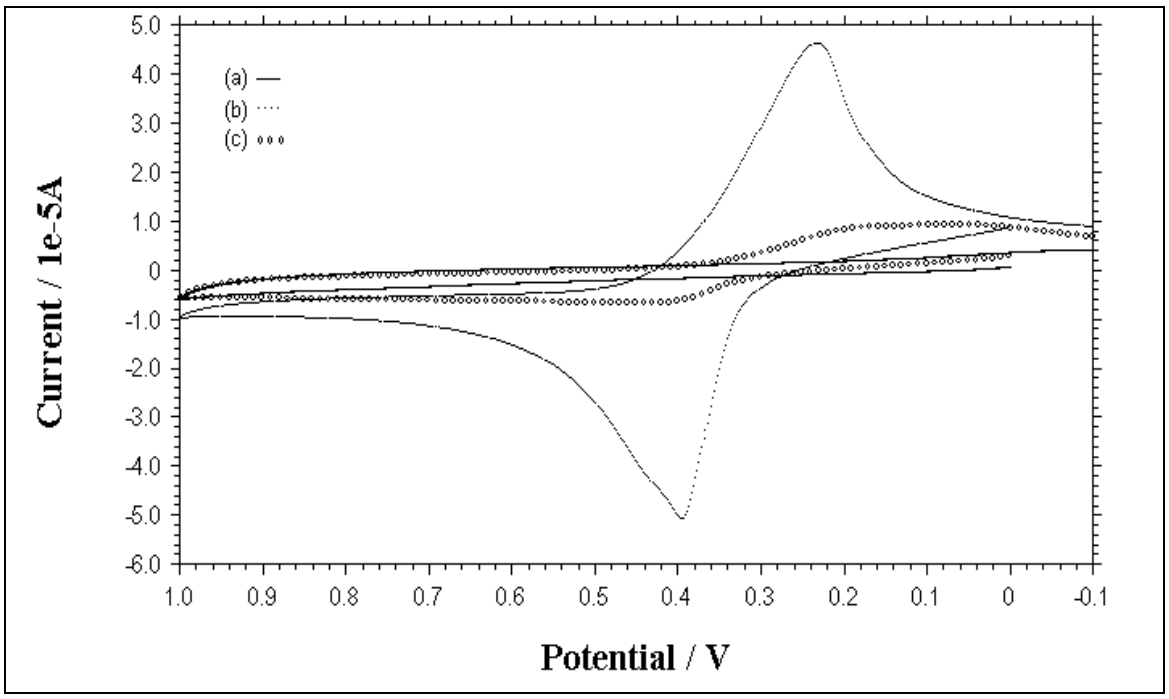

Figure 9.4. CVs of (a) uncoated Pt disc electrode, (b) $PVF^{+}ClO_4^{-}$ film, (c) dsDNA immobilized $PVF^{+}ClO_4^{-}$ film in 50 mM PBS containing 0.1 M $NaClO_4$. Scan rate: 100 mV s^{-1}.

Preparation steps of electrochemical DNA biosensor are represented schematically in Scheme 9.1.

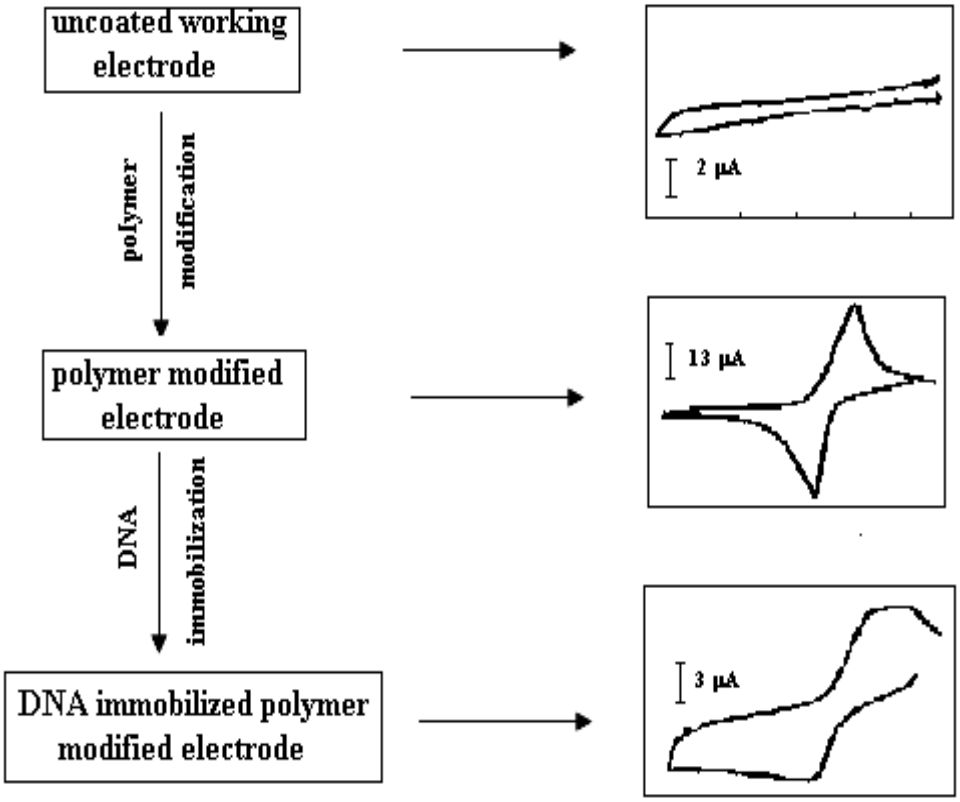

Scheme 9.1. Schematic procedure for the preparation of electrochemical DNA biosensor.

9.3. Studies Carried Out with DNA Immobilized PVF^{+} Modified Pt Electrode

In electrochemical studies Pt disc electrode was used as the first working electrode. The experimental parameters, which influenced the performance of this DNA sensing method, such as; the polymeric film thickness, the concentration of DNA, immobilization time of DNA, the concentrations of buffer solution and perchlorate ion, pH and temperature of the medium were examined and discussed in order to obtain better, more sensitive and selective electrochemical signals. After the optimum working conditions were obtained, the electrochemical behavior of DNA modified polymer electrode by using dsDNA or ssDNA was compared. The immobilization mechanism of negatively charged DNA onto the positively charged matrix was tested by reducing the polymer if it was mainly because of

electrostatic attraction or not. DNA hybridization was also investigated at optimized working conditions.

9.3.1. The effect of the polymeric film thickness

In order to investigate the effect of the polymeric film thickness on the response of the DNA biosensor, $PVF^{+}ClO_4^{-}$ film with various thicknesses was electrodeposited on the electrode surface. Firstly, cyclic voltammetric behavior of this film in 50 mM PBS containing 0.1 M $NaClO_4$ (pH 7.0) was recorded after it had immersed in buffer solution for 1 hour. Then, the electrode was immersed in dsDNA solution for 1 hour. Secondly, cyclic voltammogram of this electrode in buffer solution was recorded. The concentration of dsDNA solution was 2.5 mg mL^{-1} in each of the study.

The CVs of $PVF^{+}ClO_4^{-}$ film, dsDNA immobilized polymer film and uncoated Pt electrode in two different polymeric film thicknesses are compared in Figure 9.5 and Figure 9.6. There was an adduct measured at +0.07 V by using dsDNA immobilized polymer modified electrode when the polymer film thickness was applied as a value corresponding to the passage of a charge of 0.2 mC during the electroprecipitation of the polymer (Figure 9.5). Additional signals coming from possible adduct(s), besides to the polymer signal were attributed due to the specific interaction between DNA and PVF^{+}. In the earlier literature, it was shown that there were electrocatalytic reactions of guanine and adenine in the presence of Fe(II/III) couple. It is believed that DNA bases may possibly interact with the redox couple by giving adduct(s) (Chen et al., 2007).

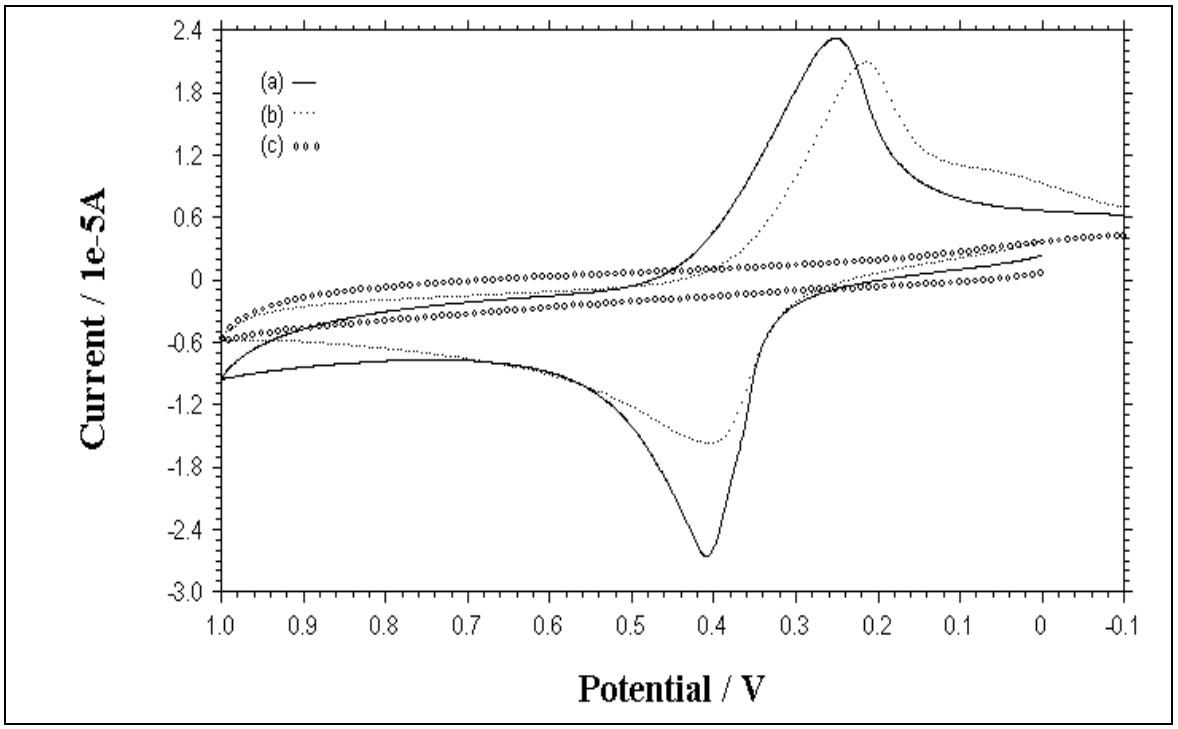

Figure 9.5. CVs of (a) $PVF^{+}ClO_4^{-}$ coated Pt electrode (b) dsDNA immobilized polymer film (c) uncoated Pt electrode in 50 mM PBS containing 0.1 M $NaClO_4$ at 0.2 mC polymeric film thickness. Scan rate: 100 mV s^{-1}.

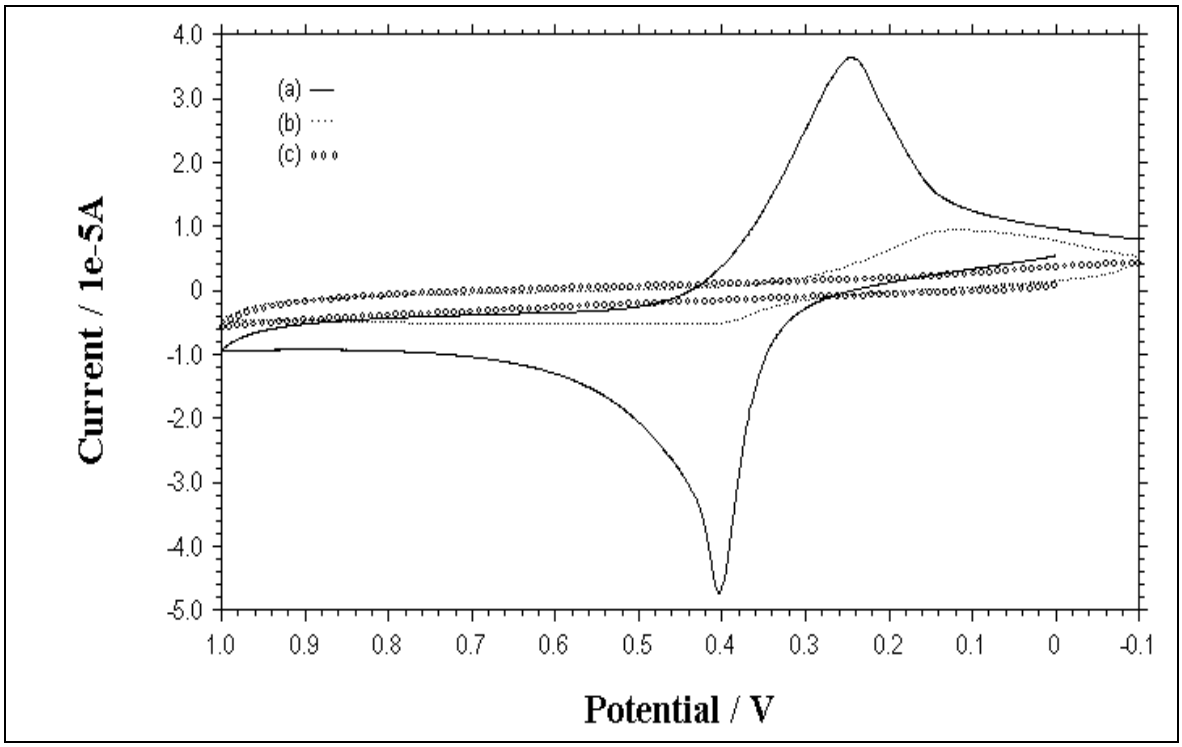

Figure 9.6. CVs of (a) $PVF^{+}ClO_4^{-}$ coated Pt electrode (b) dsDNA immobilized polymer film (c) uncoated Pt electrode in 50 mM PBS containing 0.1 M $NaClO_4$ at 1.0 mC polymeric film thickness. Scan rate: 100 mV s^{-1}.

The peak currents and peak potentials of both oxidation and reduction peaks of redox polymer changed and shifted after dsDNA was immobilized onto the polymer electrodes. The peak currents decreased due to the immobilization of dsDNA onto polymer electrodes (Figure 9.6). In Figure 9.7, histograms showing the oxidation peak currents of the polymer in different polymeric film thicknesses before (A) and after (B) dsDNA immobilization are given as a bar graphic.

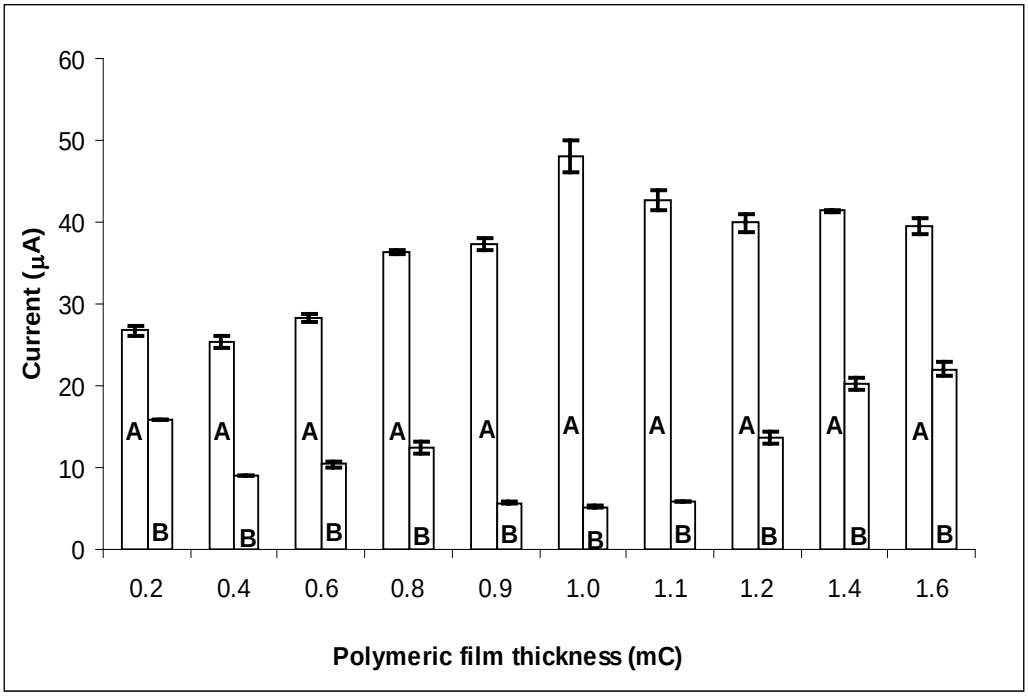

Figure 9.7. Histograms showing the oxidation peak currents of the polymer in different polymeric film thicknesses before (A) and after (B) dsDNA immobilization onto $PVF^{+}ClO_4^{-}$coated electrode.

The change in oxidation peak current between polymer electrode and dsDNA immobilized polymer electrode (ΔI) is also given in Figure 9.8. As seen from these figures, it is clear that the interaction of PVF^{+} with DNA is better at the higher thickness values of polymeric film. The amount of electroprecipitated PVF^{+} increased with increasing film thickness. Consequently, greater amount of DNA was immobilized. The oxidation and reduction peaks separation was also enlarged increasing the irreversibility of the polymer. It was found that there was a decrease observed at the peak current of polymer when the polymer film thickness were increased up to a value corresponding to the passage of a charge of 1.0 mC during the electroprecipitation of the polymer. After the polymer film

thickness value exceeded 1.0 mC, DNA immobilization may possibly be restricted due to the diffusion limitations of dsDNA into the inner regions of the porous polymer film matrix. These results were found similiar to earlier reports presenting the influence of polymer film thickness (Kuralay et al., 2005, 2006). The % decreases at the response of dsDNA immobilized polymer modified electrode were calculated as 40.88 %, 65.73 %, 89.08 %, 86.32 % and 65.83 for the film thickness values corresponding to the passage of charges of 0.2, 0.8, 1.0, 1.1 and 1.2 mC, respectively. The optimum polymeric film thickness was chosen as 1.0 mC for further experiments by using DNA immobilized polymer electrodes.

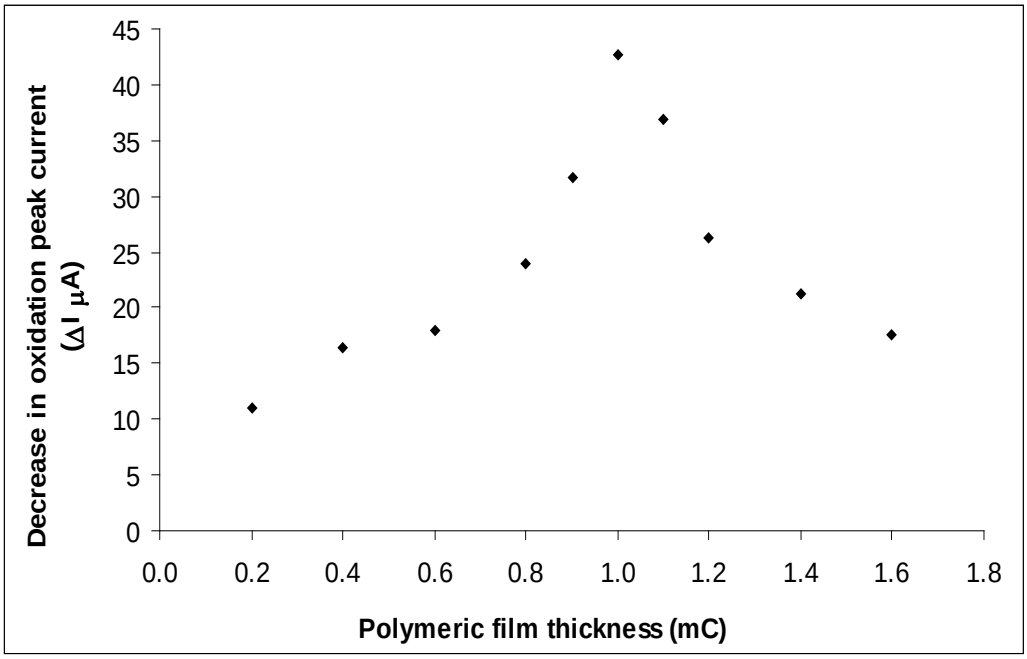

Figure 9.8. The change in oxidation peak current between polymer electrode and dsDNA immobilized polymer electrode with polymeric film thickness.

9.3.2. The effect of the concentration of dsDNA

The effect of dsDNA concentration used in the solution during the immobilization step on the response of the electrode was determined using CV technique. dsDNA concentrations varying from 0.5 and 4.0 mg mL^{-1} were used in the experiments. Optimum polymeric film thickness (1.0 mC) and 1 hour immobilization time were also used. Firstly, cyclic voltammetric behavior of the $PVF^{+}ClO_4^{-}$ film in phosphate buffer solution was recorded after the electrode had immersed in buffer solution for 1 hour. Then the prepared $PVF^{+}ClO_4^{-}$ films were

immersed in dsDNA solutions which had different concentrations. Secondly, cyclic voltammograms of these electrodes in 50 mM PBS containing 0.1 M $NaClO_4$ were recorded. The CVs of (a) $PVF^+ClO_4^-$ film, (b) $PVF^+ClO_4^-$ film after immersing into 0.5 mg mL^{-1} dsDNA solution and (c) $PVF^+ClO_4^-$ film after immersing into 2.5 mg mL^{-1} dsDNA solution are given in Figure 9.9. By the immobilization of dsDNA onto PVF^+ matrix, the oxidation and the reduction peaks of the polymer shifted and the peak currents decreased since dsDNA covered the electroactive sites of PVF^+.

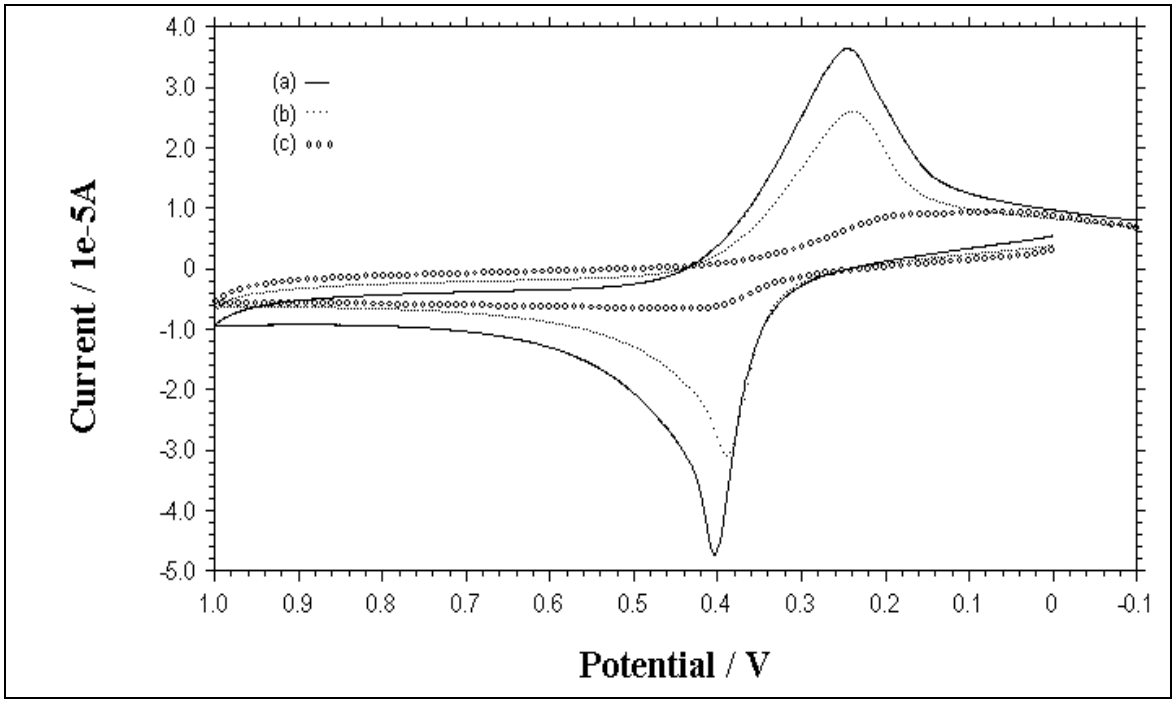

Figure 9.9. CVs of (a) $PVF^+ClO_4^-$ film (b) $PVF^+ClO_4^-$ film after immersing into 0.5 mg mL^{-1} dsDNA solution (c) $PVF^+ClO_4^-$ film after immersing into 2.5 mg mL^{-1} dsDNA solution. Scan rate: 100 mV s^{-1}.

The oxidation signals of polymer before (A) and after (B) dsDNA immobilization are given in Figure 9.10 as bar graphic. The changes in oxidation peak current of polymer electrode are also given in Figure 9.11. As seen from these figures clearly, up to a concentration level of 2.5 mg mL^{-1} dsDNA, the oxidation and reduction peaks of the polymer decreased. At this concentration value, polymer surface reached its saturation and no appreciable difference was observed in oxidation peak current. So 2.5 mg mL^{-1} solution was used as optimum dsDNA concentration in the study. The decreases in oxidation and reduction peak current

of the polymer were 86.2 % and 75.2 %, respectively at this concentration value. The detection limit corresponds to as 16.20 μg mL^{-1} for dsDNA immobilized polymer modified electrode using CV technique.

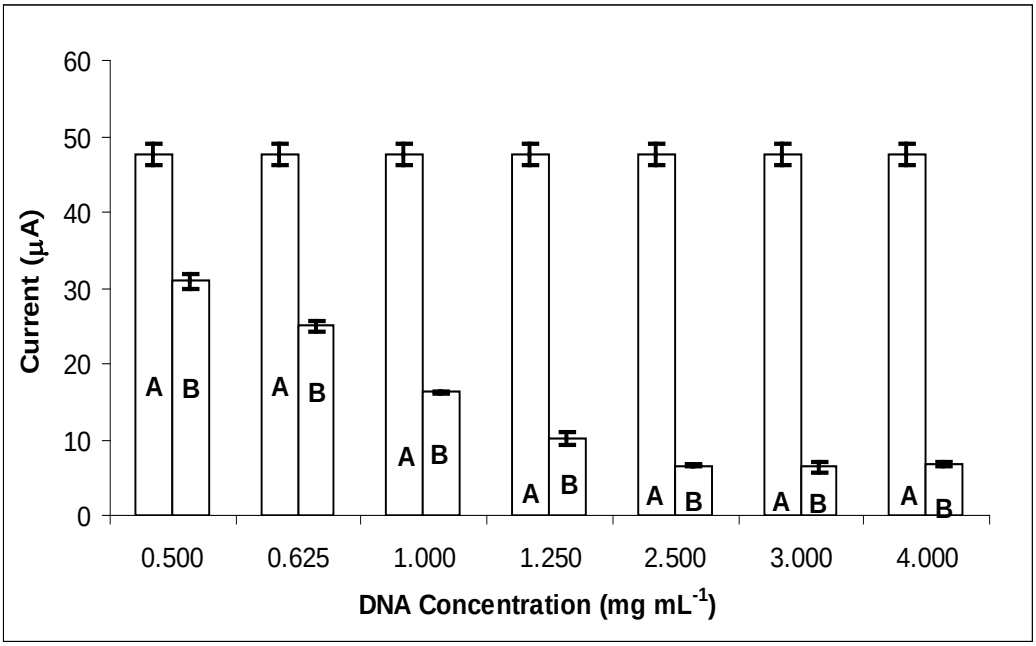

Figure 9.10. Histograms showing the changes at the oxidation peak currents of polymer; before (A) and after (B) dsDNA immobilization in different concentrations onto PVF^{+} modified electrode.

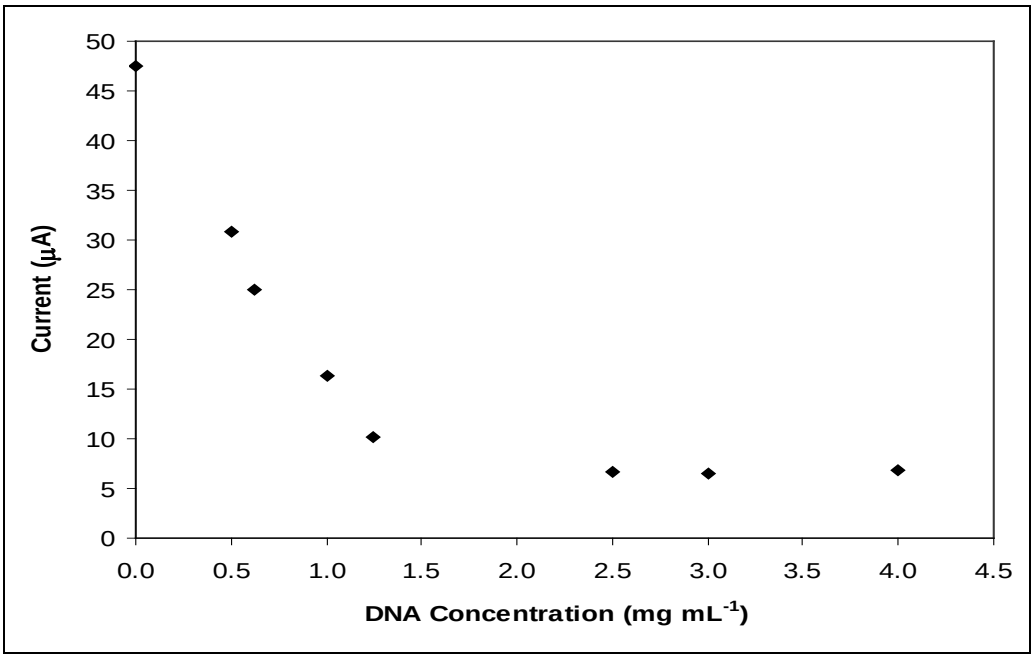

Figure 9.11. Changes in oxidation peak current of polymer with dsDNA concentration.

In order to support DNA immobilization, active surface areas were calculated as was described in the literature (Abaci et al., 2005) and it was determined that active surface areas decreased with increasing of dsDNA concentration in immobilization solution due to binding of dsDNA to the polymer surface (Figure 9.12). This result supported our earlier findings.

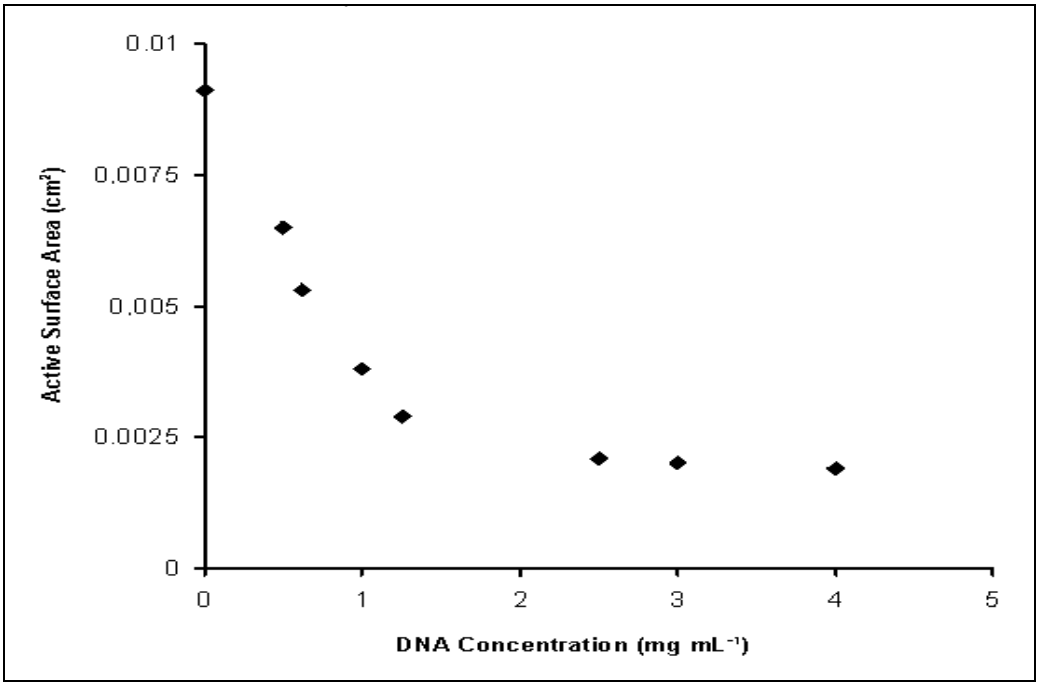

Figure 9.12. Graphic representing the changes of electroactive surface areas after dsDNA immobilization onto PVF^+ modified electrode at different concentrations.

The effect of dsDNA concentration based on the decrease in the oxidation peak of the redox polymer was also recorded using DPV technique which is more sensitive than CV technique (Figure 9.13). The oxidation signal of polymer was recorded in various dsDNA concentrations in the concentration range of 50 to 2000 $\mu g\ mL^{-1}$ (Figure 9.13A). It was obtained that the oxidation peak current of polymer decreased when the dsDNA concentration was increased from 50 to 1500 $\mu g\ mL^{-1}$ ($R^2 = 0.9910$) (Figure 9.13B). Then it was levelled off because of the fact that the polymeric structure reached its saturation value at this concentration value. With the increasing concentration of dsDNA in immobilization solution, more dsDNA was immobilized onto the PVF^+ surfaces, and the peak currents decreased due to less-conductive character of dsDNA. The detection limit corresponds to 1.56 $\mu g\ mL^{-1}$ for dsDNA immobilized polymer modified electrode.

No extra redox indicator was necessary for monitoring the changes in different DNA concentrations, since PVF^{+} directly report the event with improved selectivity at low potentials by itself (Kuralay et al., 2008, 2009a).

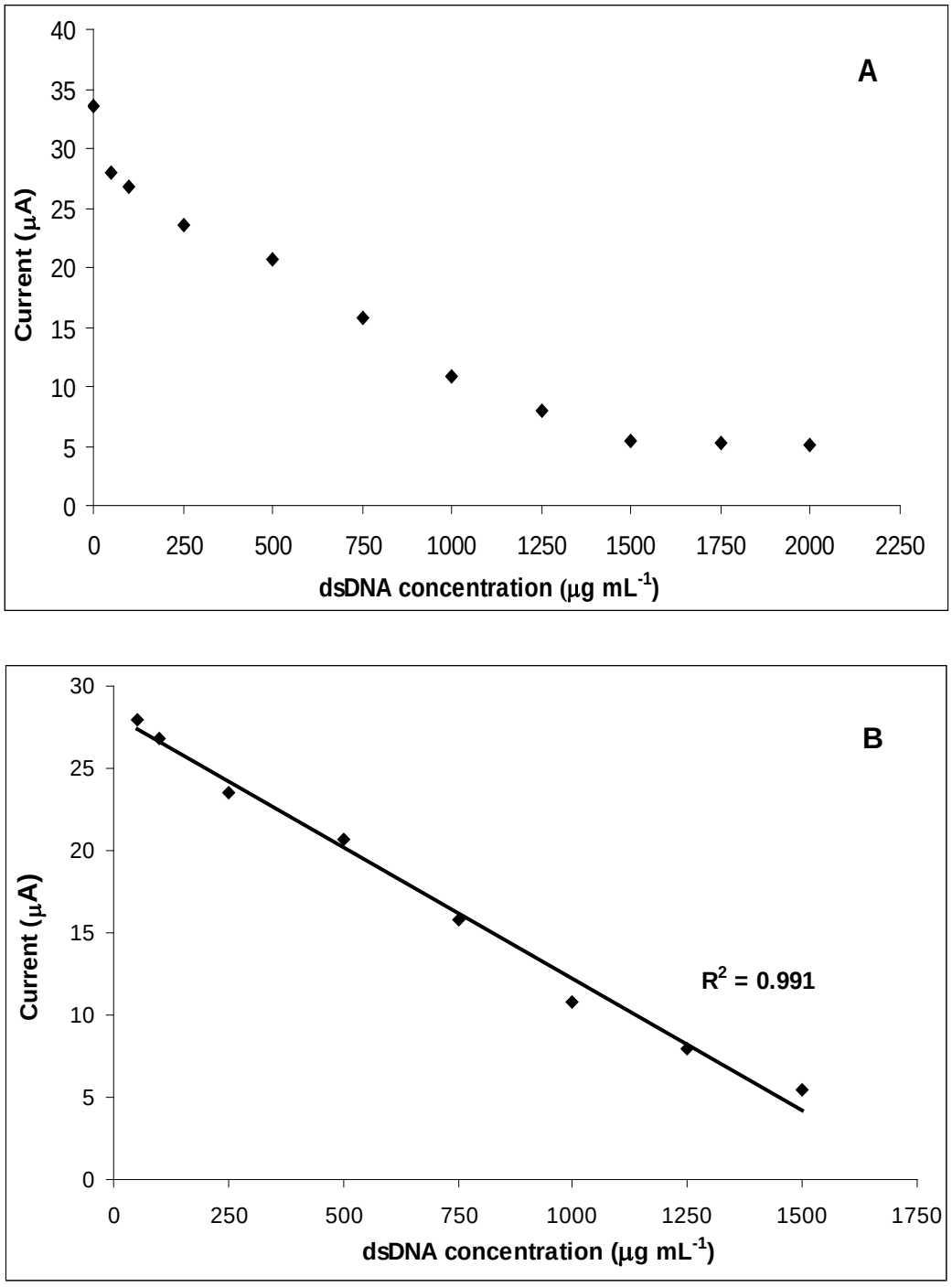

Figure 9.13. Changes in oxidation peak current of the polymer with different dsDNA concentrations.

9.3.3. The effect of immobilization time of dsDNA

The immobilization time of dsDNA is one of the important parameters for investigating the optimum working conditions of the polymer-based biosensor. For the determination of the effect of immobilization time of dsDNA onto the positively charged polymeric matrix, $PVF^{+}ClO_4^{-}$ films with a polymeric film thickness of 1.0 mC were immersed in 2.5 mg mL^{-1} dsDNA solution for different immobilization times. Firstly, cyclic voltammetric behavior of $PVF^{+}ClO_4^{-}$ film in buffer solution was recorded after it had immersed in buffer solution for several periods of time. Then, $PVF^{+}ClO_4^{-}$ film was immersed in dsDNA solution for the same period of time. Secondly, cyclic voltammetric behavior of the dsDNA immobilized film was recorded in 50 mM PBS containing 0.1 M $NaClO_4$ at pH 7.0. The oxidation peak currents of polymer were recorded in the absence (A) and the presence (B) of dsDNA in various DNA immobilization times onto PVF^{+} modified electrode. The histograms are shown in Figure 9.14. The change in oxidation peak current between polymer electrode and dsDNA immobilized polymer electrode (ΔI) is also given in Figure 9.15.

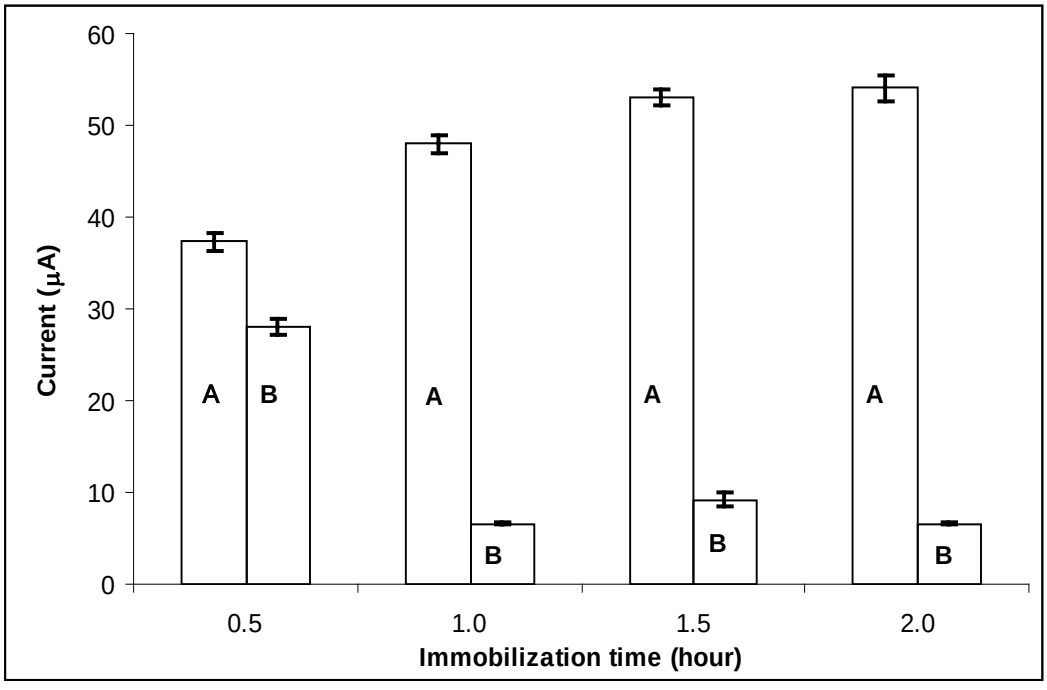

Figure 9.14. Histograms showing the changes at the oxidation peak currents of polymer in the absence (A) and the presence of (B) dsDNA in different immobilization times onto PVF^{+} modified electrode.

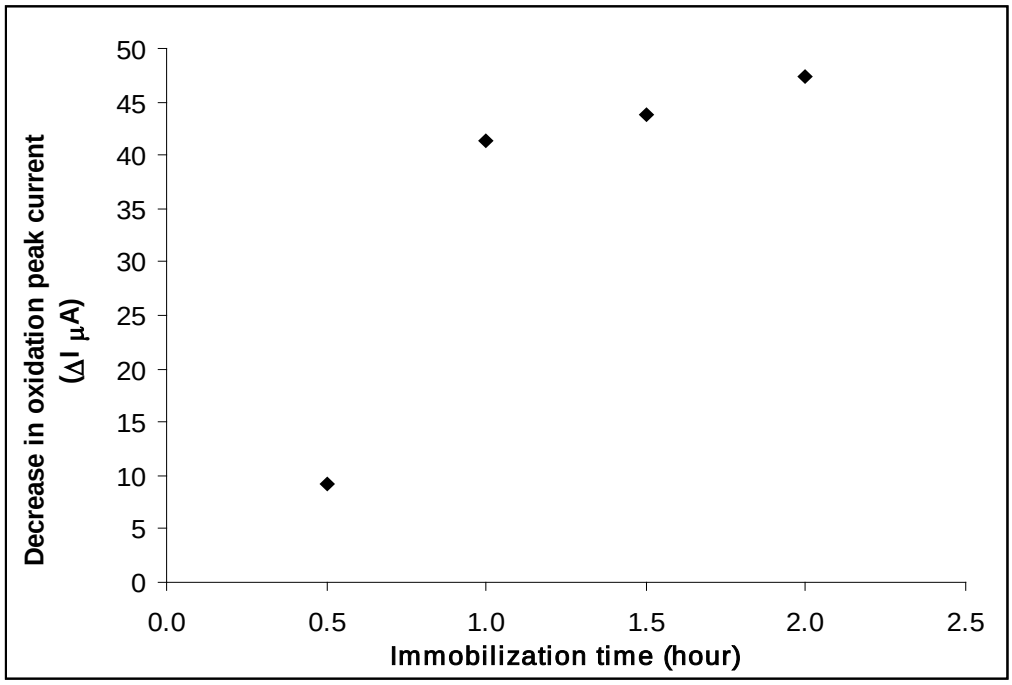

Figure 9.15. The change in oxidation peak current between polymer electrode and dsDNA immobilized polymer electrode in different dsDNA immobilization times.

This parameter also showed that there was an interaction between the positively charged polymeric matrix and the negatively charged DNA. As seen from these figures, most decrease at the oxidation peak of polymer was observed in 2 hours immobilization time of DNA. Almost same level of decrease was obtained at the polymer signal in 1.0 hour and 1.5 hours. The difference of ΔI values corresponding to 1 hour and 2 hours immobilization time was small. Thus, 1 hour immobilization time was used in the study. The CVs of (a) $PVF^{+}ClO_4^{-}$ film, (b) $PVF^{+}ClO_4^{-}$ film after immersing into 2.5 mg mL^{-1} dsDNA solution for 1 hour are given in Figure 9.16. The oxidation and reduction peaks of the polymer changed after DNA immobilization.

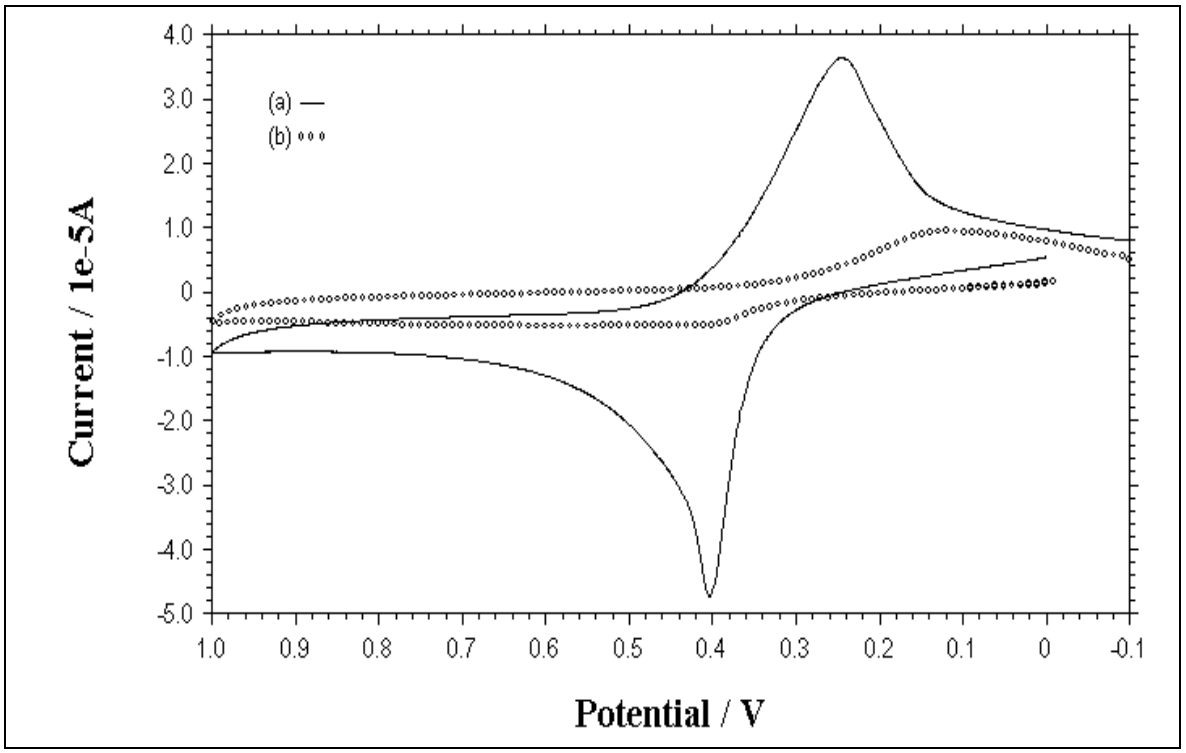

Figure 9.16. CVs of (a) $PVF^{+}ClO_4^{-}$ film (b) $PVF^{+}ClO_4^{-}$ film after immersing into 2.50 mg mL^{-1} dsDNA solution for 1 hour in 50 mM PBS containing 0.1 M $NaClO_4$. Scan rate: 100 mV s^{-1}.

The effect of the immobilization times of 1 hour and 2 hours was also determined at a low concentration value (0.5 mg mL^{-1}) of dsDNA concentration. The response of this concentration value was poor when compared with other dsDNA concentrations. The response for this concentration value might be high at longer immobilization time values. For checking this assumption, the effect of the immobilization time of 2 hours with 0.5 mg mL^{-1} of dsDNA solution was investigated. It is clearly seen from Figure 9.17 that the interaction between the polymer and dsDNA at 0.5 mg mL^{-1} concentration value was better at 2 hours than 1 hour. So it can be said that the interaction for the polymer and dsDNA can be increased by changing the parameters. There is an interaction between the positively charged matrix and the negatively charged biomolecule, even at low concentration values. The CVs of (a) $PVF^{+}ClO_4^{-}$ film, (b) $PVF^{+}ClO_4^{-}$ film after immersing into 0.50 mg mL^{-1} dsDNA solution for 2 hours are given in Figure 9.18.

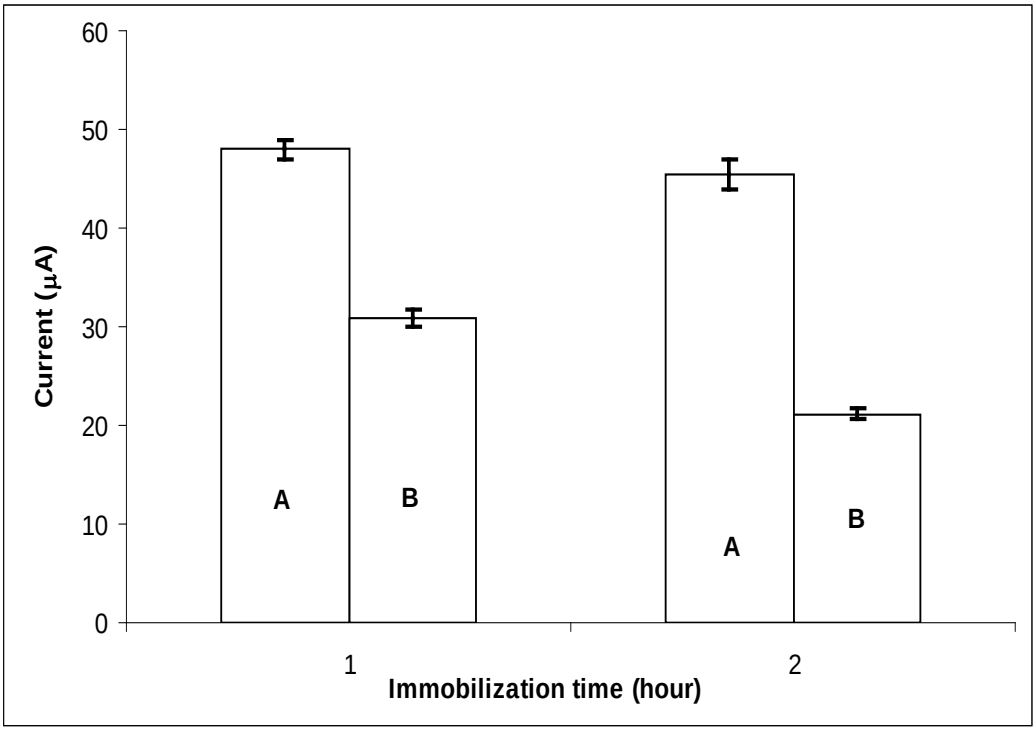

Figure 9.17. Histograms showing the changes at the oxidation peak currents of polymer; before (A) and after (B) immersing into 0.5 mg mL^{-1} dsDNA solution for 1 and 2 hours.

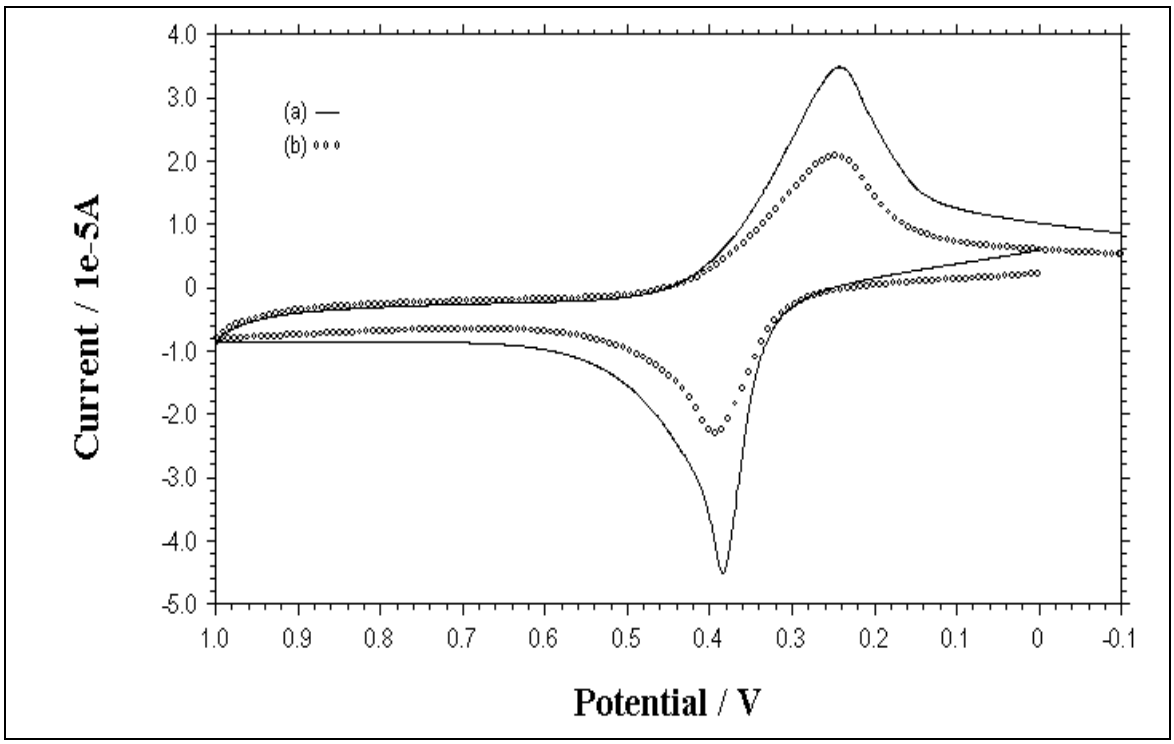

Figure 9.18. CVs of (a) $PVF^{+}ClO_4^{-}$ film (b) $PVF^{+}ClO_4^{-}$ film after immersing into 0.5 mg mL^{-1} solution for 2 hours in 50 mM PBS containing 0.1 M $NaClO_4$. Scan rate: 100 mV s^{-1}.

Electrochemical behaviors of polymer modified and dsDNA immobilized polymer modified electrodes at different immobilization times in 2.5 mg mL^{-1} dsDNA solution were also investigated by using DPV technique. There was a well-developed peak at +0.35 V by using polymer modified electrode (Figure 9.19a). After the modified electrodes were immersed into dsDNA solution for 15, 30 minutes, 1 and 2 hours, the DPVs of these films were recorded (Figure 9.19b, c, d, e, respectively). After DNA immobilization, a significant decrease at the oxidation peak currents was observed by using DPV in similar to the results obtained by using CV studies. There were additional signals coming from possible adduct(s), besides to the polymer signal in the different immersion times, such as, 1 and 2 hours. There was also a significant shift at the oxidation peak potential of polymer in 2 hours immersion time. Additional signals coming from possible adduct(s), besides to the polymer signal might be attributed due to the specific interaction between DNA molecule and PVF^{+}. DNA bases interact with iron forms in the structrure of polymer to form electroactive complexes. Adduct(s) seen in Figure 9.19 probably arised electrooxidation of these complex species. It is known from our previous studies, this polymer shows electrocatalytic effect (Gülce et al., 1997; Sönmez Çelebi et al., 2008a, b).

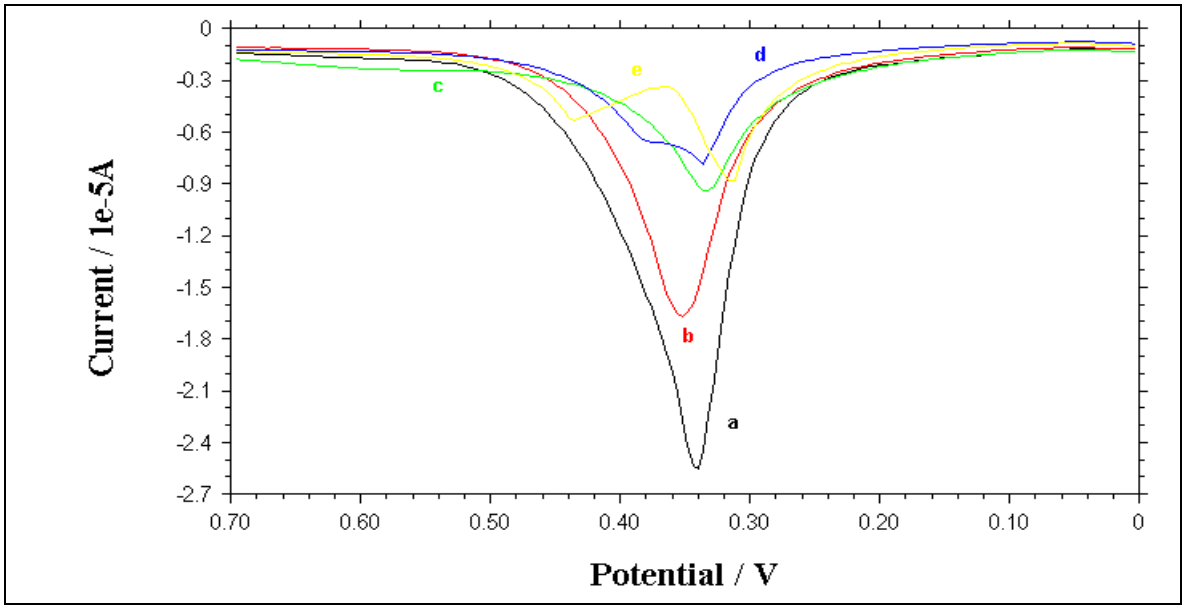

Figure 9.19. DPVs of (a) $PVF^{+}ClO_4^{-}$ film (b) $PVF^{+}ClO_4^{-}$ film after 15 minutes DNA immobilization (c) $PVF^{+}ClO_4^{-}$ film after 30 minutes DNA immobilization (d) $PVF^{+}ClO_4^{-}$ film after 1 hour DNA immobilization (e) $PVF^{+}ClO_4^{-}$ film after 2 hours DNA immobilization in 50 mM PBS containing 0.1 M $NaClO_4$. Pulse amplitude: 50 mV.

9.3.4. The effect of buffer solution

The effect of various concentrations of pH 7.0 PBS containing 0.1 M $NaClO_4$ on the response of the electrode was investigated by using $PVF^+ClO_4^-$ and dsDNA immobilized PVF^+ electrodes. Buffer concentrations varying from 10 mM to 125 mM were used in the experiments. 0.1 mC polymeric film thickness was used. The immersion time in 2.5 mg mL^{-1} dsDNA solution was 1 hour. Firstly, CV of the $PVF^+ClO_4^-$ film in buffer solutions was recorded after it had immersed in buffer solutions with different concentrations for 1 hour. Then CV of dsDNA immobilized electrode was recorded for each buffer concentration. It was determined that the oxidation peak current of the dsDNA immobilized polymer decreased with increasing phosphate buffer concentration. The changes in oxidation peak current are given in Figure 9.20. After the concentration value of 50 mM was reached, the decrease in oxidation peak current value did not change appreciably. PBS concentrations lower than 50 mM gave relatively poor results because of the insufficient buffer capacity. Thus, it was concluded that the polymeric structure reached its saturation level at this concentration value. The related histograms are also given in Figure 9.21.

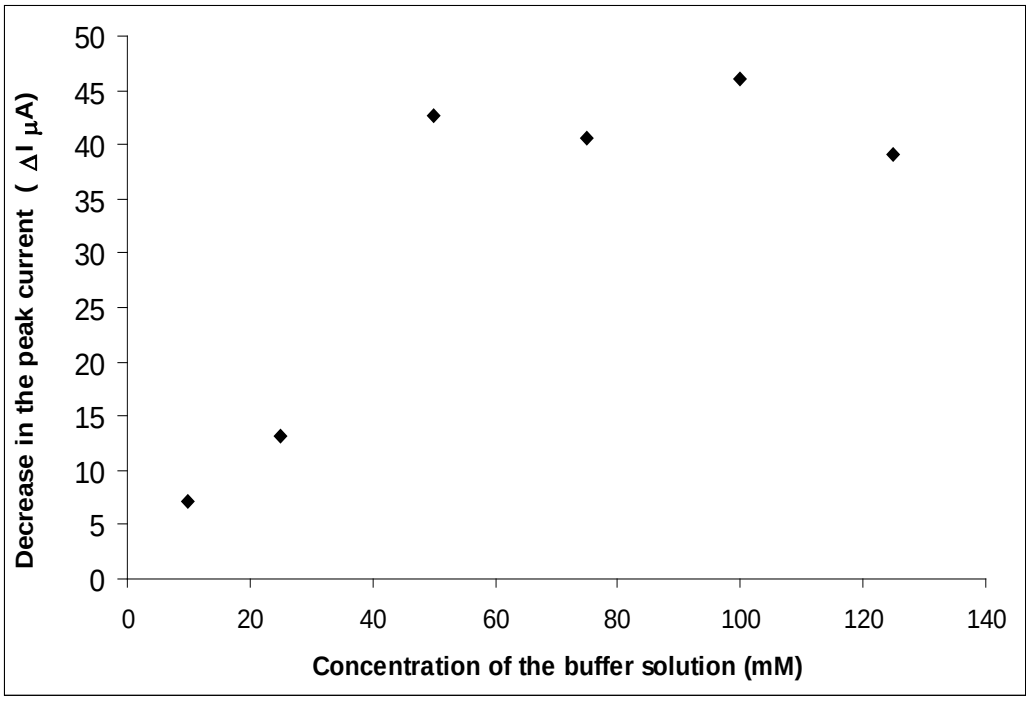

Figure 9.20. The change in oxidation peak current between polymer electrode and dsDNA immobilized polymer electrode with different concentrations of PBS.

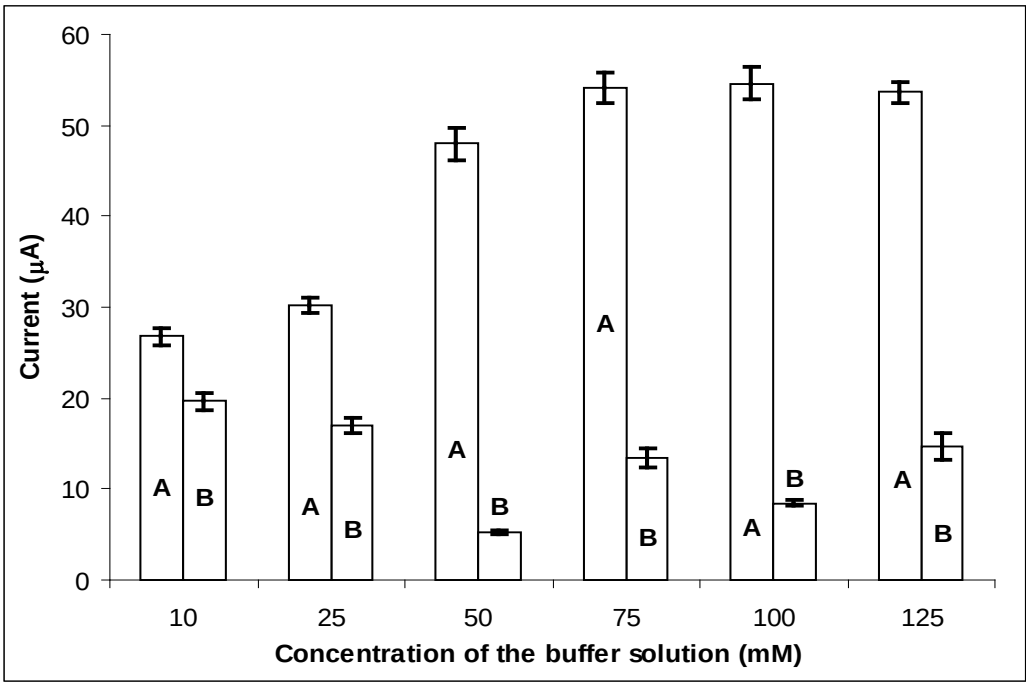

Figure 9.21. Histograms of oxidation peak currents of the polymer at different PBS concentrations: Responses of the polymer electrode (A), dsDNA immobilized polymer electrode (B)**.**

The response of this modified electrode was also examined using 50 mM acetate (ABS, pH 4.8) and 50 mM borate (BBS, pH 9.0) buffer solutions in order to compare the electrode performance at the same concentration level of PBS. The CVs of (a) $PVF^{+}ClO_4^{-}$ film, (b) $PVF^{+}ClO_4^{-}$ film after immersing into 2.50 mg mL^{-1} dsDNA solution in PBS, BBS and ABS are given in Figures 9.22, 9.23 and 9.24, respectively. It was found that the decrease at the oxidation peak current of polymer was found in a higher ratio by using PBS in comparison to the ones by using ABS and BBS. The decrease % at the response of dsDNA immobilized polymer modified electrode was calculated as 89.1 % in PBS, 66.9 % in BBS and 56.1 % in ABS. Due to the significant decrease obtained by using PBS, experiments were then performed using PBS in similiar to the ones in the literature (Saudi et al., 2000).

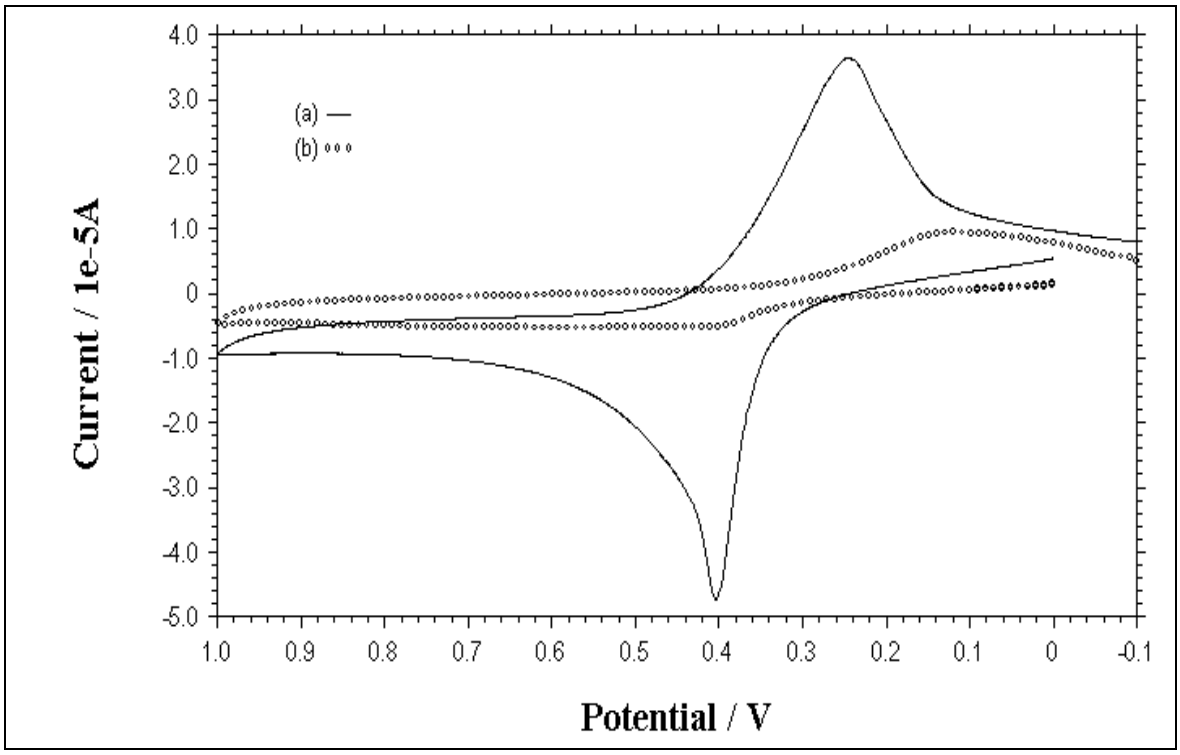

Figure 9.22. CVs of (a) $PVF^{+}ClO_4^{-}$ film (b) $PVF^{+}ClO_4^{-}$ film after immersing into dsDNA solution in 50 mM PBS containing 0.1 M $NaClO_4$. Scan rate: 100 mV s^{-1}.

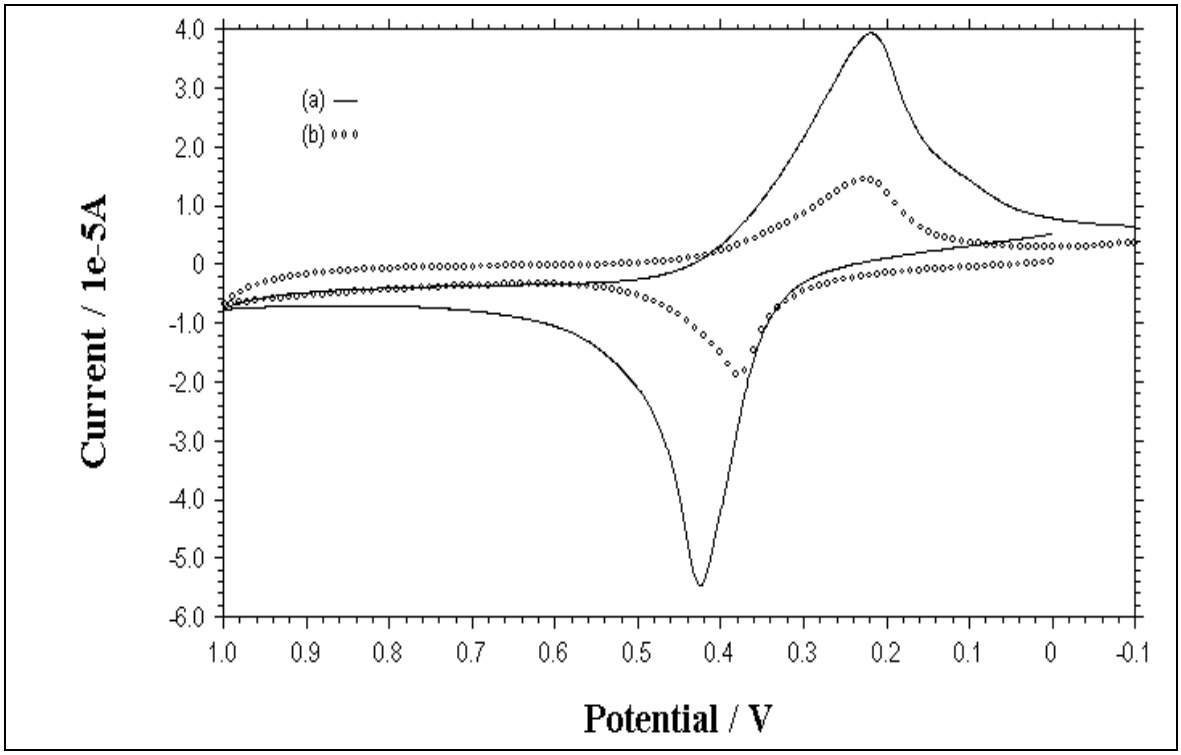

Figure 9.23. CVs of (a) $PVF^{+}ClO_4^{-}$ film (b) $PVF^{+}ClO_4^{-}$ film after immersing into dsDNA solution in 50 mM BBS containing 0.1 M $NaClO_4$. Scan rate: 100 mV s^{-1}.

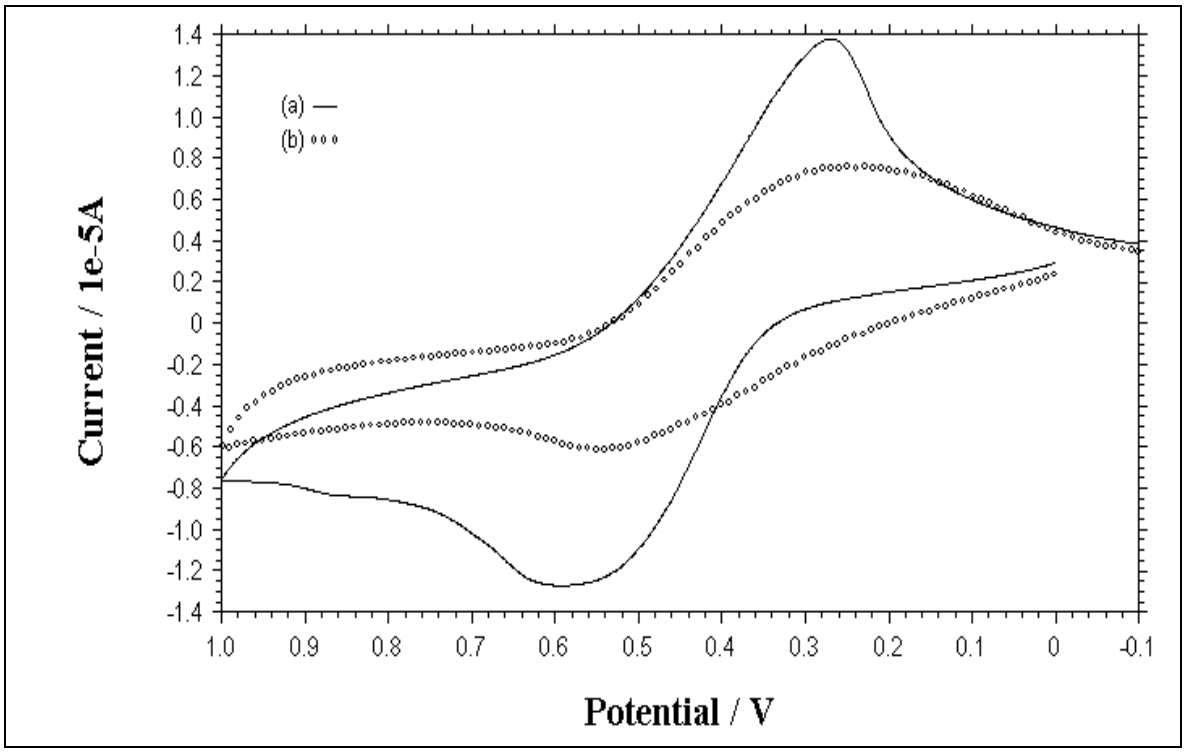

Figure 9.24. CVs of (a) $PVF^{+}ClO_4^{-}$ film (b) $PVF^{+}ClO_4^{-}$ film after immersing into dsDNA solution in 50 mM ABS. Scan rate: 100 mV s^{-1}.

9.3.5. The effect of the concentration of perchlorate ion

To investigate the effect of the perchlorate ion concentration on the response of the electrode, $PVF^{+}ClO_4^{-}$ film at 1.0 mC polymeric film thickness was electrodeposited on Pt electrode surface. The concentration of dsDNA solution was 2.5 mg mL^{-1} in each of the study. Also, phosphate buffer solution was 50 mM at pH 7.0. Perchlorate ion concentrations varying from 0.025 M to 0.150 M were used in the experiments. The CVs of (a) $PVF^{+}ClO_4^{-}$ film, (b) $PVF^{+}ClO_4^{-}$ film after immersing into dsDNA solution in PBS containing 0.025 M and 0.100 M perchlorate ion are given in Figures 9.25 and 9.26, respectively.

As shown in Figure 9.27, the decrease in the oxidation peak currents of the polymer (ΔI) increased up to a concentration value of 0.100 M. After this concentration value, the decrease in the oxidation peak currents of the polymer decreased slowly. The optimum perchlorate ion concentration was obtained as 0.100 M for the suitable ionic strength. The related histograms are also given in Figure 9.28.

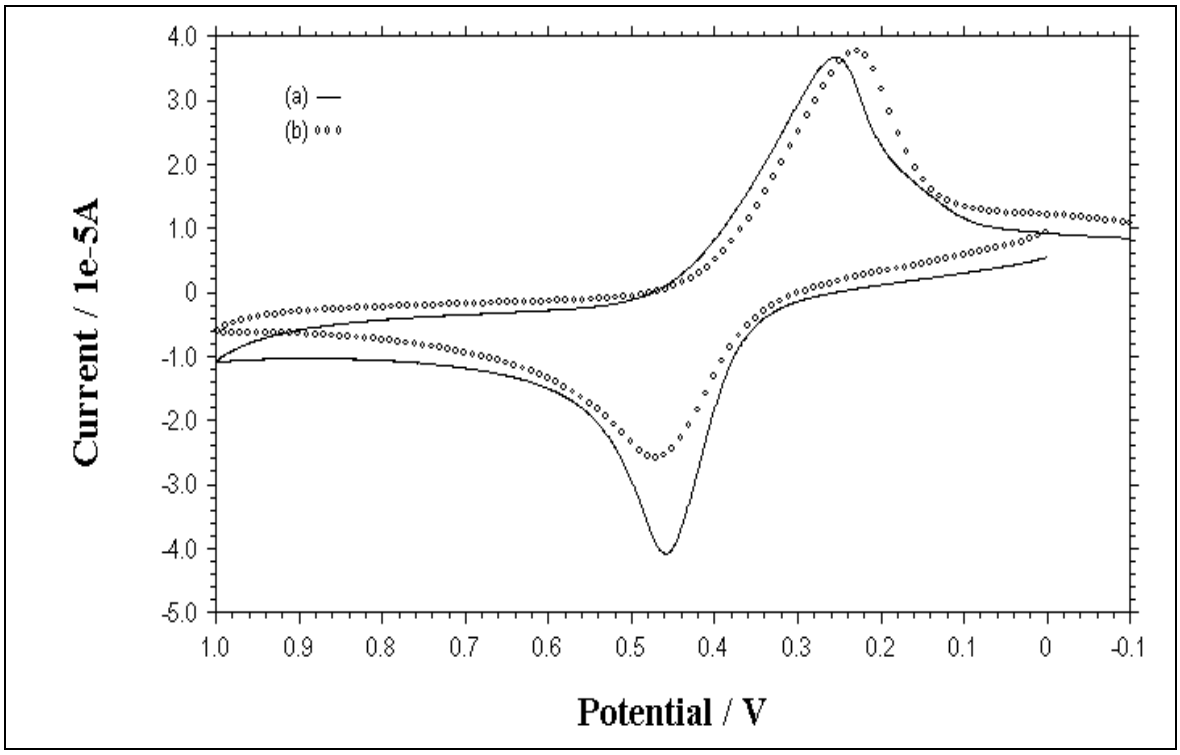

Figure 9.25. CVs of (a) $PVF^{+}ClO_4^{-}$ film (b) $PVF^{+}ClO_4^{-}$ film after immersing into dsDNA solution in 50 mM PBS containing 0.025 M perchlorate ion. Scan rate: 100 mV s^{-1}.

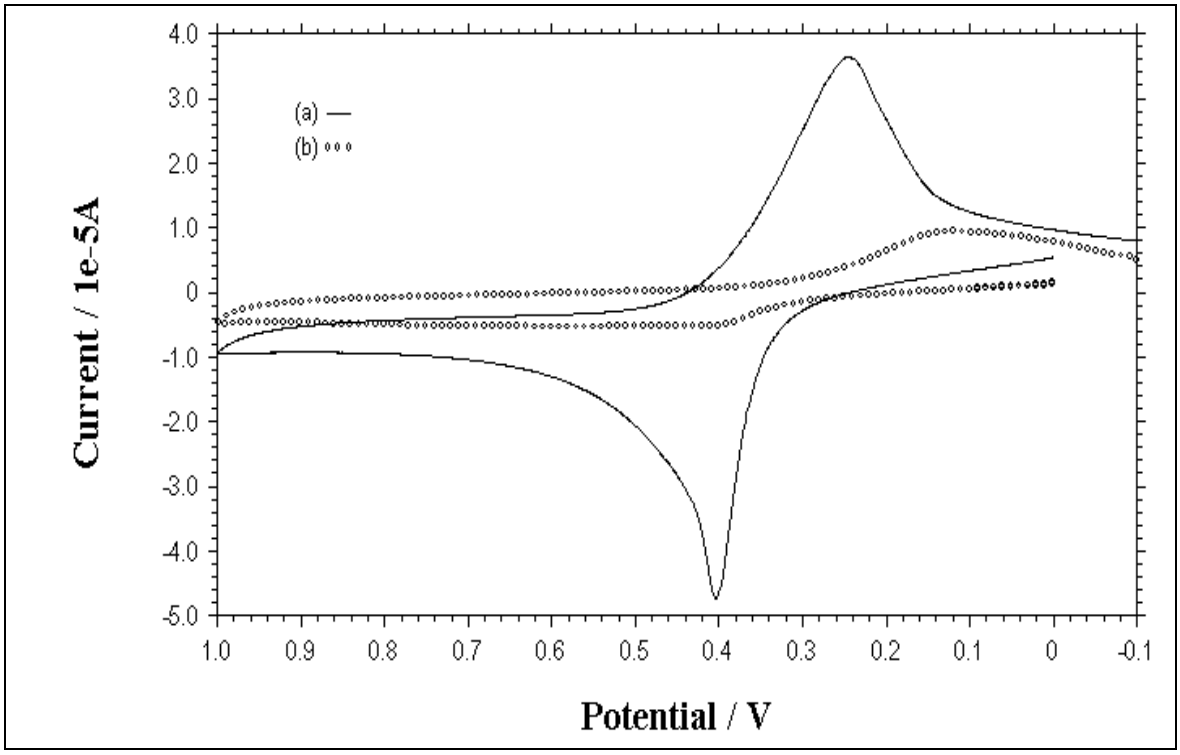

Figure 9.26. CVs of (a) $PVF^{+}ClO_4^{-}$ film (b) $PVF^{+}ClO_4^{-}$ film after immersing into dsDNA solution in 50 mM PBS containing 0.100 M perchlorate ion. Scan rate: 100 mV s^{-1}.

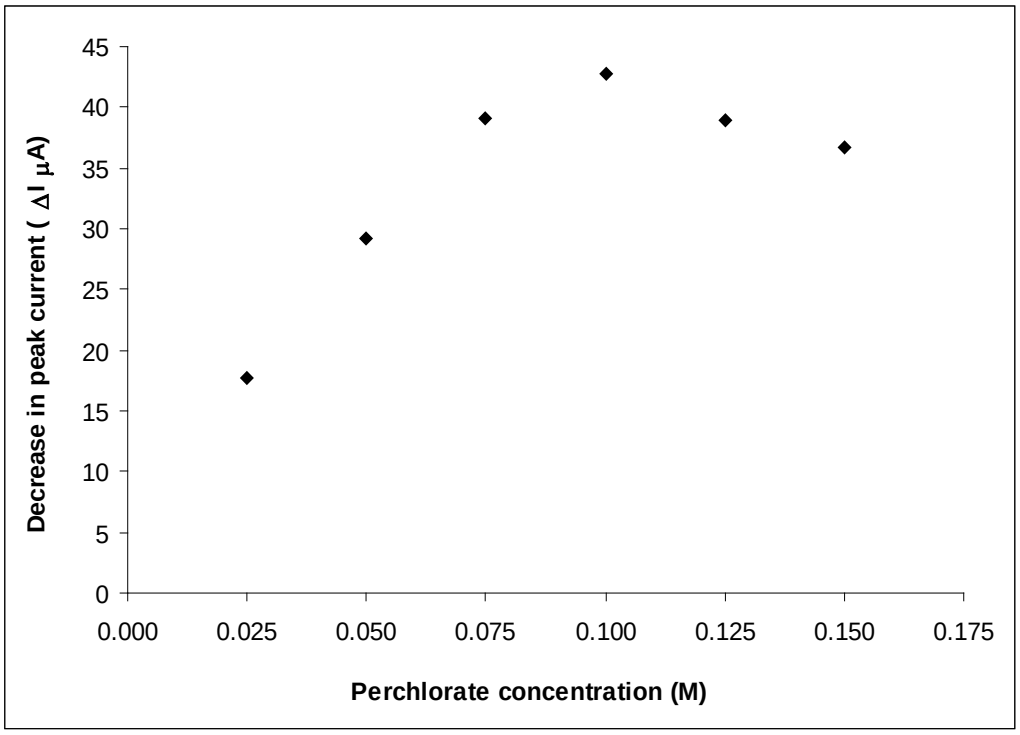

Figure 9.27. The change in oxidation peak current between polymer electrode and dsDNA immobilized polymer electrode with various perchlorate ion concencentrations.

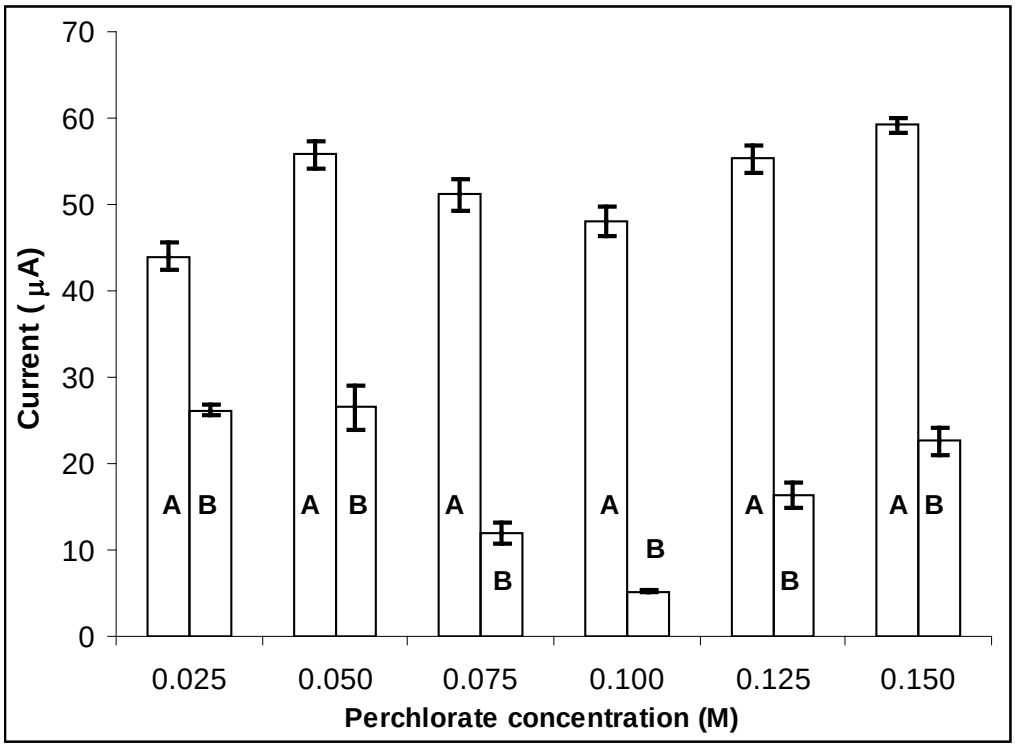

Figure 9.28. Histograms of oxidation peak currents of the polymer at various perchlorate ion concentrations: Responses of the polymer electrode (A), dsDNA immobilized polymer electrode (B).

9.3.6. The effect of pH of the medium

The effect of pH on the response of this biosensing system was determined using 50 mM PBS containing 0.1 M $NaClO_4$ at 1.0 mC polymeric film thickness with 1 hour immersion in 2.5 mg mL^{-1} dsDNA solution at a pH range of 6.0 to 9.0 (Figure 9.29a). A blank experiment (without dsDNA) in the same pH range was also carried out for polymer modified electrode and these points were also included in the same figure (Figure 9.29b). As seen from these results the most decrease in oxidation peak of the polymer was obtained at pH 7.0, which was chosen as optimum pH for further experiments. The related histograms are also given in Figure 9.30.

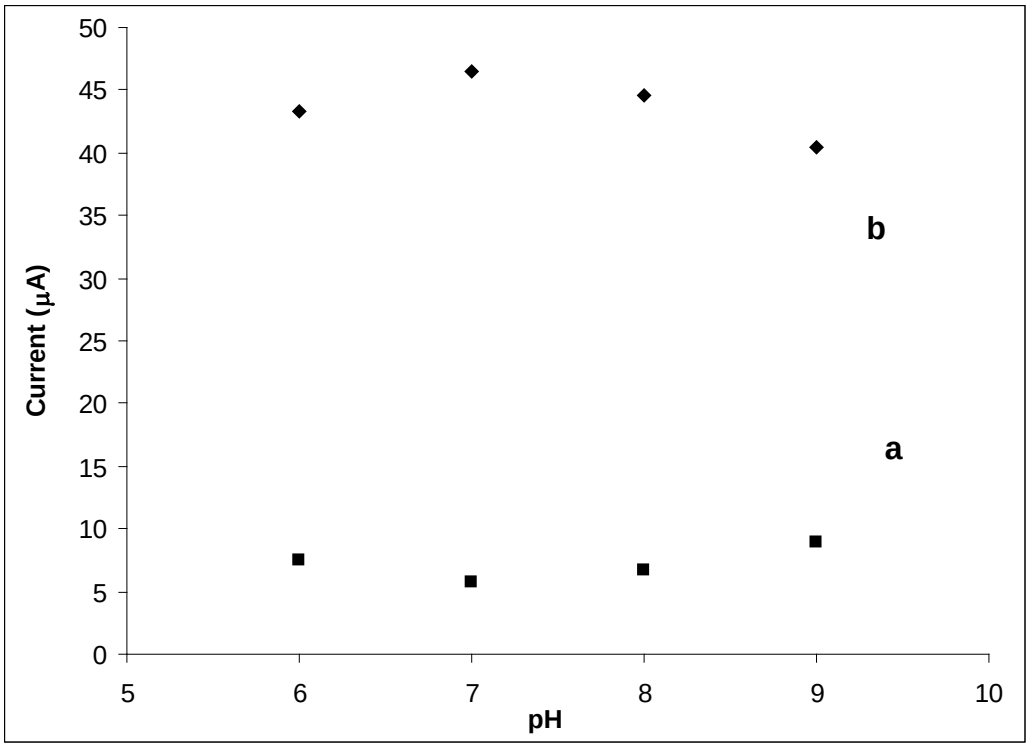

Figure 9.29. The effect of pH on the response of (a) dsDNA immobilized polymer film (b) polymer film.

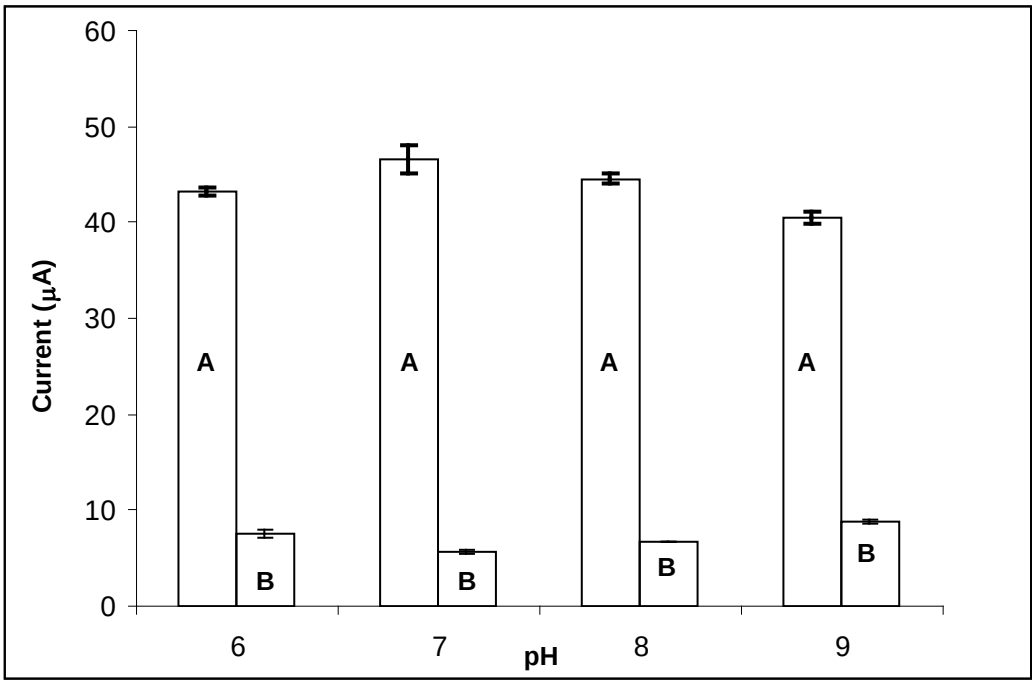

Figure 9.30. Histograms of oxidation peak currents of the polymer at different pH values: Responses of the polymer electrode (A), dsDNA immobilized polymer electrode (B)**.**

9.3.7. The effect of temperature of the medium

The effect of temperature on the response of the polymer electrode and dsDNA immobilized polymer electrode was determined using 50 mM PBS containing 0.1 M $NaClO_4$ at pH 7.0. The polymeric film thickness corresponded to 1.0 mC and dsDNA solution was 2.5 mg mL^{-1} for each experiment. The response of the electrodes was measured at a temperature range of 15 and 45 °C. Firstly, CV of the $PVF^+ClO_4^-$ film was recorded at constant temperature after it had immersed in buffer solution for 1 hour. Then CV of dsDNA immobilized electrode was recorded. As seen in Figure 9.31, the maximum decrease in oxidation peak current (ΔI) so the interaction of the positively charged matrix with the negatively charged DNA biomolecule was obtained at 30 °C. Thus, further experiments were carried out at room temperature which is nearly equal to 30 °C. The CVs of (a) $PVF^+ClO_4^-$ film, (b) $PVF^+ClO_4^-$ film after immersing into dsDNA solution in PBS containing 0.1 M $NaClO_4$ at 25, 30 and 35 °C are given in Figures 9.32, 9.33 and 9.34, respectively.

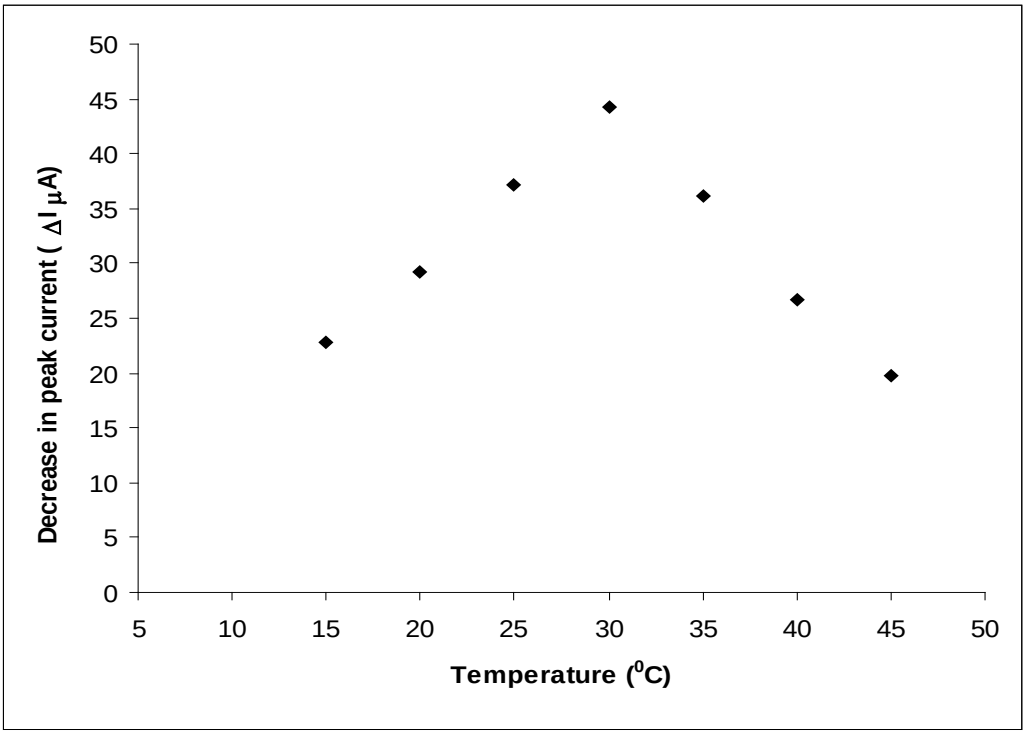

Figure 9.31. The change in oxidation peak current between polymer electrode and dsDNA immobilized polymer electrode at different temperature values.

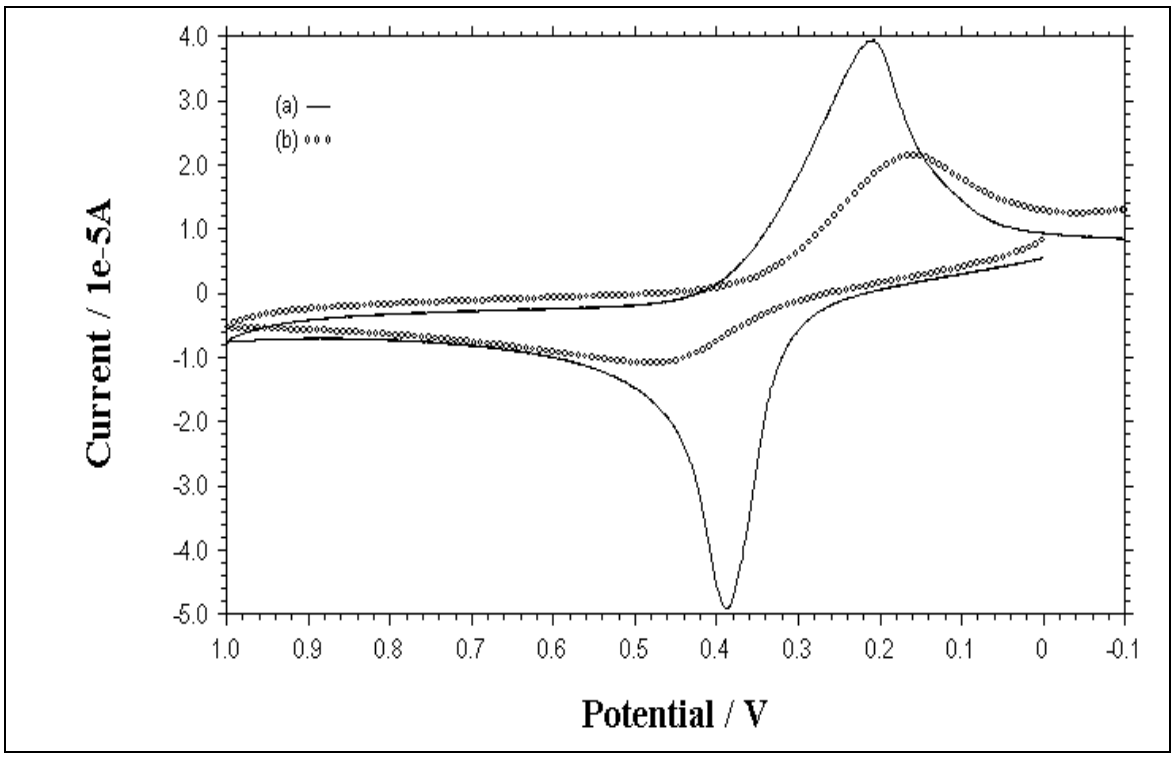

Figure 9.32. CVs of (a) $PVF^{+}ClO_4^{-}$ film (b) $PVF^{+}ClO_4^{-}$ film after immersing into dsDNA solution in 50 mM PBS containing 0.1 M $NaClO_4$ at 25 °C. Scan rate: 100 mV s^{-1}.

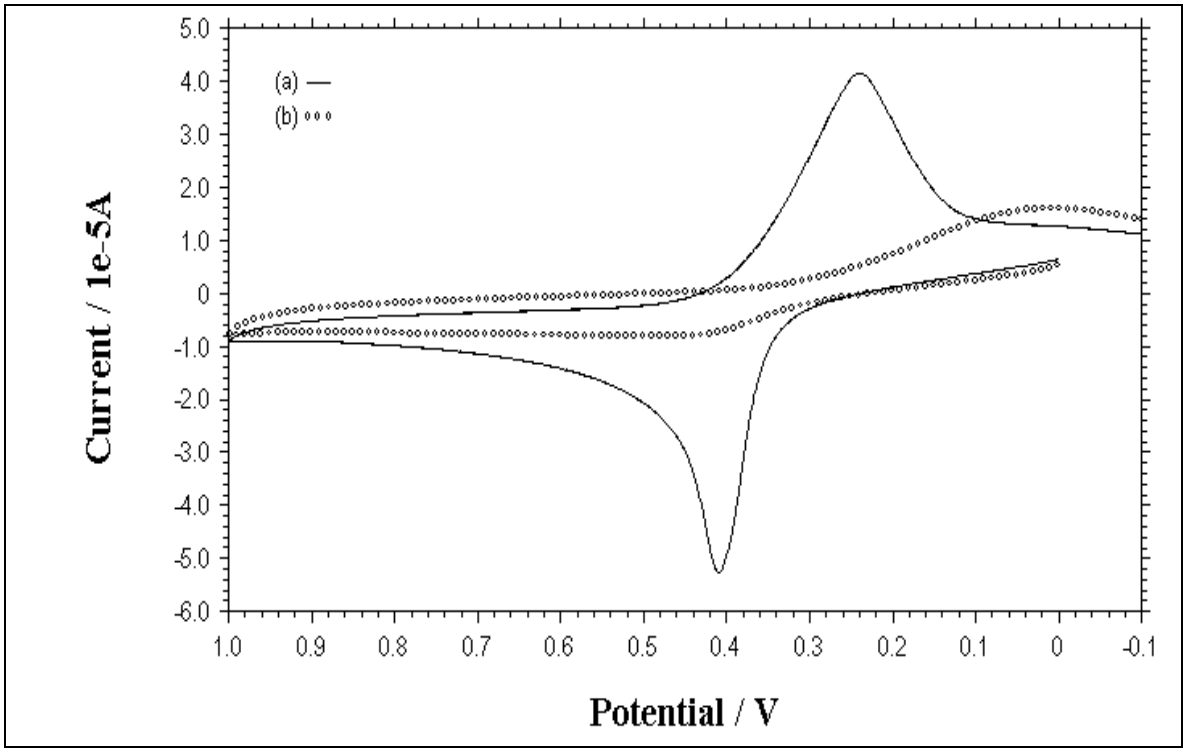

Figure 9.33. CVs of (a) $PVF^{+}ClO_4^{-}$ film (b) $PVF^{+}ClO_4^{-}$ film after immersing into dsDNA solution in 50 mM PBS containing 0.1 M $NaClO_4$ at 30 °C. Scan rate: 100 mV s^{-1}.

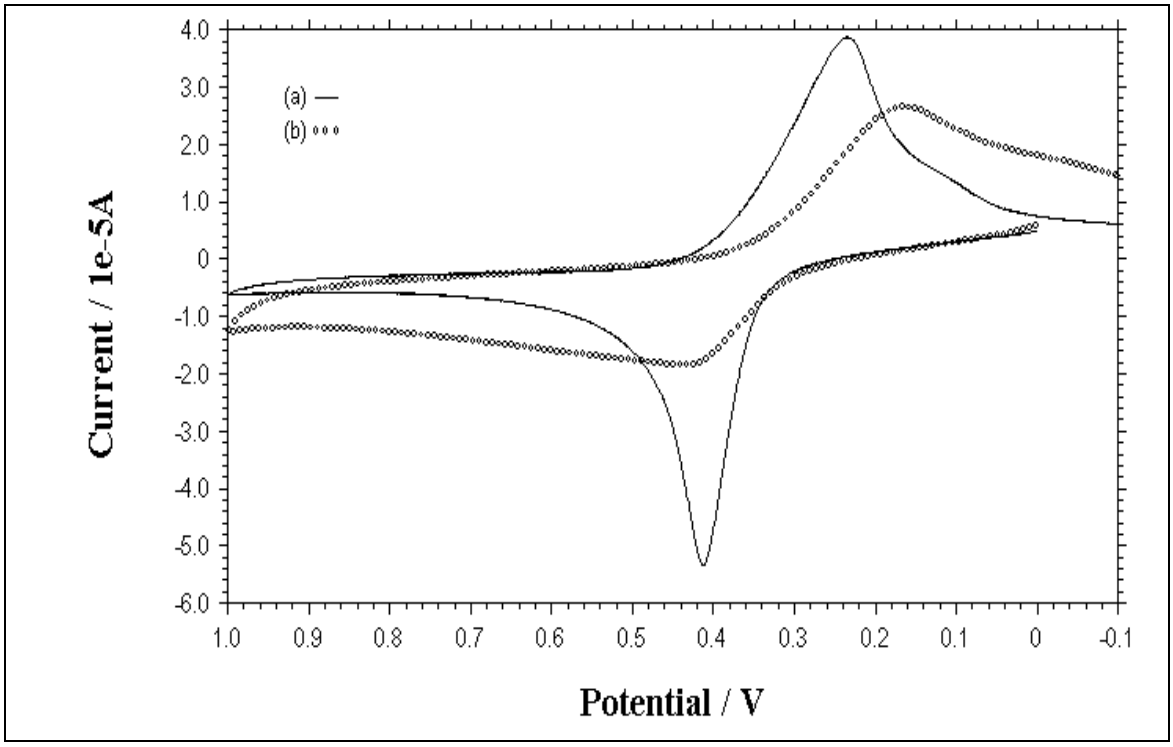

Figure 9.34. CVs of (a) $PVF^{+}ClO_4^{-}$ film (b) $PVF^{+}ClO_4^{-}$ film after immersing into dsDNA solution in 50 mM PBS containing 0.1 M $NaClO_4$ at 35 °C. Scan rate: 100 mV s^{-1}.

9.3.8. Release behavior of the polymer

The electrostatic interaction between negatively charged DNA and positively charged polymer matrix were examined. Firstly, the Pt electrode was modified with $PVF^{+}ClO_4^{-}$ film. Then, dsDNA was immobilized onto modified surface as described before. After modification of dsDNA, the polymer surface was hold on +0.2 V vs. Ag/AgCl in ABS. At the end of this procedure the PVF^{+} system reduced to PVF (Gülce et al., 1995a, 1997) by releasing the negatively charged biomolucule into the buffer solution. The solution which presumably contained dsDNA due to releasing procedure described above was tested with DPV using Au and PG electrodes. The electrochemical behaviors of ABS and dsDNA in ABS at Au electrode are shown in Figure 9.35a and Figure 9.35b, respectively. As can be seen from this figure, there are two signals at +1.0 V vs. SCE and +1.2 V vs. SCE which can be predicted to belong to the electroactive DNA bases, guanine and adenine or their adducts reported in the similar studies (Kerman et al., 2003; Chen et al., 2007). The electrochemical behaviors of ABS and dsDNA in ABS at PG electrode are shown in Figure 9.36a and Figure 9.36b, respectively. As seen from the figure, a well-defined peak observed at +1.06 V and a small peak at +0.76 V was measured because of dsDNA released from PVF structure. Thus, it can be concluded that negatively charged dsDNA could release from the neutral form of the polymer to the buffer solution. These electrochemical experiments showed that there was an electrostatic interaction between dsDNA and PVF^{+} molecule.

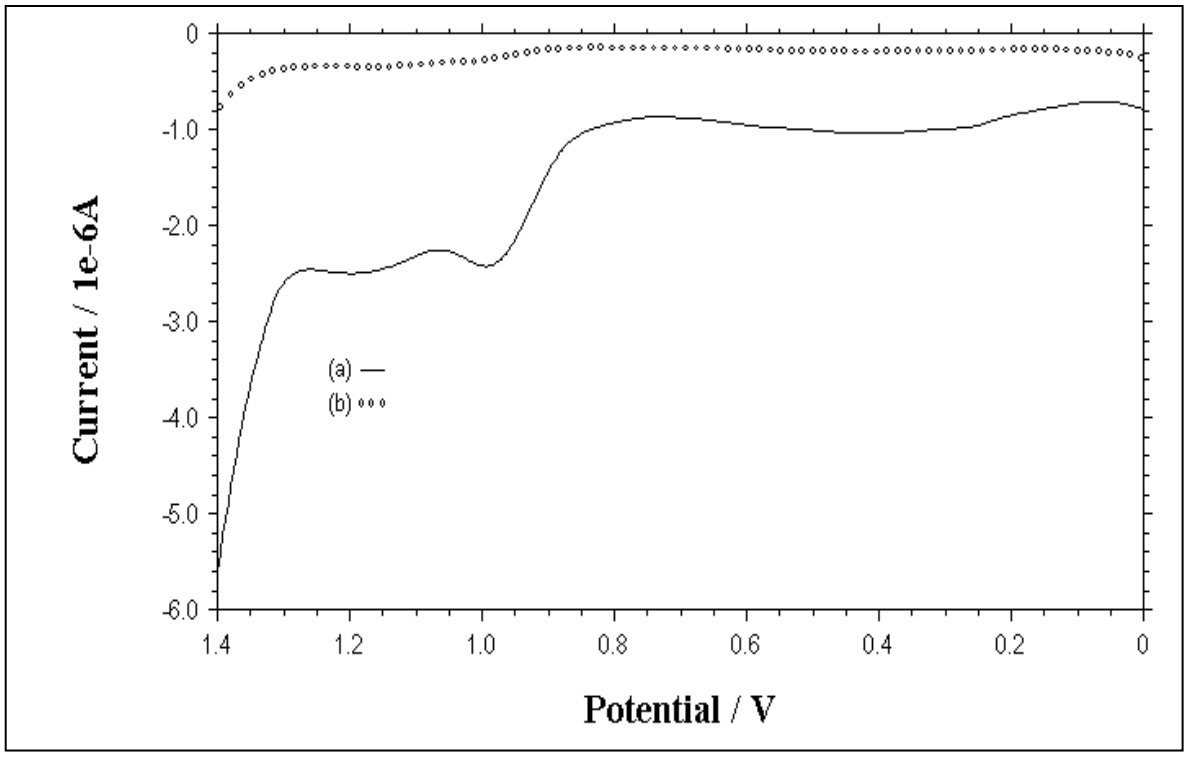

Figure 9.35. The electrochemical behavior of Au electrode in 50 mM ABS (a) with dsDNA (b) without dsDNA. Pulse amplitude: 50 mV.

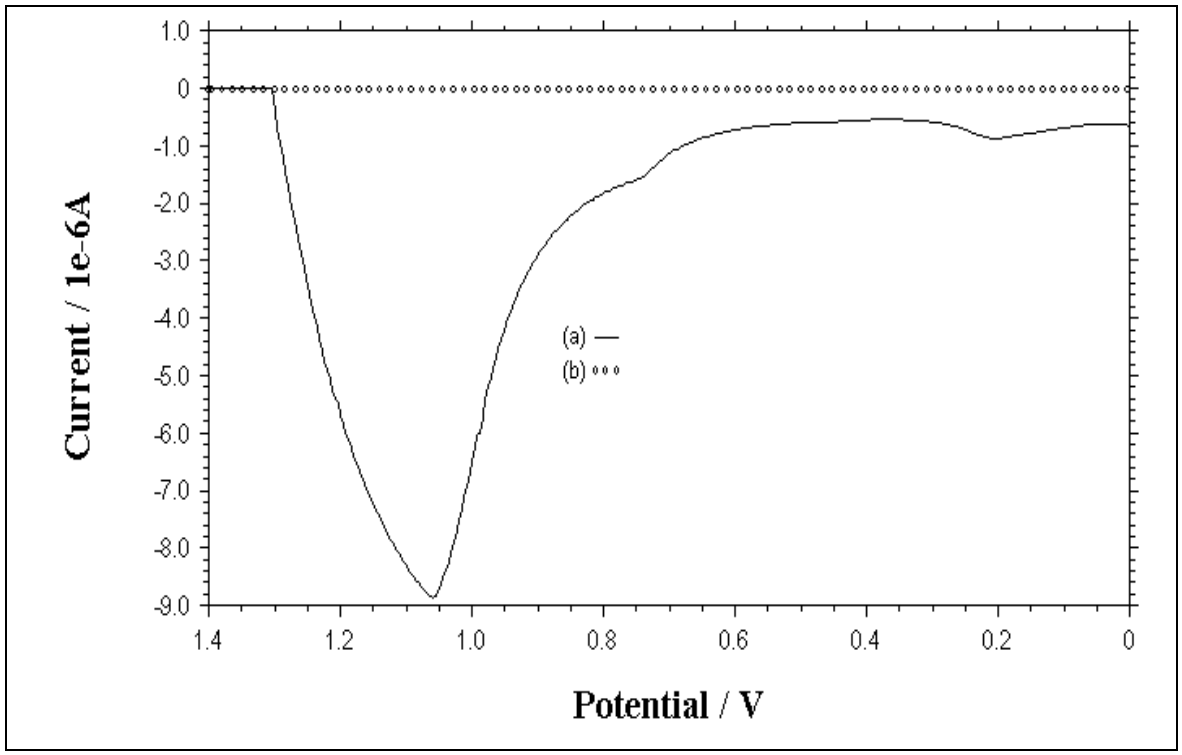

Figure 9.36. The electrochemical behavior of PGE electrode in 50 mM ABS (a) with dsDNA (b) without dsDNA. Pulse amplitude: 50 mV.

9.3.9. The comparison of electrochemical behavior of dsDNA and ssDNA immobilized polymer modified electrodes

The electrochemical behaviors of dsDNA and ssDNA immobilized polymer electrodes were also investigated for further applications. The voltammograms obtained by polymer, ssDNA immobilized polymer and dsDNA immobilized polymer electrodes in 50 mM PBS containing 0.1 M $NaClO_4$ at pH 7.0 are given in Figures 9.37a, b, c and 9.38a, b, c, respectively. The polymeric film thickness corresponded to 1.0 mC, immobilization time was 1 hour and DNA solution was 2.5 mg mL^{-1} for each experiment. The decrease in oxidation peak current of polymer was calculated as 88.5 % from the response of dsDNA immobilized polymer modified electrode, on the otherhand, this decrease was found as 61.8 % by using ssDNA immobilized polymer modified electrode (Figure 9.39). Thus, it was observed that dsDNA could incorporated easier into the positively charged polymeric matrix in comparison to ssDNA. The interaction between dsDNA and the positively charged polymer matrix is stronger than the one between ssDNA and polymer matrix. There was a peak observed at about +1.28 V vs. SCE, which reflected the oxidation signal of adenine in the CV of dsDNA immobilized polymer modified electrode as seen in Figure 9.37c in parallel to the reported results (Chen et al., 2007). Similiarly, the peaks were also appeared at about +1.30 V and +1.22 V vs. SCE, respectively in the DPVs of ssDNA and dsDNA immobilized polymer electrodes (Figure 9.38b and c).

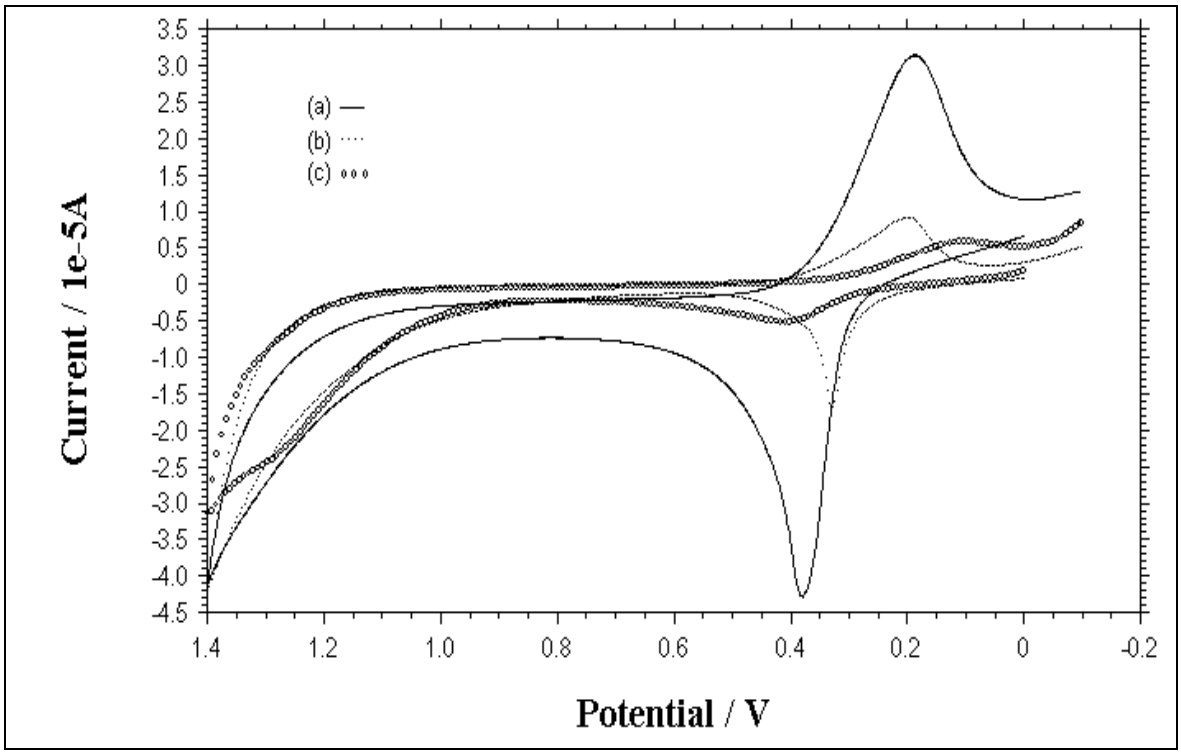

Figure 9.37. CVs of (a) $PVF^{+}ClO_4^{-}$ film (b) $PVF^{+}ClO_4^{-}$ film after immersing into ssDNA solution (c) $PVF^{+}ClO_4^{-}$ film after immersing into dsDNA solution in 50 mM PBS containing 0.1 M $NaClO_4$. Scan rate: 100 mV s^{-1}.

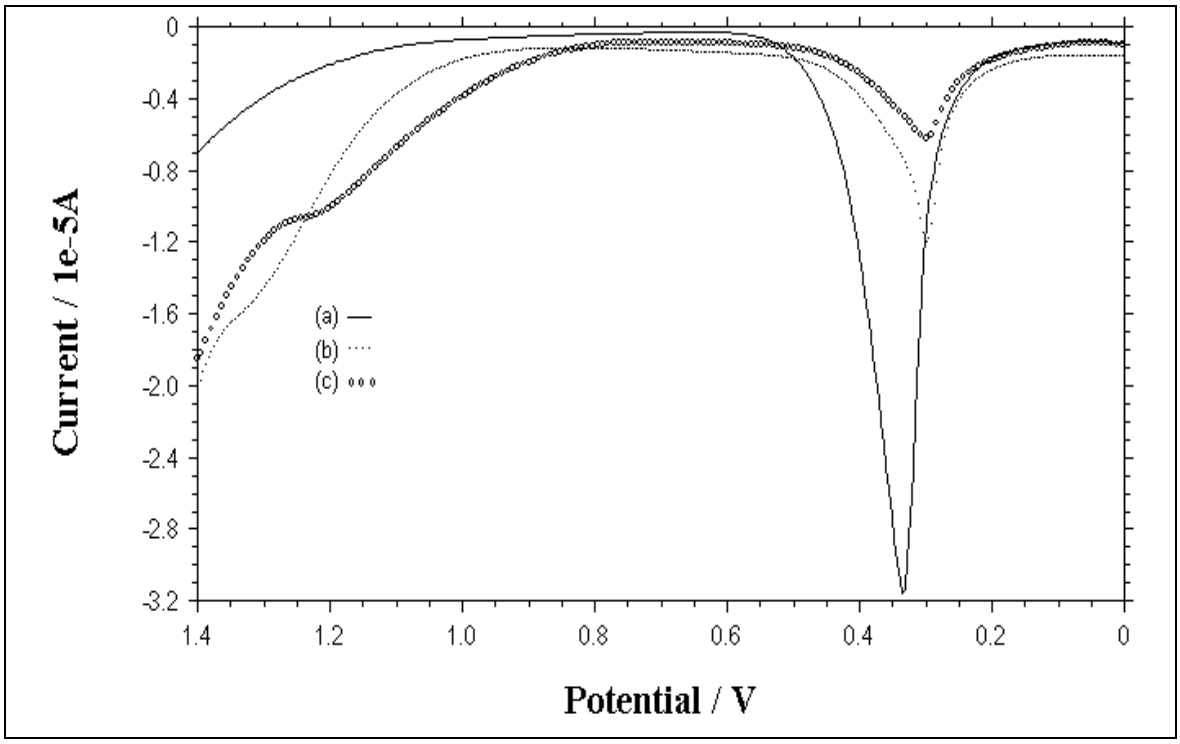

Figure 9.38. DPVs (a) $PVF^{+}ClO_4^{-}$ film (b) $PVF^{+}ClO_4^{-}$ film after immersing into ssDNA solution (c) $PVF^{+}ClO_4^{-}$ film after immersing into dsDNA solution in 50 mM PBS containing 0.1 M $NaClO_4$. Pulse amplitude: 50 mV.

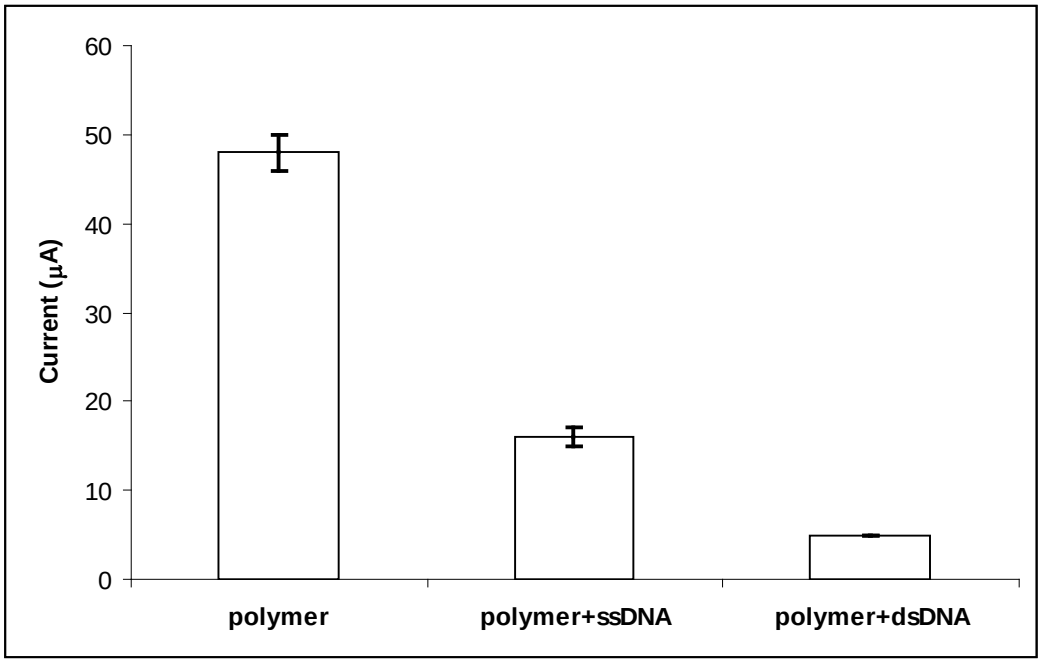

Figure 9.39. Histograms showing the oxidation peak currents of polymer electrode in the absence or presence of ssDNA or dsDNA.

9.3.10. Application of the polymer modified electrode

Probe ODN immobilized polymer electrode was prepared dropping the ODN solution onto the polymer modified Pt electrode surface with a polymeric film thickness of 1.0 mC. The electrode was kept for 1 hour before electrochemical measurements. This working electrode is named as probe. For hybridization target, NC and MM ODN solutions were dropped onto the probe and kept for 1 hour. After immobilization of nucleic acid onto the polymer electrode, the electrode was washed by using PBS for 10 seconds. The oxidation peak current of polymer, and electroactive DNA base, adenine, were measured by using DPV scanning between +0.0 V and +1.4 V vs. SCE at pulse amplitude of 50 mV. Firstly, oxidation peak current of probe and then target, NC and MM immobilized probe were measured.

The effect of different ODN modifications on the response of this DNA sensing method after ODN immobilization step was examined with different ODNs in respect to their binding performance onto the positively charged polymer matrix. The changes at the oxidation peak current of polymer with 100 μg mL^{-1} thiol linked, amino linked, phosphate linked and unmodified ODNs are given

respectively in Figure 9.40a, b, c, d. The maximum decrease in the oxidation peak current and consequently, the maximum interaction with positively charged matrix was obtained with thiol linked ODN because of the higher electronegativity of thiol group comparison to other groups. Thus, thiol linked ODN was chosen for the further experiments in order to obtain higher sensitivity and selectivity by using DNA immobilized polymer modified electrode.

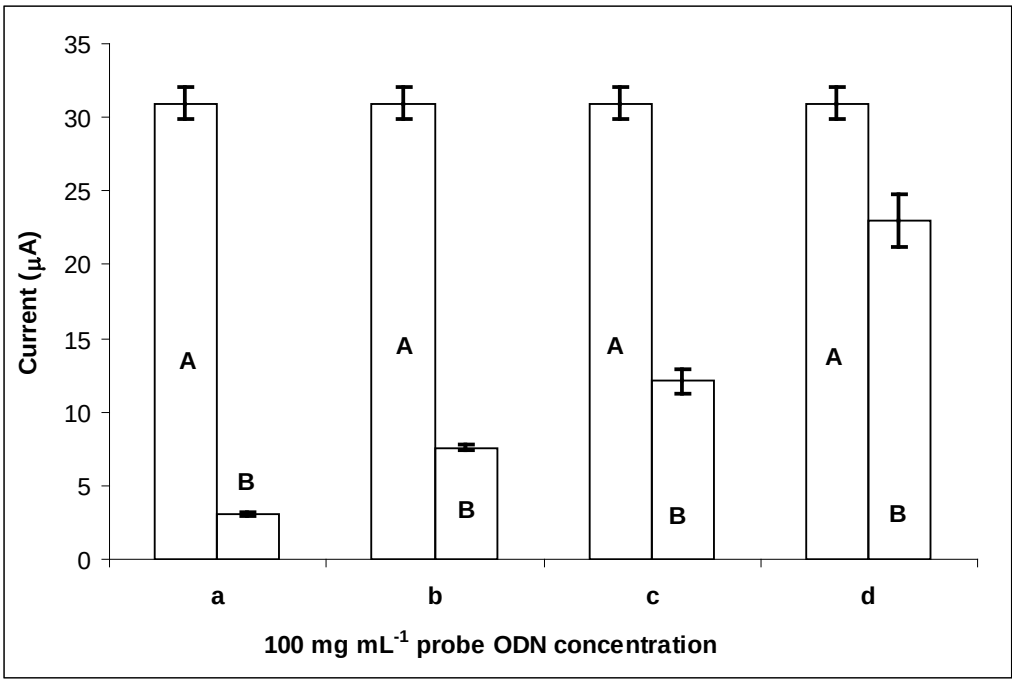

Figure 9.40. Histograms showing the changes at the oxidation peak current of polymer in the absence (A) and the presence (B) of ODNs; (a) thiol linked ODN, (b) amino linked ODN, (c) phosphate linked ODN, (d) unmodified ODN.

9.3.10.1. Hybridization studies carried out with thiol linked probe

The effect of thiol linked ODN concentration on the oxidation peak currents of polymer and DNA base, adenine, was studied in various ODN concentration from 25 to 170 μg mL^{-1}. The oxidation peak current of the polymer was decreased gradually and then levelled off, when the concentration of ODN was increased to 150 μg mL^{-1} (Figure 9.41 shown with P). On the other hand, the adenine oxidation peak current was increased and then levelled off (Figure 9.41 shown with A). The optimum immobilization concentration for 20-mer thiol linked ODN was found as 150 μg mL^{-1}. The DPVs at three different concentrations of thiol linked ODN were shown in Figure 9.42.

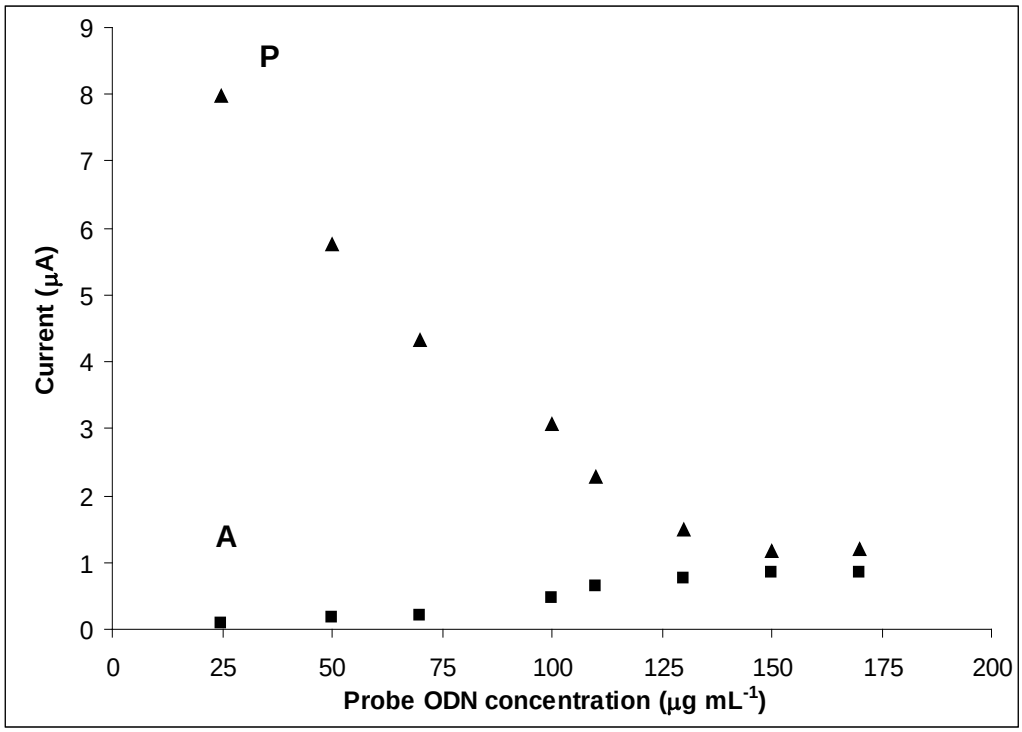

Figure 9.41. The effect of thiol linked ODN with various concentrations on the response coming from PVF^{+} and DNA. Plot showing both oxidation peak currents of polymer (P) and adenine (A).

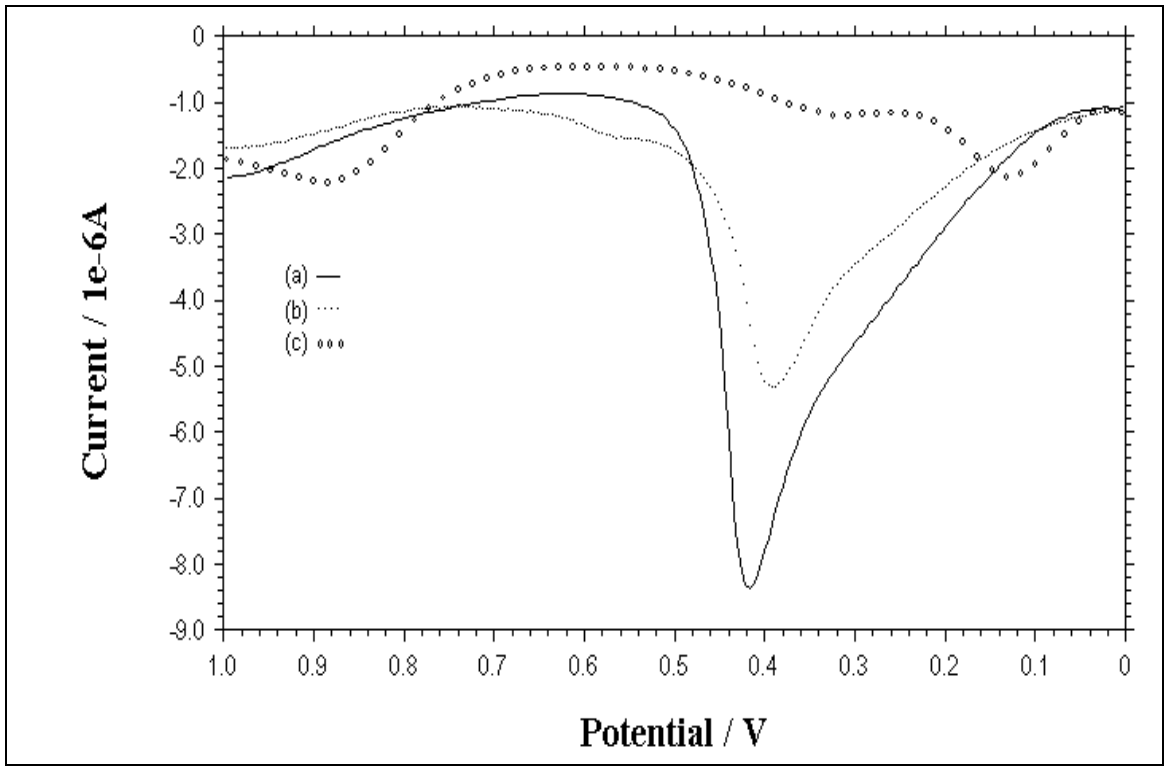

Figure 9.42. DPVs of (a) 25 μg mL^{-1} thiol linked ODN (b) 70 μg mL^{-1} thiol linked ODN (c) 150 μg mL^{-1} thiol linked ODN. Pulse amplitude: 50 mV.

For the application of DNA immobilized polymer modified electrode, an electrochemical sensing of DNA hybridization was studied. The changes at the oxidation peak current of the polymer were monitored in the presence of thiol linked probe alone and the hybridization between probe and target / NC / MM sequences, respectively (Figure 9.43a, b, c, d). The oxidation peak current of the polymer decreased as a result of DNA hybridization between probe and its complementary sequence, target (Figure 9.43a and b). Due to the specific binding of thiol linked probe with its complementary at polymer matrix, a significant decrease (58.4 %) at oxidation peak current of polymer was observed in the presence of DNA hybridization. The selectivity in hybridization of thiol linked probe with other ODNs, such as; NC and MM sequences was also checked (Figure 9.43c and d). A negligible decrease (3.4 % and 6.6 %, respectively) was obtained in the case of hybridization between probe and NC, or probe and MM similar to the results obtained in the literature (Sanchez-Pomales et al., 2007; Prabhakar et al., 2008a, b; Degefa and Kwak, 2008). Related histograms are also given as Figure 9.44.

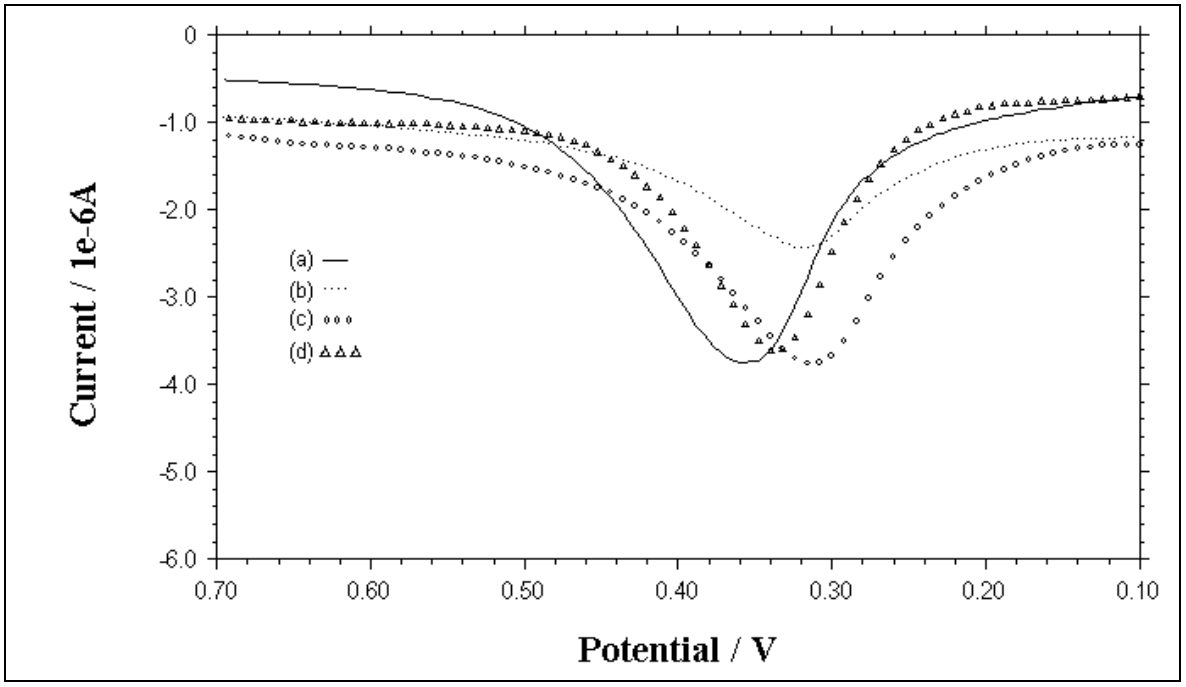

Figure 9.43. DPVs showing the oxidation peak of the polymer (a) 100 μg mL^{-1} probe alone, (b) after hybridization between probe and 100 μg mL^{-1} complementary, (c) interaction between probe and 100 μg mL^{-1} NC, (d) interaction between probe and 100 μg mL^{-1} MM. Pulse amplitude: 50 mV.

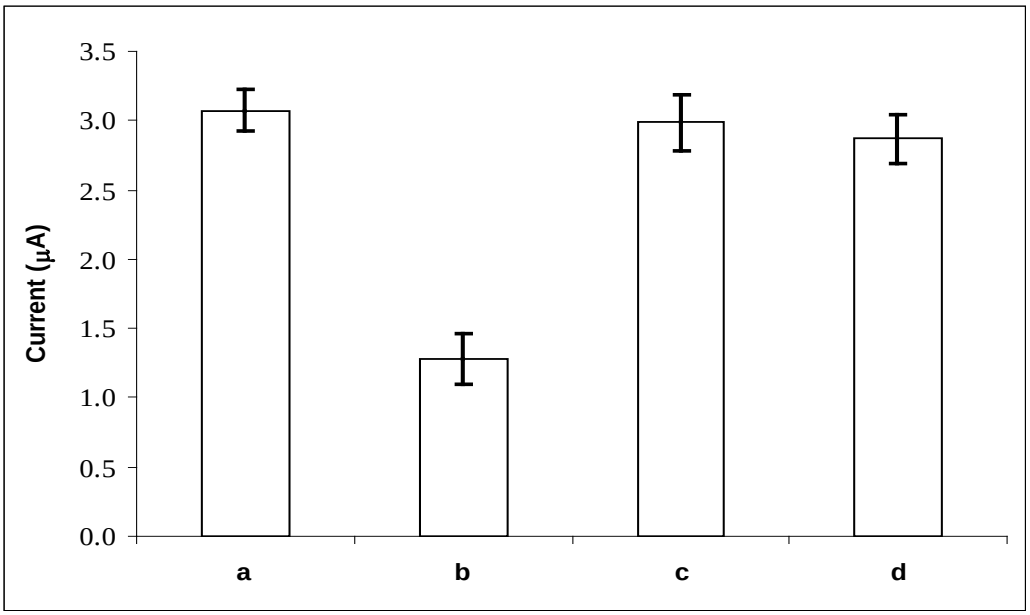

Figure 9.44. Histograms showing the oxidation peak current of the polymer (a) 100 μg mL^{-1} probe alone, (b) after hybridization between probe and 100 μg mL^{-1} complementary, (c) interaction between probe and 100 μg mL^{-1} NC, (d) interaction between probe and 100 μg mL^{-1} MM.

The effect of target concentration on the oxidation peak current of polymer was also studied in various target concentration from 25 to 150 μg mL^{-1}. The peak current decreased gradually and then levelled off, when the concentration of target was increased to 100 μg mL^{-1} (Figure 9.45).

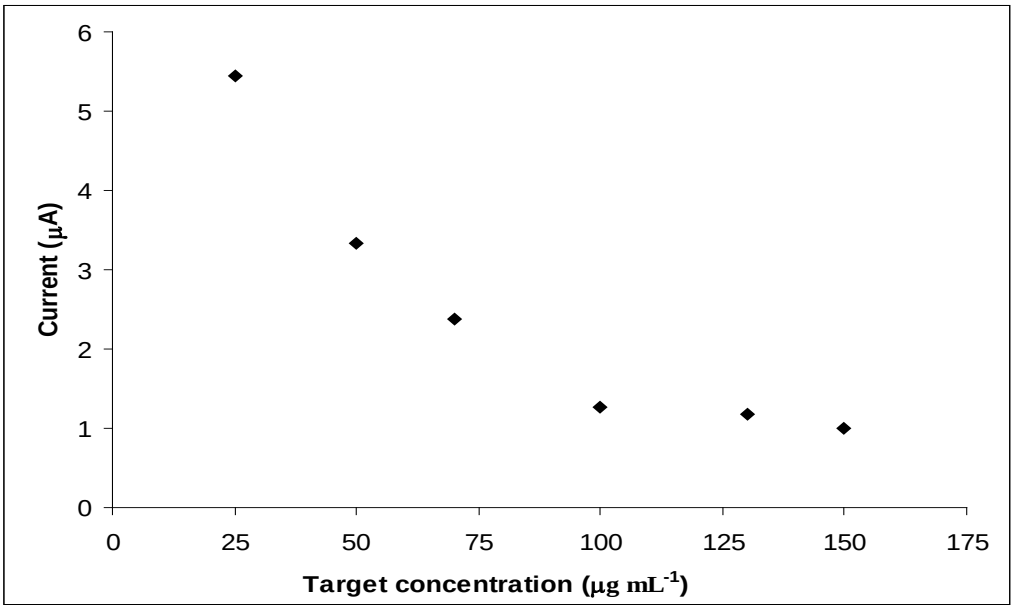

Figure 9.45. The effect of target concentration to the response of PVF^{+}.

9.3.10.2. Hybridization studies carried out with amino linked probe

The effect of 20-mer amino linked ODN concentration on the oxidation peak current of polymer was studied in various probe ODN concentration from 25 to 225 μg mL^{-1} (Figure 9.46). The oxidation peak current decreased gradually and then levelled off, when the concentration of ODN was increased to 175 μg mL^{-1}. The optimum concentration for 20-mer amino linked ODN was found as 175 μg mL^{-1}.

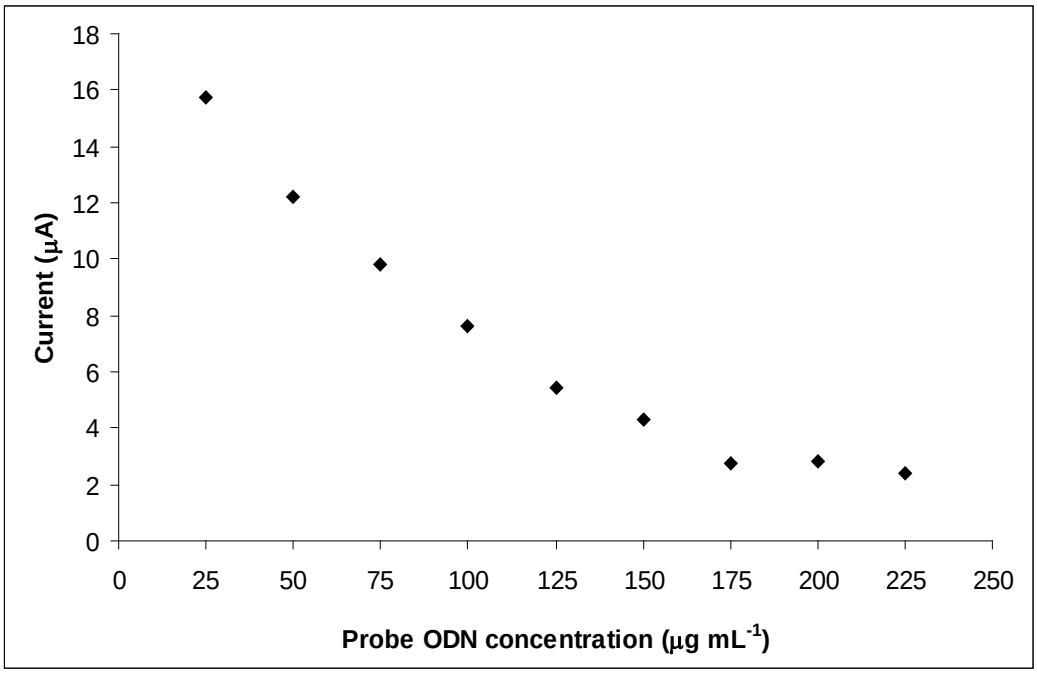

Figure 9.46. The effect of amino linked probe concentration to the response of PVF^{+}.

The detection of DNA hybridization was studied using amino linked probe. The changes at the oxidation peak current of the polymer were monitored in the presence of 100 μg mL^{-1} amino linked probe alone and the hybridization between probe and target / NC / MM sequence, respectively (Figure 9.47a, b, c, d). The oxidation peak current of the polymer decreased as a result of DNA hybridization between probe and its complementary sequence, target (Figure 9.47a and b). Due to the specific binding of amino linked probe with its complementary on polymer electrode, a significant decrease (45.5 %) at polymer response was observed in the presence of DNA hybridization. The selectivity in hybridization of amino linked probe with other ODNs, such as; NC and MM sequences was also checked

(Figure 9.47c and d). A decrease (0.8 % and 11.7 %, respectively) was obtained in the case of hybridization between probe and NC, or probe and MM.

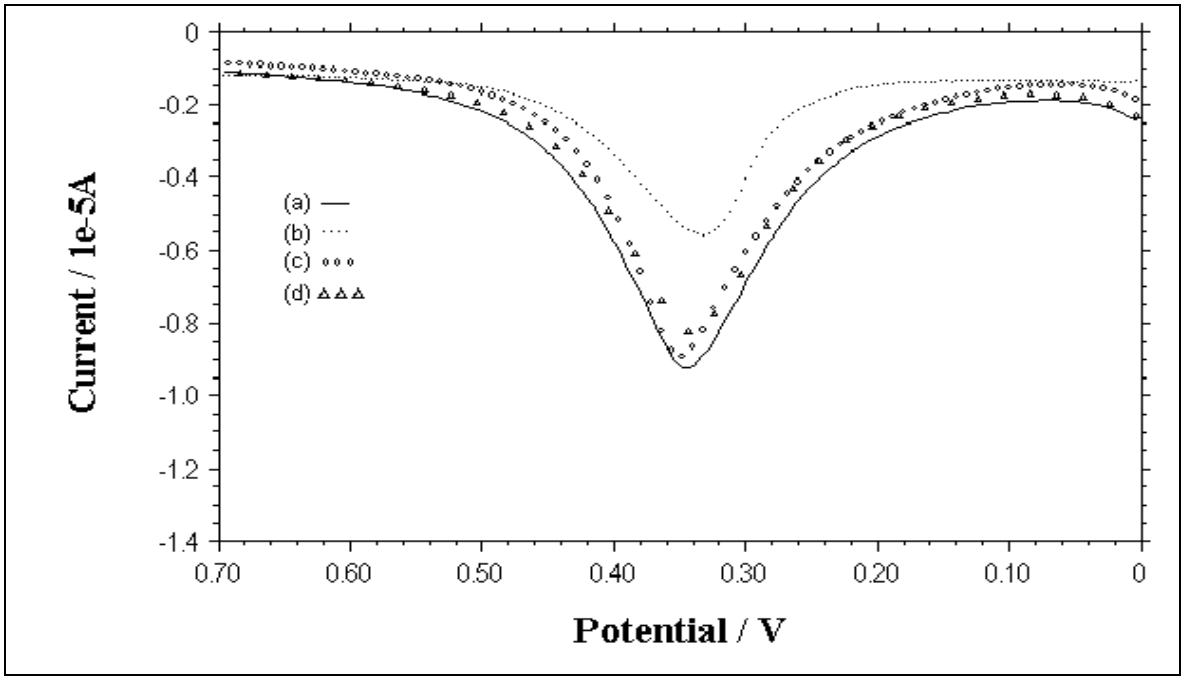

Figure 9.47. DPVs showing the oxidation peak of the polymer (a) 100 μg mL^{-1} probe alone, after hybridization between probe and (b) 100 μg mL^{-1} its complementary (target), (c) 100 μg mL^{-1} NC, and (d) 100 μg mL^{-1} MM. Pulse amplitude: 50 mV.

The effect of target concentration on the oxidation peak current of the polymer was also studied in various target concentration from 25 to 175 μg mL^{-1}. The oxidation peak current of polymer decreased gradually and then levelled off, when the concentration of ODN was increased to 125 μg mL^{-1} (Figure 9.48).

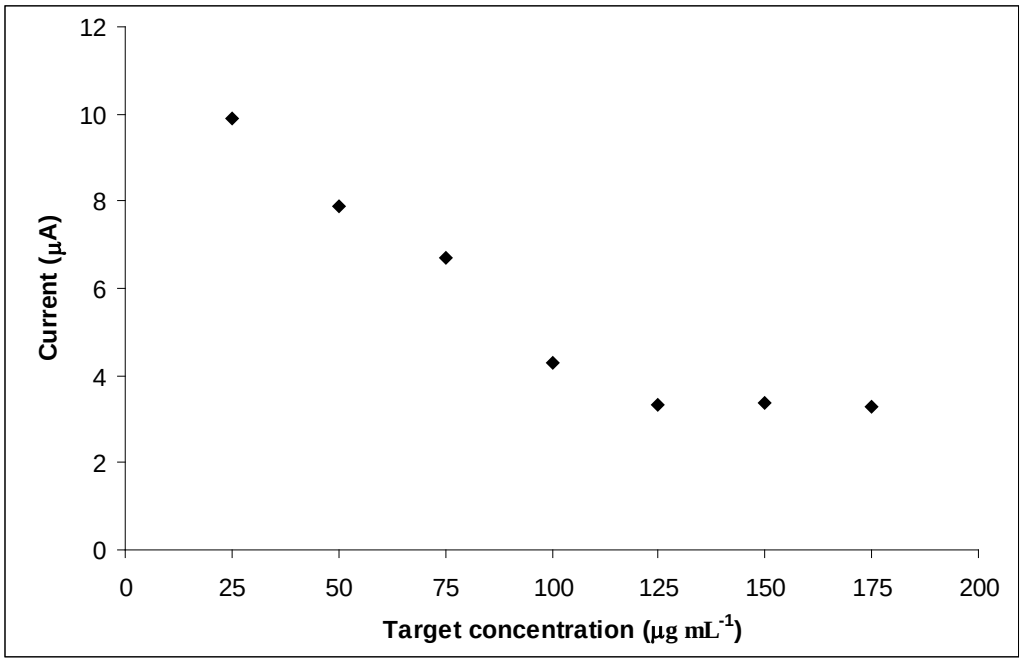

Figure 9.48. The effect of target concentration to the response of PVF^+.

9.4. Studies Carried Out with DNA Immobilized PVF^+ Modified Au Electrode

Electrochemical behaviors of DNA immobilized polymer modified Au disc working electrode were investigated by CV and DPV techniques. The experimental parameters, which influence the performance of this DNA sensing method, such as; the polymeric film thickness, the concentration of DNA, immobilization time of DNA, pH of the medium were examined and discussed in order to obtain better, more sensitive and selective electrochemical measurements. After the optimum working conditions were obtained, the electrochemical behavior of DNA modified polymer electrode by using dsDNA or ssDNA was compared. DNA hybridization was also investigated at optimized working conditions.

9.4.1. The effect of the polymeric film thickness

In order to investigate the effect of the polymeric film thickness on the response of the DNA biosensor similar to the Pt working electrode procedure, $PVF^+ClO_4^-$ films with various thicknesses were electrodeposited on the Au electrode. Firstly, cyclic voltammetric behaviors of these films in 50 mM PBS containing 0.1 M $NaClO_4$ (pH 7.0) were recorded after they had immersed in buffer solution for 1 hour. Then, these electrodes were immersed in dsDNA solution for 1 hour. Secondly, cyclic

voltammograms of these electrodes in buffer solution were recorded. The concentrations of dsDNA solution was 2.5 mg mL^{-1} in each of the study.

The change in oxidation peak current between polymer electrode and dsDNA immobilized polymer electrode (ΔI) is given in Figure 9. 49. As seen from this figure, it is clear that the interaction of PVF^{+} with dsDNA increases until 1.0 mC polymeric film thickness. It was found that there was a decrease observed at the oxidation peak current of polymer when the polymer film thickness were increased up to a value corresponding to the passage of a charge of 1.0 mC during the electroprecipitation of the polymer. After the polymer film thickness value exceeded 1.0 mC, DNA immobilization may possibly be restricted due to the diffusion limitations of dsDNA into the inner regions of the porous polymer film matrix. These results were found similiar to earlier reports presenting the influence of polymer film thickness (Kuralay et al., 2005, 2006). The % decreases at the response of dsDNA immobilized polymer modified electrode were calculated as 26.60 %, 65.19%, 79.98 %, 78.84 % and 76.64 % for the film thickness values corresponding to the passage of charges of 0.2, 0.8, 1.0, 1.1 and 1.2 mC, respectively. The optimum polymeric film thickness was chosen as 1.0 mC for further experiments by using dsDNA immobilized polymer modified Au electrodes. The peak currents and peak potentials of both oxidation and reduction peaks of redox polymer changed and decreased due to the immobilization of dsDNA onto polymer electrodes (Figure 9.50).

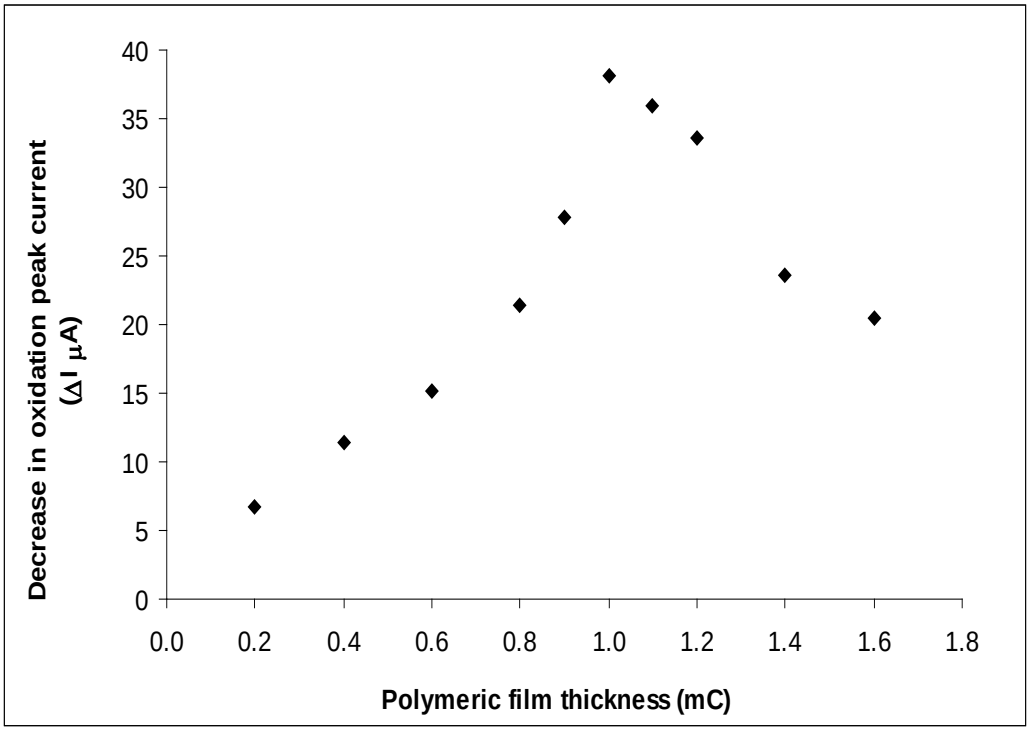

Figure 9.49. The change in oxidation peak current between polymer modified Au electrode and dsDNA immobilized polymer modified Au electrode at different polymeric film thicknesses.

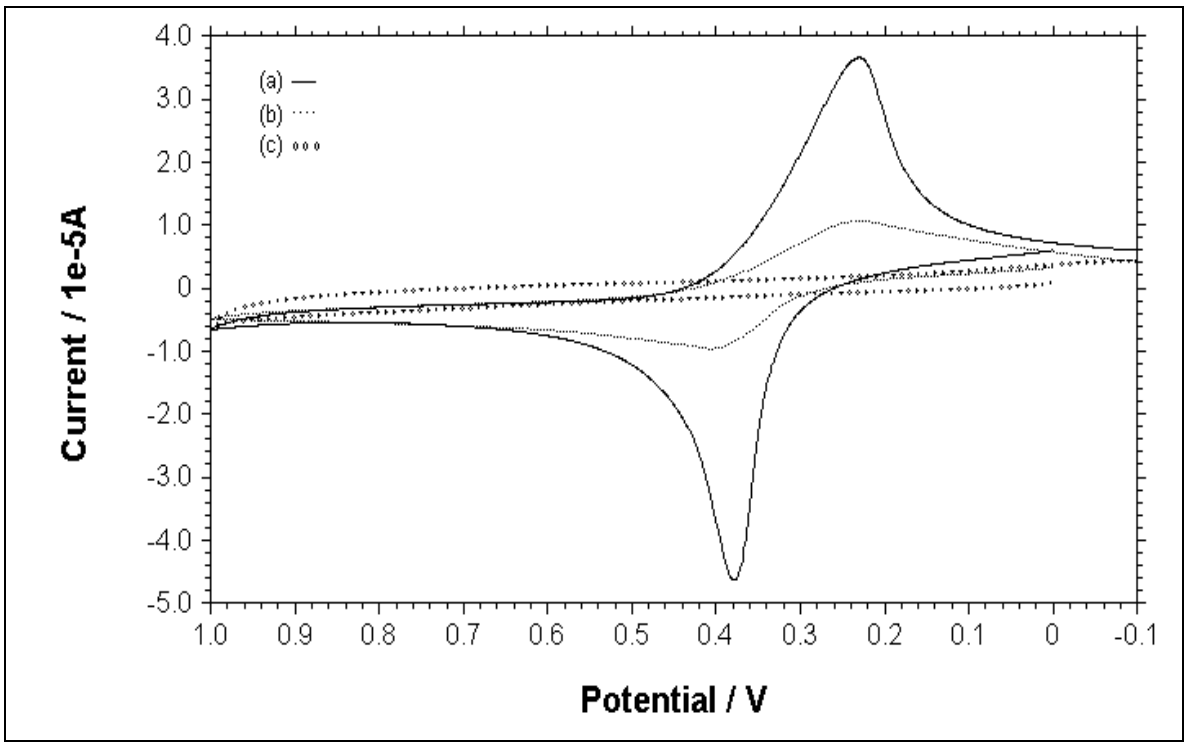

Figure 9.50. CVs of (a) $PVF^{+}ClO_4^{-}$ coated Au electrode (b) dsDNA immobilized polymer film (c) uncoated Au electrode in 50 mM PBS containing 0.1 M $NaClO_4$ at 1.0 mC polymeric film thickness. Scan rate: 100 mV s^{-1}.

9.4.2. The effect of the concentration of dsDNA

The effect of dsDNA concentration used in the solution during the immobilization step on the response of the electrode was determined using DPV technique. dsDNA concentrations varying from 50 to 2000 μg mL^{-1} were used in the experiments. Optimum polymeric film thickness (1.0 mC) and 1 hour immobilization time were also used. Firstly, differential pulse voltammetric behavior of the $PVF^{+}ClO_4^{-}$ film in 50 mM PBS containing 0.1 M $NaClO_4$ was recorded after the electrode had immersed in buffer solution for 1 hour. Then the prepared $PVF^{+}ClO_4^{-}$ film was immersed in dsDNA solutions which had different concentrations. Secondly, DPV of this electrode in 50 mM PBS containing 0.1 M $NaClO_4$ was recorded. The DPVs of (a) $PVF^{+}ClO_4^{-}$ film, (b) $PVF^{+}ClO_4^{-}$ film after immersing into 250 μg mL^{-1} dsDNA solution (c) $PVF^{+}ClO_4^{-}$ film after immersing into 750 μg mL^{-1} dsDNA solution and (d) $PVF^{+}ClO_4^{-}$ film after immersing into 1250 μg mL^{-1} dsDNA solution are given in Figure 9.51. By the immobilization of dsDNA onto PVF^{+} matrix, the oxidation peak currents of the polymer decreased since dsDNA covered the electroactive sites of PVF^{+}. The changes in oxidation peak are also given in Figure 9.52 (R^2 = 0.9891). As seen from this figure, up to a concentration level of 1250 μg mL^{-1} dsDNA, the oxidation peaks of the polymer decreased. After this concentration value no appreciable difference was observed. So 1250 μg mL^{-1} solution concentration was used for further experiments. The decrease in oxidation peak current of the polymer was 81.03 % at this concentration value. The detection limit corresponds to as 12.00 μg mL^{-1} for dsDNA immobilized polymer modified electrode.

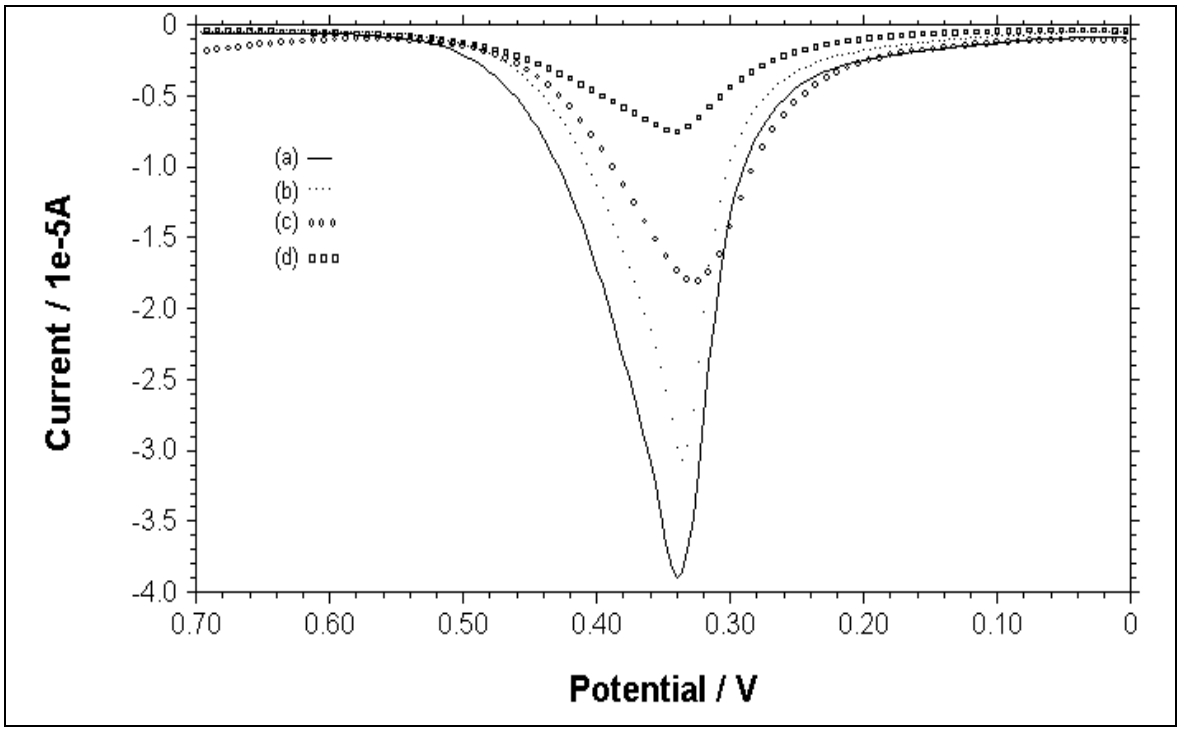

Figure 9.51. DPVs of (a) $PVF^{+}ClO_4^{-}$ film, (b) $PVF^{+}ClO_4^{-}$ film after immersing into 250 μg mL^{-1} dsDNA solution (c) $PVF^{+}ClO_4^{-}$ film after immersing into 750 μg mL^{-1} dsDNA solution and (d) $PVF^{+}ClO_4^{-}$ film after immersing into 1250 μg mL^{-1} dsDNA solution. Pulse amplitude: 50 mV.

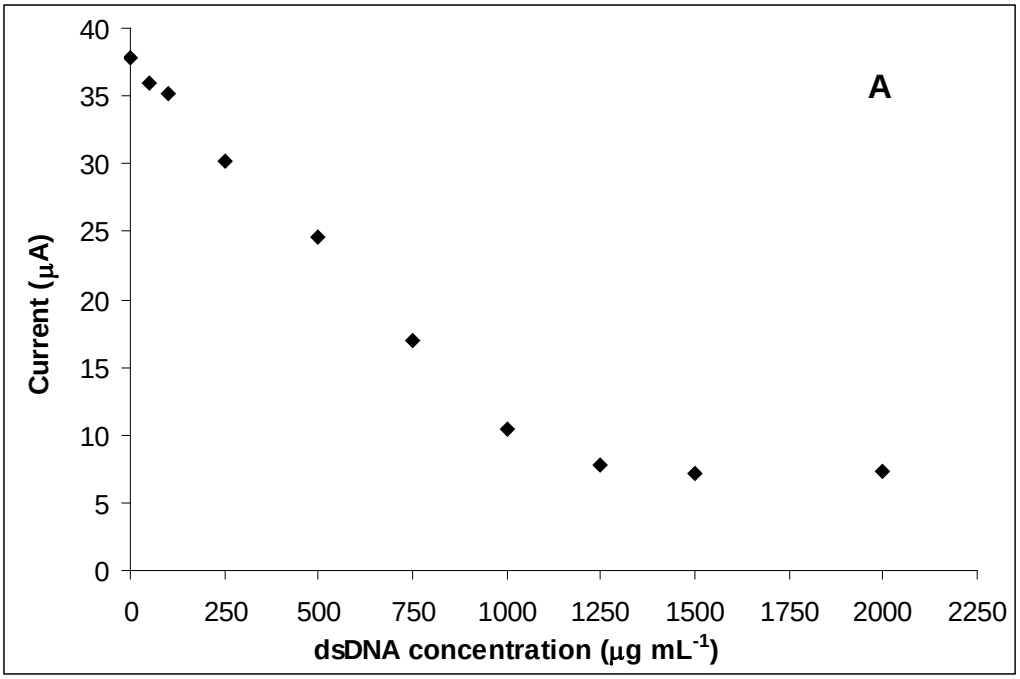

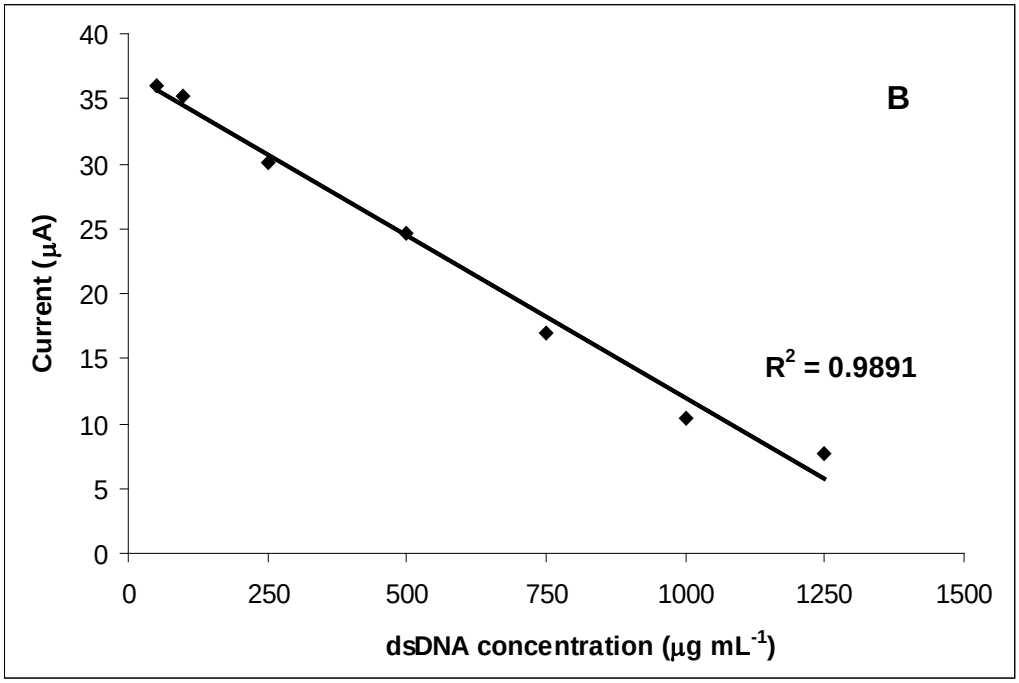

Figure 9.52. Changes in oxidation peak current of the polymer electrode in different dsDNA concentrations.

9.4.3. The effect of the immobilization time of dsDNA

For the determination of the effect of immobilization time of dsDNA onto the positively charged polymeric matrix, $PVF^{+}ClO_4^{-}$ films with a polymeric film thickness of 1.0 mC were immersed in 1250 μg mL^{-1} dsDNA solution for different immobilization times. Firstly, differential pulse voltammetric behavior of $PVF^{+}ClO_4^{-}$ film in 50 mM PBS containing 0.1 M $NaClO_4$ at pH 7.0 was recorded after it had immersed in buffer solution for several periods of time. Then, $PVF^{+}ClO_4^{-}$ film was immersed in dsDNA solution for the same periods of time. Secondly, DPV of the dsDNA immobilized film was recorded. The change in oxidation peak current between polymer electrode and dsDNA immobilized polymer electrode in different dsDNA immobilization times are given in Figure 9.53. As seen from this figure, after 1 hour immobilization time almost same level of decrease in oxidation peak current of the polymer was obtained. Thus, 1 hour immobilization time was choosen as optimum immobilization time for polymer modified Au electrode. The DPVs of (a) $PVF^{+}ClO_4^{-}$ film, (b) $PVF^{+}ClO_4^{-}$ film after immersing into dsDNA solution for 1 hour are given in Figure 9.54. The oxidation peak of the polymer changed after DNA immobilization because of the interaction between polymer and dsDNA.

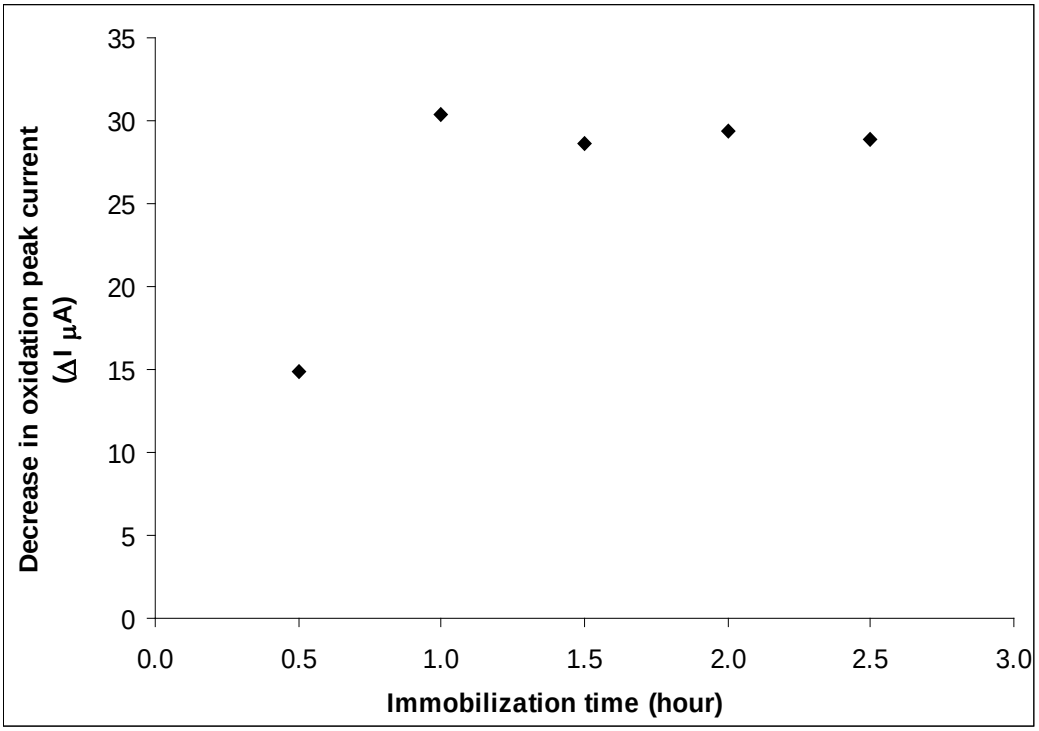

Figure 9.53. The change in oxidation peak current between polymer electrode and dsDNA immobilized polymer modified Au electrode with different DNA immobilization times.

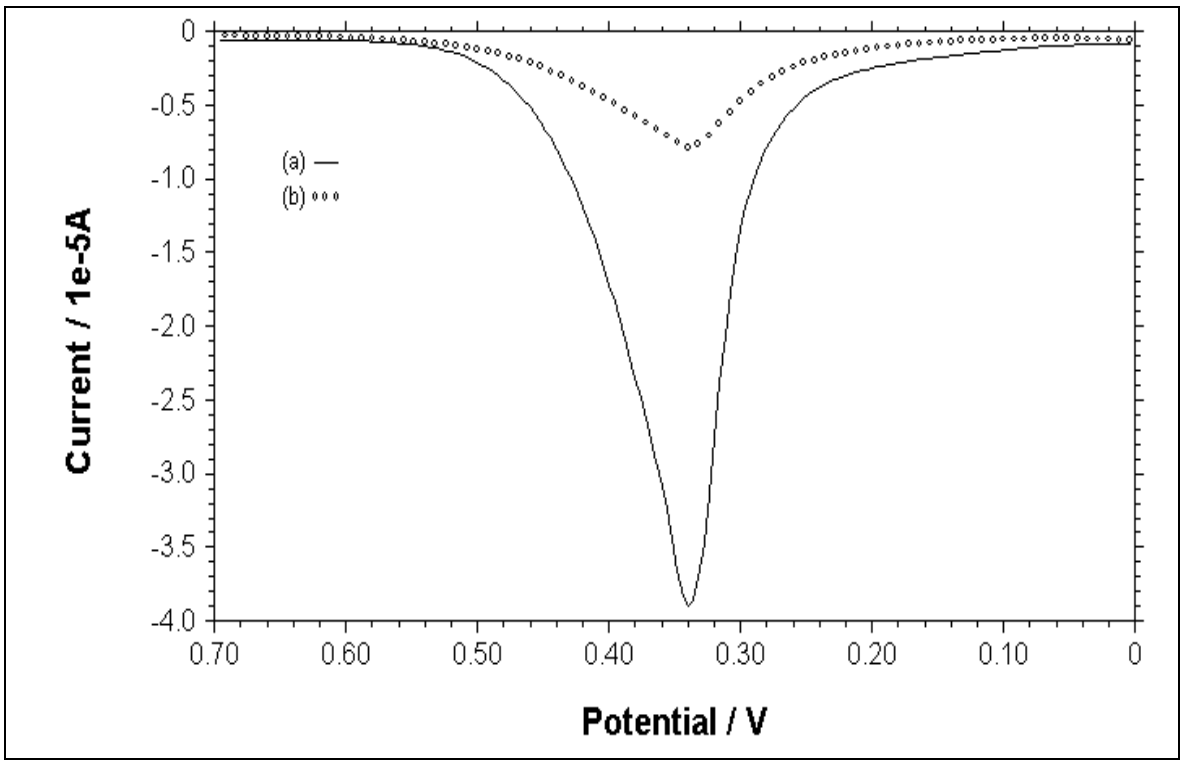

Figure 9.54. DPVs of (a) $PVF^{+}ClO_4^{-}$ coated Au electrode (b) $PVF^{+}ClO_4^{-}$ film after immersing into 1250 μg mL^{-1} dsDNA solution for 1 hour in 50 mM PBS containing 0.1 M $NaClO_4$. Pulse amplitude: 50 mV.

9.4.4. The effect of pH of the medium

The response of this modified electrode was also examined using 50 mM ABS (pH 4.8) in order to compare the electrode performance at the same concentration level of PBS. The CVs of (a) $PVF^{+}ClO_4^{-}$ film, (b) $PVF^{+}ClO_4^{-}$ film after immersing into 2.50 mg mL^{-1} dsDNA solution in PBS and ABS are given in Figures 9.55 and 9.56, respectively. It was found that the decrease at the oxidation peak current of polymer was found in a higher ratio by using PBS in comparison to the one by using ABS. The decreases % at the response of dsDNA immobilized polymer modified electrode were calculated as 80.13 % in PBS and 60.86 % in ABS.

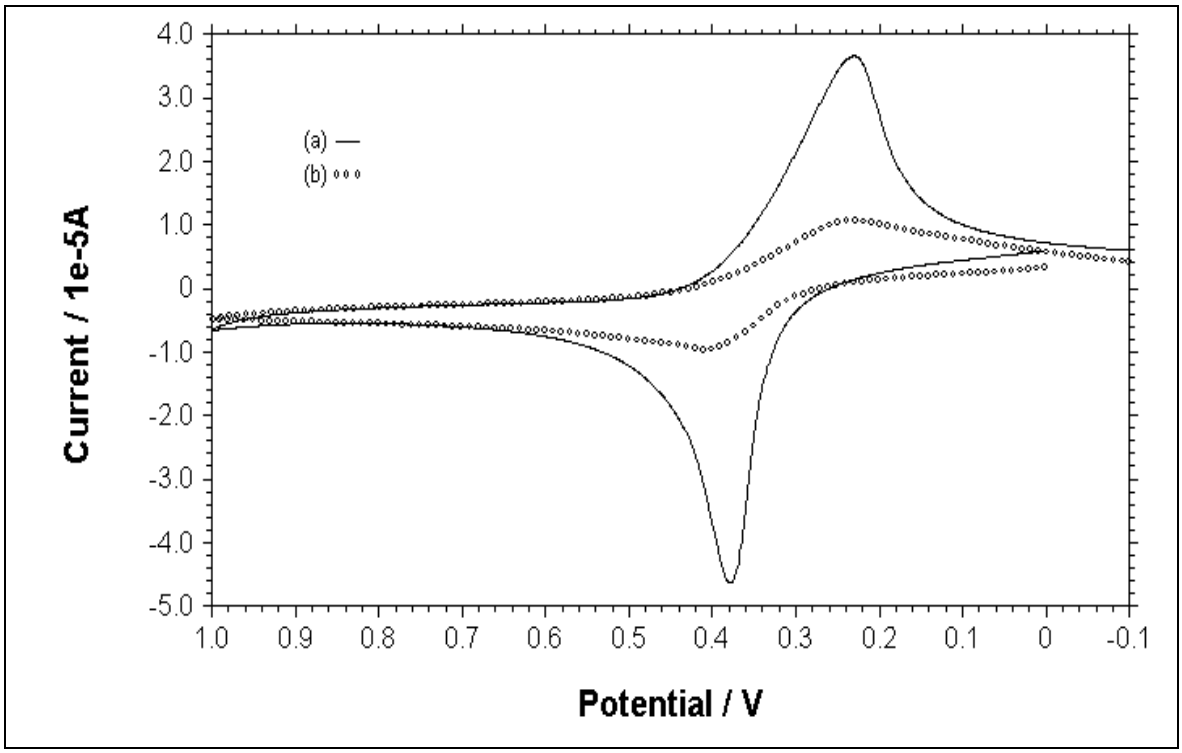

Figure 9.55. CVs of (a) $PVF^{+}ClO_4^{-}$ coated Au electrode (b) $PVF^{+}ClO_4^{-}$ film after immersing into dsDNA solution in 50 mM PBS containing 0.1 M $NaClO_4$. Scan rate: 100 mV s^{-1}.

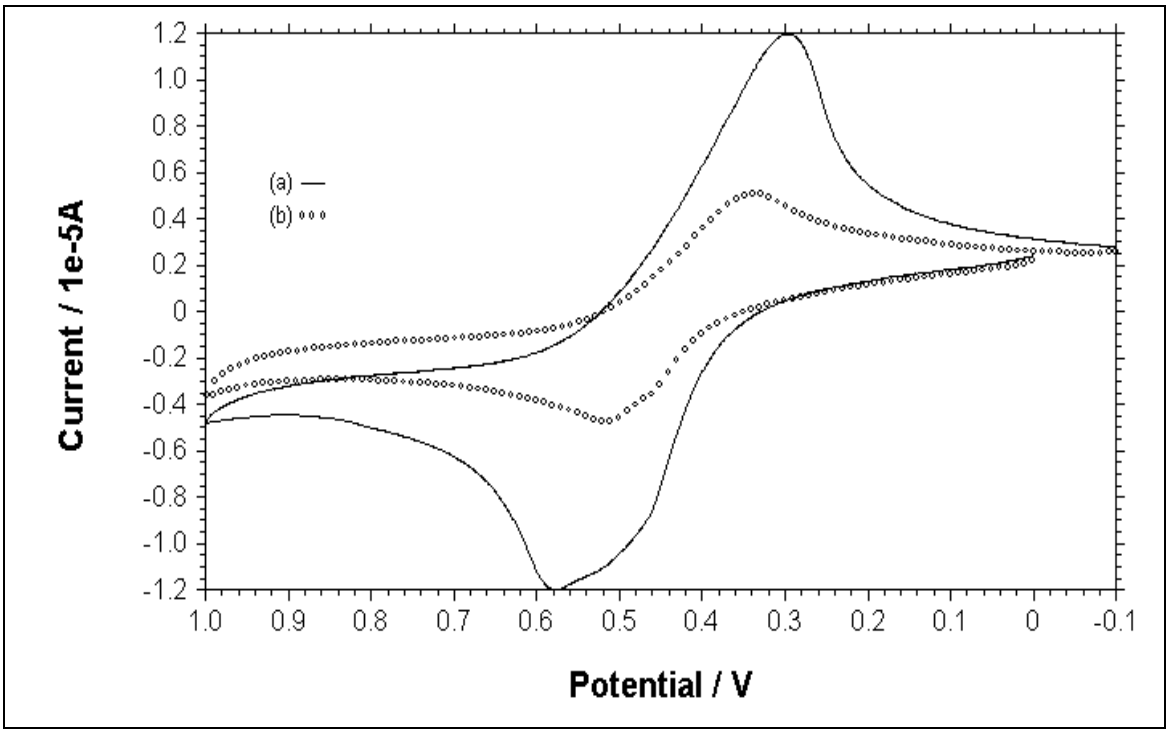

Figure 9.56. CVs of (a) $PVF^{+}ClO_4^{-}$ coated Au electrode (b) $PVF^{+}ClO_4^{-}$ film after immersing into dsDNA solution in 50 mM ABS. Scan rate: 100 mV s^{-1}.

9.4.5. The Comparison of Electrochemical Behavior of dsDNA and ssDNA Immobilized Polymer Modified Au Electrodes

The electrochemical behaviors of dsDNA and ssDNA immobilized polymer modified Au electrodes were investigated. The voltammograms obtained using 50 mM PBS containing 0.1 M $NaClO_4$ at pH 7.0 by polymer, ssDNA immobilized polymer and dsDNA immobilized polymer electrodes are given respectively, in Figures 9.57a, b, c and 9.58a, b, c. The polymeric film thickness corresponded to 1.0 mC, immobilization time was 1 hour and DNA solution concentration was 1250 μg mL^{-1} for each experiment. It was observed that the interaction between dsDNA and the positively charged polymer matrix was stronger than the interaction between ssDNA and polymer matrix similar to the results obtained with polymer modified Pt working electrode. The decrease in oxidation peak current of the polymer was calculated as 79.98 % from the response of dsDNA immobilized polymer modifed electrode, on the otherhand, the decrease was found as 56.67 % by using ssDNA immobilized polymer modified electrode (Figure 9.57). There was a small peak observed at about +0.92 V vs. SCE, which reflected the oxidation signal of guanine in the DPV of ssDNA immobilized polymer modified electrode

(Figure 9.58b). There was also a small peak observed at about + 0.91 V vs. SCE, which reflected the oxidation signal of guanine in the DPV of dsDNA immobilized polymer modified electrode (Figure 9.58c).

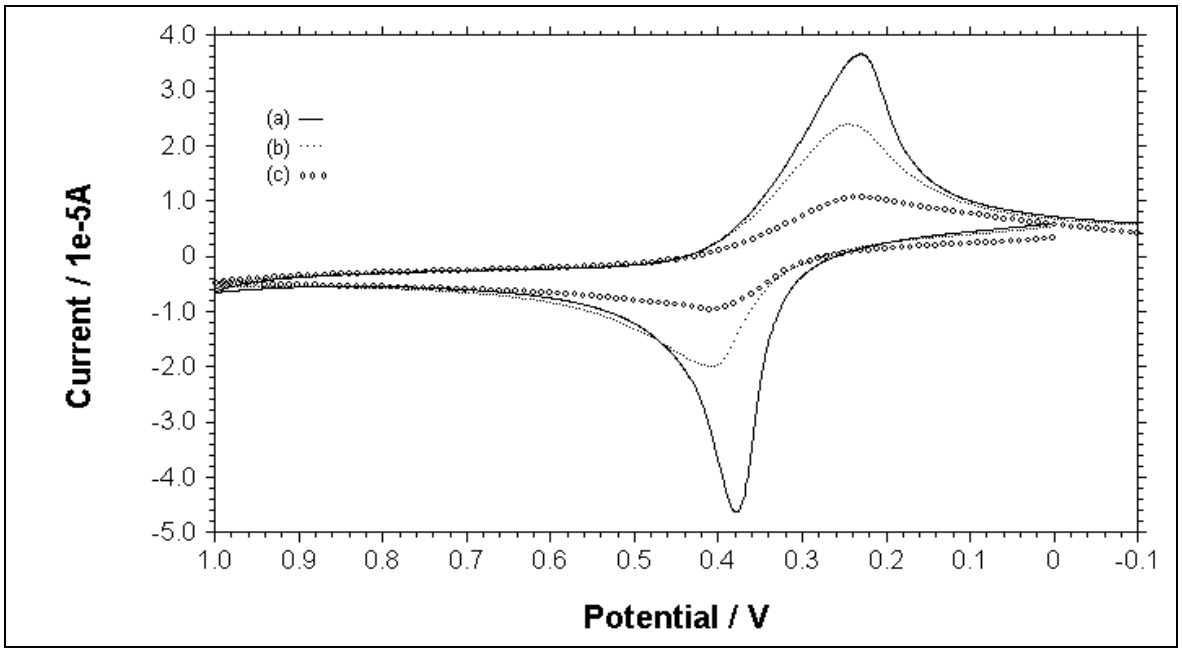

Figure 9.57. CVs of (a) $PVF^{+}ClO_4^{-}$ film (b) $PVF^{+}ClO_4^{-}$ film after immersing into ssDNA solution (c) $PVF^{+}ClO_4^{-}$ film after immersing into dsDNA solution in 50 mM PBS containing 0.1 M $NaClO_4$. Scan rate: 100 mV s^{-1}.

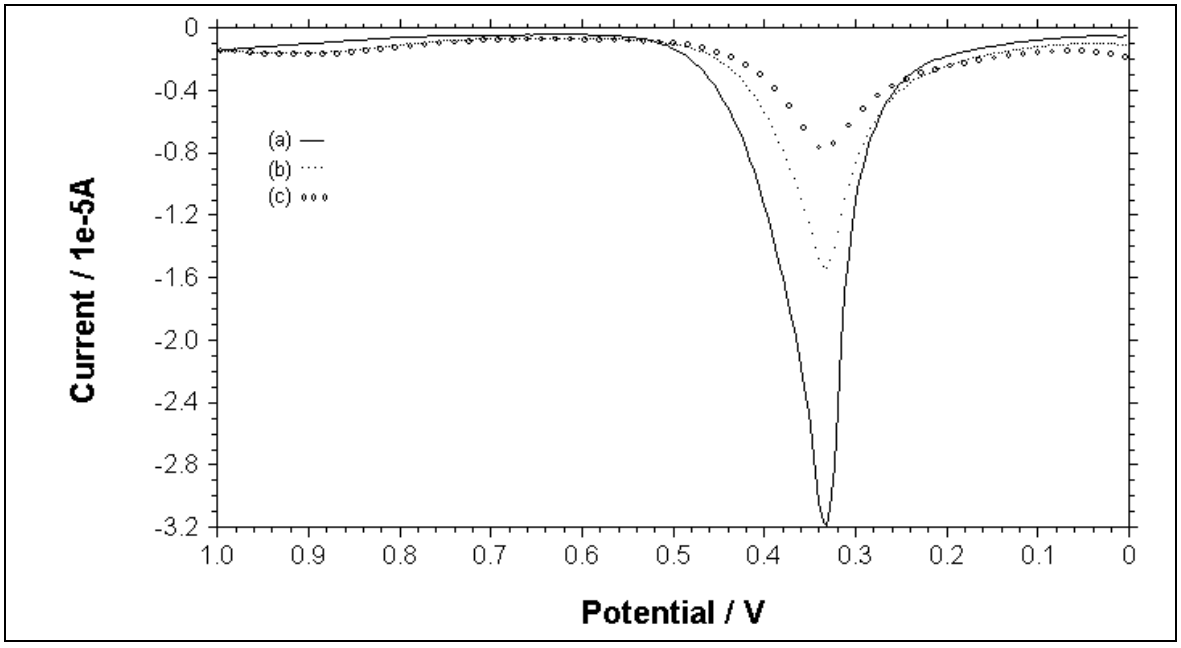

Figure 9.58. DPVs (a) $PVF^{+}ClO_4^{-}$ film (b) $PVF^{+}ClO_4^{-}$ film after immersing into ssDNA solution (c) $PVF^{+}ClO_4^{-}$ film after immersing into dsDNA solution in 50 mM PBS containing 0.1 M $NaClO_4$. Pulse amplitude: 50 mV.

The CVs were recorded in 50 mM ABS (pH 4.8) for polymer, ssDNA immobilized polymer and dsDNA immobilized polymer electrodes, respectively (Figure 9.59a, b, c). As can be seen from this figure, the oxidation peak current of the polymer decreased due to the less conductive character of DNA molecule. It was also observed that the interaction between dsDNA and the positively charged polymer matrix was stronger than the interaction between ssDNA and polymer matrix supporting the earlier results. The DPVs were also recorded for polymer, ssDNA immobilized polymer, dsDNA immobilized polymer electrodes and uncoated Au electrode, respectively (Figure 9.60a, b, c, d). The peaks at +0.98 V vs. SCE in the DPV of dsDNA immobilized polymer modified electrode and +1.01 V vs. SCE in the DPV of ssDNA immobilized polymer modified electrode could be predicted to belong to the electroactive DNA base, guanine reported in the similar studies (Kerman et al., 2003; Chen et al., 2007). As seen in Figure 9.60b and Figure 9.60c, peak currents in the DPV of dsDNA immobilized polymer modified electrode were greater than the peak currents in the DPV of ssDNA immobilized polymer modified electrode.

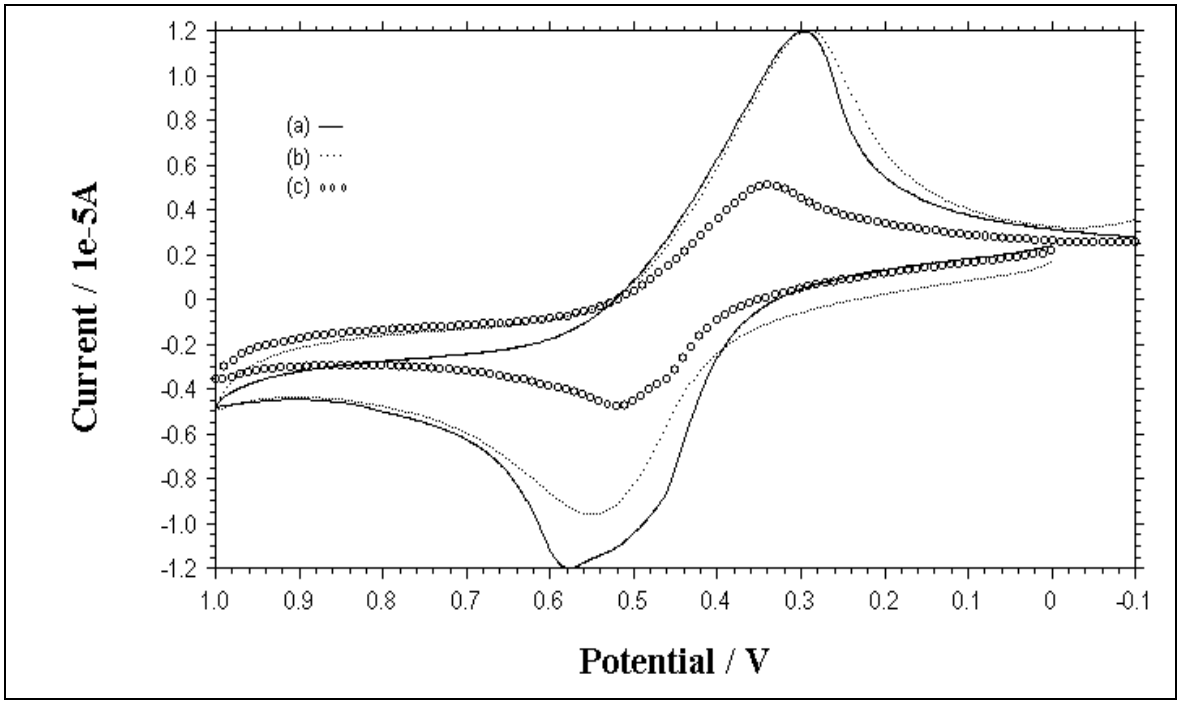

Figure 9.59. CVs of (a) $PVF^{+}ClO_4^{-}$ film (b) $PVF^{+}ClO_4^{-}$ film after immersing into ssDNA solution (c) $PVF^{+}ClO_4^{-}$ film after immersing into dsDNA solution in 50 mM ABS. Scan rate: 100 mV s^{-1}.

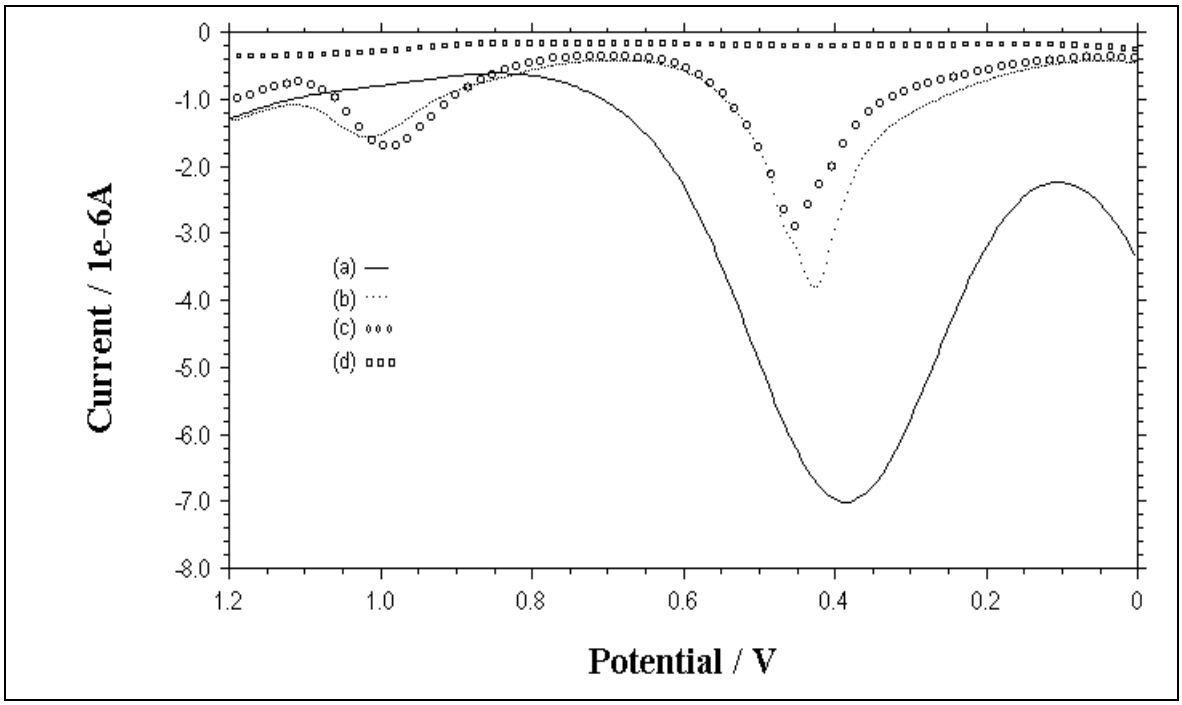

Figure 9.60. CVs of (a) $PVF^{+}ClO_4^{-}$ film (b) $PVF^{+}ClO_4^{-}$ film after immersing into ssDNA solution (c) $PVF^{+}ClO_4^{-}$ film after immersing into dsDNA solution in 50 mM ABS. Scan rate: 100 mV s^{-1}.

9.4.6. Application of the polymer modified Au electrode

Probe ODN immobilized polymer electrodes were prepared dropping the ODN solutions onto the polymer modified Au electrode with a polymeric film thickness of 1.0 mC and kept for 1 hour. For hybridization target, NC and MM ODN solutions were dropped onto the probe immobilized polymer modified electrode and kept for 1 hour. After immobilization of nucleic acid onto the polymer electrode, the electrode was washed with buffer solution for 10 seconds. The oxidation peak currents of polymer, and guanine were measured by using DPV scanning between +0.0 V and +1.0 V vs. SCE at pulse amplitude of 50 mV. Firstly, oxidation peak currents of probe and then target, NC and MM immobilized probe were measured.

The effect of different ODN modifications on the response of this DNA sensing method after ODN immobilization step was examined with different ODNs in respect to their binding performance onto the positively charged polymer matrix. The changes at the oxidation peak current of polymer with 100 μg mL^{-1} thiol linked, amino linked, phosphate linked and unmodified ODNs are given

respectively in Figure 9.61a, b, c, d. The maximum decrease in the peak current and consequently, the maximum interaction with positively charged matrix was obtained with thiol linked ODN because of the higher electronegativity of thiol group comparison to other groups. Thus, thiol linked ODN was chosen for the further experiments in order to obtain higher sensitivity and selectivity by using DNA immobilized polymer modified Au electrode.

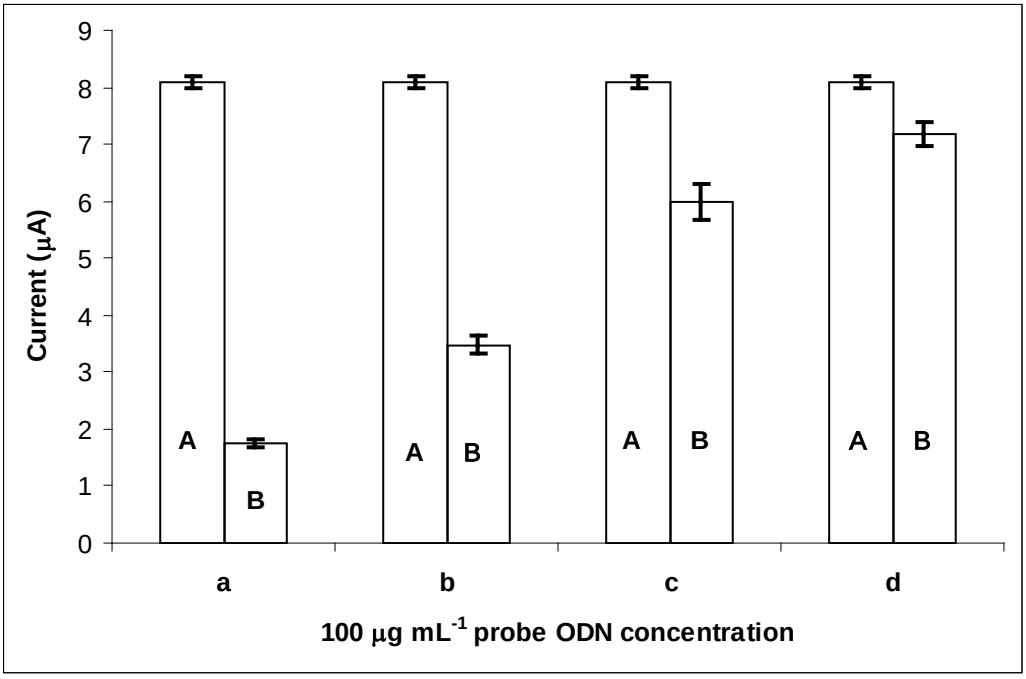

Figure 9.61. Histograms showing the changes at the oxidation peak current of polymer in the absence (A) and the presence (B) of ODNs; (a) thiol linked ODN, (b) amino linked ODN, (c) phosphate linked ODN, (d) unmodified ODN.

9.4.6.1. Hybridization studies carried out with thiol linked probe

The effect of thiol linked ODN concentration on the oxidation peak currents of polymer was studied in various ODN concentration from 12.5 to 200 μg mL^{-1}. The oxidation peak current of polymer decreased gradually and then levelled off, when the concentration of ODN was increased to 175 μg mL^{-1} (Figure 9.62). The optimum immobilization concentration for 20-mer thiol linked ODN was found as 175 μg mL^{-1}. The DPVs at three different concentrations of thiol linked ODN were shown in Figure 9.63.

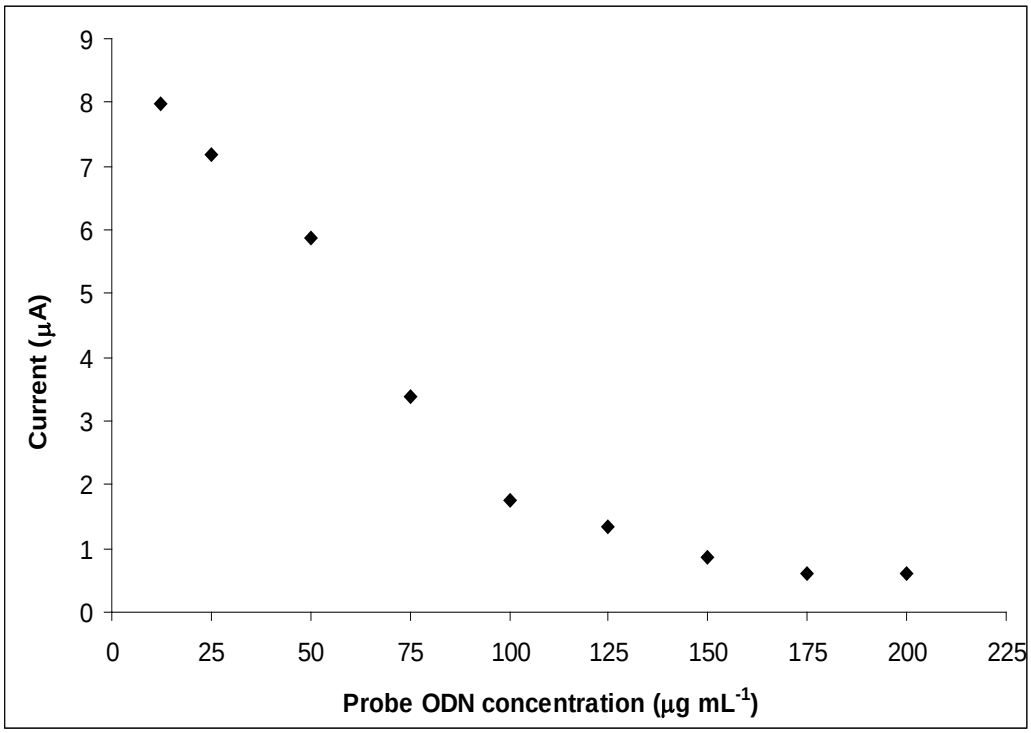

Figure 9.62. The effect of thiol linked ODN concentration to the response of PVF^{+}.

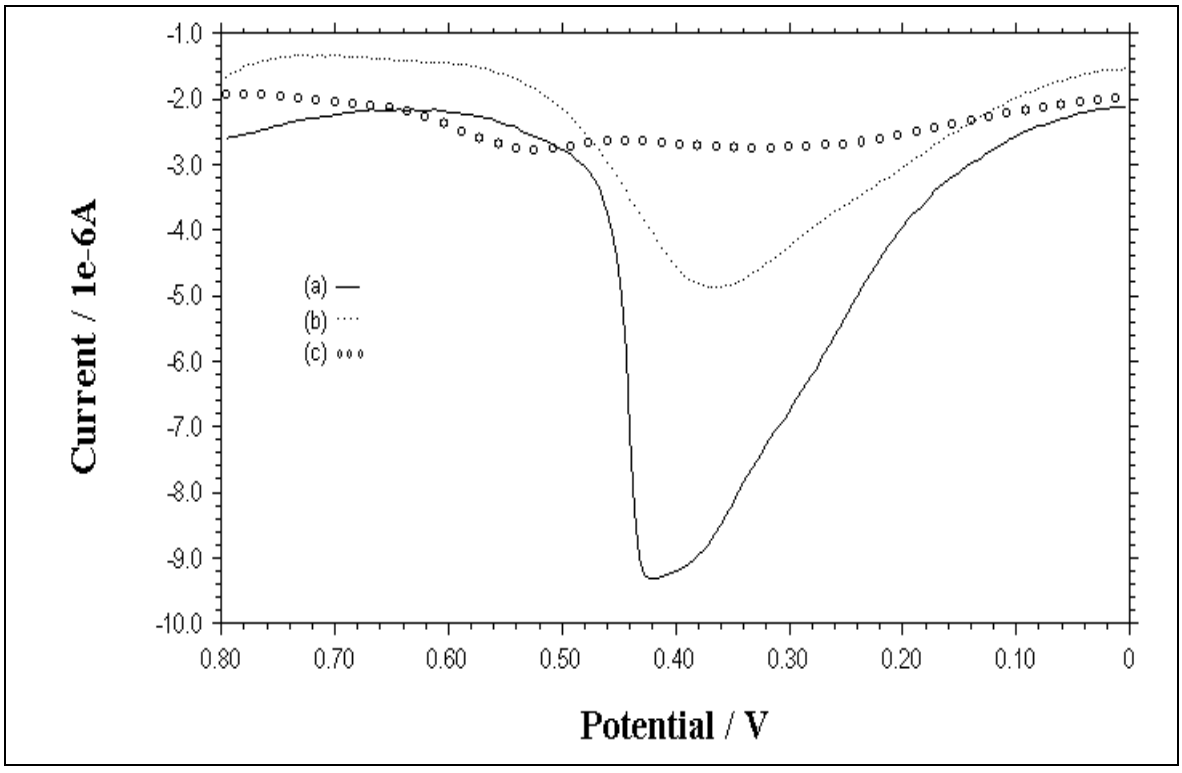

Figure 9.63. DPVs of (a) 25 μg mL^{-1} thiol linked ODN (b) 75 μg mL^{-1} thiol linked ODN (c) 150 μg mL^{-1} thiol linked ODN. Pulse amplitude: 50 mV.

For the application of DNA immobilized polymer modified electrode, an electrochemical sensing of DNA hybridization was studied. The changes at the oxidation peak current of the polymer were monitored in the presence of thiol linked probe alone and the hybridization between probe and target / NC / MM sequences, respectively (Figure 9.64a, b, c, d). The oxidation peak current of polymer decreased as a result of DNA hybridization between probe and its complementary sequence, target (Figure 9.64a and b). Due to the specific binding of thiol linked probe with its complemantary at the polymer matrix, a significant decrease (53.7 %) at oxidation peak current of the polymer was observed in the presence of DNA hybridization. The selectivity in hybridization of thiol linked probe with NC and MM sequences was also checked (Figure 9.64c and d). A small decrease (2.2 % and 10.2 %, respectively) was obtained in the case of hybridization between probe and NC, or probe and MM similar to the results obtained in the literature (Sanchez-Pomales et al., 2007; Prabhakar et al., 2008a, b; Degefa and Kwak, 2008). Related histograms are also given in Figure 9.65.

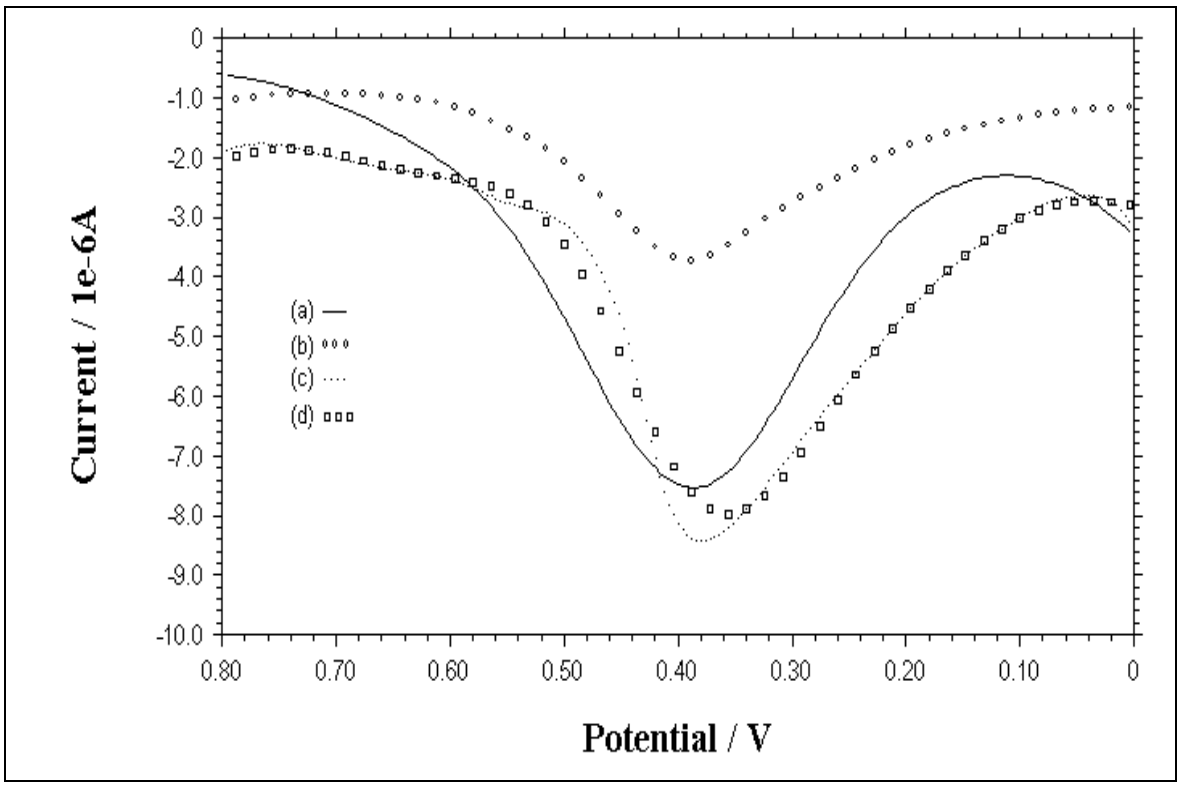

Figure 9.64. DPVs showing the oxidation peak of the polymer (a) 50 μg mL^{-1} probe alone, (b) after hybridization between probe and 50 μg mL^{-1} complementary, (c) interaction between probe and 50 μg mL^{-1} NC, (d) interaction between probe and 50 μg mL^{-1} MM. Pulse amplitude: 50 mV.

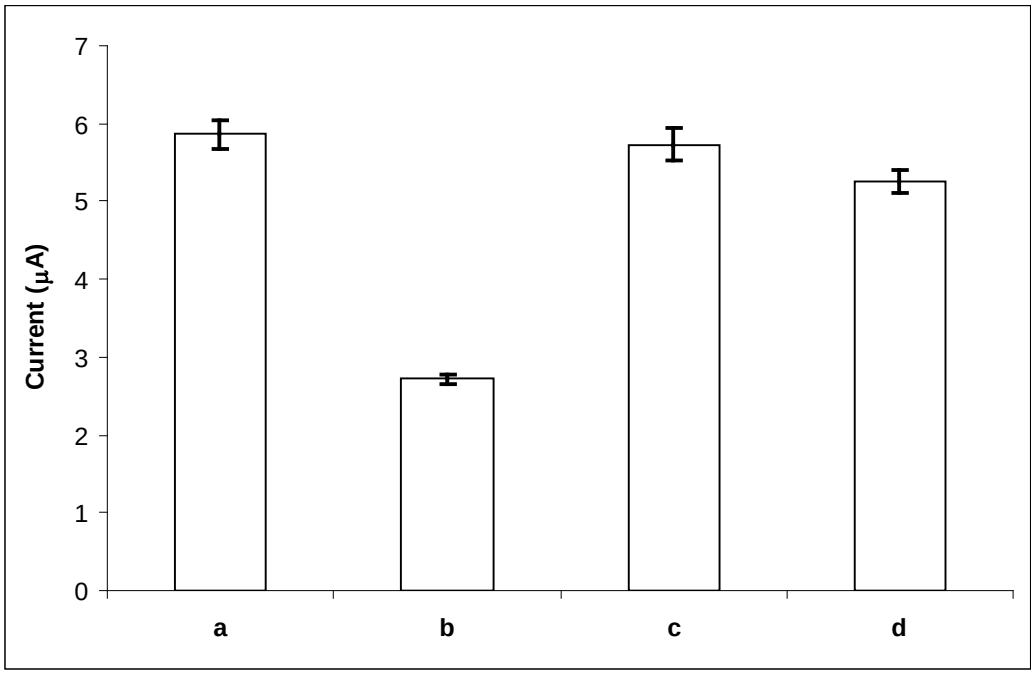

Figure 9.65. Histograms showing the oxidation peak current of the polymer (a) 50 μg mL^{-1} probe alone, (b) after hybridization between probe and 50 μg mL^{-1} complementary, (c) interaction between probe and 50 μg mL^{-1} NC, (d) interaction between probe and 50 μg mL^{-1} MM.

The effect of target concentration on the oxidation peak current of polymer and guanine was also studied in various target concentration from 12.5 to 125 μg mL^{-1}. The polymer oxidation peak current decreased gradually and then levelled off, when the concentration of target was increased to 75 μg mL^{-1} (Figure 9.66 shown with P). On the other hand, the guanine oxidation peak current increased and then levelled off (Figure 9.66 shown with G). The optimum immobilization concentration for target ODN was found as 75 μg mL^{-1}. The DPVs at three different concentrations of target ODN were shown in Figure 9.67. The peaks at about +0.90 V vs. SCE could be attributed to guanine oxidation (Kerman et al., 2003).

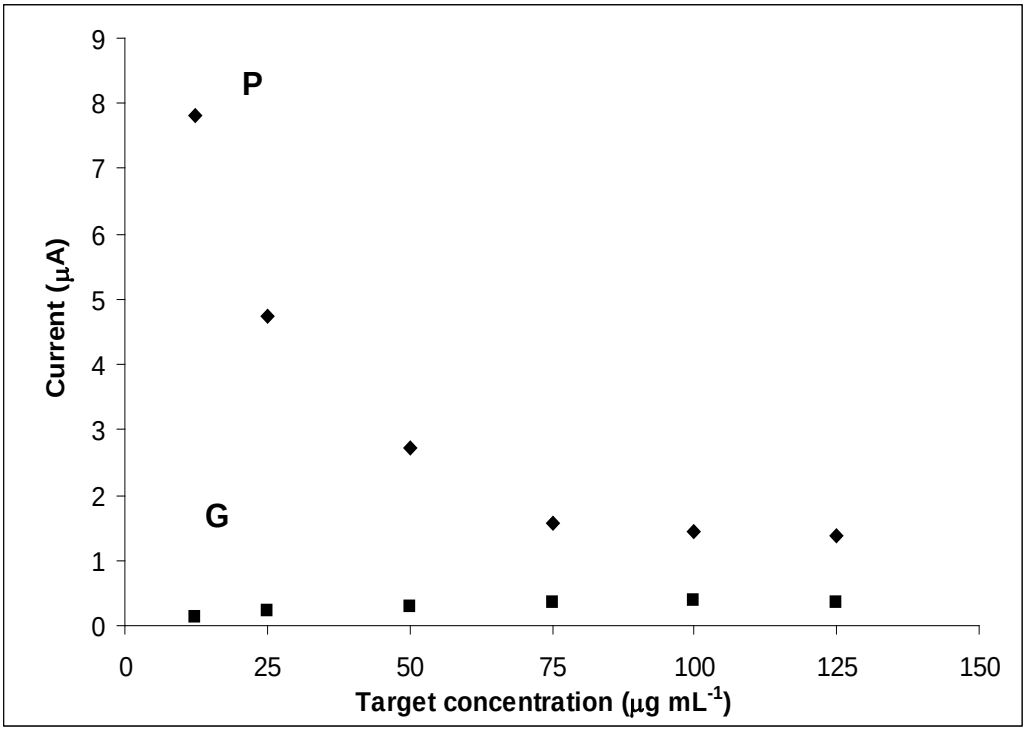

Figure 9.66. The effect of target concentration to the response of PVF^+ and guanine. Plot showing both oxidation peak currents of polymer (P) and guanine (G).

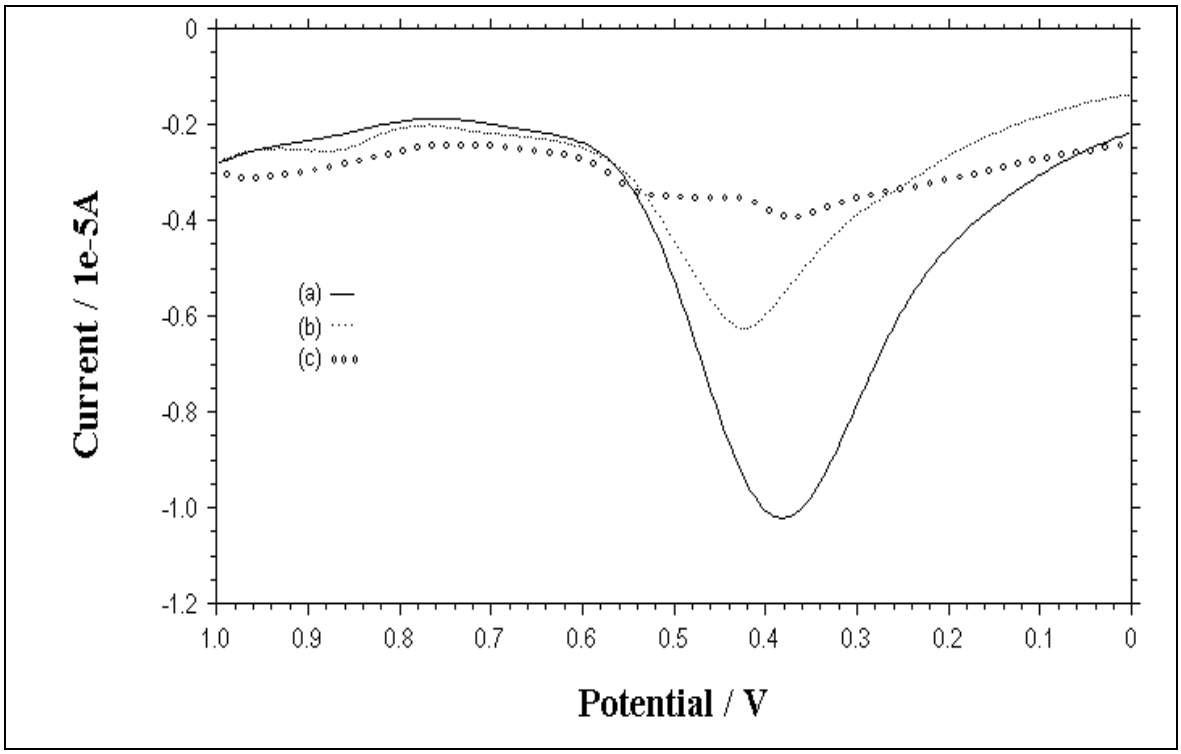

Figure 9.67. DPVs of (a) 12.5 μg mL^{-1} target ODN (b) 25 μg mL^{-1} target ODN (c) 75 μg mL^{-1} target ODN. Pulse amplitude: 50 mV.

9.5. Studies Carried Out with DNA Immobilized PVF^+ Modified Disposable Pencil Graphite (PG) Electrode

In electrochemical studies disposable pencil graphite (PG) electrode was used as the third working electrode. The experimental parameters, which influence the performance of this DNA sensing method, such as; the polymeric film thickness, immobilization time of DNA were examined in order to obtain better, more sensitive and selective electrochemical signal. After the optimum working conditions were obtained, the electrochemical behavior of DNA modified polymer electrode by using dsDNA or ssDNA was compared. DNA hybridization was also performed at optimized working conditions.

9.5.1. The effect of the polymeric film thickness

In order to investigate the effect of the polymeric film thickness on the response of the DNA biosensor, $PVF^+ClO_4^-$ film with various thicknesses was electrodeposited on the PG electrode. Firstly, cyclic voltammetric behavior of this film in 50 mM PBS containing 0.1 M $NaClO_4$ (pH 7.0) was recorded after it had immersed in buffer solution for 30 min. Then, this electrode was immersed in dsDNA solution for 30 min. Secondly, cyclic voltammogram of this electrode was recorded. The concentration of dsDNA solution was 500 $\mu g\ mL^{-1}$ in each of the study. The change in oxidation peak current between polymer electrode and dsDNA immobilized polymer electrode (ΔI) is given in Figure 9. 68. It was found that the currents of both oxidation and reduction peaks of polymer decreased after dsDNA immobilization with various polymeric film thicknesses. The decrease at the oxidation peak of PVF^+ enhanced with an increasing film thickness up to a value corresponding to the passage of a charge of 2.0 mC. After this value, DNA immobilization may possibly be restricted due to the diffusion limitations of dsDNA into the inner regions of the porous polymer film (Kuralay et al., 2005, 2006).

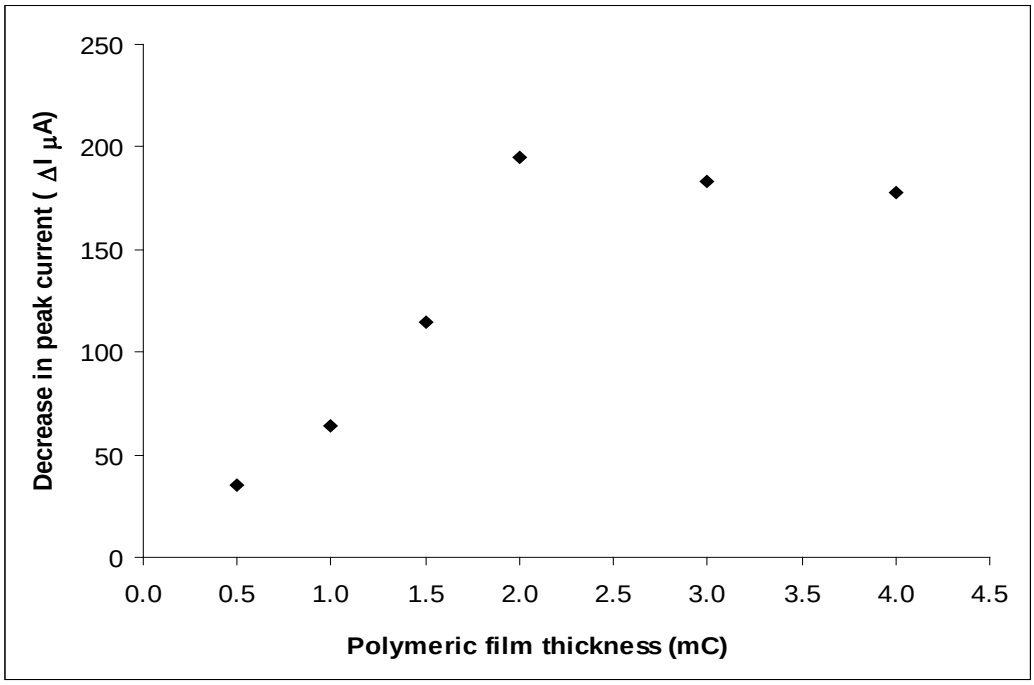

Figure 9.68. The change in oxidation peak current between polymer modified PG electrode and dsDNA immobilized polymer modified PG electrode at different polymeric film thicknesses.

9.5.2. The effect of immobilization time of dsDNA

For the determination of the effect of immobilization time of dsDNA onto the positively charged polymeric matrix, $PVF^{+}ClO_4^{-}$ film with a polymeric film thickness of 2.0 mC was immersed in dsDNA solution for different immobilization times. Firstly, differential pulse voltammetric behavior of $PVF^{+}ClO_4^{-}$ film was recorded after it had immersed in 50 mM PBS containing 0.1 M $NaClO_4$ (pH 7.0) for several periods of time. Then, $PVF^{+}ClO_4^{-}$ film was immersed in dsDNA solution for the same periods of time. Secondly, DPV of the dsDNA immobilized film was recorded in buffer solution. The concentration of dsDNA solution was 500 $\mu g\ mL^{-1}$ in each of the study. The change in oxidation peak current between polymer electrode and dsDNA immobilized polymer electrode in different dsDNA immobilization times are given in Figure 9.69. As seen from this figure, after 30 min immobilization time almost same level of decrease in oxidation peak current was obtained. Thus, 30 min immobilization time was choosen as optimum immobilization time for polymer modified PG electrode.

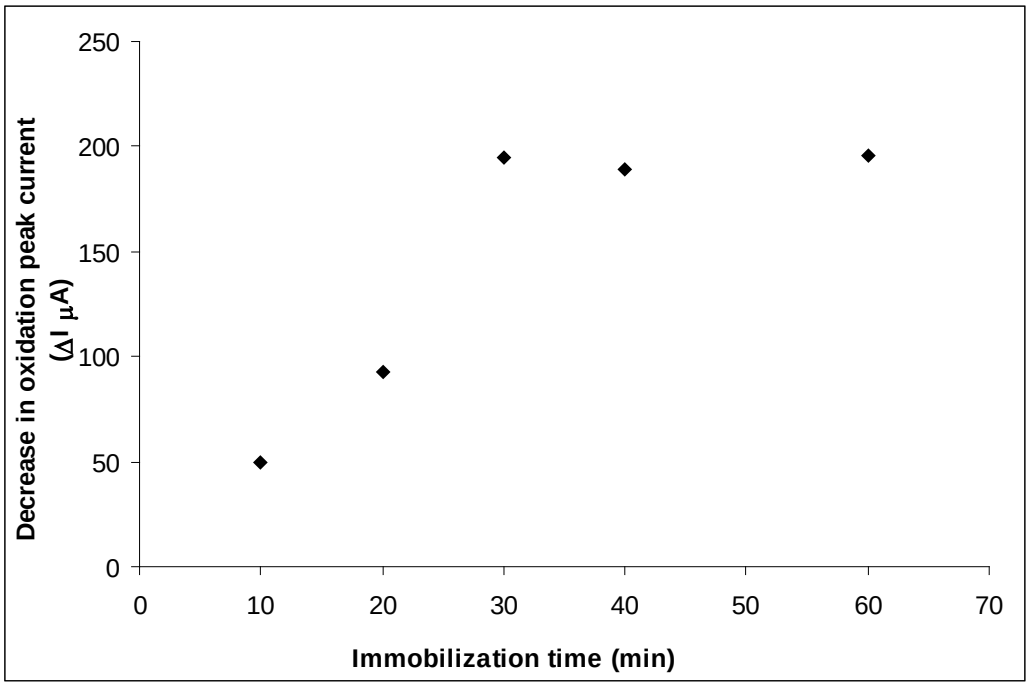

Figure 9.69. The change in oxidation peak current between polymer electrode and dsDNA immobilized polymer modified PG electrode for different DNA immobilization times.

9.5.3. The comparison of electrochemical behavior of dsDNA and ssDNA immobilized polymer modified PG electrodes

The electrochemical behaviors of dsDNA and ssDNA immobilized polymer electrodes were also investigated at polymer modified PG electrodes. The CVs obtained using 50 mM PBS containing 0.1 M $NaClO_4$ at pH 7.0 by polymer, ssDNA immobilized polymer and dsDNA immobilized polymer modified electrodes are given respectively, in Figures 9.70a, b, c. The polymeric film thickness corresponded to 2.0 mC, immobilization time was 30 min and DNA solution was 500 μg mL^{-1} for each experiment. It was observed that the interaction between dsDNA and the positively charged polymer matrix was stronger than the interaction between ssDNA and polymer matrix similar to the results obtained with polymer modified Pt and Au working electrodes. The oxidation peak current decreased about 84.2 % for dsDNA immobilized polymer modified electrode and 55.8 % for ssDNA immobilized polymer modified electrode. The small peak observed at about +0.79 V in the CV of dsDNA immobilized polymer modified PG electrode reflected the oxidation peak of guanine (Figure 9.70c). There was also an adduct measured at +0.04 V vs. SCE attributed due to the specific interaction

between DNA and polymer in the presence of Fe(II/III) couple (Chen and Wang, 2007; Kuralay et al., 2009b).

A peak obtained at +0.34 V in the DPV is related to the oxidation of polymer (Figure 9.71a). After the modified electrode was immersed into ssDNA or dsDNA solution, the DPV of this film was recorded, respectively (Figure 9.75b and c). After DNA immobilization, a significant decrease at the peak currents was observed similar to the results obtained by using CV studies. There was a shift in the oxidation peak potential of the polymer.

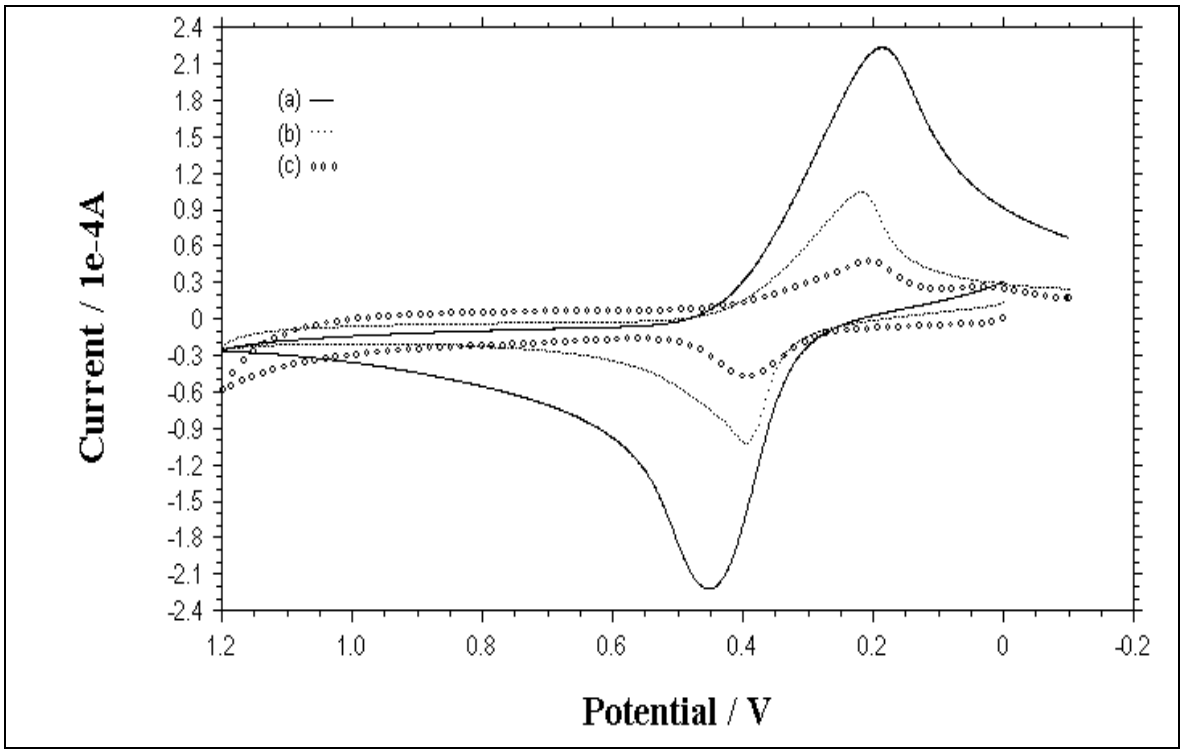

Figure 9.70. CVs of (a) $PVF^{+}ClO_4^{-}$ film (b) $PVF^{+}ClO_4^{-}$ film after immersing into ssDNA solution (c) $PVF^{+}ClO_4^{-}$ film after immersing into dsDNA solution in 50 mM PBS containing 0.1 M $NaClO_4$. Scan rate: 100 mV s^{-1}.

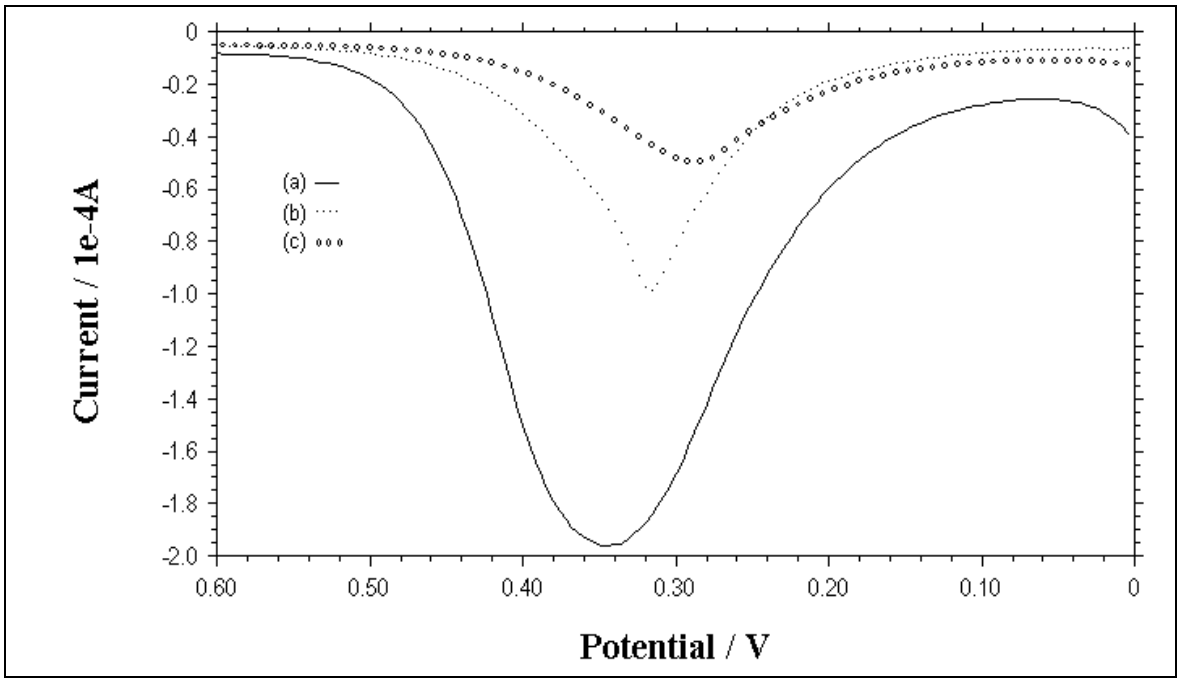

Figure 9.71. DPVs (a) $PVF^{+}ClO_4^{-}$ film (b) $PVF^{+}ClO_4^{-}$ film after immersing into ssDNA solution (c) $PVF^{+}ClO_4^{-}$ film after immersing into dsDNA solution in 50 mM PBS containing 0.1 M $NaClO_4$. Pulse amplitude: 50 mV.

9.5.4. Application of the polymer modified PG electrode

Probe ODN immobilized polymer electrode was prepared immersing the PVF^{+} modified electrode with a polymeric film thickness of 2.0 mC into ODN solution and kept for 30 min. For hybridization target, NC and MM ODN solutions were dropped onto the probe immobilized polymer modified electrode and kept for 30 min. After immobilization of nucleic acid onto the polymer electrode, the electrode was washed by using PBS for 10 seconds. The oxidation peak current of polymer, guanine and adenine were measured by using DPV scanning between +0.0 V and +1.4 V vs. SCE at pulse amplitude of 50 mV. Firstly, oxidation peak current of probe and then target, NC and MM immobilized probe were measured.

The effect of different ODN modifications on the response of this DNA sensing method after ODN immobilization step was examined with different ODNs in respect to their binding performance onto the positively charged polymer matrix. The changes at the oxidation peak current of polymer with 100 $\mu g\ mL^{-1}$ thiol linked, amino linked, phosphate linked and unmodified ODNs are given respectively in Figure 9.72a, b, c, d. The maximum decrease in the peak current and consequently, the maximum interaction with positively charged matrix was

obtained with thiol linked ODN because of the higher electronegativity of thiol group comparison to other groups. Thus, thiol linked ODN was chosen for the further experiments in order to obtain higher sensitivity and selectivity by using DNA immobilized polymer modified electrode. Histograms representing oxidation peak current of adenine obtained with thiol linked, amino linked, phosphate linked and unmodified ODNs are also given respectively in Figure 9.73a, b, c, d. As seen from this figure the oxidation peak current of adenine was maximum with thiol linked ODN.

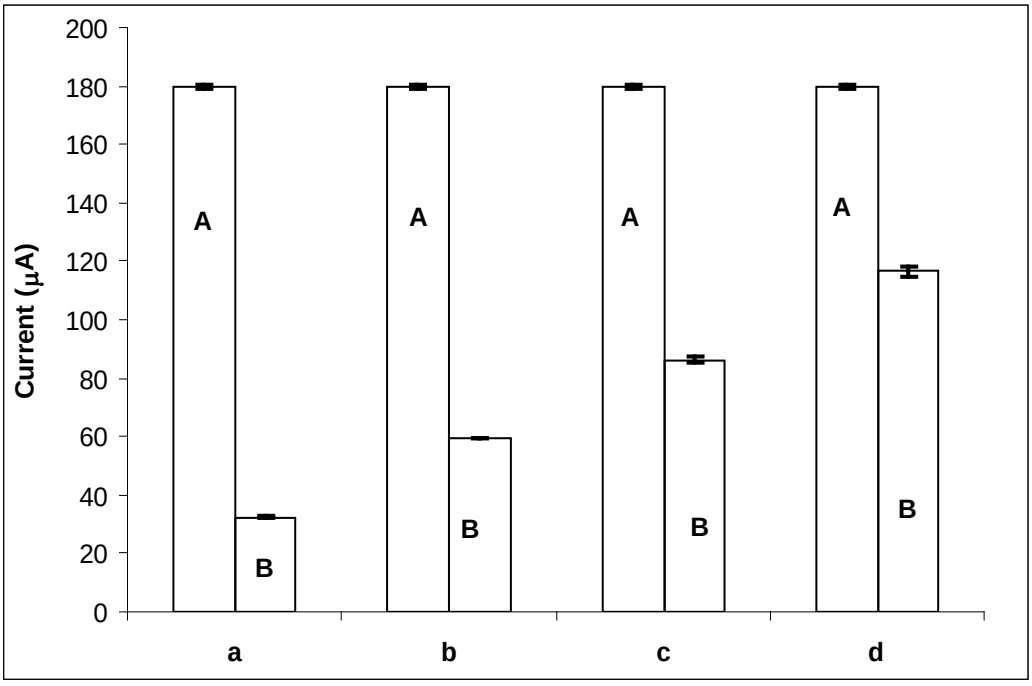

Figure 9.72. Histograms showing the changes at the oxidation peak current of polymer in the absence (A) and the presence (B) of ODNs; (a) thiol linked ODN, (b) amino linked ODN, (c) phosphate linked ODN, (d) unmodified ODN.

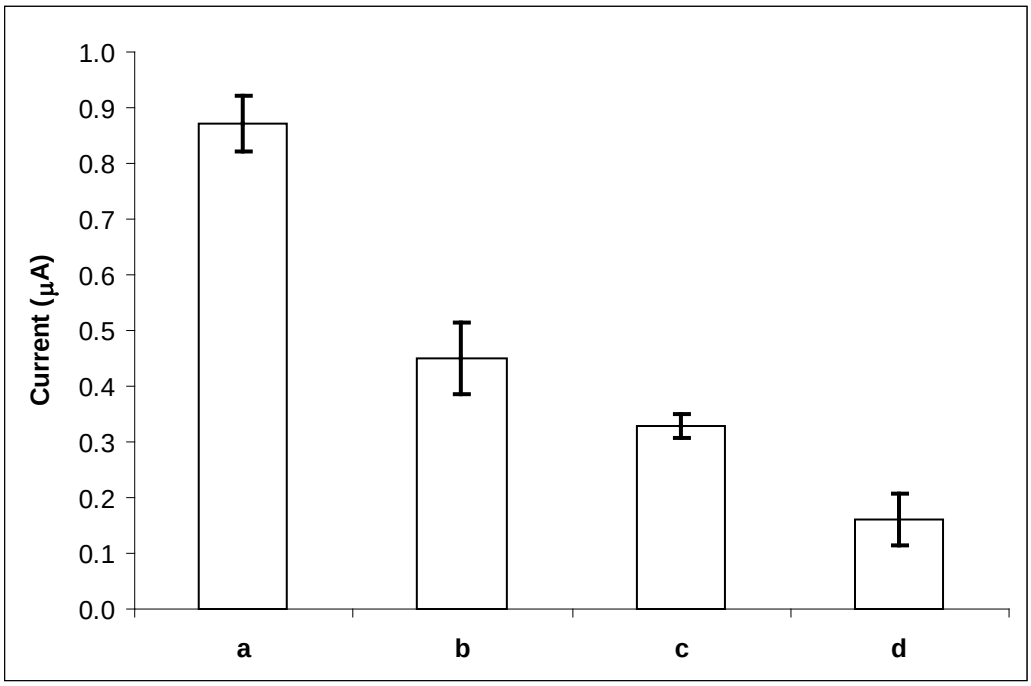

Figure 9.73. Histograms representing oxidation peak currents of adenine obtained with (a) thiol linked ODN, (b) amino linked ODN, (c) phosphate linked ODN, (d) unmodified ODN.

9.5.4.1. Hybridization studies carried out with thiol linked probe

The effect of thiol linked ODN concentration on the oxidation peak currents of polymer was studied in various ODN concentration from 25 to 200 μg mL^{-1}. The oxidation peak current of polymer decreased gradually and then levelled off, when the concentration of ODN was increased to 175 μg mL^{-1} (Figure 9.74). The optimum immobilization concentration for 20-mer thiol linked ODN was found as 175 μg mL^{-1}.

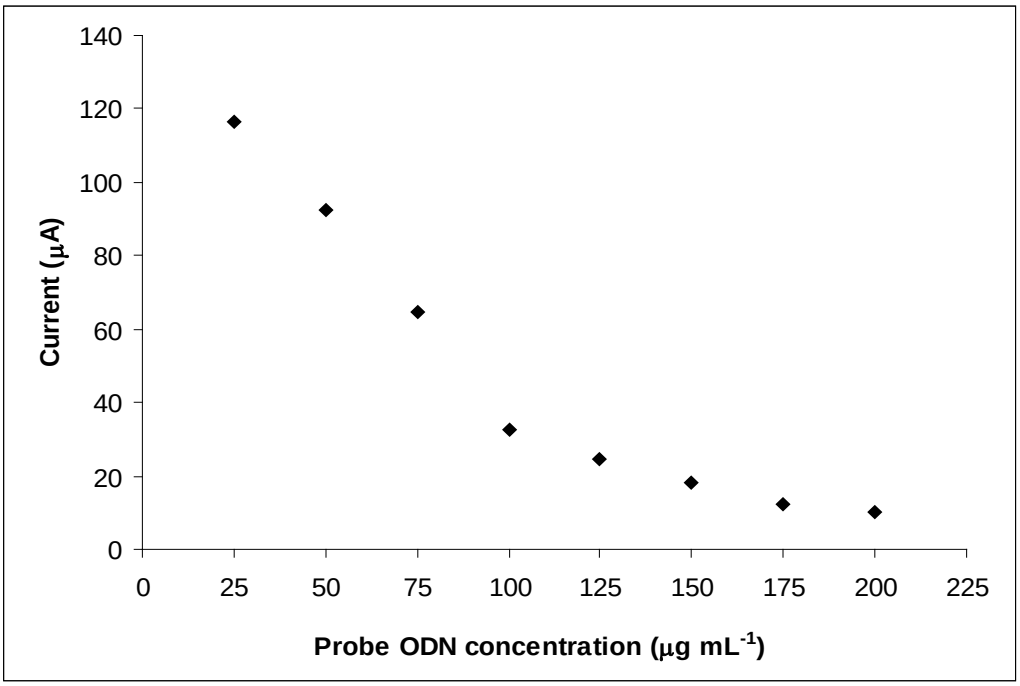

Figure 9.74. The effect of thiol linked ODN concentration to the response of PVF^{+}.

DNA hybridization was also studied. The changes at the oxidation peak current of the polymer were monitored in the presence of thiol linked probe alone and the hybridization between probe and target / NC / MM sequences, respectively (Figure 9.79a, b, c, d). Due to the specific binding of thiol linked probe with its complementary sequence (target) at the polymer matrix, oxidation peak current of polymer decreased (20.1 %) in the presence of DNA hybridization (Figure 9.75a and b). In the presence of target sequence it was also seen that there was a significant shift in the oxidation peak potential of the polymer. The oxidation of guanine was observed at 0.71 V in the case of hybridization of probe which didn't contain guanine base and target. The selectivity in hybridization of thiol linked probe with NC and MM sequences was also checked (Figure 9.75c and d). A small decrease was obtained in the hybridization between probe and NC (3.3 %), or probe and MM (4.2 %) (Sanchez-Pomales et al., 2007; Prabhakar et al., 2008a, b; Degefa and Kwak, 2008). Related histograms are also given in Figure 9.76.

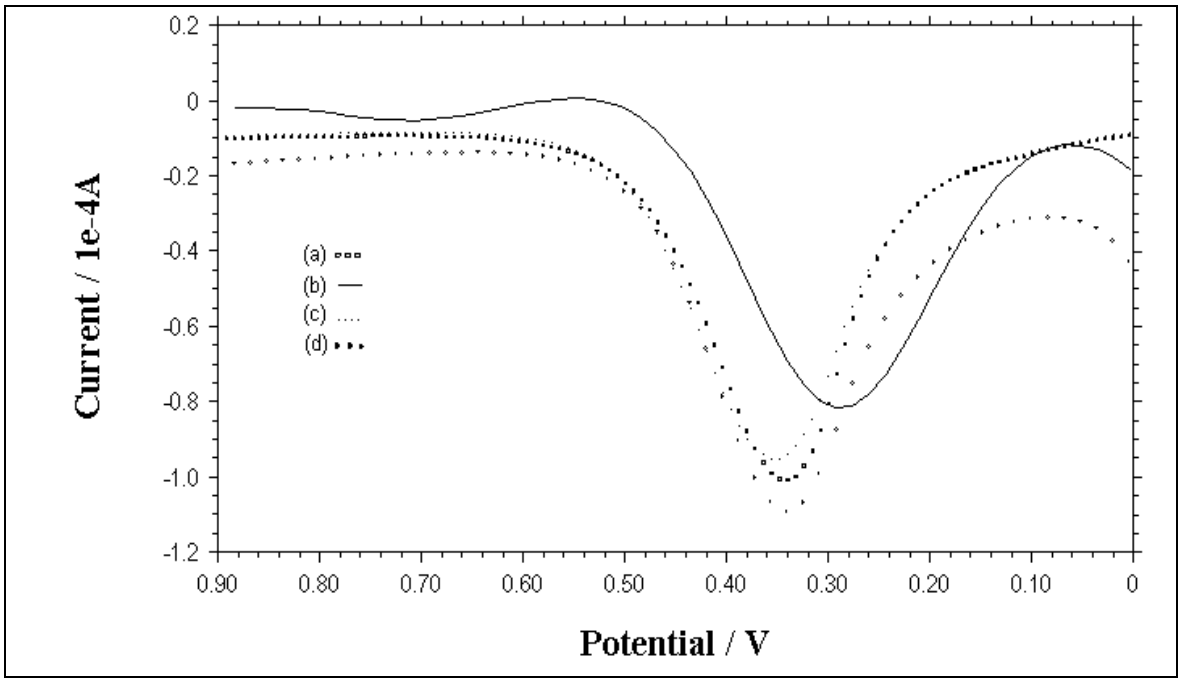

Figure 9.75. DPVs showing the oxidation peak of the polymer (a) 50 μg mL^{-1} probe alone, (b) after hybridization between probe and 50 μg mL^{-1} complementary, (c) interaction between probe and 50 μg mL^{-1} NC, (d) interaction between probe and 50 μg mL^{-1} MM. Pulse amplitude: 50 mV.

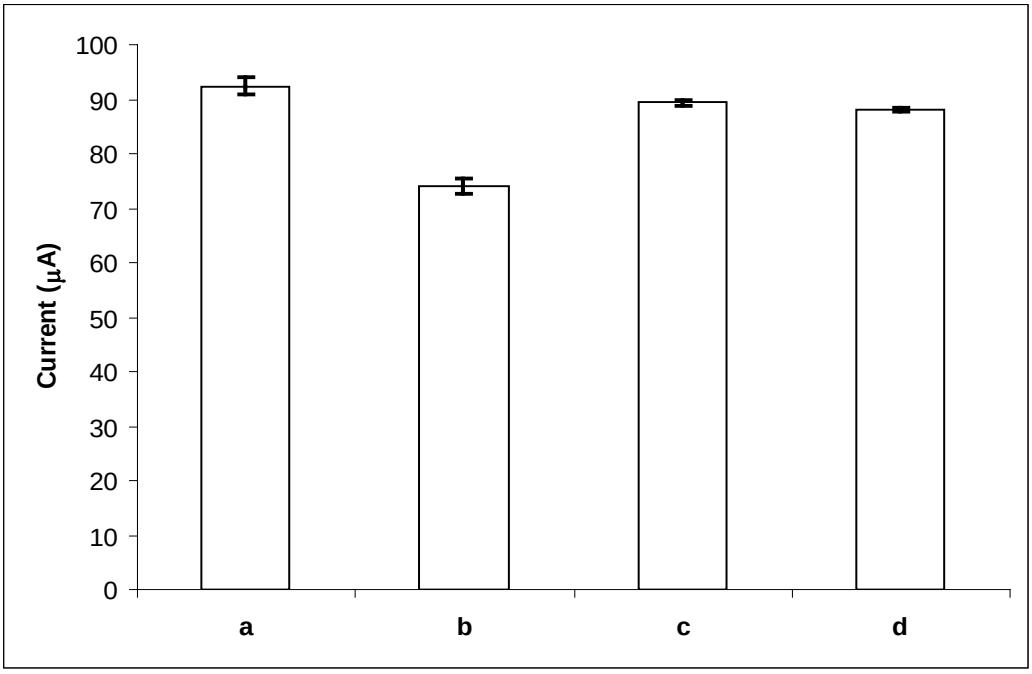

Figure 9.76. Histograms showing the oxidation peak current of the polymer (a) 50 μg mL^{-1} probe alone, (b) after hybridization between probe and 50 μg mL^{-1} complementary, (c) interaction between probe and 50 μg mL^{-1} NC, (d) interaction between probe and 50 μg mL^{-1} MM.

The effect of target concentration on the oxidation peak current of polymer was also studied at various target concentrations from 25 to 175 μg mL^{-1}. The oxidation peak current of polymer decreased gradually and then levelled off, when the concentration of target was increased to 125 μg mL^{-1} (Figure 9.77). The related voltammograms at three different concentrations of target ODN were shown in Figure 9.78. As seen from this figure, guanine and adenine oxidation peak currents were enhanced with increasing target concentration. It is also clear that their oxidation peak potentials shifted with increasing target concentration indicating more interaction of DNA with Fe(II/III) redox couple (Chen and Wang, 2007).

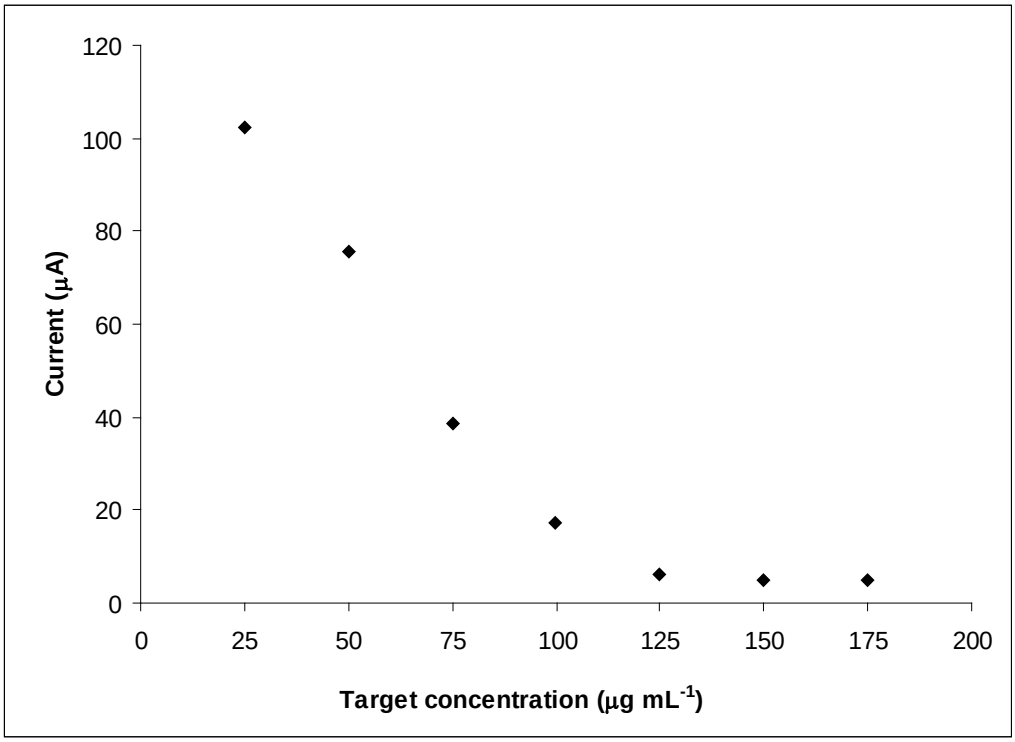

Figure 9.77. The effect of target concentration to the response of PVF^{+}.

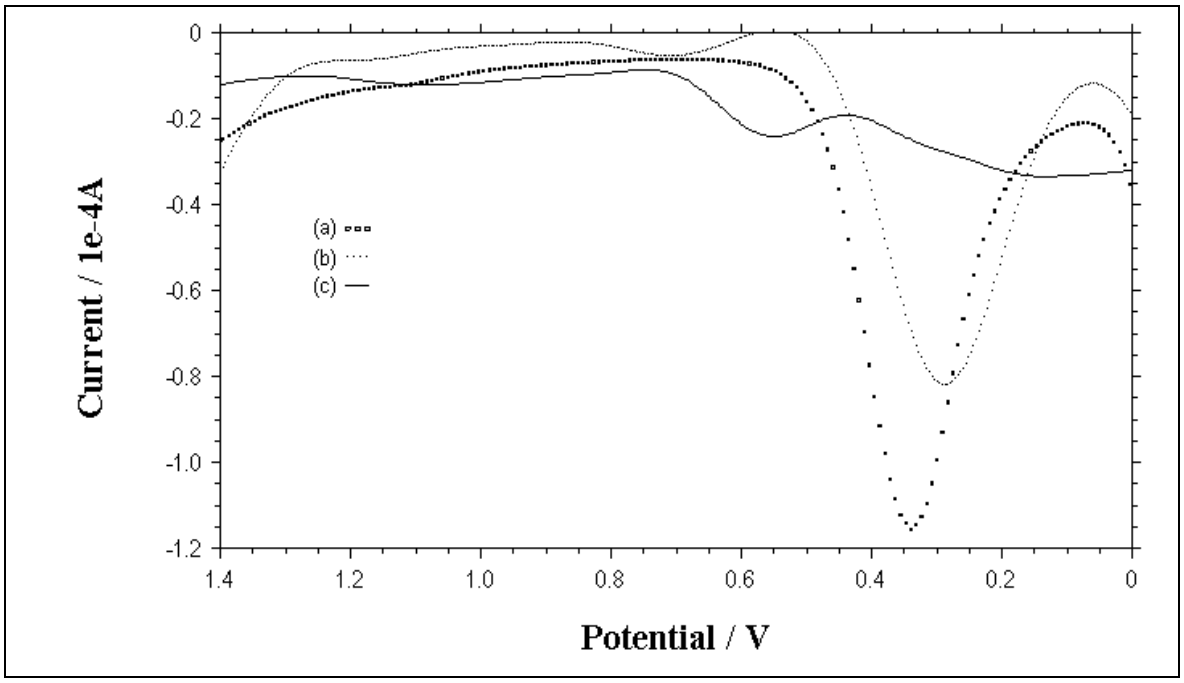

Figure 9.78. DPVs of (a) 25 μg mL^{-1} (b) 50 μg mL^{-1} (c) 125 μg mL^{-1} target ODN.

9.6. Characterization of Polymer Modified Electrodes

In this part of the study, polymer modified and DNA immobilized polymer modified electrodes were characterized by scanning electron microscopy (SEM), scanning tunneling microscopy (STM), raman spectroscopy, X-ray photoelectron spectroscopy (XPS), fourier transform infrared-attenuated total reflentance (ATR) spectroscopy and alternating current (AC) impedance spectroscopy.

9.6.1. Scanning electron microscopy (SEM) analysis

The surface morphologies of $PVF^+ClO_4^-$ and dsDNA immobilized PVF^+ films onto Pt foil electrode were examined by SEM analysis to verify the explanation given above for DNA immobilization. A low and a high magnitude SEM images of $PVF^+ClO_4^-$ are shown in Figure 9.79A. As can be seen from this figure, $PVF^+ClO_4^-$ film had regular globular shape with a diameter of approximately 600 nm. However some parts of the regular structure of $PVF^+ClO_4^-$ film became irregular because of dsDNA immobilization (Figure 9.79B). When the immersion time of the modified electrode was extended, it was observed that irregularities in the image increased (Figure 9.79C). SEM analysis showed that some PVF^+ sites were blocked by DNA immobilization and this observation confirmed the previous electrochemical results.

(A)

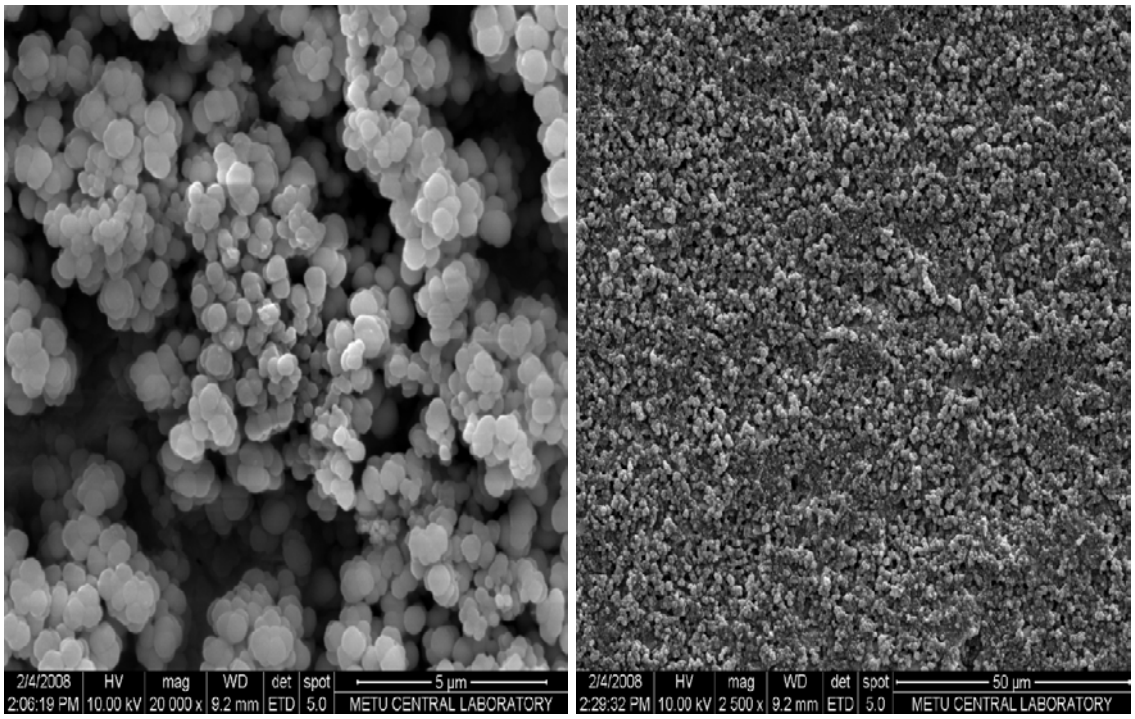
2/4/2008 | HV | mag | WD | det | spot | 5 µm
2:06:19 PM | 10.00 kV | 20 000 x | 9.2 mm | ETD | 5.0 | METU CENTRAL LABORATORY
2/4/2008 | HV | mag | WD | det | spot | 50 µm
2:29:32 PM | 10.00 kV | 2 500 x | 9.2 mm | ETD | 5.0 | METU CENTRAL LABORATORY

(B)

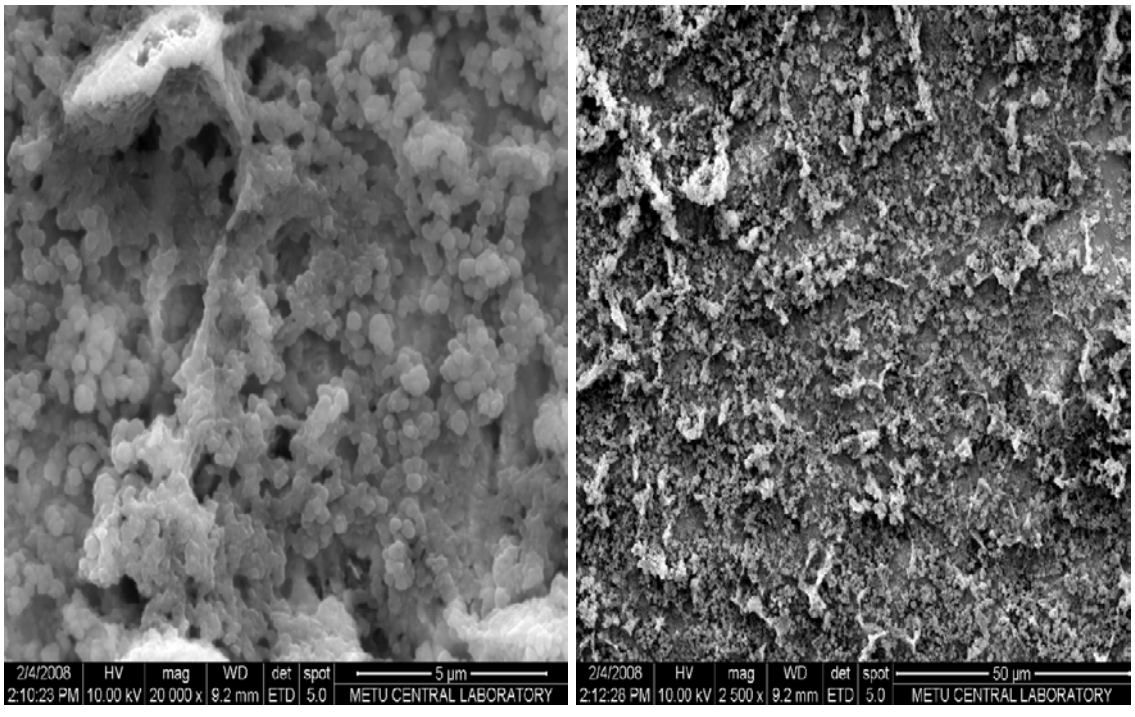
2/4/2008 | HV | mag | WD | det | spot | 5 µm
2:10:23 PM | 10.00 kV | 20 000 x | 9.2 mm | ETD | 5.0 | METU CENTRAL LABORATORY
2/4/2008 | HV | mag | WD | det | spot | 50 µm
2:12:26 PM | 10.00 kV | 2 500 x | 9.2 mm | ETD | 5.0 | METU CENTRAL LABORATORY

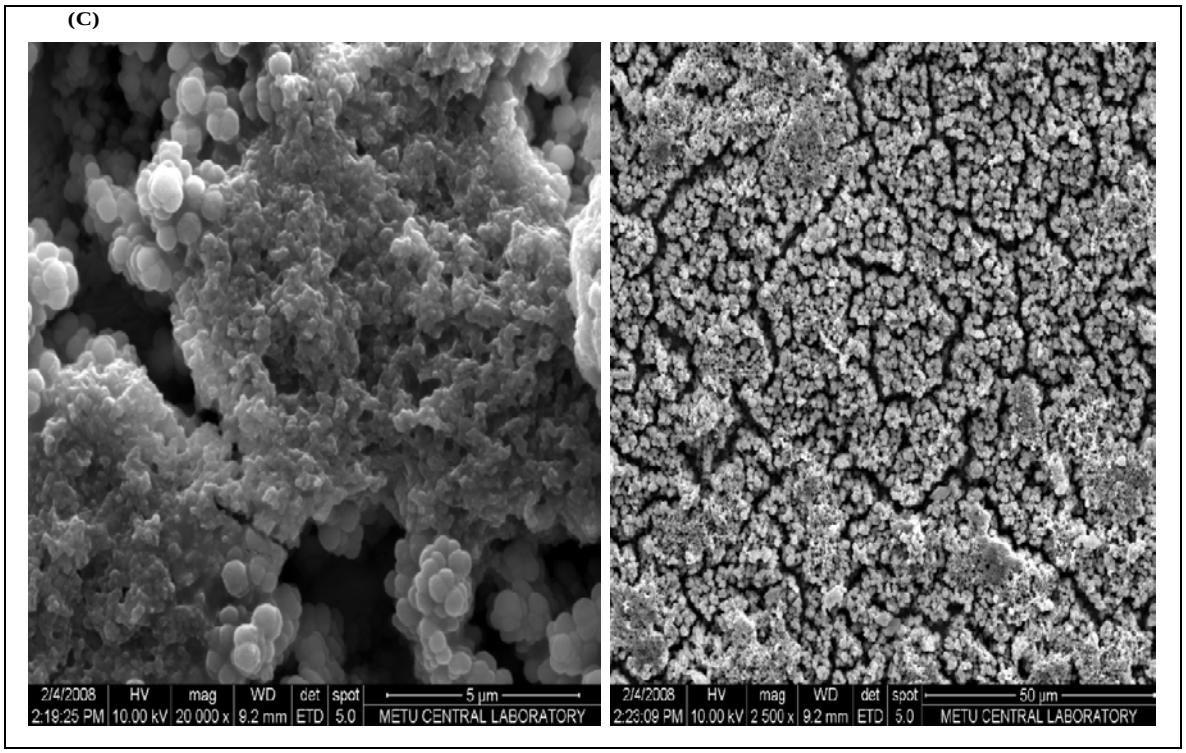

Figure 9.79. SEM images of polymer film (A) before (B) after immersing into 2.5 mg mL^{-1} dsDNA solution 1 hour (C) after immersing into 2.5 mg mL^{-1} dsDNA solution 2 hour.

9.6.2. Scanning tunneling microscopy (STM) images

Figure 9.80A and B exhibit the surface morphologies of $PVF^{+}ClO_4^{-}$ films onto Pt foil electrode examined by STM before and after dsDNA immobilization, respectively. These images show that the Pt surface completely covered with polymer films. In Figure 9.80B, there were highly ordered long grains with about 50 nm width oriented horizontally to each other. However, in Figure 9.80b, it is observed that ordered structure was changed and surface was covered with irregular film. Thus, it is proposed that, some region of the polymer surface was blocked by dsDNA layer and the regular structure of $PVF^{+}ClO_4^{-}$ film was corrupted.

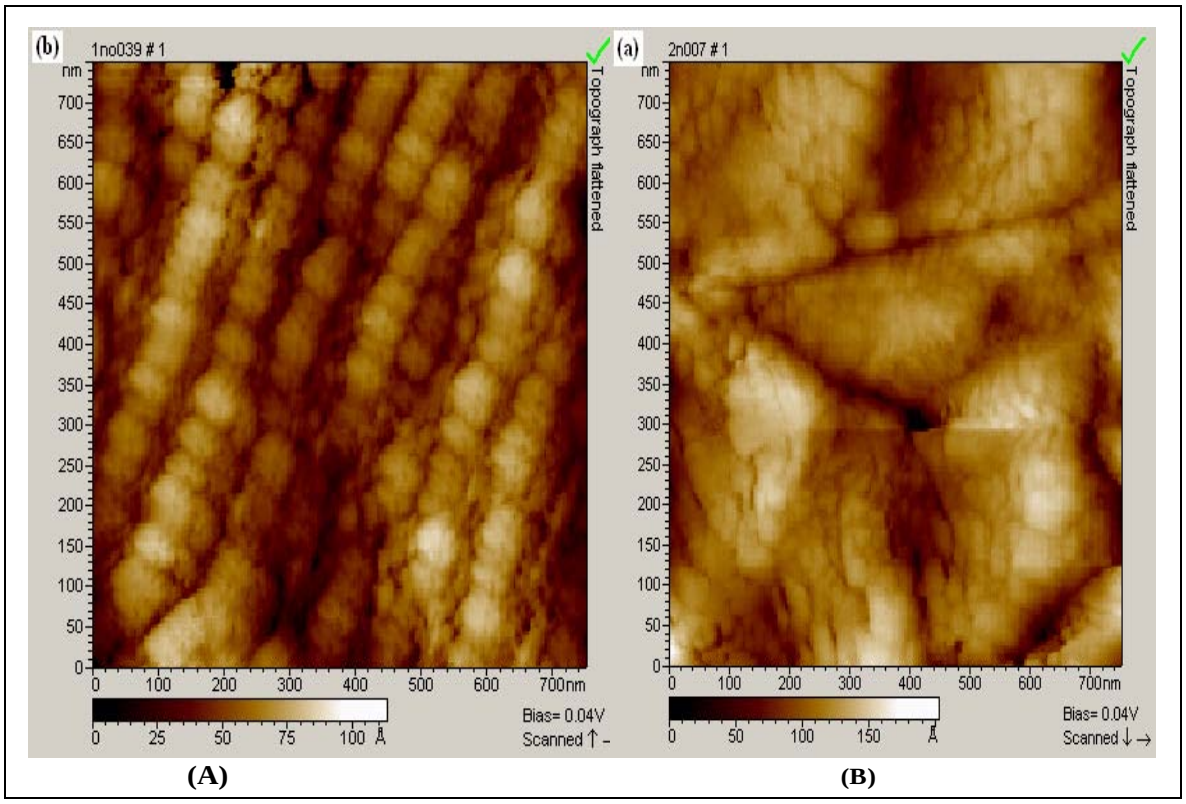

Figure 9.80. STM images of $PVF^{+}ClO_4^{-}$ films (A) before (B) after immersing into 2.5 mg mL^{-1} dsDNA solution for 1 hour.

9.6.3. Raman spectra

$PVF^{+}ClO_4^{-}$ films before and after immersing into dsDNA solution were subjected to Raman spectroscopy, respectively (Figure 9.81 and B). When these spectra were carefully analyzed, it was observed that the bands in the wave number region of approximately 1060 cm^{-1} and 1100 cm^{-1} changed after dsDNA immobilization. This change in bands are mainly related to symmetric stretching vibrations of the deoxyribose-phosphate backbone of DNA molecule, indicating that phosphate groups can be immobilized on the positively charged matrix. It is also seen that there was small peak at about 1550 cm^{-1} in the Raman spectrum of DNA immobilized $PVF^{+}ClO_4^{-}$ film which was assigned to the vibration of nitrogen containing DNA bases (Zhao et al., 1999). Thus, it can be concluded that dsDNA was immobilized onto the polymer modified electrode both by phosphate groups and bases.

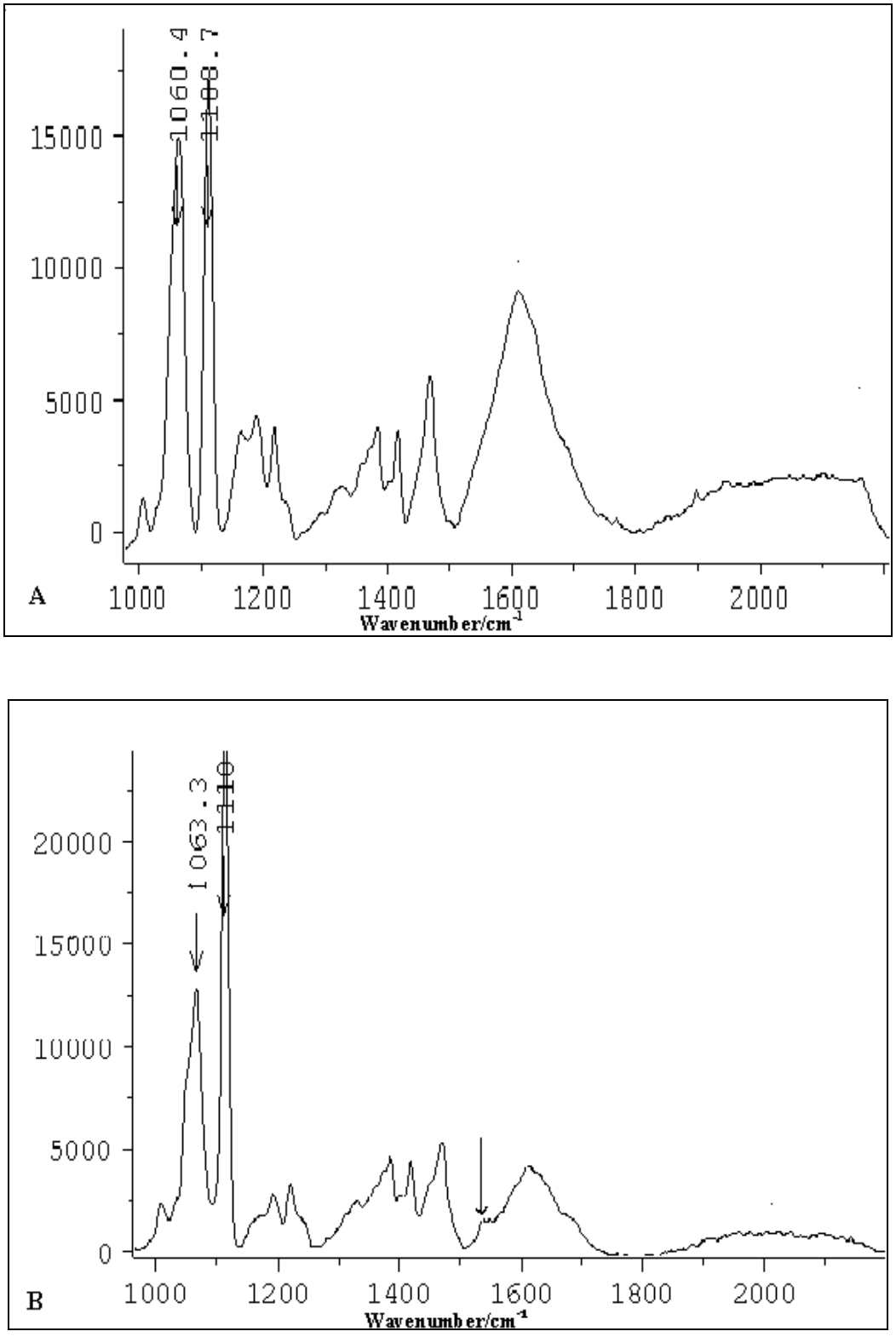

Figure 9.81. Raman spectra of $PVF^{+}ClO_4^{-}$ films (A) before and (B) after immersing into 2.5 mg mL^{-1} dsDNA solution for 1 hour.

9.6.4. X-ray photoelectron spectroscopy (XPS) spectra

Figure 9.82A, B and C shows the wide energy range of XPS spectra of the polymer modified, dsDNA immobilized polymer modified and ssDNA immobilized polymer modified electrodes, respectively. The main peaks due to elements, atom % and ranges are also given in Table 9.1 for polymer modified electrode, in Table 9.2 for dsDNA immobilized polymer modified electrode and in Table 9.3 for ssDNA immobilized polymer modified electrode. The best evidences of DNA immobilization onto polymer modified electrode were the presence of the P and N peaks which found in the structure of DNA (Figure 9.82B and C). These results are parallel to the results found in the literature (Zhao, et al., 1999) and our Raman studies. It is concluded that ds/ssDNA were immobilized onto the surface of polymer modified electrode both by phosphate groups and N containing DNA bases. It is also found that the interaction of polymer with dsDNA was better than the interaction of polymer with ssDNA supporting the electrochemical results.

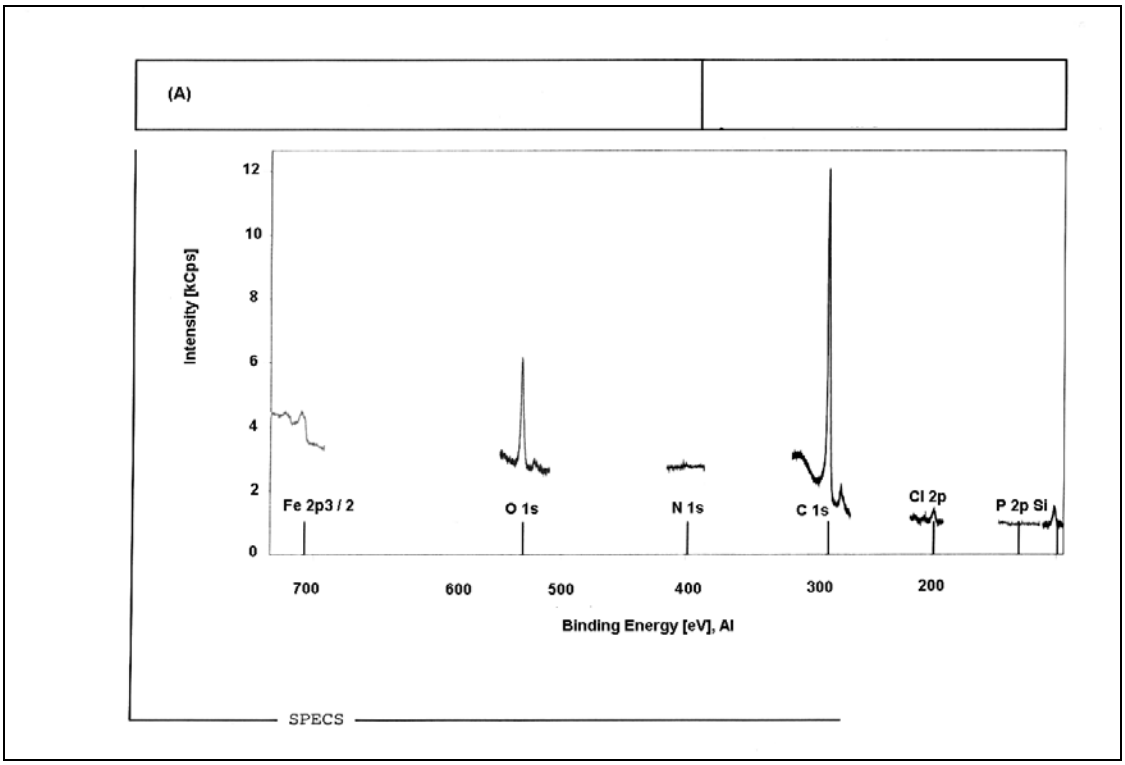

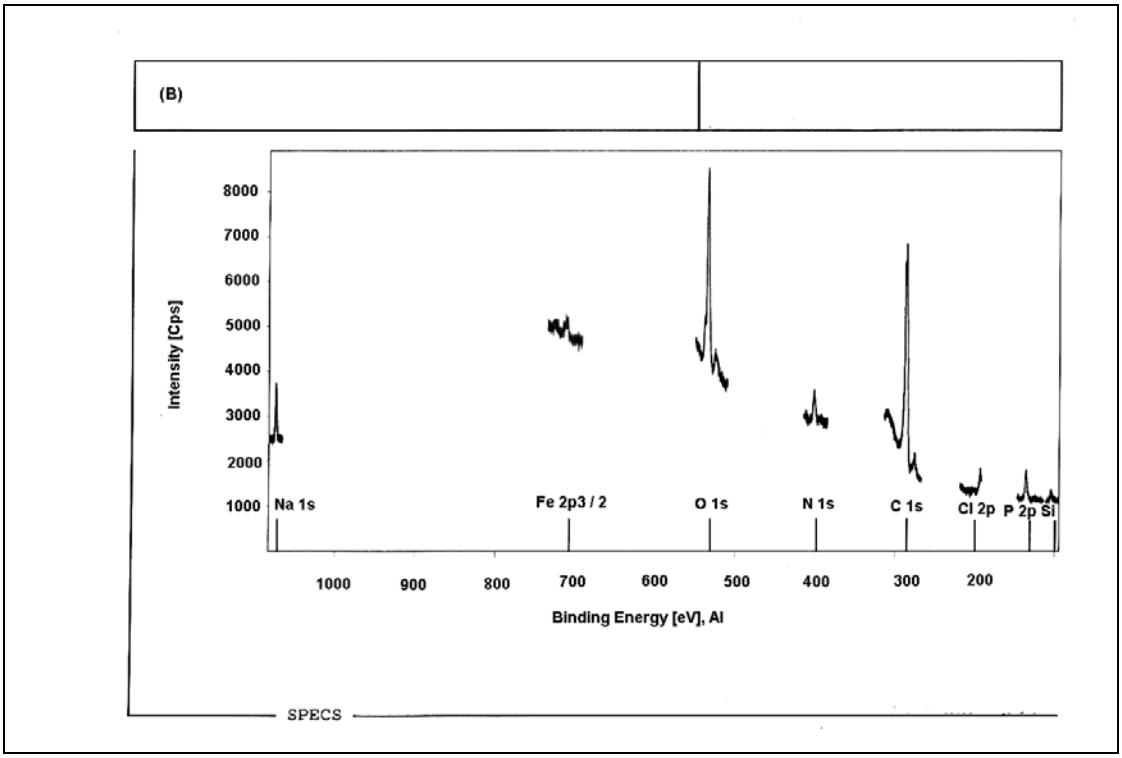

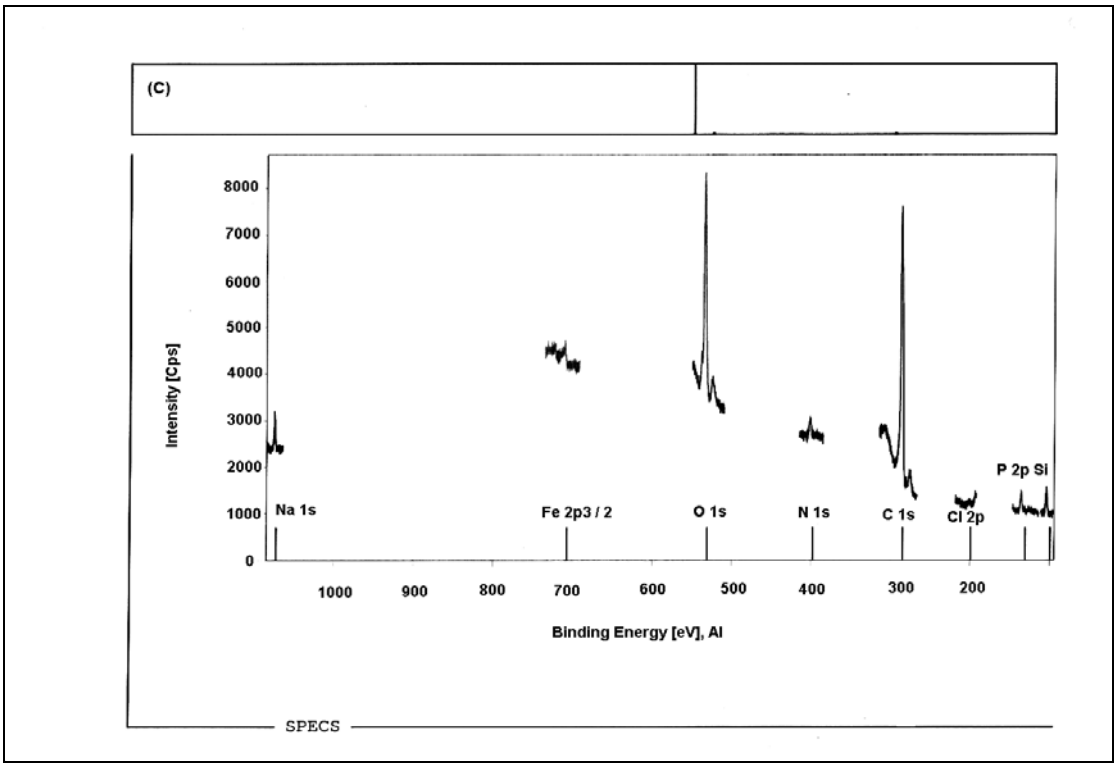

Figure 9.82. XPS spectra of $PVF^{+}ClO_4^{-}$ film (A) before, (B) after immersing into 2.5 mg mL^{-1} dsDNA solution for 1 hour (C) after immersing into 2.5 mg mL^{-1} ssDNA solution for 1 hour.

Table 9.1. Data for polymer modified electrode

Element	Atom %	Range
C	78.8	292.7 - 279.2
N	0.2	398.1 - 396.6
O	13.2	538.6 - 526.8
Si	5.4	108 - 98.2
P	0.0	130 - 130
Cl	1.2	204 - 195.5
Fe	1.2	714.3 - 705.8

Table 9.2. Data for dsDNA immobilized polymer modified electrode

Element	Atom %	Range
C	63.0	293.9 - 282
N	4.6	408.3 - 397
O	23.9	541.6 -527.7
Na	3.2	1079.1 - 1070.7
Si	2.2	109.8 - 98.2
P	3.1	141.2 - 129.2
Cl	0.0	205.3 - 198.7

Table 9.3. Data for ssDNA immobilized polymer modified electrode

Element	Atom %	Range
C	64.5	294.2 - 281.5
N	3.3	408 - 397
O	23.2	542.2 - 528.7
Na	1.9	1079.1 - 1070.7
Si	4.5	110.2 -98.2
P	2	141.5 - 129.2
Cl	0.0	205.2 - 197
Fe	0.5	714.1 -706

9.6.5. Fourier transform infrared-attenuated total reflentance (ATR) spectroscopy

Fourier transform infrared-attenuated total reflentance (ATR) spectra of polymer film and dsDNA immobilized polymer film are given in Figure 9.83A and 9.83B, respectively. The peaks in the spectrum of $PVF^{+}ClO_4^{-}$ that appeared about 623 and 1093 cm^{-1} were due to the presence of ClO_4^{-} ion in the polymer structure (Kuralay et al., 2005). In the spectrum of dsDNA immobilized polymer film, intensity of the peaks that belonged to ClO_4^{-} decreased due to the anion exchange occurred between counter anion and negatively charged phosphate backbone of DNA molecule.

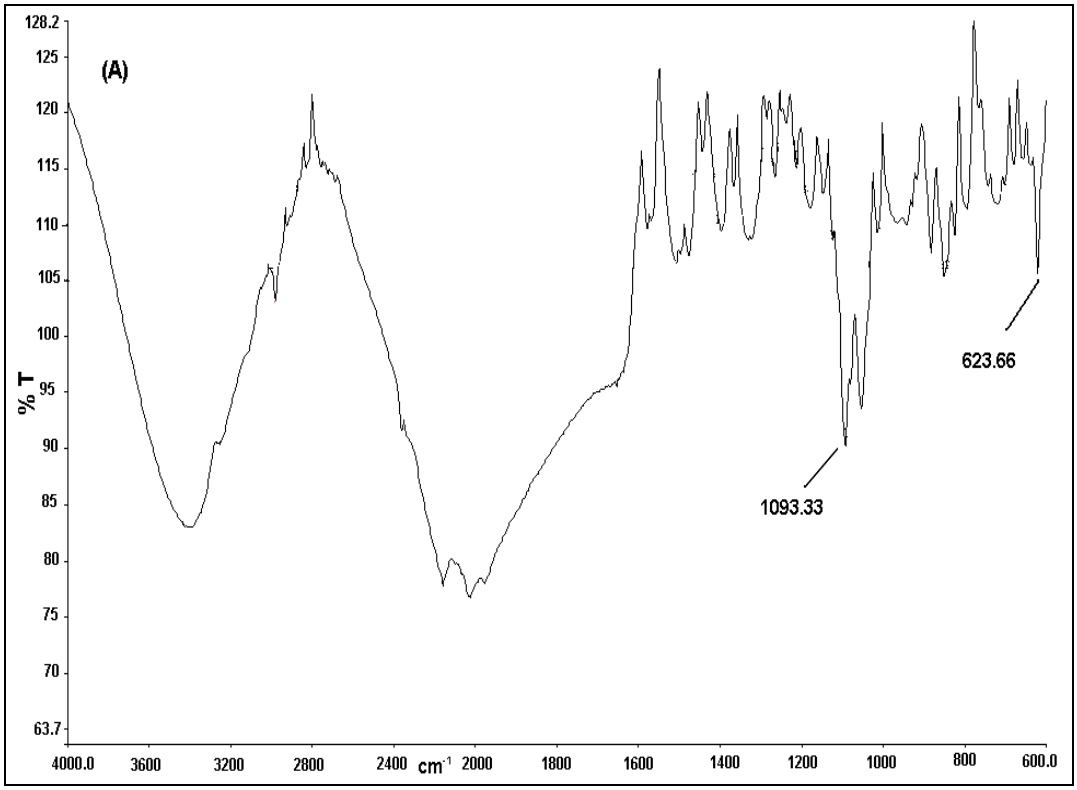

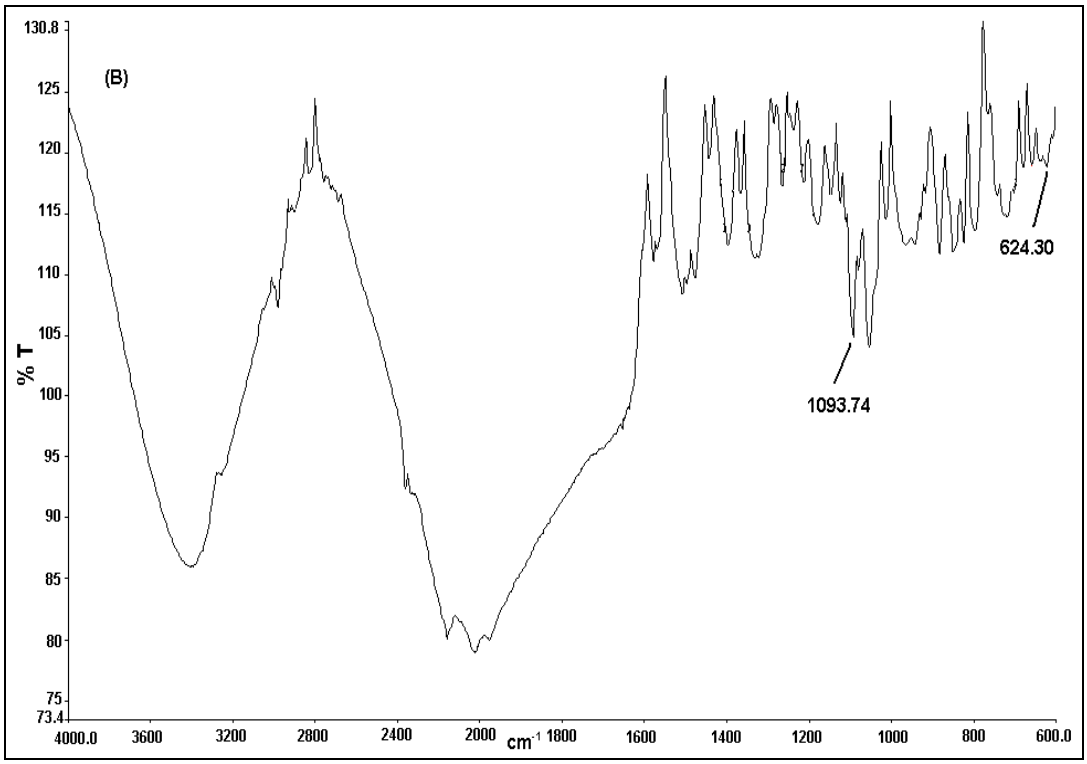

Figure 9.83. ATR spectra of $PVF^{+}ClO_4^{-}$ film (A) before, (B) after immersing into 2.5 mg mL^{-1} dsDNA solution for 1 hour.

9.6.6. Alternating current (AC) impedance spectroscopy

AC impedance, which has been used as an effective and rapid method to measure the impedance value of the electrode surface during the process of the frequency variation was also used to identify and differentiate the immobilization of ss/dsDNA on the polymer modified electrode (Jiang et al., 2008). In the Nyquist plot of impedance spectra, the semicircle portion at higher frequencies correspond to the charge-transfer limited process and linear portion seen at lower frequencies may be ascribed to the diffusion process (Arora et al., 2007). The diameter of the semicircle represents the charge-transfer resistance (R_{ct}) at the electrode surface (Degefa and Kwak, 2008). AC impedance measurements were controlled at the open-circuit value; +0.4 V and the frequency was varied over the range 10^{5}-10^{-2} Hz with amplitude of 5 mV in 50 mM PBS containing 0.1 M $NaClO_4$. Figure 9.84a, b, c shows the impedance spectra of polymer modified electrode, ssDNA immobilized polymer modified electrode and dsDNA immobilized polymer electrode, respectively. There was an increase obtained at the R_{ct} values after DNA immobilization onto the surface of the polymer modified electrode that indicated the enhanced resistance to the charge-transfer occured at the electrode

surface. These results presented in Figure 9.84 were found in a good agreement with the results obtained by using voltammetric methods; CV and DPV techniques.

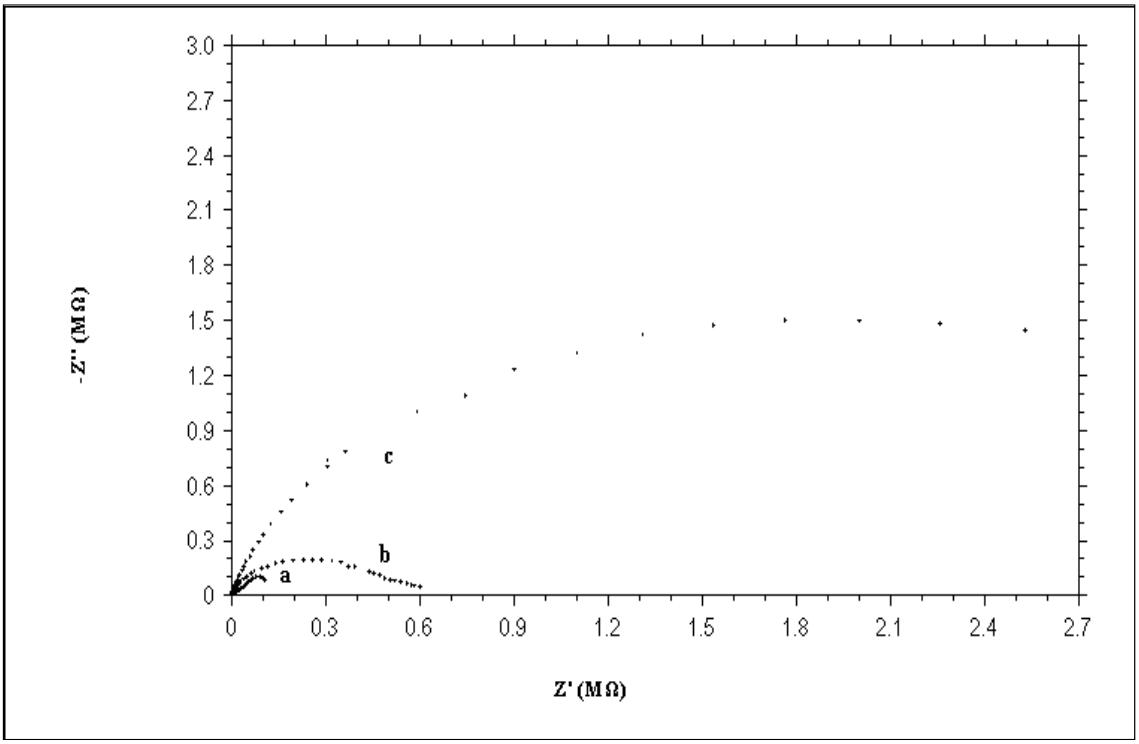

Figure 9.84. AC impedance spectra of $PVF^{+}ClO_4^{-}$ film (a) before, (b) after immersing into 2.5 mg mL^{-1} ssDNA solution for 1 hour, (c) after immersing into 2.5 mg mL^{-1} dsDNA solution for 1 hour in PBS containing 0.1 M $NaClO_4$.

9.7. Interaction of Anticancer Drug Mitomycin C (MC) and ds/ssDNA Immobilized Polymer Modified Electrodes

In this part of the study, the interaction of anticancer drug Mitomycin C (MC) and dsDNA immobilized polymer modified electrode or ssDNA immobilized polymer modified electrode was investigated. Firstly, DPV of dsDNA or ssDNA was immobilized onto polymer modified Pt working electrode was recorded in 50 mM PBS containing 0.1 M $NaClO_4$ after immersing the electrode in 2500 μg mL^{-} DNA solution for 1 hour. Then, ds/ssDNA immobilized Pt electrode was immersed into 100 μg mL^{-1} MC solution and kept for 1 hour and DPV of this system was recorded. The interaction of MC with dsDNA and ssDNA immobilized polymer modified electrodes are given in Figure 9.85 and Figure 9.86, respectively. A significant decrease was observed at the interaction of dsDNA or ssDNA with the polymer matrix after the interaction between MC and DNA. This decrease was

attributed to the binding of MC to DNA by shielding of oxidizable groups of electroactive DNA bases and electrostatic interaction occured between polymer and phosphate backbone of DNA (Rauf et al., 2005; Karadeniz et al., 2007b).

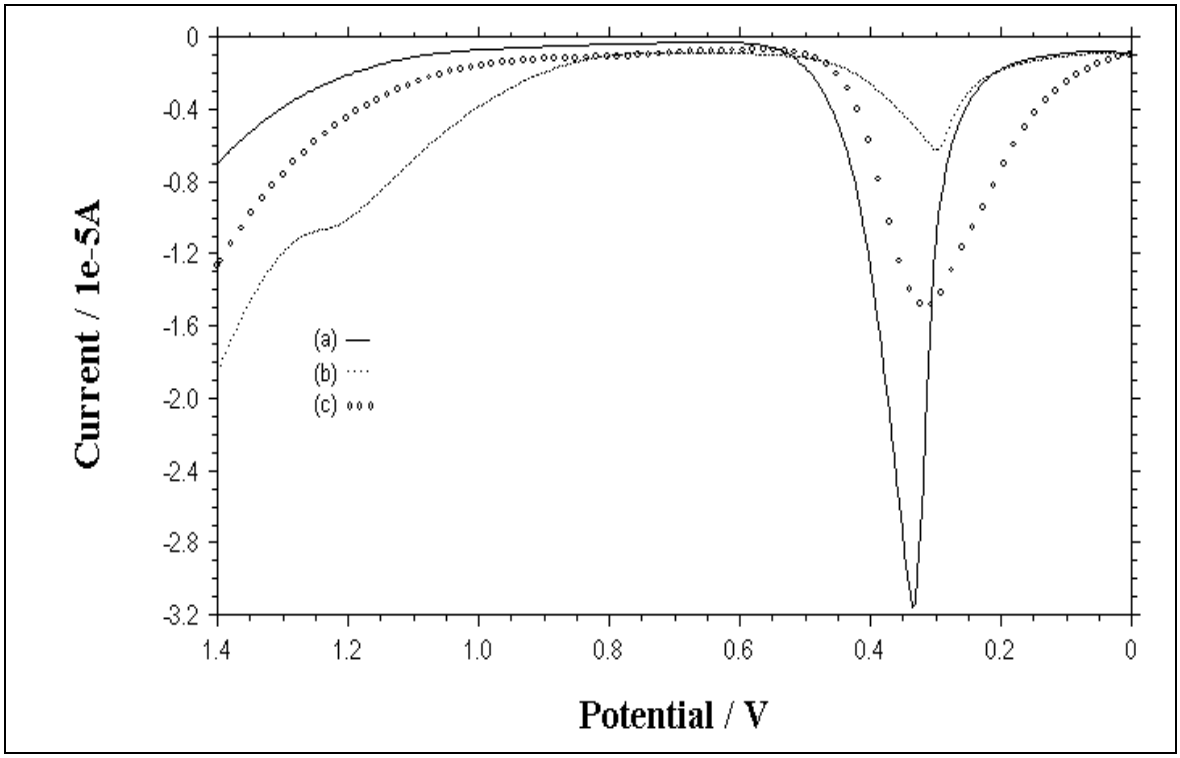

Figure 9.85. DPVs of (a) $PVF^{+}ClO_4^{-}$ film (b) $PVF^{+}ClO_4^{-}$ film after immersing into 2500 μg mL^{-} dsDNA solution (c) dsDNA immobilized polymer film after immersing into 100 μg mL^{-1} MC in 50 mM PBS containing 0.1 M $NaClO_4$. Pulse amplitude: 50 mV.

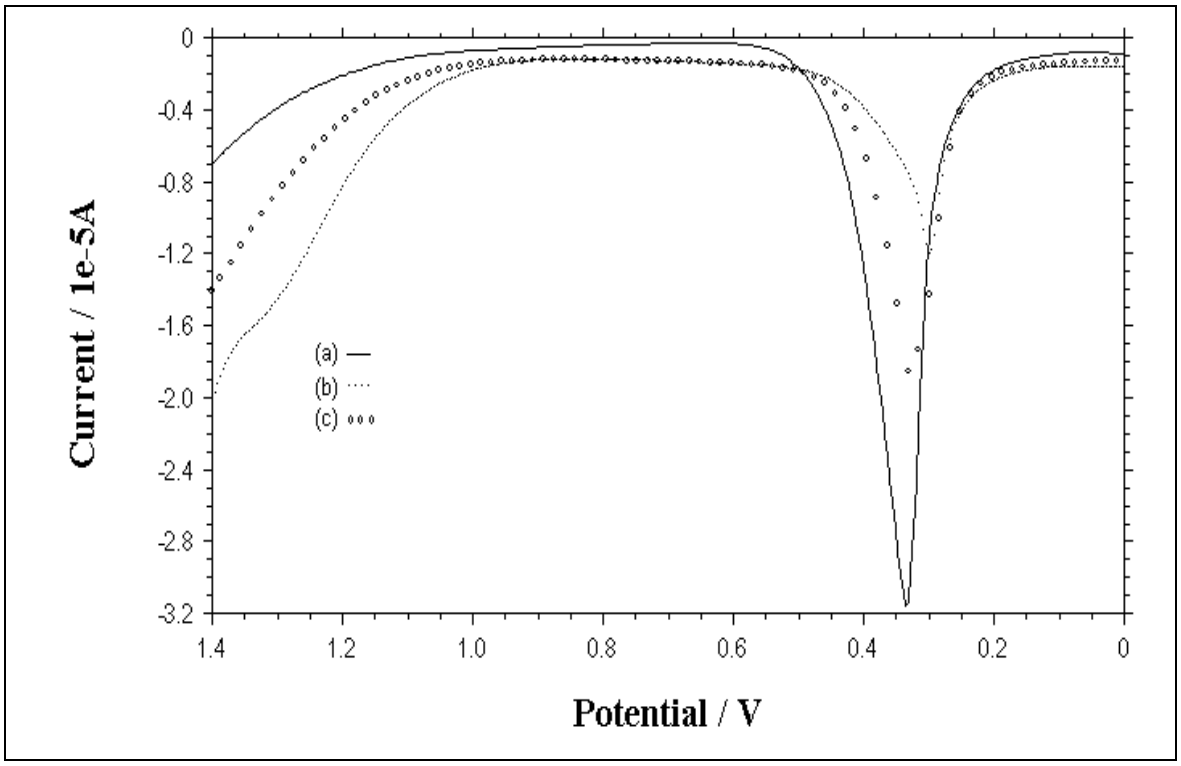

Figure 9.86. DPVs of (a) $PVF^{+}ClO_4^{-}$ film (b) $PVF^{+}ClO_4^{-}$ film after immersing into 2500 μg mL^{-} ssDNA solution (c) ssDNA immobilized polymer film after immersing into 100 μg mL^{-1} MC in 50 mM PBS containing 0.1 M $NaClO_4$. Pulse amplitude: 50 mV.

10. CONCLUSIONS

In this work, preparation, application and characterization of electrochemical DNA biosensor based on PVF^+ modified electrodes was discussed. Electrodeposition of $PVF^+ClO_4^-$ onto the working electrode was performed in the solution of PVF including methylene chloride/TBAP solvent/supporting electrolyte system at +0.7 V vs. Ag/AgCl. The thicknesses of the polymer films were controlled by the charge passed during the electroprecipitation of oxidized form of the polymer onto the electrode.

Immobilization of dsDNA and ssDNA were performed immersing the polymer modified working electrode into ds/ssDNA solution by stirring. ODNs were immobilized onto polymer modified Pt and Au electrodes by dropping ODN solutions. ODN immobilized polymer modified PG electrode was performed immersing the polymer modified working electrode into PG solution.

The changes at the oxidation peak of polymer and electroactive DNA bases, adenine and guanine, were sensitively monitored by using CV and DPV techniques in the absence/presence of DNA. The oxidation peak current of the polymer decreased after DNA immobilization due to less conductive character of DNA molecule.

The electrochemical behavior of PVF^+ modified Pt electrode was investigated in the absence or presence of DNA. The investigation of parameters influencing DNA immobilization onto $PVF^+ClO_4^-$ film was studied in terms of optimum analytical conditions; the effects of; the polymeric film thickness, concentration of dsDNA, immobilization time of dsDNA, the concentration of PBS solution, different buffer solutions, pH and temperature of the medium, the concentration of ClO_4^- ion. The optimum conditions were found as 1.0 mC polymeric film thickness, 2.5 mg mL^{-1} DNA concentration, 1 hour immobilization time of dsDNA, pH 7.0 50 mM PBS containing 0.1 M $NaClO_4$ and 30 °C. The detection limit corresponds to 1.56 $\mu g\ mL^{-1}$ for dsDNA immobilized polymer modified Pt electrode using DPV technique.

Electrostatic interaction between the positively charged polymer and negatively charged DNA was tested by reducing the polymer at + 0.2 V vs. Ag /AgCl.

After the optimum working conditions were obtained, the electrochemical behavior of DNA immobilized polymer modified Pt electrode by using dsDNA or ssDNA was compared. It was found that the interaction of dsDNA was stronger than ssDNA with polymer matrix.

The effect of different ODN modifications on the response of polymer modified Pt electrode was examined with thiol linked, amino linked, phosphate linked and unmodified ODNs in respect to their binding performance onto the positively charged polymer matrix. Thiol linked ODN gave the best binding performance. The optimum immobilization concentration for 20-mer thiol linked ODN was found as 150 $\mu g\ mL^{-1}$. The optimum concentration for 20-mer amino linked ODN was found as 175 $\mu g\ mL^{-1}$.

DNA hybridization was studied with thiol linked and amino linked ODNs at polymer modified Pt electrode. The optimum immobilization concentration for target ODN was found as 100 $\mu g\ mL^{-1}$ using thiol linked probe. The optimum immobilization concentration for target ODN was found as 125 $\mu g\ mL^{-1}$ using amino linked probe.

The electrochemical behavior of PVF^{+} modified Au electrode was investigated in the absence or presence of DNA. The investigation of parameters influencing DNA immobilization onto $PVF^{+}ClO_4^{-}$ film was studied in terms of optimum analytical conditions; the effects of; the polymeric film thickness, concentration of dsDNA, immobilization time of dsDNA and pH of the medium. The optimum conditions were found as 1.0 mC polymeric film thickness, 1.25 mg mL^{-1} DNA concentration, 1 hour immobilization time of dsDNA and pH 7.0 PBS containing 0.1 M $NaClO_4$. The detection limit corresponds to as 12.00 $\mu g\ mL^{-1}$ for dsDNA immobilized polymer modified Au electrode using DPV technique.

After the optimum working conditions were obtained, the electrochemical behavior of DNA immobilized polymer modified Au electrode by using dsDNA or ssDNA

was compared. It was found that the interaction of dsDNA was stronger than ssDNA with polymer matrix.

The effect of different ODN modifications on the response of polymer modified Au electrode was examined with thiol linked, amino linked, phosphate linked and unmodified ODNs in respect to their binding performance onto the positively charged polymer matrix. Thiol linked ODN gave the best binding performance. The optimum immobilization concentration for 20-mer thiol linked ODN was found as 175 $\mu g\ mL^{-1}$.

DNA hybridization was studied with thiol linked ODN at polymer modified Au electrode. The optimum immobilization concentration for target ODN was found as 75 $\mu g\ mL^{-1}$.

The electrochemical behavior of PVF^{+} modified PG electrode was investigated in the absence or presence of DNA. The investigation of parameters influencing DNA immobilization onto $PVF^{+}ClO_4^{-}$ film was studied in terms of optimum analytical conditions; the effects of; the polymeric film thickness and immobilization time of dsDNA. The optimum conditions were founds as 2.0 mC polymeric film thickness, and 30 min immobilization time of dsDNA.

After the optimum working conditions were obtained, the electrochemical behavior of DNA immobilized polymer modified PG electrode by using dsDNA or ssDNA was compared. It was found that the interaction of dsDNA was stronger than ssDNA with polymer matrix.

The effect of different ODN modifications on the response of polymer modified PG electrode was examined with thiol linked, amino linked, phosphate linked and unmodified ODNs in respect to their binding performance onto the positively charged polymer matrix. Thiol linked ODN gave the best binding performance. The optimum immobilization concentration for 20-mer thiol linked ODN was found as 175 $\mu g\ mL^{-1}$.

DNA hybridization was studied with thiol linked ODN at polymer modified PG electrode. The optimum immobilization concentration for target ODN was found as 125 $\mu g\ mL^{-1}$.

SEM images of $PVF^{+}ClO_4^{-}$ and dsDNA immobilized PVF^{+} films were compared. Some parts of the regular structure of $PVF^{+}ClO_4^{-}$ films became irregular after dsDNA was immobilized onto polymer film. SEM analysis showed that some PVF^{+} sites were blocked by DNA immobilization.

The surface morphologies of $PVF^{+}ClO_4^{-}$ films were examined by STM before and after dsDNA immobilization. These images showed that the Pt surface completely covered with polymer films. It was observed that ordered structure of $PVF^{+}ClO_4^{-}$ films changed and surface was covered with irregular film after dsDNA immobilization. Thus, it was concluded that, some region of the polymer surface was blocked by dsDNA.

$PVF^{+}ClO_4^{-}$ films before and after immersing into dsDNA solution were subjected to Raman spectroscopy. When these spectra were carefully analyzed, it was observed that the bands in the wave number region of approximately 1060 cm^{-1} and 1100 cm^{-1} changed after DNA immobilization indicating that phosphate groups were immobilized on the positively charged matrix. There was also a small peak at about 1550 cm^{-1} in the Raman spectrum of DNA immobilized $PVF^{+}ClO_4^{-}$ film which was assigned to nitrogen containing DNA bases.

XPS spectra of the polymer modified, dsDNA immobilized polymer modified and ssDNA immobilized polymer modified electrodes were compared. The best evidences that DNA had been immobilized onto polymer modified electrode were the presence of the P and N peaks. It was found that the interaction of polymer with dsDNA was better than the interaction of polymer with ssDNA.

ATR spectra of polymer film and dsDNA immobilized polymer film were also compared. The peaks in the spectrum of $PVF^{+}ClO_4^{-}$ that appeared about 623 and 1093 cm^{-1} were due to the presence of ClO_4^{-} ion in the polymer structure. In the spectrum of dsDNA immobilized polymer film, intensity of these peaks decreased

due to the anion exchange occurred between counter anion and negatively charged phosphate backbone of DNA molecule.

AC impedance spectra of polymer modified electrode, ssDNA immobilized polymer modified electrode and dsDNA immobilized polymer electrode in 50 mM PBS containing 0.1 M $NaClO_4$ were recorded. There was an increase obtained at the R_{ct} values after DNA immobilization onto the surface of the polymer modified electrode that had been indicating the enhanced resistance to the charge-transfer occured at the electrode surface. It was found that the resistance to the charge-transfer was higher in the case of dsDNA.

In the last part, the interaction of MC with dsDNA/ssDNA immobilized polymer modified electrode was investigated. It was found that the interaction of dsDNA or ssDNA with positively charged matrix decreased after the interaction of drug with DNA.

The preparation of DNA immobilized polymer modified electrode presented here was simple, easy, fast and cheap when compared with similar studies in the literature. This electrochemical approach for DNA detection and hybridization by using polymer based electrode showed a good selectivity and sensitivity. It was found that the level of nonspecific immobilization on these polymer modified electrode was sufficiently low, thus it was easy to distinquish DNA hybridization. There was no need to use or bind any extra electroactive species, or mediator, since this polymer system had already a good electroactivity.

REFERENCES

Abaci, S., Pekmez, K., Yildiz, A., 2005, The influence of nonstoichiometry on the electrocatalytic activity of PbO_2 for oxygen evolution in acidic media, Electrochemistry Communications, 7, 328-332.

Abruna, H.D., 1988, Coordination chemistry in two dimensions: Chemically modified electrodes, Coordination Chemistry Reviews, 86, 135-189.

Arora, K., Prabhakar, N., Chand, S., Malhotra, B.D., 2007, Ultrasensitive DNA hybridization biosensor based on polyaniline, Biosensors & Bioelectronics, 23, 613-620.

Arrigan, D.W.M., 1994, Voltammetric determination of trace metals and organics after accumulation at modified electrodes, Analyst, 119, 1953-1966.

Aso, C., Kunitake, T., Nakashima, T., 1969, Cationic polymerization and copolymerization of vinylferrocene, Macromolecular Chemistry, 124, 232-239.

Aydın, G., Çelebi, S.S., Özyörük, H., Yıldız, A., 2002, Amperometric enzyme electrode for L(+)-lactate determination using immobilized L(+)-lactate oxidase in poly(vinylferrocenium) film, Sensors and Actuators B, 87, 8-12.

Bard, A.J. and Faulkner, L.R., 2001, Electrochemical Methods: Fundamentals and Applications, 2nd Edition, Wiley, New York.

Beilstein, A.M. and Grinstaff, M.W., 2001, Synthesis and characterization of ferrocene-labelled oligodeoxynucleotides, Journal of Organometallic Chemistry, 637-639, 398-406.

Billova, S., Kizek, R., Palecek, E., 2002, Differential pulse adsorptive stripping voltammetry of osmium-modified peptides, Bioelectrochemistry, 56, 63-66.

Cai, H., Wang, Y., Piang, He, Fang, Y., 2002, Electrochemical detection of DNA hybridization based on silver-enhanced gold nanoparticle label, Analytica Chimica Acta, 469, 165-172.

Chaubey, A. and Malhotra, B.D., 2002, Mediated biosensors, Biosensors & Bioelectronics, 17, 441-456.

Chang, Z., Chen, M., Fan, H., Zhao, K., Zhuang, S., He, P., Fang, Y., 2008, Multilayer membranes via layer-by-layer deposition of PDDA and DNA with Au nanoparticles as tags for DNA biosensing, Electrochimica Acta, 53, 2939-2945.

Chen, S.M. and Wang, C.H., 2007, Electrochemical properties of guanine, adenine, guanosine-5'-monophosphate, ans ssDNA by Fe(II) bis(2,2':6',2"-terpyridine), Fe(II) tris(1,10-phenanthroline), and poly-Fe(II) tris(5-amino-1,10-phenanthroline), Bioelectrochemistry, 70, 452-461.

Connor, D.J.O., Sexton, B.A., Smart, R.S.C., 2003, Surface Analysis Methods in Materials Science, Springer-Verlag, New York.

Cougnon, C., Gautier, C., Pilard, J.F., Casse, N., Chenais, B., 2008, Redox and ion-exchange properties in surface-tethered DNA-conducting polymers, Biosensors & Bioelectronics, 23, 1171-1174.

Davis, J., Vaughan, D.H., Cardosi, M.F., 1995, Elements of biosensor construction, Enzyme and Microbial Technology, 17, 1030-1035.

Degefa, T.H. and Kwak, J., 2008, Electrochemical impedance sensing of DNA at PNA self assembled monolayer, Journal of Electroanalytical Chemistry, 612, 37-41.

Edwards, G.A., Bergren, A.J., Porter, M.D., 2007, Chemically modified electrodes, Handbook of Electrochemistry, ed. Zoski, C.G., USA, Elsevier, 295-327.

Erdem, A., Kerman, K., Meric, B., Ozsoz, M., 2000a, Methylene blue as a novel electrochemical hybridization indicator, Electroanalysis, 13, 219-223.

Erdem, A., Pabuccuoglu, A., Meric, B., Kerman, K., Özsöz, M., 2000b, Electrochemical biosensor based on horseradish peroxidase for the determination of oxidizable drugs, Turkish Journal of Medical Sciences, 30, 349-354.

Erdem, A. and Özsöz, M., 2001a, Voltammetry of the anticancer drug mitoxantrone and DNA, Turkish Journal of Chemistry, 25, 469-475.

Erdem, A. and Ozsoz, M., 2001b, Interaction of the anticancer drug epirubicin with DNA, Analytica Chimica Acta, 437, 107-114.

Erdem, A. and Ozsoz, M., 2002, Electrochemical DNA biosensors based on DNA-drug interactions, Electroanalysis 14, 965-974.

Erdem, A., Papakonstantinou, P., Murphy, H., 2006, Direct DNA hybridization at disposable graphite electrodes modified with carbon nanotubes, Analytical Chemistry, 78, 6656-6659.

Fan, C., Song, H., Hu, X., Li, G., Zhu, J., Xu, X., Zhu, D., 1999, Voltammetric response and determination of DNA with a silver electrode, Analytical Biochemistry, 271, 1-7.

Fang, B., Jiao, S., Li, M., Qu, Y., Jiang, X., 2008, Label-free electrochemical detection of DNA using ferrocene-containing cationic polythiophene and PNA probes on nanogold modified electrodes, 23, 1175-1179.

Fojta, M., Kubicarova, T., Palecek, E., 2000, Electrode potential-modulated cleavage of surface-confined DNA by hydroxyl radicals detected by an electrochemical biosensor, Biosensors & Bioelectronics, 15, 107-115.

Fojta, M., Havran, L., Kubicarova, T., Palecek, E., 2002, Electrode potential-controlled DNA damage in the presence of copper ions and their complexes, Bioelectrochemistry, 55, 25-27.

Fojta, M., Havran, L., Kizek, R., Billova, S., Palecek, E., 2004, Multiply osmium-labeled reporter probes for electrochemical DNA hybridization assays: detection of trinucleotide repeats, Biosensors & Bioelectronics, 20, 985-994.

Fojta, M., Kostecka, P., Trefulka, M., Havran, L. and Palecek, E., 2007, "Multicolor" electrochemical labeling of DNA hybridization probes with osmium tetroxide complexes, Analytical Chemistry, 79, 1022-1029.

Gerard, M., Chaubey, A., Malhotra, B.D., 2002, Application of conducting polymers to biosensors, Biosensors & Bioelectronics, 17, 345-359.

Gooding, J.J., 2002, Electrochemical DNA hybridization biosensors, Electroanalysis, 14, 1149-1156.

Gülce, H., Özyörük, H., Yıldız, A., 1995a, Electrochemical response of poly(vinylferrocenium)-coated Pt electrodes to some anions in aqueous media, Electroanalysis, 7, 178-183.

Gülce, H., Çelebi, S.S., Özyörük, H., Yıldız, A., 1995b, Amperometric enzyme electrode for sucrose determination prepared from glucose oxidase and invertase co-immobilized in poly(vinylferrocenium), Journal of Electroanalytical Chemistry, 397, 217-223.

Gülce, H., Özyörük, H., Çelebi, S.S., Yıldız, A., 1995c, Amperometric enzyme electrode for aerobic glucose monitoring prepared by glucose oxidase immobilized in poly(vinylferrocenium), Journal of Electroanalytical Chemistry, 394, 63-70.

Gülce, H., Çelebi, S.S., Özyörük, H., Yıldız, A., 1997, Electroanalysis and electrocatalysis using poly(vinylferrocenium) perchlorate coated electrodes, Pure & Applied Chemistry, 69, 173-177.

Gülce, H., Ataman, İ, Gülce, A., Yıldız, A., 2002a, A new amperometric enzyme electrode for galactose determination, Enzyme and Microbial Technology, 30, 41-44.

Gülce, H., Gülce, A., Yıldız, A., 2002b, A novel two-enzyme amperometric electrode for lactose determination, Analytical Sciences, 18, 147-150.

Gülce, H., Gülce, A., Kavanoz, M., Çoşkun, H., Yıldız, A., 2002c, A new amperometric enzyme electrode for alcohol determination, Biosensors & Bioelectronics, 17, 517-521.

Gülce, H., Aktaş, Y.S., Gülce, A., Yıldız, A., 2003, Polyvinylferrocenium immobilized enzyme electrode for choline analysis, Enzyme and Microbial Technology, 32, 895-899.

Gündoğan-Paul, M., Çelebi, S.S., Özyörük, H., Yıldız, A., 2002a, Amperometric enzyme electrode for organic peroxides determination prepared from horseradish peroxidase immobilized in poly(vinylferrocenium) film, Biosensors & Bioelectronics, 17, 875-881.

Gündoğan-Paul, M., Özyörük, H., Çelebi, S.S., Yıldız, A., 2002b, Amperometric enzyme electrode for hydrogen peroxide determination prepared with horseradish peroxidase immobilized in poly(vinylferrocenium) (PVF^+), Electroanalysis, 14, 505-511.

Havran, L., Fojta, M., Palecek, E., 2004, Voltammetric behavior of DNA modified with osmium tetroxide 2,2'-bipyridine at mercury electrodes, Bioelectrochemistry, 63, 239-243.

Inzelt, G. and Bacskai, J., 1992, Electrochemical quartz crystal microbalance study of the swelling of poly(vinylferrocene) films, Electrochimica Acta, 37, 647-654.

Inzelt, G. and Szabo, L., 1986, The effect of the nature and the concentration of counter ions on the electrochemistry of poly(vinylferrocene) polymer film electrodes, Electrochimica Acta, 31, 1381-1387.

Jelen, F., Kourilova, A., Pecinka, P., Palecek, E., 2004, Microanalysis of DNA by stripping transfer voltammetry, Bioelectrochemistry, 63, 249-252.

Jiang, C., Yang, T., Jiao, K., Gao, H., 2008, A DNA electrochemical sensor with poly-L-lysine/single-walled carbon nanotubes films and its application for the highly sensitive EIS detection of PAT gene fragment and PCR amplification of NOS gene, Electrochimica Acta, 53, 2917-2924.

Karadeniz, H., Gulmez, B., Erdem, A., Jelen, F., Ozsoz, M., Palecek, E., 2006, Echinomycin and cobalt-phenanthroline as redox indicators of DNA hybridization at gold electrodes, Frontiers in Bioscience, 11, 1870-1877.

Karadeniz, H., Erdem, A., Caliskan, A., Pereira, C.M., Pereira, E.M., Ribeiro, J.A., 2007a, Electrochemical sensing of silver tags labelled DNA immobilized onto disposable graphite electrodes, Electrochemistry Communications, 9, 2167-2173.

Karadeniz, H., Alparslan, L., Erdem, A., Karasulu, E., 2007b, Electrochemical investigation of interaction between mitomycin C and DNA in a novel drug-delivery system, Journal of Pharmaceutical and Biomedical Analysis, 45, 322-326.

Kaufman, F.B. and Engler, E.M., 1979, Solid-State spectroelectrochemistry of. cross-linked donor bound polymer films, J. American Chemical Society, 101, 547-549.

Kerman, K., Ozkan, D., Kara, P., Meric, B., Gooding, J.J., Ozsoz, M., 2002, Voltammetric determination of DNA hybridization using methylene blue and

self-assembled alkanethiol monolayer on gold electrodes, Analytica Chimica Acta, 462, 39-47.

Kerman, K., Morita, Y., Takamura, Y., Tamiya, E., 2003, Label-free electrochemical detection of DNA hybridization on gold electrode, Electrochemistry Communications, 5, 887-891.

Kizek, R., Havran, L., Fojta, M., Palecek, E., 2002, Determination of nanogram quantities of osmium-labeled single stranded DNA by differential pulse sripping voltammetry, Bioelectrochemistry, 55, 119-121.

Komarova, E., Aldissi, M., Bogomolova, A., 2005, Direct electrochemical sensor for fast reagent-free DNA detection, Biosensors & Bioelectronics, 21, 182-189.

Kumar, R.S. and Arunachalam, S., 2007, DNA binding and antimicrobial studies of some polyethyleneimine-copper(II) complex samples containing 1,10-phenanthroline and 1-theronine as co-ligands, Polyhedron, 26, 3255-3262.

Korri-Youssoufi, H. and Makrouf, B., 2001, Electrochemical biosensing of DNA hybridization by electroactive ferrocene functionalized polypyrrole, Synthetic Metals, 119, 265-266.

Kuralay, F., Özyörük, H., Yıldız, A., 2005, Potentiometric enzyme electrode for urea determination using immobilized urease in poly(vinylferrocenium) film, Sensors and Actuators B, 109, 194-199.

Kuralay, F., Özyörük, H., Yıldız, A., 2006, Amperometric enzyme electrode for urea determination using immobilized urease in poly(vinylferrocenium) film, Sensors and Actuators B, 114, 500-506.

Kuralay, F., Özyörük, H., Yıldız, A., 2007, Inhibitive determination of Hg^{2+} ion by an amperometric urea biosensor using poly(vinylferrocenium) film, Enzyme and Microbial Technology, 40, 1156-1159.

Kuralay, F., Erdem, A., Abacı, S., Özyörük, H., Yıldız, A., 2008, Electrochemical biosensing of DNA immobilized poly(vinylferrocenium) modified electrode, Electroanalysis, 20, 2563-2570.

Kuralay, F., Erdem, A., Abacı, S., Özyörük, H., Yıldız, A., 2009a, Characterization of redox polymer based electrode and electrochemical behavior for DNA detection, Analytica Chimica Acta, 643, 83-89.

Kuralay, F., Erdem, A., Abacı, S., Özyörük, H., Yıldız, A., 2009b, Poly(vinylferrocenium) modified disposable pencil graphite electrode for DNA hybridization, Electrochemistry Communications, 11, 1242-1246.

Lehninger, A.L., Nelson, D.L., Cox, M.M., 1982, Principles of Biochemistry, 2nd Edition, Worth Publishers, New York.

Li, J., Liu, Q., Liu, Y., Liu, S., Yao, S., 2005, DNA biosensor based on chitosan film doped with carbon nanotubes, Analytical Biochemistry, 346, 107-114.

Liu, Y. and Hu, N., 2007, Loading/release behavior of (chitosan/DNA)$_n$ by layer-by-layer films toward negatively charged anthraquinone and its application in electrochemical detection of natural DNA damage, Biosensors & Bioelectronics, 23, 661-667.

Lucarelli, F., Marrazza, G., Turner, A.P.F., Mascini, M., 2004, Carbon and gold electrodes as electrochemical transducers for DNA hybridization sensors, Biosensors & Bioelectronics, 19, 515-530.

Malhotra, B.D., Chaubey, A. 2003, Biosensors for clinical diagnostics industry, Sensors and Actuators B, 91, 117-127.

Mello, L.D. and Kubota, L.T., 2002, Review of the use of biosensors as analytical tools in the food and drink industries, Food Chemistry, 77, 237-256.

Millan, K.M. and Mikkelsen, S.R., 1993, Sequence-selective biosensor for DNA based on electroactive hybridization indicators, Analytical Chemistry, 65, 2317-2323.

Miwa, T., Jin, L.T., Mizuike, A., 1984, Differential-pulse anodic stripping voltammetry of copper with a chemically-modified glassy carbon electrode, Analytica Chimica Acta, 160, 135-140.

Muguruma, H. and Karube, I., 1999, Plasma-polymerized films for biosensors, Trends in Analytical Chemistry, 18, 62-68.

Mugweru, A. and Rusling, J.F., 2001, Catalytic square-wave voltammetric detection of DNA with reversible metallopolymer-coated electrodes, Electrochemistry Communications, 3, 406-409.

Murray, R.W., 1984, Chemically modified electrodes, Electroanalytic Chemistry, ed. Bard, A.J., Marcel Dekker, New York, 13, 191-368.

Nakayama, M., Ihara, T., Nakano, K., Maeda, M., 2002, DNA sensors using a ferrocene-oligonucleotide conjugate, Talanta, 56, 857-866.

Navarro, A.E., Spinelli, N. Chaix, C., Moustrou, C., Mandrand, B., Brisset, H., 2004, Supported synthesis of ferrocene modified oligonucleotides as new electroactive DNA probes, Bioorganic and Medicinal Chemistry Letters, 14, 2439-2441.

Niemeyer, C.M., 2001, Semi-synthetic nucleic acid-protein conjugates: applications in life sciences and nanobiotechnology, Reviews in Molecular Biotechnology, 82, 47-66.

Ostatna, V. and Palecek, E., 2006, Self-assembled monolayers of thiol-end-labeled DNA at mercury electrodes, Langmuir, 22, 6481-6484.

Özcan, A., Şahin, Y., Özsöz, M., Turan, S., 2007, Electrochemical oxidation of ds-DNA on polypyrrole nanofiber modified pencil graphite electrode, Electroanalysis, 19, 2208-2216.

Özer, B.C., Özyörük, H., Çelebi, S.S., Yıldız, A., 2007, Amperometric enzyme electrode for free cholesterol determination prepared with cholesterol oxidase immobilized in poly(vinyferrocenium) film, Enzyme and Microbial Technology, 40, 262-265.

Palecek, E., Fojta, M., Tomschik, M., Wang, J., 1998, Electrochemical biosensors for DNA hybridization and DNA damage, Biosensors & Bioelectronics, 13, 621-628.

Palecek, E. and Fojta, M., 2001, Detecting DNA hybridization and damage, Analytical Chemistry, 73, 74A-83A.

Palecek, E., 2002a, Preface, Talanta, 56, 807.

Palecek, E., 2002b, Past, present and future of nucleic acids electrochemistry, Talanta, 56, 809-819.

Palecek, E. and Jelen, F., 2005, Electrochemistry of nucleic acids, Perspectives in Bioanalysis, 1, 73-173.

Peerce, P.J. and Bard, A.J., 1980, Polymer films on electrodes: Part II. Film structure and mechanism of electron transfer with electrodeposited poly(vinylferrocene), J. Electroanalytical Chemistry, 112, 97-115.

Pejcic, B. and De Marco, R., 2006, Impedance spectroscopy: Over 35 years of electrochemical sensor optimization, Electrochimica Acta, 51, 6217-6229.

Peterson, J.I. and Vurek, G.G., 1984, Fiber optic sensors for biomedical applications, Science, 224, 12-127.

Piro, B., Haccoun, J., Pham, M.C., Tran, L.D. Rubin, A., Perrot, H., Gabrielli, C., 2005, Study of the DNA hybridization transduction behavior of quinone-containing electroactive polymer by cyclic voltammetry and electrochemical impedance spectroscopy, Journal of Electroanalytical Chemistry, 577, 155-165.

Prabhakar, N., Singh, H., Malhotra, B.D., 2008a, Nucleic acid immobilized polypyrrole-polyvinylsulphonate film for Mycobacterium tuberculosis detection, Electrochemistry Communications, 10, 821-826.

Prabhakar, N., Sumana, G., Arora, K., Singh, H., Malhotra, B.D., 2008b, Improved electrochemical nucleic acid biosensor based on polyaniline-polyvinyl sulphonate, Electrochimica Acta, 53, 4344-4350.

Ramanavicius, A., Ramanaviciene, A., Malinauskas, A., 2006, Electrochemical sensors based on conducting polymer-polypyrrole, Electrochimica Acta, 51, 6025-6037.

Rauf, S., Gooding, J.J., Akhtar, K., Ghauri, M.A., Rahman, M., Anwar, M.A., Khalid, A.M., 2005, Electrochemical approach of anticancer drugs-DNA interaction, Journal of Pharmaceutical and Biomedical Analysis, 37, 205-217.

Ren, X. and Pickup, P.G., 1994, Strong dependence of the electron-hopping rate in poly-tris(5-amino-1,10-phenanthroline)iron(III/II) on the nature of the counter-anion, J. Electroanalytical Chemistry, 365, 289-292.

Qi, H., Li, X., Chen, P., Zhang, C., 2007, Electrochemical detection of DNA hybridization based on polypyrrole/ss-DNA/multi-wall carbon nanotubes paste electrode, Talanta, 72, 1030-1035.

Salimi, A., Korani, A., Hallaj, R., Khoshnavazi, R., Hadadzadeh, H., 2009, Immobilization of $[Cu(bpy)_2]Br_2$ complex onto a glassy carbon electrode modified with α-$SiMo_{12}O_{40}^{4-}$ and single walled carbon nanotubes: Application to nanomolar detection of hydrogen peroxide and bromate, Analytica Chimica Acta, 635, 63-70.

Sanchez-Pomales, G., Santiago-Rodriguez, L., Rivera-Velez, N.E., Cabrera, C.R., 2007, Control of DNA self-assembled monolayers surface coverage by electrochemical desorption, Journal of Electroanalytical Chemistry, 611, 80-86.

Saoudi, B., Despas, C., Chehimi, M., Jammul, N., Delemar, M., Bessiere, J., Walcarius, A., 2000, Study of DNA adsorption on polypyrrole: interest of dielectric monitoring, Sensors and Actuators B, 62, 35-42.

Senthil Kumar, R., Arunachalam, S., 2007, DNA binding and antimicrobial studies of some polyethylene-copper(II) complex samples containing 1,10-phenanthroline and L-theronine as co-ligands, Polyhedron, 26, 3255-3262.

Shirota, Y., Kakuta, T., Mikawa, H., 1984, Electrochemical oxidation of poly(vinylferrocene) with concurrent precipitation on the electrode: Preparation of an electronically conducting polymer, Macromolecular Chemistry, 5, 337-340.

Skoog D.A., Leary, J.J., 1992, Principles of Instrumental Analysis, 4th Edition, Saunders College Publishing, New York.

Sönmez Çelebi, M., Pekmez, K., Özyörük, H., Yıldız, A., 2008a, Preparation and physical/electrochemical characterization of Pt/poly(vinyferrocenium) electrocatalyst for methanol oxidation, Journal of Power Sources, 183, 8-13.

Sönmez Çelebi, M., Pekmez, K., Özyörük, H., Yıldız, A., 2008b, Electrochemical synthesis of Pd particles on poly(vinyferrocenium), Catalysis Communications, 9, 2175-2178.

Storhoff, J.J., Mirkin, C.A. 1999, Programmed materials synthesis with DNA, Chemical Reviews, 99, 1849-1862.

Stryer, L., 1995, Biochemistry, 4th Edition, W.H. Freeman and Company, New York, 75-93.

Tang, T.C. and Huang, H.J., 1999, Electrochemical studies of the intercalation of ethidium bromide to DNA, Electroanalysis, 11, 1185-1190.

Takenaka, S., 2005, Threading intercalators as redox indicators, Perspectives in Bioanalysis, 1, 345-367.

Thevenot, D.R., Klara, T., Durst, R.A., Wilson, G.S., 2001, Electrochemical biosensors: recommended definitions and classification, Biosensors & Bioelectronics, 16, 121-131.

Umana, M., Rolison, D.R., Nowak, R., Daum, P., Murray, R.W., 1980, X-Ray photoelectron spectroscopy of metal, metal oxide and carbon electrode surfaces chemically modified with ferrocene and ferrocenium, Surface Science, 101, 295-309.

Wang, J., 1994, Selectivity coefficients for amperometric biosensors, Talanta, 41, 857-863.

Wang, J., Ozsoz, M., Cai, X., Rivas, G., Shiraishi, H., Grant, D.H., Chicharro, J., Palecek, E., 1998, Interactions of antitumor drug daunomycin with DNA in solution and at the surface, Bioelectrochemistry and Bioenergetics, 45, 33-40.

Wang, J., 2000, From DNA biosensors to gene chips, Nucleic Acids Research, 28, 3011-3016.

Wang, J., Kawde, A.N., Erdem, A., Salazar, M., 2001, Magnetic bead-based label-free electrochemical detection of DNA hybridization, Analyst, 126, 2020-2024.

Wang, J., Kawde, A.N., 2002, Amplified label-free electrical detection of DNA hybridization, Analyst, 127, 383-386.

Wang, J., 2002, Electrochemical nucleic acid biosensors, Analytica Chimica Acta, 469, 63-71.

Wang, J., 2005, Electrochemical nucleic acid biosensors, Perspectives in Bioanalysis, 1, 175-194.

Yang, M., McGovern, M.E., Thompson, M., 1997, Genosensor technology and the detection of interfacial nucleic acid chemistry, Analytica Chimica Acta, 346, 259-275.

Yosypchuk, B., Fojta, M., Havran, L., Heyrovsky, M., Palecek, E., 2006, Voltammetric behavior of osmium-labeled DNA at mercury meniscus-modified solid amalgam electrodes. Detecting DNA hybridization, 18, 186-194.

Yu, L., Sathe, M., Zeng, X., 2005, EQCM study of the redox processes of polyvinylferrocene film in L-glutamine solution, J. Electrochemical Society, 152, E357-E363.

Zhao, Y.D., Pang, D.W. Hu, S., Wang, Z.L., Cheng, J.K., Qi, Y.P., Dai, H.P., Mao, B.W., Tian, Z.Q., Lou, J., Lin, Z.H., 1999, DNA-modified electrodes Part 3: spectroscopic characterization of DNA-modified gold electrodes, Analytica Chimica Acta, 388, 93-101.

Zhu, N., Zhang., A., Wang, Q., He, P., Fang, Y., Electrochemical detection of DNA hybridization using methylene blue and electro-deposited zirconia thin films on gold electrodes, Analytica Chimica Acta, 510, 163-168.

CURRICULUM VITAE

Name Surname	:	Filiz Kuralay
Place of Birth	:	Ordu
Date of Birth	:	1978
Marital Status	:	Single

Education and Academic Position

High School	1993-1996	Trabzon Yomra Science High School	Ordu
BSc	1996-2001	Hacettepe University, Department of Chemistry	Ankara
MSc	2001-2003	Institute of Sciences of Hacettepe University	Ankara

Job Experience

2001 - onwards	Research Assistant at Hacettepe University, Department of Chemistry